UNIVERSITAT POLITÈCNICA DE VALÈNCIA

DEPARTMENT OF MECHANICAL AND MATERIALS ENGINEERING

PROGRAMA DE DOCTORADO INGENIERÍA Y PRODUCCIÓN INDUSTRIAL

RĪGAS TEHNISKĀ UNIVERSITĀTE

RIGA TECHNICAL UNIVERSITY

FACULTY OF MECHANICAL ENGINEERING, TRANSPORT AND AERONAUTICS

INSTITUTE OF MECHANICAL ENGINEERING, DEPARTMENT OF MATERIAL PROCESSING TECHNOLOGY

Author: Andris Logins

High speed milling technological regimes, process condition and technological equipment condition influence on surface quality parameters of difficult to cut materials

Scientific advisors: Dr.sc.ing. Professor
Toms Torims

Dr.sc.ing. Professor
Pedro Rosado Castellano

Dr.sc.ing. Professor
Santiago Carlos Gutiérrez Rubert

Valencia, January, 2021

Abstract

Surface quality of machined parts highly depends on the surface texture that reflects the marks, left by the tool during the cutting process. The traditional theoretical approaches indicate that these marks are related to the cutting parameters (cutting speed, feed, depths of cut…), the machining type, the part material, the tool geometry, etc. But, different machining type and material selection can give a variable result. In nowadays, more progressively, High Speed milling techniques have been applied on hard-to-cut materials more and more extensively. High-speed milling has often been applied in injection mold manufacturing processes, where surface roughness is a significant criterion in product quality demands. It is equally applicable to automotive, general industrial engineering and even in toy manufacturing, where plastic parts with a high-quality surface finish have been produced using the injection molding techniques. High-speed milling involves a considerable number of process parameters that may affect the 3D surface topography formation. The influence of some factors has been widely studied by several researchers. They have proposed different approaches to mathematical models used to predict the final surface roughness and texture in milling processes. But, the lack of knowledge in the processes of HSM cutting doesn't allow to predict results of machined surface topography efficiently.

Supported by the previous work done in Master Thesis, the author conclude that only statistical analysis is an insufficient tool for surface topography prediction with variable process parameters. The hypothesis that surface topography parameters depends on the traces left by the tool, determined by working conditions and environmental properties, led to the development of a custom research methodology. This research work shows how the parameters combination, tool axis inclination, tool geometric deflection, cutting tool geometry and environment vibrational behavior, influence on 3D surface topography parameter Sz.

Author developed methodology and several mathematical models were used for milling process analysis. The general model was divided in multiple parts, where additional process parameters influence has been described and included in general model proposed. The reliability of experimentally obtained measurements, calculations and predicted surface topography values have been tested with a statistical validation process. 3D surface topography measurements are compared with statistical correlation methods. Each part of analysis is followed by a mathematical approach of the 3D surface topography parameter Sz. The incremental process followed allows the author to develop a general mathematical model, step by step, adding the components that affect surface topography formation the most.

In the first part of the research new samples were developed, with more conventional shape of cutting tool, to analyze the cutting parameter influence on surface topography formation. End milling procedure with flat end milling tools was selected. First, tool geometry, combined with multiple cutting feed rates, is analyzed to distinguish the main parameters that affect surface

topography. A prediction model is introduced with a basic topography height component, performed by cutting tool geometry.

Next, specifically designed experiments were conducted, varying technological parameters. That starts with cutting tool axis inclination against the milling table analysis. The specimens of analysis are samples with 4 contrary aimed straight cutting paths. Linear paths in different directions give a chance to analyze milling machine spindle axis topography, as well as marks left from cutting tool back cutting edge.

Considering the deviations of cutting marks observed in the images of the surface topography obtained through the measurements, the milling equipment and cutting tool dynamical behavior analysis were introduced. Vibrations produce deviations in the milling table and cutting tool. These deviations were detected and included in the mathematical model to complete the prediction model accuracy.

Finally, the prediction model of the topography parameter Sz was tested with increased number of process parameters. Measured and predicted Sz values were compared and analyzed statistically. Results revealed high predicted topography deviation on samples manufactured with different machines and with different feed rates.

Relevant conclusions about the manufacturing equipment accuracy have been drawn and they state that cutting tool's footprint is directly related with surface topography parameters. Besides, footprint influence is affected by cutting tool geometry, tool stiffness and equipment accuracy. Tool geometry forms the basis of Sz parameter – surface height deviation. Developed prediction model justify and ANOVA analysis confirms, that the most important influence on Sz parameter formation is done by cutting feed rate. Besides, feed rate leave direct influence on cutting tool stiffness and milling system dynamical behavior. Local cutting tool vibrations do not have any influence on surface parameter mean values. In general, developed mathematical model to predict Sz topography parameter local vibrations are an improvement of existing ones. The conclusions reached are basis for practical recommendations, applicable in industry.

Resumen

La calidad superficial en las piezas mecanizadas depende del acabado superficial, resultado de las marcas dejadas por la herramienta durante el proceso de corte. Las aproximaciones teóricas tradicionales indican que estas marcas están relacionadas con los parámetros de corte (velocidad de corte, avance, profundidad de corte…), el tipo de máquina, el material de la pieza, la geometría de la herramienta, etc. Pero no todos los tipos de mecanizado y selección de materiales pueden dar un resultado ambiguo. Hoy en día, de manera progresiva, se están utilizando las técnicas de fresado de Alta Velocidad sobre materiales de difícil mecanizado cada vez más. El fresado de Alta Velocidad se utiliza a menudo en los procesos de fabricación de moldes para inyección de plástico, donde la rugosidad superficial es un criterio significante exigido en la calidad del producto. De la misma forma se exige en el sector del automóvil, en la

ingeniería industrial en general o incluso en la fabricación de juguetes, donde las piezas de plástico con una alta calidad en su acabado superficial han sido producidas usando técnicas de inyección en moldes. El fresado de Alta Velocidad implica a un considerable número de parámetros del proceso que pueden afectar a la formación topográfica 3D de la superficie. La influencia de algunos factores ha sido ampliamente estudiada por varios investigadores. Ellos han propuesto diferentes aproximaciones de modelos matemáticos para predecir la textura y rugosidad superficial final en los procesos de fresado. Pero, la falta de conocimiento en los procesos de mecanizado de Alta Velocidad no permite predecir eficientemente resultados de rugosidad superficial en piezas mecanizadas.

Respaldado por el trabajo previo hecho en el Trabajo Fin de Máster, el autor concluye que solo el análisis estadístico es una herramienta insuficiente para la predicción de la rugosidad superficial con parámetros del proceso variables. La hipótesis de que los parámetros de rugosidad superficial dependen de las huellas dejadas por la herramienta, determinadas por las condiciones de trabajo y las propiedades del entorno, condujo al desarrollo de una metodología de investigación personalizada. Este trabajo de investigación muestra como la combinación de los parámetros, inclinación del eje de la herramienta, deflexión geométrica de la herramienta y comportamiento vibracional del entorno, influencian sobre el parámetro de rugosidad superficial 3D, Sz.

La metodología desarrollada por el autor y varios modelos matemáticos fueron usados en el proceso de análisis del fresado. El modelo general fue dividido en varias partes, donde se ha descrito la influencia de parámetros del proceso adicionales, siendo incluidos en el modelo general propuesto. La confiabilidad de las mediciones obtenidas experimentalmente, cálculos y valores de rugosidad superficial predichos han sido comprobados con un proceso de validación estadístico. Las medidas de la topografía 3D de la superficie son comparadas con métodos de correlación estadística. Cada parte del análisis es acompañada por una aproximación matemática para el parámetro de rugosidad 3D, Sz. El proceso incremental seguido permite al autor desarrollar un modelo matemático general, paso a paso, añadiendo los componentes que más afectan a la formación de la topografía de la superficie.

En la primera parte de la investigación se desarrollaron nuevas muestras, con una forma más convencional de la herramienta de corte, para analizar la influencia de los parámetros de corte sobre la formación de la topografía de la superficie. Se seleccionó un proceso de fresado con herramientas de punta plana. Primero, se analiza la geometría de la herramienta, combinada con múltiples avances, para distinguir los principales parámetros que afectan a la rugosidad superficial. Se introduce un modelo de predicción con un componente básico para la altura de la rugosidad, obtenida por la geometría de la herramienta de corte.

A continuación, se llevan a cabo experimentos más específicamente diseñados, variando parámetros tecnológicos. Esto empieza con el análisis de la inclinación del eje de la herramienta contra la mesa de fresado. Los especímenes de análisis son muestras con cuatro recorridos de

corte rectos con corte en sentido contrario. Las trayectorias lineales con diferentes direcciones dan la oportunidad de analizar la inclinación del husillo de fresado en la máquina. Un análisis visual reveló diferencias entre direcciones de corte opuestas, así como marcas dejadas por el filo posterior de la herramienta.

Considerando las desviaciones de las marcas de corte observadas en las imágenes de rugosidad superficial obtenidas a partir de las medidas, se introdujo un análisis sobre el comportamiento dinámico del equipo y de la herramienta de corte. Las vibraciones producen desviaciones en la mesa de fresado y en la herramienta de corte. Estas desviaciones fueron detectadas e incluidas en el modelo matemático para completar la precisión en la predicción del modelo.

Finalmente, el modelo de predicción del parámetro de rugosidad Sz fue comprobado con un mayor número de parámetros del proceso. Los valores de Sz medidos y predichos, fueron comparados y analizados estadísticamente. Los resultados revelaron una mayor desviación de la rugosidad predicha en las muestras fabricadas con diferentes máquinas y con diferentes avances.

Importantes conclusiones sobre la precisión del equipo de fabricación han sido extraídas y de ellas se desprende que la huella de la herramienta de corte está directamente relacionada con los parámetros de la topografía de la superficie. Además, la influencia de la huella está afectada por la geometría de la herramienta de corte, la rigidez de la herramienta y la precisión del equipo. La geometría de la herramienta conforma la base del parámetro S_z, desviación de la altura de la superficie. Las conclusiones alcanzadas son la base para recomendaciones prácticas, aplicables en la industria.

Resum

La qualitat superficial en les peces mecanitzades depèn de l'acabat superficial, resultat de les marques deixades per l'eina durant el procés de tall. Les aproximacions teòriques tradicionals indiquen que aquestes marques estan relacionades amb els paràmetres de tall (velocitat de tall, avanç, profunditat de tall...), el tipus de màquina, el material de la peça, la geometria de l'eina, etc. Però no tots els tipus de mecanitzat i selecció de materials poden donar un resultat ambigu. Avui en dia, de manera progressiva, s'estan utilitzant les tècniques de fresat d'Alta Velocitat sobre materials de difícil mecanització cada vegada més. El fresat d'Alta Velocitat s'utilitza sovint en els processos de fabricació de motlles per a injecció de plàstic, on la rugositat superficial és un criteri significant exigit en la qualitat del producte. De la mateixa manera s'exigeix en el sector de l'automòbil, en l'enginyeria industrial en general o fins i tot en la fabricació de joguines, on les peces de plàstic amb una alta qualitat en el seu acabat superficial han estat produïdes usant tècniques d'injecció en motlles. El fresat d'Alta Velocitat implica un considerable nombre de paràmetres del procés que poden afectar la formació topogràfica 3D de la superfície. La influència d'alguns factors ha estat àmpliament estudiada per diversos investigadors. Han proposat diferents aproximacions de models matemàtics per predir la textura i rugositat superficial final en els processos de fresat. Però, la manca de coneixement en els

processos de mecanitzat d'Alta Velocitat no permet predir eficientment resultats de rugositat superficial en peces mecanitzades.
Recolzat pel treball previ fet en el Treball Fi de Màster, l'autor conclou que només l'anàlisi estadístic és una eina insuficient per a la predicció de la rugositat superficial amb paràmetres variables del procés. La hipòtesi que els paràmetres de rugositat superficial depenen de les empremtes deixades per l'eina, determinades per les condicions de treball i les propietats de l'entorn, va conduir al desenvolupament d'una metodologia d'investigació personalitzada. Aquest treball de recerca mostra com la combinació dels paràmetres, inclinació de l'eix de l'eina, deflexió geomètrica de l'eina i comportament vibracional de l'entorn, influencien sobre el paràmetre de rugositat superficial 3D, Sz.
La metodologia desenvolupada per l'autor i diversos models matemàtics van ser usats en el procés d'anàlisi del fresat. El model general va ser dividit en diverses parts, on s'ha descrit la influència de paràmetres addicionals del procés, sent inclosos en el model general proposat. La fiabilitat de les mesures obtingudes experimentalment, càlculs i valors de rugositat superficial predits han estat comprovats amb un procés de validació estadístic. Les mesures de la topografia 3D de la superfície són comparades amb mètodes de correlació estadística. Cada part de l'anàlisi és acompanyada per una aproximació matemàtica per al paràmetre de rugositat 3D, Sz. El procés incremental seguit permet a l'autor desenvolupar un model matemàtic general, pas a pas, afegint els components que més afecten a la formació de la topografia de la superfície.
En la primera part de la investigació es van desenvolupar noves mostres, amb una forma més convencional de l'eina de tall, per analitzar la influència dels paràmetres de tall sobre la formació de la topografia de la superfície. Es va seleccionar un procés de fresat amb eines de punta plana. Primer, s'analitza la geometria de l'eina, combinada amb múltiples avanços, per distingir els principals paràmetres que afecten la rugositat superficial. S'introdueix un model de predicció amb un component bàsic per a l'altura de la rugositat, obtinguda a través de la geometria de l'eina de tall.

A continuació, es duen a terme experiments més específicament dissenyats, variant paràmetres tecnològics. Això comença amb l'anàlisi de la inclinació de l'eix de l'eina contra la taula de fresat. Els espècimens d'anàlisi són mostres amb quatre recorreguts de tall rectes amb tall en sentit contrari. Les trajectòries lineals amb diferents direccions donen l'oportunitat d'analitzar la inclinació del fus de fresat en la màquina. Una anàlisi visual revelà diferències entre direccions de tall oposades, així com marques deixades pel tall posterior de l'eina.

Considerant les desviacions de les marques de tall observades en les imatges de rugositat superficial obtingudes a partir de les mesures, es va introduir una anàlisi sobre el comportament dinàmic de l'equip i de l'eina de tall. Les vibracions produeixen desviacions en la taula de fresat i en l'eina de tall. Aquestes desviacions van ser detectades i incloses en el model matemàtic per completar la precisió en la predicció de el model.

Finalment, el model de predicció de el paràmetre de rugositat Sz va ser comprovat amb un major nombre de paràmetres del procés. Els valors de Sz mesurats i predits, van ser comparats i analitzats estadísticament. Els resultats van revelar una major desviació de la rugositat predita en les mostres fabricades amb diferents màquines i amb diferents avanços.

Importants conclusions sobre la precisió de l'equip de fabricació han estat extretes i d'elles es desprèn que l'empremta de l'eina de tall està directament relacionada amb els paràmetres de la topografia de la superfície. A més, la influència de la empremta està afectada per la geometria de l'eina de tall, la rigidesa de l'eina i la precisió de l'equip. La geometria de l'eina conforma la base del paràmetre Sz, desviació de l'altura de la superfície. Les conclusions assolides són la base per recomanacions pràctiques, aplicables en la indústria.

.

Table of Contents

Abstract 1
Resumen 2
Resum 4
LIST OF ABBREVIATIONS 10
1. INTRODUCTION 13
1.2. Hypothesis 19
1.3. Research objective and tasks to do 20
2. STATE OF THE ART: ANALYSIS OF SCIENTIFIC PUBLICATIONS 22
2.1. Surface roughness and topography prediction models – review 22
2.1.1. Empirical models 25
2.1.2. Artificial network analysis and non-traditional methods 31
2.2. Theoretical models 44
2.2.1. Geometrical models 44
2.2.2. Vibration model 55
2.3. Conclusions and assumptions about the state of the art 60
3. DESCRIPTION OF THE 3D SURFACE TOPOGRAPHY STANDARD 62
3.1. Height parameter group 62
3.2. Spatial parameter group 63
3.3. Functional parameter group 64
4. OUTLINE OF THE PREVIOUS WORK AND BASIS OF THE RESEARCH 65
4.1. Objective of the previous work 65
4.2. Applied methodology of previous work 65
4.3. Results of previous work with relevance to this research 70
4.4. Conclusions of previous work 73
5. RESEARCH METHODOLOGY 75
5.1. Introduction 75
5.2. Research strategy 75
5.3. Research method and approach 75
5.4. Data collection and treatment methods 77
5.4.1. Surface topography measurements 78
5.4.2. Surface microscope imaging 81
5.4.3. Obtained data management 82
5.5. Selection of significant samples 83

5.6. Research process description 83
6. EXPERIMENTAL PLANNING OF THE HSM MODEL: a case study of flat end milling ..84
6.1. Material selection for the experiment 85
6.2. Machining equipment selection 85
6.3. Selection of cutting conditions 87
6.4. Design of Experiment 88
6.5. Experimental execution and measurements 90
6.6. Analysis of the flat-end milling model 91
6.6.1. Numerical analysis 92
6.6.2. Visual analysis 93
6.6.3. Oscillation marks at surface topography 98
6.7. Theoretical model: discussion of the results 100
6.8. Conclusions 102
7. ANALYSIS OF THE FLAT END MILLING MODEL – SAMPLES WITH CONTRARY AIMED CUTTING DIRECTIONS 104
7.1. Design of the Experiment 104
7.1.1. Selection of the cutting tool movement strategy 104
7.1.2. Cutting conditions and Design of Experiment 107
7.1.3. Material and machining equipment selection 108
7.2. Experimental execution 110
7.3. Analysis of experimental results 112
7.3.1. Numerical analysis 112
7.3.2. ANOVA analysis of the influence of cutting feed rate, radial cutting depth and cutting direction on S_Z formation 116
7.3.3. Visual analysis 121
7.4. Theoretical model of contrary cutting directions 122
7.4.1. Cutting force model influence on cutting tool deflection 122
7.4.2. Cutting tool axis inclination model 133
7.5. Complete surface topography height prediction model 135
7.6. Conclusions 140
8. ANALYSIS OF THE FLAT-END MILLING MODEL – VIBRATION COMPONENT 142
8.1. Experimental execution and measurements 142
8.1.1 Performance of FEM analysis to detect the cutting tool's natural frequency of cutting tool 143
8.1.2 Measurements of the milling table's Natural Frequencies 145

8.2. Visual analysis 147
8.3. Theoretical model of milling table vibrations 150
8.4. Theoretical model: discussion of results 154
9. DATA VALIDATION MODEL AND RESEARCH RESULTS 157
9.1. Material and milling equipment selection 157
9.2. Cutting conditions and Design of Experiments 158
9.3. Experiment execution, surface topography and natural frequency measurements 160
9.4. Analysis of vibration data and result validation 164
9.4.1. Descriptive statistics of measurement data 164
9.4.2. ANOVA analysis of the influence of cutting feed rate, radial cutting depth and cutting direction influence on S_Z formation 168
9.4.3. Visual analysis 174
9.5. Theoretical model: discussion of results 177
9.5.1. Cutting force and cutting tool deflection component 177
9.5.2. Tool deflection 182
9.5.3. Milling head inclination 185
9.5.4. Vibration component 190
9.6. Validation of predicted surface topography 196
10. REVIEW AND CONCLUSIONS 199
11. RECOMMENDATIONS FOR DIE AND MOLD MANUFACTURUNG INDUSTRY AND FUTURE WORKS 202
12. PUBLICATIONS AND CONFERENCES RELATED WITH THE RESEARCH 203
REFERENCES 204
APPENDIXES 219
A - Copy of publications 219
B - Design of experiments 220
C - Surface topography measurements and images 221
D - Mathematical calculation of minimum surface, cutting forces and tool deflection, cutting tool inclination and vibration model 234
E - Vibration analysis of KONDIA B500 and GENTIGER GT66V High speed milling machines 242

LIST OF ABBREVIATIONS

2D	*- 2 dimensions;*
3D	*- 3 dimensions;*
$a_{e,}$	*- cutting width;*
A_d	*- axial depth of cut*
AI	*- Artificial Intelligence;*
AISI	*- American Iron and Steel Institute;*
ANOVA	*– Analysis of Variance;*
ANN	*- Artificial Neural Network;*
ASCII	*- American Standard Code for Information Interchange;*
a_p	*- cutting depth;*
BCBN	*- cubic boron nitride;*
BNN	*- Bayesian Neural network;*
C	*- circle length;*
c	*- damping ratio (in case of vibration analysis);*
CAD	*- Computer Aided Design;*
CAE	*- Computer Aided Engineering;*
CAM	*- Computer Aided Manufacturing;*
CNC	*- Computer Numerical Control;*
CP	*- circular cutting path;*
CW	*- Clockwise;*
CCW	*- Counter clockwise;*
DIN	*- DIN*
DoF	*- degrees of freedom;*
fz, fa	*- feed per tooth;*
fn	*- natural frequency;*
fm	*- counting frequency;*
ft	*- rotation frequency;*
fex	*- excitation frequency;*
Fx	*- cutting force at X axis;*
Fy	*- cutting force at Y axis;*
Fz	*- cutting force at Z axis;*
Ft	*- cutting force in tangential direction;*
Fn	*- cutting force in normal direction;*
Fa	*- cutting force in axial direction;*
FE	*- finite element;*
FEM	*- Finite Element Modelling, Finite Element Method;*
FRF	*- Frequency response function;*
GA	*- genetic algorithm;*
GEP	*- Gene Expression Programming;*
GP	*- genetic programming;*
GRNN	*- generalized regression neural network;*
HS	*- high speed;*
HSM	*– high-speed milling;*
HSS	*- high speed steel;*

Hz - *the hertz (frequency);*
k - *spring tension coefficient;*
Kt, Kn, Ka - *tangential, normal and axial cutting coefficients, accordingly;*
LP - *linear cutting path;*
LS-SVM - *Least Squares Support Vector Machine;*
M_t, M_n, M_z - *tangential, normal and axial material stiffness coefficients, accordingly;*
m - *mass;*
MMR - *material removal rate;*
MRA - *Multiple Regression analysis;*
n - *spindle speed;*
N - *tool revolutions (counting);*
NA - *not available;*
NaN - *not a number;*
NC - *Numerical Control;*
ODE - *ordinary differential equation;*
P - *overlap value;*
PCD - *polycrystalline diamond;*
PSO - *particle swarm optimization;*
R - *ball nose radius;*
Ra - *arithmetic mean roughness;*
R_d, *RCD* - *radial depth of cut;*
RSM - *response surface method;*
Sa - *arithmetic mean surface height;*
Sdc(mr) - *inverse areal material ratio of the scale-limited surface;*
Sds - *summit density;*
Sku - *kurtosis of the scale-limited surface;*
Sq - *root mean square height of the scale-limited surface;*
Sp - *max peak height;*
Std - *surface texture direction;*
STp - *height of the bearing area ratio curve;*
Str - *texture aspect ratio;*
Ssc - *mean summit curvature;*
Ssk - *surface skewness;*
Svi - *valley fluid retention index;*
SVM - *support vector machines;*
S_Z - *surface height on scale limited area;*
T - *period (frequency);*
t - *uncut chip thickness;*
tc - *uncut chip volume;*
tg, tan - *tangent of an angle;*
TiAlN - *miracle coating (Titanium, Aluminium, Nitrogen);*
TLP - *two linear cutting paths;*
V_c - *cutting speed;*
V_f - *feed speed;*
Vm(h) - *material volume left;*
Vmp - *surface peak material volume;*

Vv	*- void volume;*
ISO	*- International Standards Organization;*
WC	*- tungsten carbide;*
δ_d	*- plastic deformation;*
δ_z	*- surface height differential on Z axis;*
δz_{vib}	*- vibration amplitude;*
θ	*- tool immersion angle;*
λ	*- tool inclination dependency on vibration angle;*
ω	*- angular frequency (2*π);*
ζ	*- damping ratio;*
$\Theta x, \Theta y$	*- tool axis inclination angle in relation to machine coordinates;*

1. INTRODUCTION

Currently, various kinds of engineering applications are calling for new, more lightweight, more rigid and harder types of materials. One task of the engineers who work in the material development field is to develop these kinds of materials. Another task is to develop the machining and post-treatment technology, to finish the products made from these new materials. Die and mold manufacturing is one of the areas for the application of materials with high rigidity and hardness. In die and mold manufacturing, hardened steels, alloys and titanium have typically been used. In their manufacture, one of most important aspects is the surface quality of the final product. The quality of the final plastic product depends on manufactured tool (mold) or ancillary equipment surface shape, aspect and roughness. Therefore, injection mold surface roughness and shape will directly influence the final plastic product surface topography.

Plastics and plastic products are used everywhere - household appliances, automotive industry, toys, tools, etc. and for some of them the surface quality and external appearance plays a major role in convincing customers to acquire the product. To obtain the requirements of final product surface quality, molds have to be prepared accordingly. To prepare dies and molds for plastic injections, the metal has to be machined, but difficult-to-cut material machining encounters the problem of low machining efficiency when obtaining the required surface quality. Attempts to improve productivity have led to a shorter machining tool lifetime and higher machining expenses.

One of the main goals for every manufacturer is to decrease manufacturing costs and increase productivity and the quality of their products. This is the area where engineers need to work and develop the technology to machine difficult-to-cut materials more effectively. After a quarter of a century of continuous developments and innovations in the multiple disciplines composing high-speed machining (HSM), the technology has reached maturity. Industrial users today are finally taking advantage of all the economic and technical benefits provided by high-speed machining. As a result, manufacturing industries have now acquired all the necessary means to work in this new, high-speed environment, which essentially contributes to reducing production costs. High-speed machining is being used extensively worldwide in all sectors of production engineering, especially in the aerospace, automotive, instrumental (dies and molds), electro-technical and medical sectors, and even in woodworking and composite material processing [1]. Until recently, high-speed machining was applied in machining aluminum and titanium alloys for manufacturing complicated parts used in the aircraft industry [2]. Recently, with the advances in cutting tool technologies, HSM has also been employed for machining alloy steels for making dies and molds used in the production of a wide range of automotive components, as well as plastic molding parts. The most extensively used type of HSM in die and mold manufacturing is end milling. Increased end-milling speeds allow

manufacturers to Likewise, end-milling operations are one of most commonly used milling operations in old production.[3] [4]

High Speed Milling has often been applied in injection mold manufacturing processes, where surface roughness is a significant criterion in product quality demands. Machining materials used for mould manufacturing is a complicated task. Hardened or difficult-to-cut material machining usually encounters the problem of low machining productivity, poor surface quality and roughness, short tool lifetime and high machining expenses. To improve surface roughness of the hardened tool, die mold steels and alloys, it is necessary to apply modern, effective machining techniques, which can provide required surface quality and roughness parameters. Furthermore, it is possible to decrease machining costs in finishing processes, such as polishing, by selecting appropriate cutting conditions in preliminary milling operations [5]. These quality parameters have to comply with existing standards and parameter values as required by die mold manufacturers.

High-speed machining is an effective machining method used in modern tool and die-cast material processing, to increase the efficiency, quality and accuracy of the machined surface and to reduce costs and machining time. In the entire spectrum of high-speed machining, high-speed milling is the leading and most widely used technological process in numerous applications. Spindle speeds vary in range from 10,000 to 60,000 r/min and more. [6] A significant amount of data was obtained as regards the impact of the high cutting speeds on:

1. the type of chip produced;
2. cutting forces and power;
3. temperature changes;
4. tool wear and failure;
5. surface finish and integrity;
6. the economics of the process [6]–[8].

Most advantages of HSM technology are related with its time consumption during the machining process and obtained surface quality. Therefore, because of the high speed of the material removal, a large amount of heat is removed from the machining zone through the chip and the use of coolant. One of the most important discoveries about HSM was that when a certain cutting speed reached, the heat reduces in the chip-tool interface, even in cutting without coolant (Fig. 1.1) [9]. This is reached by using relatively low cut width 10-15% of tool diameter down to as little as 5%, and small feed values, depending on where the most effective point is for the spindle’s max r/min. These low radial depths allow better chip clearance and time for the cutting tool to cool down in the air, allowing for much higher productivity, especially on harder materials [9]. High cutting depth is used to increase the material removal rate (MRR) at the same time as using low cutting

width and small feed rate. That allows more efficient use of the cutting tool length and longitude cutting edges. Low radial cutting depths and feed rates allow using smaller cutting tools, to machine tiny cavities.

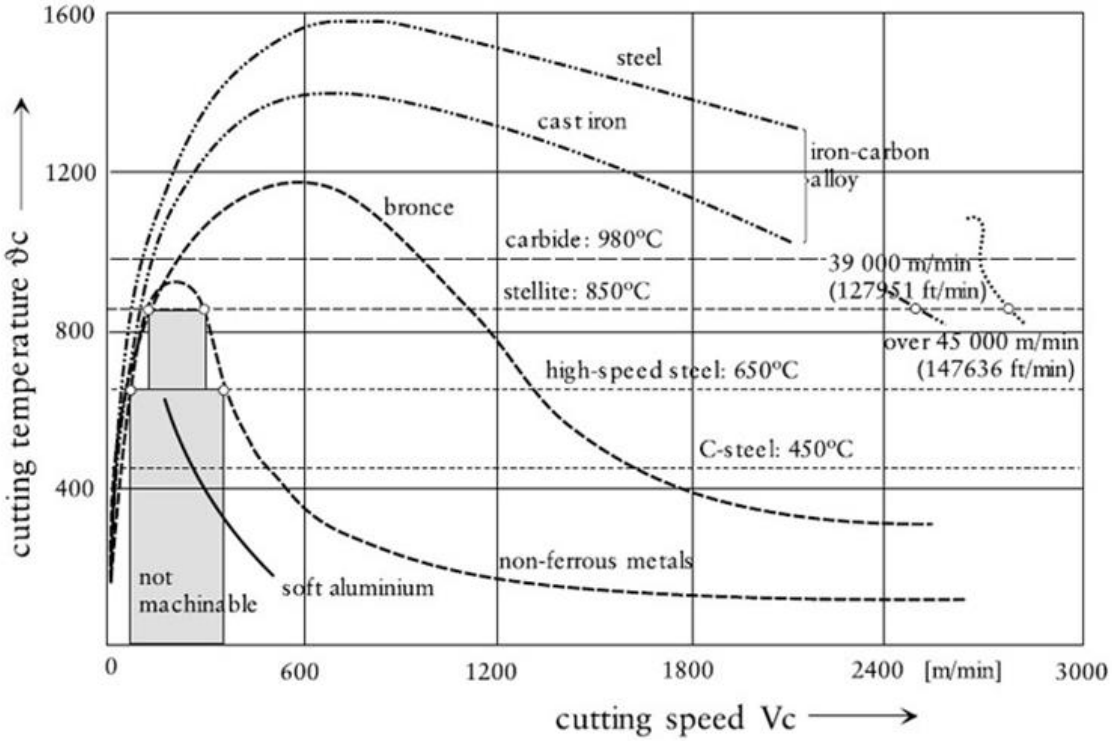

FIG. 1.1. Cutting speed and temperature relation at chip-tool interface [9]

The temperature on the chip-tool interface remains lower than in the conventional milling process. It helps to avoid thermal influence stress on the machined surface. By applying a specified combination of cutting regimes, it is possible to obtain lower surface roughness values. Accordingly, the number of operations needed to finish the part decreases. This helps to save time and energy during the manufacturing process. Less tool changes are necessary to finish the part.

Another advantage is that the cutting force influence is decreased by increasing the cutting speed. Cutting forces tends to decrease, by increasing cutting speed and decreasing the cutting width. Kronenberg [10] found scientific proof that cutting force initially increases while increasing the cutting speed and then drops sharply to rise again later. Moreover, studies showed that by increasing the cutting speed, the flowing chip gradually turns into a discontinuous chip [10]. This effect may result in tool deformations and influence surface topography formation during the cutting process. This technology is associated with significant improvements in machine tools and constructions, spindles and controllers [2]. New generation machines were introduced with improved construction, stiffness and high-speed resistant parts.

However the advantages and potential of high-speed manufacturing are not always

fully exploited. Industry largely depends on empirical recommendations and experience-based technological regimes. The reason for this is a regrettable lack of knowledge and availability of researchers' recommendations, which are not only of scientific value but can also be applied in real-life conditions. Furthermore, initial investment in manufacturing equipment and knowledge is substantial. It requires technologically highly advanced machines with high accuracy and stability. HSM tool manufacturing technology is expensive. Usually, the tools have to reach certain requirements in terms of resistance against excessive tool wear and high strength. Therefore special tungsten carbide tools with friction-reducing coatings are used for HSM. Also, HSM requires experience, in order to correctly use CAM (Computer Aided Manufacturing) software and to precisely describe tool moving paths. Otherwise, an incorrect tool path and excessively wide cutting width may lead to tool and workpiece damage [6], [10], [11]. Basically, manufacturers have to learn the appropriate cutting conditions and select a suitable machining environment to successfully and economically use HSM for die and mold manufacturing. Therefore, the industry has to be provided with the necessary support from technical universities, in order to improve the use of the aforementioned technology and to bridge the gap between researchers and industrial production engineers.

One of the less devolved areas is related to an understanding of how high-speed machining technological parameters, especially in combinations with extreme cutting parameters, affect the formation of surface micro-topography. In particular, it involves correlations between conventional or high-speed milling and 3D surface roughness parameters. Surface roughness parameters are currently regulated by several ISO standards as well as numerous national standards. This leads to a situation where a variety of standards are used by industrially developed countries. On top of those applicable to all sectors of production engineering, there is a well-established practice of surface roughness parameter measurement. Today the most commonly used parameter is Ra – arithmetic mean roughness. It is important to note that most of the said standards and technical specifications are based on 2D surface roughness, where the surface roughness is measured by profilometers using the contact method. In the majority of production enterprises, industrial measurement equipment is based on 2D profile contact gauges and subsequent subtraction of surface roughness parameters from the linear readings.

Nevertheless, every workpiece is a spatial object, thus to obtain complete measurements, the object has to be analyzed and mathematically described as a 3D object. Accordingly, the surface topography should be perceived as a spatial object and estimated with the appropriate quality values. Since 2012, an international ISO standard ISO 25178-2:2012 Geometrical product specifications - Surface texture: terms, definitions and surface texture parameters, has specified 3D surface roughness parameters. Surface quality, including 3D surface texture, is an important indicator with respect to machined surfaces. Surface roughness is a means of defining the characteristics of mechanically machined surfaces. In recent years, most researchers in different scientific fields have adopted 3D

surface topology as a reference in process analysis. Surface topology provides a broader view of the machined surface quality. 3D surface topology is directly related to the 2D surface roughness measured in orthogonal planes. Topology measurements and analysis are important when undertaking complex machining operations, to ensure a high-quality machined surface.

Relevance of the research

To ensure high quality injection mould surfaces, whilst avoiding external finishing operations, it is important to take the principle machining technological factors into account. Good knowledge of the surface formation process could reveal the benefits of applying HSM in difficult-to-cut material machining. But the lack of knowledge in HSM cutting processes doesn't allow the results of machined surfaces to be predicted efficiently. The authors of this research field are interested in developing the model to select the appropriate cutting conditions that guarantee the mould quality with a minimal machining cost. In this field, much research is available, dealing with the mathematical modelling of the cutting process; however, most of them result in differences between measured and modelled surface roughness parameters. To reduce this error, it is important to detect the most important parameters in the cutting process, which affect the surface formation process and then calculate the correlation function between the cutting conditions and surface texture parameters. These factors are related not only to cutting conditions, but also to other factors (tool-sharpening error, concavity angle on the bottom face, vibrations, etc.) which cannot be modified directly. Furthermore, these factors intervene during the finishing processes rather than in the rough machining. To develop a surface topography prediction model, such factors as tool deformation errors, formed by increased cutting forces during the machining process, tool alignment position and tool-sharpening error, are important. A combination of tool manufacturing errors and coupling inaccuracies could generate tool radial run-out errors, i.e. discrepancies between the theoretical axis and the tool's real axis.

Literature analysis in this field reveals that there have been a number of empirically-based research projects, where authors try to eliminate the impact of model accuracy errors in their developed models. Due to the changes in the machining environment (machine manufacturer, tool chuck, tool manufacturer and material), the model accuracy is highly variable. Sometimes, these models are not at all applicable for other types of milling machines, due to other factors influencing the milling processes. To improve the accuracy of the predicted surface topography models, it is important to include all of the most significant cutting conditions, taking into consideration the environmental and material properties, and the dynamic behavior of the milling factor.

Subject of the research

A well-developed surface topography prediction model should be based on

theoretical knowledge of the cutting process. Conventional, low-speed cutting processes have been modeled by various authors, including Martellotti, M.E. [12] and Kline W.A. [13], for more than half a century. Even so, a high speed milling process model that can characterize the machined surface still encounters difficulties and inaccuracies. Most of them are related to a failure to include the most important cutting parameters.

The die and mold manufacturing industry is facing this problem—the lack of knowledge about the surface topography formation process under HSM operations. This is the point where the idea for the research project originated. Matrival is one of most important die and mold design and manufacturing companies in the Valencia Community, in Spain, where the Universitat Politècnica de València is located. This company is facing the issue described above. The company is working with molds for the automotive industry as well as with molds for toys and household goods manufacturing. Manufacturers are interested in this research field to understand if it will be useful to relate HSM and 3D surface texture measurements, to effectively machine difficult-to-cut materials with HSM technology and relate the cutting parameters with 3D surface topography. The manufacturer cooperates with the Universitat Politècnica de València in this research and development. Currently this research involves the scientific collaboration between several universities, due to their potential for research and development in this field. The Universitat Politècnica de València (Valencia, Spain) and Riga Technical University (Riga, Latvia) cooperate in sample preparation and development. Part of the surface texture measurement, surface micro-hardness measurement and research work has been done in these universities. Also involved is Tallinn University of Technology (Tallinn, Estonia), where all the 3D surface texture measurements were performed using an optical surface topography measurement device.

Basic methodology of the research

An understanding of the difficulties in this field was achieved through analysis of relevant literature. The literature review revealed that there are problems with development of a reliable mathematical prediction model, suitable for every machine, under different cutting conditions. Extensive empirical research of a very large number of samples could decrease the error number in the prediction model. But this wouldn’t give the authors any kind of reliable information in terms of how the process of HSM cutting has been affected by the environmental behavior of the cutting system.

Therefore, a mathematical model to predict surface topography is under development, including machine-tool-workpiece system inaccuracies and the properties of the dynamic behaviour of the cutting system. Basically, in the result of this research project, a mathematical surface topography prediction model is prepared to represent the machine accuracy, surface topography formation and 3D surface topography parameter S_Z values, according to the cutting conditions, environmental conditions, material, etc. 3D surface topography parameters from the experimental samples provide results to compare and

analyze with the mathematical prediction model. This model involves the software tool for manufacturers to improve the quality of machined part surfaces, taking into account the behavioural properties of their machining equipment. The dynamic (vibration) effect, tool deflection and alignment, a combination of tool geometry and sharpening inaccuracy (relative to the plane of the tool path) are the parameters under review. The author is investigating the vibrations in the milling system to clarify whether they affect the cutting process and contribute to the surface topography prediction model. Local cutting tool vibrations and overall machining equipment vibrations are analyzed.

Finally, relevant conclusions are drawn. All the recommendations for industry are based on mathematical results and conclusions from the research. The mathematical results' significance is checked using analytical methods. The research results' validation process includes research publications in a number of highly respected International Scientific Conferences and scientific journals. A list of these publications is provided in Appendix A.

Venue and scientific collaboration

The practical part, more specifically the sample preparation and machining for this research, was carried out in the CNC (Computer Numerical Control) workshop at the Universitat Politècnica de València, Department of Mechanical and Materials Engineering in Spain. All the samples in this research have been processed with machining equipment located in the university's workshop laboratory. Afterwards, the surface topography measurements were taken in the Tallinn University of Technology (TUT), Department of Mechanical and Industrial Engineering, in Estonia. In this university, an optical surface topography measurement device is available which facilitates the surface topography measurement process, compared with the contact method. Surface microscope photography and geometrical dimension measurements were carried out in the Department of Material Processing Technology of Riga Technical University (RTU), Faculty of Transport and Mechanical Engineering, Institute of Mechanical Engineering Technologies. All of this work was compiled during the doctorate dual-studies at UPV and RTU universities.

1.2. Hypothesis

The surface roughness, measured with different standardized parameters, is directly related to the topography of the surface. In the mechanical machining processes, the obtained topography is primarily related to the tool's footprint, based on the paths followed by the tool. These paths are related to the kinematic parameters of the movement, as well as to dynamic characteristics resulting from the efforts and deformations produced. It is possible to establish a mathematical model according to physical behaviour models, which relates the topography obtained with the actual paths of

the tool. These paths can be determined based on working conditions (spindle speed, cut feed, number of teeth, etc.) and based on the dynamic behaviour model of the tool-part-machine chain.

1.3. Research objective and tasks to do

To fulfil the hypothesis put forward, the author of this research has to detect the challenges in the field of surface topography prediction and HSM. Conclusions of said analysis should provide the basis for developing the experimental and measurement methodology and to compare it with developed mathematical surface prediction model as the result.

The main goal of this research project is to develop the mathematical methodology based on calculation model for high speed end milling operations, to determine the surface 3D topography parameter S_z values.

To obtain the aforementioned goal, the following primarily tasks are set for this research:

1. The literature analysis is a way to obtain new knowledge about challenges in the field of high-speed milling process behavior and its impact on surface quality from a topological point of view. The result of literature analysis provide the conclusions about the status of knowledge of similar research undertaken by other authors. This analysis should represent the models developed by other authors and the difficulties they encountered while working on their models. Also, the advantages and disadvantages in their developed models have to be described and analyzed to understand the particular features and factors determining the accuracy of their developed models. Based on this information, the author of this research work will determine the most influential process parameters.
2. Analysis of the surface topography parameters and choice of the most relevant surface topography parameters, which describe the machined surface. The author refers to surface topography 3D standard parameters in this research. In industry, commonly used surface roughness parameters, related with the ISO 4287:1998 standard are Ra, Rz and others. There is no direct link between the application of different cutting process parameters and surface topography parameters referred to in the ISO 25178:2012 standard, which is a new area to be investigated. There are a number of topography parameters, but the representative ones used for this case study have to be detected with correlation analysis.
3. Milling experiments have to be planned and conducted, in order to test the hypothesis. In this way, milling strategies, cutting conditions, cutting process parameters, etc. can be selected. To develop an accurate surface prediction model, a considerable number of experiments have to be performed to analyze data and results obtained from them.

4. Finite element methodology (FEM) has to be applied for analysis in cases where conventional methods are useless to detect the cutting process parameters. FEM applied for dynamic cutting process analysis will provide information about cutting tool and milling table vibrations. FEM is also used to obtain cutting force values, as measurements of cutting forces are complicated, time consuming and expensive process. Therefore, all available FEM options should be used to get the most detailed possible picture of the cutting process in this research.
5. The surface topography parameters have to be represented with a mathematical prediction model. This model should be constructed using the most significant milling process parameters, including all the most relevant milling process inaccuracies. The typical parameters considered in manufacturing technological process planning are material properties and such cutting conditions as feed rate, cutting depth, spindle speed, etc. To develop a reliable surface topography model, it is important to consider more than the basic process parameters. This task will lead the authors to work on process parameter detection and selection to update the model with the most important factors acting on the cutting process. It is no easy task to identify which milling process parameters and factors are the most important. Literature analysis should lead the authors to select the process parameters for ANOVA analysis. Results of this analysis will create the basis for the mathematical prediction model.
6. Comparative analysis between the results of the mathematical model with real surface topography parameter measurements, taken from experimentally machined samples, has to be performed. Experimental sample measurements will validate the mathematical model and identify its accuracy. Detecting all the particularities in the cutting process and applying them in the mathematical model requires a preliminary analysis of the machined samples. Therefore, all the analysis has to be done within two loops. The first loop will cover the measurement analysis and the machine's accuracy in terms of the particular parameters obtained from it. The second loop will be conducted to validate the statements and results.
7. The expected result of this thesis is to develop sound conclusions and practical recommendations that can be implemented in the die and mold manufacturing industry. All the added value of this research work lies in the conclusions drawn from the mathematical results and the recommendations made to manufacturers who work with HSM technology in the industrial field. The results of mathematical topography prediction model analysis will provide the conclusions of the research work. These conclusions will confirm or refute the hypothesis and statements proposed at the start of this work, but as with any result, they will provide important information for the application of HSM with hard-to-cut materials. Also, these conclusions should be taken as a basis for useful and reliable advice and practical recommendations for the die and mold manufacturing industry, where HSM technology has been used as the

main manufacturing process.

8. To propose new lines of research and future works. If the results of this research reveal some flaws in the model's development, it could be improved in the further research.

2. STATE OF THE ART: ANALYSIS OF SCIENTIFIC PUBLICATIONS

In the scientific field, there exists a considerable amount of research work related to cutting conditions, technological parameters and the influence of the cutting tool and equipment used on the various characteristic parameters describing surface quality. Each of these studies applies its own approach model to determine specific surface quality parameters.

Surface roughness is a way of defining the topological characteristics of mechanically machined surfaces. In recent years, most researchers have adopted 3D surface topography as a reference in process analysis. 3D surface topography provides more information about the machined surface; thereby researchers and manufacturers have more information to make assumptions about how the surface has been generated. Surface topography measurements could be important part on analysis of surface quality in particular. Although 2D surface topography can provide the author with surface peak maximum and valley minimum values, 3D topography analysis could provide the author with information about the surface error directions and slopes, and their behaviour in contact with other surfaces – liquid or solid. These statements are important when it comes to complex machining operations, where it is important not only to know surface height parameters, but also direction and path angle. Some of these complex operations are related to mold manufacturing. Also it is well known that insert cavities for dies and molds are one of most complex engineering part, usually made from one piece of solid material. To ensure high molded part surface finish quality, good molded plastic material flow over the thin channels of the complete mold assembly is required. It is important to know which topography direction descriptive parameters as well as surface height parameters to consider during the mold machining process. 3D surface topography parameters give more information in order to know the behaviour of the final product. [3]

To fulfill the above statements, in the next subchapters we will analyze the prediction models proposed by other researchers and compare them. We will select the most appropriate and accurate model as a starting point to predict the surface topography parameters for mould materials machined with HSM technology.

2.1. Surface roughness and topography prediction models – review

There are many different surface roughness and topography prediction methods used in the literature. Statistical analysis is one of most famous. Cutting technological parameters, process factors and dynamics have been used as input factors for regression models. At the same time, several authors apply the same input factors on the geometrical models to try and reconstruct the surface from a geometrical point of view. In recent years, with improvements in computer and software technologies, Finite Element methods have become a popular tool to develop surface

topography prediction models in science. These methods are summarized in this chapter and the factor influence will be analyzed, to select their application in new model development. [3], [14]–[21]

Many factors influence the final surface topography parameters. Several research works have studied different factors, such as cutting conditions, material type, equipment condition and dynamics of the cutting system. [22] They use these factors to develop the behaviour models in order to predict surface roughness or topography.

There are also works where researchers review and make a classification of the applied techniques to predict the surface roughness or topography. The latest review of the various methodologies to predict surface topography was published by P.G. Benardos et.al. [22] In this work they considered different methods in order to classify the papers by other authors according to the approach used to predict the surface roughness and topography. They classify these models by approaches based on machining theory, experiments, design of experiments and artificial intelligence. Most of the input factors used in all of these approaches are basic cutting conditions like feed rate, cutting depth, spindle speed and selection of machined material type. As P.G. Benardos outline in his research, some authors try to combine approaches to develop new models. Some authors do not consider other process parameters—what we might also call surrounding factors. These are factors like cutting tool geometry, milling equipment accuracy, stiffness, performance, etc. The combination of their effective influence on surface topography formation also depends on cutting parameters. In some cases, the authors consider different internal cutting system parameters, like vibrations or tool inclination, but don’t combine them with other important factors. They are looking only at the separate influences of these factors. These are parameters which in most cases cannot be changed, or it takes a lot of effort and resources to adjust and improve them. The result of this work provides the advantages and disadvantages as outlined.

As P.G. Benardos concludes, firstly, all the methodologies that are presented in his work can exhibit advantages and disadvantages when compared to one another, but the most promising seem to be the Theoretical and Artificial Intelligence (AI) approaches. Models created with AI seem to be the most realistic and accurate, probably demonstrating the highest level of integration with computers. This approach can be used in conjunction with other, more conventional techniques. [22]

Secondly, by changing the indirect input factors, the influence on surface topography could also be changed. Sometimes, when it is not possible to adjust these parameters, it is important to accept their existence. Accordingly, the researcher can predict the surface quality result considering the process parameters and their negative influence, and adjust the cutting conditions accordingly to improve the result. Considering all the information from previous research, we can identify the most important process parameters affecting end milling operations.

Making all of the previous assumptions, we can distinguish two groups of parameters: cutting conditions and system process parameters. Cutting conditions for every material, applied tool,

machine and processing operation (rough or final machining) can be adjusted to improve the surface quality or to decrease machining time and save resources. It is more complicated with process parameters, which cannot be affected directly. These are conditions that are brought about by operational particularities, machine behavior and other effects that can influence the cutting process and surface formation [14], [15], [23]. Some of these factors are:

- tool axis inclination;
- milling head inclination;
- tool axial deflection;
- tool run-out or sharpening errors;
- chatter or vibrations;
- etc.

From a basic idealization of the tool geometry, tool kinematics, machine alignment, etc., a relationship between surface topography and the actual input factors can be established. Some of these factors remain constant during the whole machining time and for subsequent machining operations, such as tool axis inclination, milling head inclination, spindle run-out, machine natural vibration frequency, etc. Other factors can be altered by selecting appropriate cutting conditions, to avoid excessively high cutting forces that may influence tool axial deflection, vibration, etc. The former factors are constant for the whole machining cycle, but tool deflection and vibrations change over time and depend on the tool's rotational or immersion angle λ. The instant cutting force is a variable, which depends on the tool's angular rotation or immersion angle λ. Cutting force coefficients can be represented as a function of cutting conditions and material properties. [14], [15], [24]

A large amount of research has been undertaken to identify the impact of conventional milling and the HSM process on surface roughness, topography and tool kinematics, to identify problems that occur during machining processes, such as severe tool wear, tool deformations, high cutting temperatures etc. [5], [25], [26]. The authors of this research sought to examine the influence of the technological parameter and cutting process parameter on surface 2D and 3D roughness parameters. Different approaches and models were used by other authors to make similar studies. Here we are looking at numerical modeling methods used by other authors to predict and describe surface roughness and topography. In this case we develop our own classification method.

In general from our point of view, all developed prediction models can be classified into two main groups:

Empirical ***Theoretical***

The difference between these groups is in the global assumptions and how the surface prediction models are built. Based on these two groups, we will classify and describe the actual models in this review of literature. Every group contains subgroups of models that use either the

same principles or similar approaches of data treatment to obtain the resulting predicted surface parameter value.

2.1.1. Empirical models

Empirical models, also called Response Surface Methodology (RSM) models, in general are models based on statistical analysis of input data. Empirical models start with the execution of a variety of experiments with different parameter values to define the influence of factors as input data variables. From experiments the results are measured. Using different statistical techniques, a model is fitted relating result data to input data. In empirical models, authors use either Regression approaches to define input parameters as exponential regression coefficients, or the Polynomial regression approach model, where polynomial input variables are multiplied by coefficients.

In the next sub-chapters, we will discuss two types of Empirical models used by other researchers. One type is regression models, where regression analysis is used to relate experimental measurements with input factors, which include Exponential and Polynomial regression models. The second type of empirical methods is Artificial Intelligence methods. Here, different kind of newly discovered methods, such as Artificial neural networks, Taguchi, optimization and Genetic programming methods have been used to relate experimental measures with input factors. One author compares the advantages and disadvantages of the proposed models.

Exponential regression models - Design of experiments

The most common model to describe surface topography used in research and industry is the RSM model of exponential regression coefficients. One representative example of this model was the research work [2] published J. Vivancos et al. The main goal of this work was the selection of suitable parameters for hardened steel machining. They consider that dimensional precision and surface quality are the two key factors which determine the quality of manufactured parts. Machining parameters such as spindle speed, n (r/min), feed per tooth, f_t (mm/z), axial depth of cut, a_c (mm), and radial depth of cut, R_d (mm), deeply affect both dimensional precision and surface quality. J. Vivancos presents the modelling of surface roughness in HSM of hardened steels for injection molds. From the conclusions of J. Vivancos's regression analysis, it is clear, that the most influential parameter is tool radial depth of cut. J. Vivancos considers surface quality only with a well-known profile method, based on the *ISO* 4287:1998 [27] standard. If radial cutting depth is higher, the obtained arithmetic average values of the absolute parameter R_a values are also higher.

J. Vivancos et al. also studied the impact on hardened die steel of basic, side or peripheral milling operation parameters, [28]. They tried to find impact factors, using a material with better performance than traditional die steels, which are statistically more significant for modelling the surface roughness parameter R_a. In this research they detected the most influencing technological parameters—feed per tooth, the axial depth and the cutting speed, v_c. They observed that the

higher the axial depth of cut value and the cutting speed, the lower the roughness values achieved [28]. Also, they found horizontal lines of peaks in the geometry, possibly caused by a shape error of the cutting tool edge. From the design of their experiment, it is possible to understand that axial depth of cut should be used at its highest value. This means that the length of engaged flutes is increased, and the force required for milling is also increased, while the surface roughness parameter is decreasing. This may minimize vibrations caused in the cutting process.

Other authors, M. Alauddin et al. [29], [30] also analyzed the end milling process using the regression method. They proposed first and second order models to increase the accuracy of the obtained results. They clearly assume that this is an ideal case cutting model, where tool deflection, run-out and surface errors are not considered. They proposed a model as follows:

$$\boldsymbol{R_a = cV_c^k * f_a^l * a_e^m} \quad (2.1)$$

where f_a - feed per tooth, v_c – milling speed, a_e – cutting axial depth, *c, k, l, m* - are model parameters, estimated from the experimentally approached data, accordingly: *c= 39,48, k = -0,3977, l = 0,7431 and m = 0,4779.*

Both previous authors tested their models for adequacy with ANOVA. M. Alauddin concluded that they developed an adequate and reliable model to enhance the efficiency of the slot milling operation for 190 HB (Hardness by Brinell) steel. The most important parameters, in this case, are cutting speed and axial cutting depth [29].

Otherwise, the same approach was used by author Chang-Feng YAO et al. [31]. They are looking at the HSM input parameter influence on surface roughness and how these parameters are affecting the surface fatigue behavior. The same type of exponential surface response model was used. They simulated surface formation, but only considered 2D surface texture parameters, like R_a, [27]. Firstly, they tried to develop an analytical mathematical coefficient approach for surface roughness parameters, based on the technological parameters used in the machining process. This resulted in Eq. 2.2:

$$\boldsymbol{R_a = 8,58 f_z^{0.5} * v_c^{-0.14} * a_e^{0.28}} \quad (2.2)$$

where f_z - feed per tooth, v_c – milling speed, a_e – cutting axial depth. [31].

Likewise N.S. Kumar Reddy et al. [32] define the surface roughness parameter R_a. In their work, experimental studies were conducted to see the effect of tool geometry (radial rake angle and nose radius) and cutting conditions (cutting speed and feed rate) on machining performance during the end milling of medium carbon steel.

Kumar et al. use the second order polynomial response function, where the parameters are estimated with the least square method. At the same time, Kumar et al. compare results with

Genetic algorithm used to optimize model coefficients. The obtained results enable surface topography to be predicted more precisely, with an enhanced number of input parameters. [32]

Ozcelik and M. Bayramogl in Ref. [33] used more parameter interactions to increase the accuracy of their model. They used cutting time as a tool wear representative parameter. Up to 15 different effects were used in this research: 5 main effects of cutting conditions, material and cutting time, 5 squared effects and 5 interaction effects. First and second order models were developed using the experimental results of a rotatable central composite design, and were assessed by means of various statistical tests. A model with 10 terms was found to be the best model for this specific case:

$$Ra = -1.8 + 2.19e^{-04}*X_1 + 4.13*X_3 + 0.58*X_4 + 8.67e^{-03}*X_5 - 1.23*X_8 - \quad (2.3)$$

$$-0.0965*X_9 - 6.00e^{-08}*X_{10} - 5.21e^{-04}*X_{11} + 1.05e^{-03}*X_{13} + 5.20e^{-05}*X_{14}$$

where $X_1, X_2, X_3 .., X_{14}$ - were previously defined models parameters (input parameters).

The obtained accuracy of the fitted model was around 88%, which is an average result when compared with other models.

The same approach, only for helically-milled hole surface prediction was used in ref. [34]. X. Da Qin et al. claim that this model will be helpful in selecting cutting conditions to meet surface finish requirements in helical milling operations. The accuracy of it is more than 90% and it is validated by means of variance analysis. X. Da Qin et al. conclude that with some parameter combinations, predicted surface roughness values are closer to measured ones; with other combinations the same result is not so precise.

Moreover, in very similar way J. Sun et al., R.H. Yuan et al., W. Zhang et al., D. Begic-Hajdarevic et al. and C. K. Toh et al. in ref**.** [35]–[39] used the same approach to study the factors influencing surface roughness changes. They did not predict the surface roughness or surface topography, but used the same methods to analyze the behaviour of surface roughness and surface quality, for example, plastic deformation, fatigue fracture, etc. In the majority of cases, their conclusions were similar and they proposed that the surface roughness value increases with increased feed and cutting speed and decreases with the axial depth of cut. Also, if the cutting edge radius is smaller than cutting depth, then the most important parameter was in fact the edge radius. Otherwise, H. Cao et al. [40] considered environmental media to make a statistical analysis of the effect on surface roughness. With environmental media, these authors used different combinations of cutting cooling media. Statistical analysis was performed and the authors concluded from the obtained results that cooling media behaviour affects the friction significance on the surface roughness formation process. One type of applied cooling decrease the temperature, which may increase the contact friction, on the other hand, cutting fluid with more friction-decreasing elements will decrease the friction and improve the surface roughness. Cooling and lubrication behaviour was examined also in ref. [41] by F. Jiang et al. The exponential and quadratic fit model was applied to detect the influence of technological

parameters. They compared results and drew the conclusion that the quadratic model provides higher accuracy of the predicted surface. Under cooling and lubrication conditions, again surface roughness was slightly dependent on feed per tooth and axial depth of cut.

To summarize:

Regression models and exponential regression models are good tools to detect the influence of selected cutting and process parameters on surface roughness and topography formation. A number of authors use these methods to conclude the most important factors in the cutting process. On the other hand, this method does not guarantee any prediction accuracy for changes in the impact factors or cutting environment. Indeed, without any measurements taken beforehand, it cannot be called a prediction model at all.

Part of these works can be classified under a title of 'Optimization', because the authors use different kinds of methods to optimize the result and obtain a more precise and reliable exponential regression model. Furthermore, these models are applicable to specific cases, and as the authors frequently mention, they are applicable only for the tested model, with measurements taken to validate the model.

Polynomial regression model

Polynomial models are the second largest group, after exponential regression models. These models are basically the same as the previously described exponential model. However an enhanced number of effect coefficients is fitted to the polynomial expression.

Similar statistical regression models were provided by such authors as J.Vivancos et al. Their paper presented a mathematical model of the surface roughness in high-speed milling of hardened steels for injection moulds using experiment design. The model was predicted to analyze the surface roughness. For the case of climb milling, the regression equation of the fitted model was provided by Eq. (2.4.), where the most significant parameters were included from the results obtained from the regression analysis (α = 0.05). The design factors have also been included.

$$\begin{aligned} R_{(a)} = {} & 0.683042 - 1.34515A_d - 2.49037R_d \\ & + 3.40813f_z - 0.00250345V_c + 0.00672575A_{dVc} \\ & + 14.6044R_{d2} - 17.0406R_{dfz} + 0.0057915R_{dVc} \end{aligned} \tag{2.4}$$

Where f_z = feed per tooth, v_c = milling speed, A_d = axial depth of cut and R_d = radial depth of cut.

Unlike previous authors, J. Vivancos et al. considered the ball-end milling process. Finally, they concluded that the model was reliable and had been carried out efficiently and without having to perform a large number of experiments. The authors highlight that this model is efficient to predict surface roughness values for HSM machining in the ball-end milling process.

On the other hand, Mike, S. et al. [42] proposed multiple regression models shaped like a three-way interaction equation. It is also a regression model, only considering other types of regression coefficients. The proposed multiple regression model is:

$$\mathbf{Y = 22.9468 + 10.9357 * X_{2i} + 0.004274 * X_{1i} * X_{2i} + }$$
$$\mathbf{+0.674909 * X_{1i} * X_{3i} - 69.7679 * X_{2i}X_{3i}} \qquad (2.5)$$

Where Y = surface roughness, X_{1i}, X_{2i}, $X_{3i,}$are input parameters, spindle speed, feed rate, depth of cut respectively.

Mike S. et al. claim that their model can predict the surface roughness parameter R_a with 90,29% accuracy. This multiple regression model could predict the surface roughness from testing the data set that was not included in the multiple regression analysis with an average percentage deviation of 9.97 % or accuracy of 90.03%. The feed rate was the most significant machining parameter used to predict the surface roughness in the authors' proposed multiple regression model. [42]

A similar method was used by M.Y. Wang et al. [43] to analyze the slot-end milling procedure on aluminum workpieces. The parameters considered were the cutting speed, feed, depth of cut, concavity and axial relief angles of the end cutting edge of the end mill. Also a model with and without cooling were developed. This model was more advanced, due to the increased number of input parameters. Furthermore, there appears to be a high influence from tool geometry, or more specifically of tool concavity angle, which is directly related to the most important cutting feed influence.

In the same or similar way, the authors A. Zain et al. [44], [45] and B. Lela et al. [46] used the same regression model and compared the results with either support vector machine models (SVM), or Bayesian Neural Network (BNN) model results. These methods will be described later.

D. Bajic et al. [46] used a simple regression model by Rotatable Central Composite Design (RCCD) and compared the results with the Taguchi model. They concluded that their proposed model exactly determines surface roughness, for certain cutting parameters. It was obtained by means of a response surface method and it enabled a high quality analysis of the experiment range as well as achieving optimal exact values. [46]

$$\mathbf{R_{(a)} = 4{,}9271 - 0{,}0574*v_c + 1{,}1808*\ f_z - 0{,}0273a_p +}$$
$$\mathbf{+1{,}78035*10^{-4}*v_c^2 + 11{,}6182*f_z^2 + 0{,}031243*a_p^2 -} \qquad (2.6)$$
$$\mathbf{-0{,}025*v_c*f_z - 4{,}7619*10^{-4}*V_c*a_p + 0{,}29762*f_z*a_p}$$

Where f_z = feed per tooth, v_c = milling speed, A_d = axial depth of cut and a_p = axial depth of cut.

The authors Y. Ding et al. [47] used the same approach to investigate the surface generated by face milling on 38CrSi high-strength steel. They used experiments based on 24 factorial

design and the Box-Behnken design method [48]. The milling parameters under consideration were v_c, a_p, R_d and f_z. A second-order model of surface roughness was established by using the response surface methodology (RSM). The obtained confidence level in this research is very high: 99%. Y. Ding et al. concluded that nonlinear relations exist between surface roughness and interaction terms. As in previous works, the obtained model was precise for one, exact case, and it was validated by ANOVA analysis of the same experiments. However, the result is unknown when the experiment was repeated with the model with another type of machine or different size of cutting tool.

Exactly the same type of analysis, with 16 factorial designs, was undertaken by X.W. Yu et al. [49] The same conclusions for the surface height dependence were proposed, i.e. that feed per tooth was the main factor affecting the surface roughness of aluminum alloy work-pieces. This research just provides information about how the same model had been used with different type of material. No other sound conclusions were drawn.

Other authors, such as B.C. Routara et al. [50] used the same polynomial second order model to predict,not only R_a parameters (as usual), but also other important characteristic surface roughness parameters as R_q, R_{sk}, R_{ku}, R_{sm}. Their model, in terms of the machining parameters, had been developed predict each of these five roughness parameters using response surface method on the basis of experimental results. The obtained result was within the same error as other authors, up to 15%, depending on the response surface parameter and material used.

Therefore, the second order regression model presented by S. Alam and his colleagues [51] considered analyzing the Ti-6Al-4V material with the same standard 3-parameter influence on surface roughness. After fitting the model, the following result was obtained:

$$\mathbf{R_a = 0.24 + 0.018 * A + 0.021 * B + 0.015 * C + } \\ \mathbf{+0.026 * A^2 + 0.031 * B^2 + 0.018 * C^2} \qquad (2.7)$$

Where A is cutting speed, B is axial depth of cut and C is the feed rate.

In this case, as can be seen by the coefficients in Eq. 2.7., the most important parameter appears to be cutting depth, while feed rate is less important. The author concluded that the proposed model had a confidence level of 95% and they proposed that the milling operation could replace grinding, if the achieved proposed surface roughness was similar as in their proposals. In general, to make models more reliable and applicable for other materials, machines and systems, certain other important parameters are missing, such as axial depth of cut, environmental media, etc.

To summarize:

Based on literature analysis of Polynomial regression models, the following conclusions can be extracted.

In order to simplify their research, the authors normally use only the most important and general cutting conditions as input parameters. Not all of the input parameters can be separated

by their own coefficients. Basically, this model can provide only a general, non-analytical view of the exact cutting operation, with applied material type, equipment behavior and cutting conditions. The same result cannot be repeated on other machines or materials whilst maintaining the same error level. Otherwise, the major difference between the proposed models is the number of input parameters used, their combination, and the response parameters used: surface roughness or topography parameter.

Analytical regression coefficients in the proposed works include regression of the applied material, cutting conditions and process parameters that are not detected before model development.

Furthermore, every author in their approach used their own system properties—their own tool geometry, machine and material, and did not consider the dependent process parameters, like tool deflection, inclination, machine alignment inaccuracies and vibration behaviour. Also, all of the prediction models are based on the roughness parameter response function. Therefore, without experimental data from machined samples, it is impossible to predict the surface topography considering one specific series of cutting conditions used in the cutting process.

In most cases, the authors use statistical analysis such as ANOVA or F-test to confirm the validity of the selected model. Only certain authors ran the confirmation tests to prove reliability of their models. This is essential condition to introduce the model in industry. It should be tested with different conditions and different combinations of input parameters, so as to obtain its real reliability and accuracy, which was not undertaken in most of the considered research.

2.1.2. Artificial network analysis and non-traditional methods

Artificial neural network method

Other, non-analytical models are based on cutting parameters and their coefficients, obtained by Artificial Neural Network (ANN) [52]–[55] models, to predict the surface topology or at least to analyze the importance of the applied cutting regimes on surface topography or roughness parameters. This method has been widely developed since the early 2000s. Artificial neural network is an artificial statistical analysis method, where an unknown inside layer between the Input and Output variables is trained to “learn” the behavior of the system and to calculate results by its knowledge about the system behavior. Those models are compared with other models, proposed by other authors. One famous example is the method to compare ANN with the Multiple Regression or Taguchi model. [56]

A general review of ANN was carried outv by S. Al-Zubaidi et. al [52]. They describe all the advantages and disadvantages of this method. Al-Zubaidi et al. consider ANN as one of the important methods of artificial intelligence for the modelling of nonlinear problems like complex machining processes. The authors considered the application of the ANN method to propose not only surface roughness, but also examined force, surface integrity, tool life and wear prediction,

etc. The referenced authors concluded that this method was mostly used to predict surface roughness, due to its importance in machined surface quality characterization.

An extensive explanation of Neural Networks and optimization with the Taguchi method applied to surface roughness prediction models was given by P.G. Benardos et al. [57]. At the same time, the Taguchi method was applied to analyze a wide range of input parameters and "teach" the system to predict the output variables (FIG. 2.1). The depth of cut, feed rate per tooth, cutting speed, engagement and wear of the cutting tool, use of cutting fluid and the three components of the cutting force were used as input parameters.

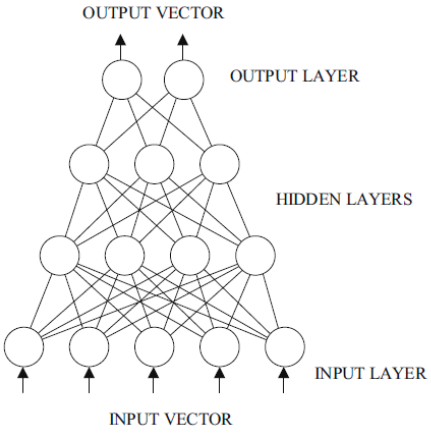

Fig. 2.1. Schematics of the Artificial neural network [57]

Each input into the neuron has an associated weight that determines the ‘‘intensity’’ of the input. The processes that a neuron performs are: multiplication of each of the inputs by its respective weight, adding up the resulting numbers for all the inputs and determination of the output according to the result of this summation and activation function. Fig. 2.2 represents how data is fed into the network through an input layer, is processed through one or more intermediate hidden layers and is finally fed out of the network through an output layer.

Based on previous approaches, Bernardos et al. describe that the most important parameters to predict surface roughness are:

- Cutter insert and solid tool arbor mounting inaccuracies;
- Variable rigidity of the workpiece-tool-machine system;
- Cutting tool wear;
- Built-up edge formation;
- Non-uniformity of cutting conditions during the cutting process.

The Total Design of Experiments system in this case included a huge number of different input factors. The orthogonal array system was complex, and as Bernardos et al. concluded, the neural network was a powerful tool to solve similar problems. They underline that the result of this research was accurate, but a wider system can be proposed to teach the model and provide a

database of advanced ANN with even more accuracy. The most important parameter was again feed rate. A higher feed rate increases the surface roughness. Currently these systems are not available for manufacturers to calculate precise surface roughness or topography parameters. Furthermore it is difficult to control the network and to follow the accuracy of every case, which means that it is difficult to identify the errors made by neural network faults. Thus a large number of training iterations are required to obtain an accurate Artificial Neural Network.

In their work E.S. Topal et al. [58] justified that additional components, such as tool radial cutting depth component, contributed to an improved ANN model, and were essential to improve the accuracy of roughness prediction model. A model including radial depth of cut was compared with a model without radial depth of cut. In this case, a high surface roughness deviation was observed between measurements and the ANN model without the radial depth of cut component. Conversely the result was more precise using the model with this component.

On the other hand, the author P.B. Huang et al. [55] applied a neural network model to analyze the in-process monitoring system response. In contrast to other authors, they proposed to decrease the variation of input parameters to increase the accuracy and reliability of the obtained models. They used a regression threshold model to sort and filter all of the provided input parameters and reduce their number to a minimum in neural network models. Architecture of this model is represented in Fig. 2.2. Inputs represent the input parameters divided into appropriate groups. A regression model worked as a data preprocessor to filter the data. The confidence interval of the regression model was applied as a threshold to categorize the data into different groups, and then the grouped data was trained to generate different neural network decision-making models.

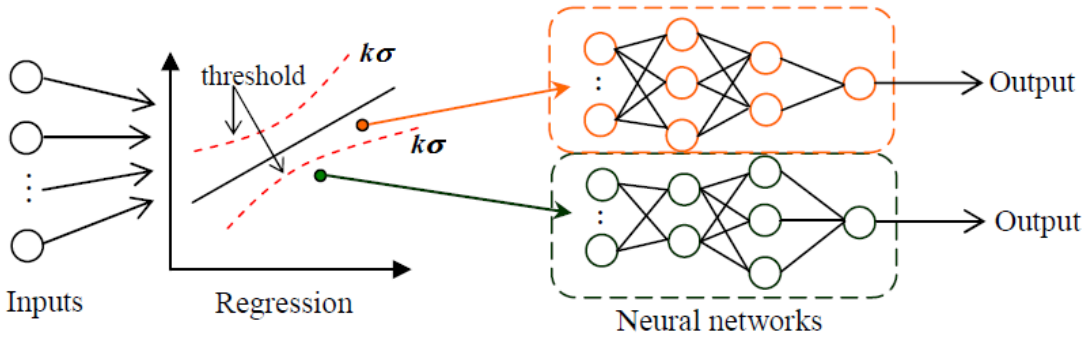

Fig. 2.2. Architecture of decision-making regression – neural network [55]

PP.B. Huang et al. proposed this as a decision-making model that can be applied in process manufacturing to perform the machining and quality inspection simultaneously. The result obtained with the Regression-Neural network model is more accurate for predicted surface roughness than a simple neural network model. However, some of the input parameters are fixed, which cannot provide reliable results for industry needs. As the authors concluded, the number of input parameters should be increased to teach the model. [55]. Considering these shortcomings, it

casts some doubt that this kind of model can be adjusted for all cutting system environmental properties.

In ref. [44], A. M. Zain et al. considered tool geometry as an important input parameter. They selected 5 different rake angle values to analyze them in an ANN model, together with other conventionally used cutting parameters, such as feed rate and cutting speed. The authors did not analyze only the input parameter influence, but also applied various neural network structures to obtain the best-fit model for surface prediction. In the authors' opinion, different structures of hidden layer connections may strongly affect the result, and it is unacceptable if they are talking about surface precision and accuracy.

In ref. [59], Y. L. Chen et al. used Generalized Regression Neural Networks (GRNN) to predict the surface. At first sight, it seems that this model is similar to the previous one. Actually, in this model none of the input parameters were separated. A typical architecture of this model is represented in Fig. 2.3, R is the radial basis Gaussian function. The first layer of the network is a radial basis hidden layer in which the number of neurons amount to the number of training samples. Each neuron's weighted input is the distance between the input vector and its weight vector, calculated with "dist". The second layer is called the special linear layer, which has a normative dot product weight faction (nprod) that can be used to calculate the vector n^2. Each element is the dot product of a row of $LW_{2,1}$ and the input vector a^1, all normalized by the sum of the elements of a^1, which provide n^2 to the linear transfer function a^2=purelin(n^2) to calculate net outputs.

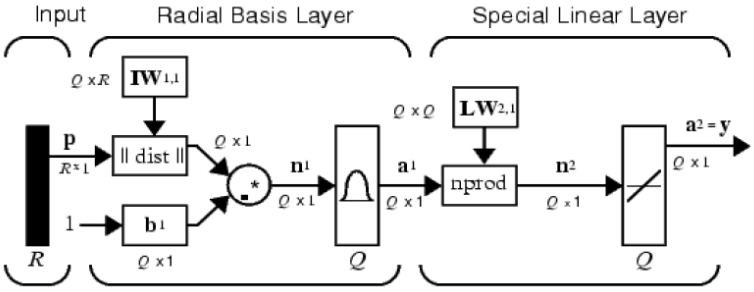

Fig. 2.3. Typical architecture of GRNN model [59]

The obtained results of the GRNN model provide better prediction accuracy than an empirical regression model. The authors also claim that this model can be better used for the dynamic control of surface roughness. [59]

An Artificial Neural Network is an adaptable system that can learn relationships through repeated presentation of data and is capable of generalizing to new, previously unseen data [60]. M. Rashid et al. in their research compare the results of Multiple Regression analysis of the end-milling process and results of the Artificial Neural Network used to predict surface roughness values. The network is given a set of inputs and corresponding desired outputs, and the network tries to learn the input-output relationship by adapting its free parameters [60].

The neural network activation function is given by following equation:

$$\boldsymbol{f(x) = \frac{1}{1+exp(-x)}} \quad (2.8)$$

Where x between the input layer and the hidden layer is:

$$\boldsymbol{x = \sum_{i=1}^{m} \omega_{ui} * u_i + \theta_j} \quad (2.9)$$

And x between the hidden layer and the output is:

$$\boldsymbol{x = \sum_{i=1}^{m} \omega_{kj} * u_j + \theta_k} \quad (2.10)$$

Where *m* - number of input nodes, *n* - number of hidden nodes, *i* - number of output nodes, *u* - input node values, *v* - hidden node values, ω - synaptic weight and θ - threshold.

The result of the analysis is similar to previously mentioned documents. The most important variable is feed rate, followed by spindle speed and axial depth of cut. Therefore, as regards the accuracy of the model, the artificial neural network provides better accuracy to predict surface roughness, with 93.58% accuracy, while Multiple Regression Analysis (MRA) accuracy is only 86.7%. [60]

In ref. [61], Y. Liu et al. use the same approaches of simple ANN to predict surface roughness on Aluminum 6061 material. Four factors in four levels were used in this research. The surface roughness Ra parameter was recognized as a response surface parameter. Cutting speed and feed rate were recognized as the most important factors, similar to other studies.

Another interesting method was applied by B.G.Y. Huang et al. [62]. In their work, the Least Squares Support Vector Machine (LS-SVM) method was used to propose the surface fractal conditions in a face-milling operation. The input parameters, as always, were cutting conditions. The output parameters of the LS-SVM were the corresponding calculated fractal parameters: fractal dimension *D* and vertical scaling parameter *G*. To analyze surface roughness, the Weierstrass-Mandelbrot (W-M) fractal function can be used in order to characterize and simulate surface profile. This function was integrated in the LS-SVM method. This model was based on model training using different obtained surface roughness parameters from identical situations. The modified W-M function is given by:

$$\boldsymbol{z(x) = L(\frac{G}{L})^{D-1} \sum_{n=0}^{n_{max}} \frac{cos(2*\pi*n*\gamma^n*x/L}{\gamma^{(2-D)n}}} \quad (2.11)$$

Where *G* is the vertical scaling parameter, *D* - the fractal dimension (1< D <2), L - the sample length of measured profile, *x* - the x-axis coordinates of the measured sample length. γ is chosen to be equal to 1.5, providing both the phase randomization and high spectral density, and n is the frequency mode, which corresponds to the reciprocal of wavelength as $\gamma_n=1/\lambda_n$ and $\lambda > 1$.

When the plot of a structure function for a measured surface profile follows a power law with *τ*, a surface profile is said to be fractal. Fractal parameters *D* and *G* can be calculated from following function:

$$\boldsymbol{S(\tau) = G^{2(D-1)} * \tau^{2(2-D)}} \quad (2.12)$$

The obtained D and G parameters are substituted into the W-M fractal function to obtain the corresponding fractal-generated roughness profiles. The result of the proposed model confirms that the predicted profiles exhibited more details than the actual measured roughness profiles, so that they could be used effectively for establishing different contact models. The authors proposed that the obtained results were similar to the measured surface in general and error is less than 5-7%. The accuracy of the obtained results depends on measured surface data points. [62]

B. Lela et al. [46] in their work compared Regression Analysis, Support Vector Machines (SVM) and Bayesian Neural Network (BNN) models. SVM is a specific class of algorithms that are referred to as kernel methods that are well-known tools for classification and regression tasks. The authors highlight that SVM and BNN models are also widely used to predict tool wear and error detection. As datasets are small, the best results obtained from a learned system are provided by the BNN method. The authors consider that BNN automatically controls the network complexity, so there is no need for any dataset validation and cross-validation procedure.

In ref. [63], M. R. Razfar et al. used the Harmony Search (HS) algorithm to improve the result of their ANN model. They used the Harmonic Search algorithm to optimize the model. A typical type of Back-Propagation (BP) neural network was used. It is designed to minimize the mean square error between the actual output of the hidden layers and the experimental output, continuously changing the vector weights between layers. Similar to the previous models, the model was fitted to (or learned) the experimentally obtained data. The HS method applied the musical procedure of seeking the best state of harmony. The authors used the following steps to complete the model:

- Step 1 - Initializing the problem and algorithm parameters
- Step 2 - Initializing the harmony memory
- Step 3 - Improvising a new harmony
- Step 4 - Updating the harmony memory
- Step 5 - Repeating Steps 3 and 4 until the termination criterion is satisfied.

The authors concluded that a good correlation between the HS model predicted parameters and measured surface parameters had been obtained. Furthermore, the HS method was not so sensitive for its setting parameters [63].

The basis of a simple BP artificial neural network algorithm was also used in ref. [64], where obviously a precise result for the exact case, with a low number of input parameters and short training times, were observed by the author J. P. Hu et al.

The ANN method has also been applied to predict the surface roughness online for high-speed machining. G. Quintana in ref. [65] proposed that it is important to monitor the cutting process, and this trend was going to develop in future years. He used a high number of input parameters as geometrical conditions, part geometry, dynamic factors, lubricants, tool and

material conditions. Some measurements, such as vibration, were taken online, during the cutting process with piezoelectric actuators. In this research, due to the high number of input parameters, an extensive number of experiments were performed. Because of the large amount of data, the obtained accuracy of the ANN model was determined to be high.

Taguchi method

Next, the Taguchi method is another optimization tool for improving the accuracy of surface prediction models [56], [66] and [67]. John L. Yang et al. [66] in their research used a Taguchi method to develop a model based on an experimental design. Unlike previous models, the Taguchi parameter design was based on two important tools. They were orthogonal arrays and signal-to-noise (S/N) ratios. Orthogonal arrays have a balanced property in which every factor setting occurs the same number of times for every setting of all the factors in the experiment. Orthogonal arrays allow researchers or designers to study many design parameters simultaneously and can be used to estimate the effects of each factor independently from the other factors. The signal-to-noise ratio is simply a quality indicator by which experimenters and designers can evaluate the effect of changing a particular design parameter on the performance of the process or product. In [66] to determine the influence of each factor, they performed analysis of variance - ANOVA.

The predicted mean value of surface roughness was:

$$\boldsymbol{A_2 + B_3 + C_1 + D_2 + 3 * (y..) =>}$$

$$\boldsymbol{66.83 + 60.67 + 51.56 + 84.94 - 3 * (80.59) = 22.26\ \mu m.} \qquad (2.13)$$

A, B, C and *D* are optimal cutting conditions that give the lowest surface roughness parameters in i^{th} experiment. and *y*.. is the mean value of the i^{th} measurement.

The proposed method can provide good results for individual milling machines with an end-mill tool. This model was valid for machining in a specific case. To adjust it to another type of machine, additional experiments have to be done and coefficients adapted for other cases. As the authors concluded, additional research was also necessary to identify other factors that influence the machining process (lubrication, materials etc.).

Similar optimization was conducted in the research of D. Bajic et al. [68]. The equation for surface roughness, as a function of cutting parameters, was obtained by means of regression analysis. The Taguchi method, with orthogonal arrays and a signal-to-noise ratio, was used to analyze the impact of various cutting parameters on surface roughness and to find the optimal levels of the cutting parameters. The most valuable advantage of the Taguchi model was the decreased model number for designing experiments.

The same Taguchi approach was used in K. Yusuf and his colleagues' work [69]. The study investigated the optimal parameters that could produce significant good surface roughness. The Taguchi design method was used to optimize the surface roughness quality in Computer Numerical Control (CNC) of end-milling operations. The control parameters were spindle speed,

feed rate, depth of cut and the type of end-milling tool. On the other hand, the noise parameters were coolant pressure and cutting patterns. Analysis of the influence of input parameters indicates that the most important parameter in the end-milling process in this case was spindle speed, type of milling tool used and feed rate.

Likewise, J. Speedie et al. [70] presented an approach based on the Taguchi and orthogonal array model. The same input parameters as in other researches were used. The applied material was 13% Austenitic Manganese Steel. The response factors for these specific experiments were surface finish, spindle load, material removal rate, cutting forces and surface hardness. The authors used the Taguchi model to predict not only surface topography parameters. The linear graph was similar in size to other research work. To validate the results, unlike in other research, the authors used confirmation experiments, where they grouped input parameters together to test other combinations of them. From the results, they concluded that the surface hardness of the machined surface increases by increasing the cutting forces, and different combinations of input parameters give different surface roughness outcomes.

Another research project with experimental result validation was carried out by Y. Wang et al. [71]. The Taguchi method was applied to design the cutting experiments for the end-milling tool on Inconel 718. The Signal-Noise (S/N) ratios were used to study the impact of input parameters. Results were based on the regression method, where exponential coefficients were determined from multiple regression analysis.

$$\mathbf{lg_R = 3.59 + 0.799lg_f + 1.20lg_a + 1.49lg_a} \quad (2.14)$$

From the verification tests, the author concluded that compared with the verification experiment, the predictive error was less than 3%, which notably indicated that the prediction model for surface roughness was significant and could be used to predict the R_a value.

Elsewhere, in T. Ding et al. [72], it was found that the axial depth of cut and the feed rate were the two dominant factors affecting the cutting forces. The Taguchi method was also used to determine the polynomial second-order model coefficients. The obtained result of the author's proposed model can provide surface roughness of less than 0,25 μm. This led to the conclusion that the milling process in this specific case is comparable with the surface grinding process. The same authors applied Taguchi optimization to improve the prediction model on the AISI H13 material. [73] The obtained conclusions were opposite to other authors. In this specific type of material, high cutting speed, in combination with high feed and low axial and radial depth of cut produced minimal surface roughness. The obtained accuracy error was 10,49% and less.

Gray relational analysis as an optimization method for face milling was considered in the research by N. Tosun et al. [74] paper. The Taguchi method was applied for Aluminum grade 7075 material, to predict the lowest surface roughness with the highest MRR (Material Removal Rate). An orthogonal array was used for the experimental design. Optimum machining parameters were determined by the Gray relational grade obtained from the Gray relational

analysis. The Gray relational grade γ_i represents the level of correlation between the reference sequence and the comparability sequence:

$$\boldsymbol{\gamma' = \frac{1}{n}\sum_{k=1}^{n} \omega_k \zeta_i(k)} \qquad \boldsymbol{\sum_{k=1}^{n} \omega_k = 1} \tag{2.15}$$

Where w_k denotes the normalized weight of factor k, but ζ is the distinguishing or identification coefficient.

The importance of the controllable factors, in the words of the authors, on the multi-performance characteristics were identified in the following order: feed rate --> cutting speed --> tool material --> cooling technique. The model represented a substantial improvement of the Taguchi method used to predict surface topography. But again, the RSM method rejected this method as being applicable to other systems without repeating the experiments and experimental surface measurements.

The Gray relational analysis method was used also in ref. [75]. B. Jiang et al. analyzed how different input parameters and other dependent parameters, such as vibrations, affected the final surface roughness for hardened steel. These experiments were conducted with the ball-end milling tool. The results show that cutting efficiency was advanced by the increase of rotational speed and row spacing, and less surface roughness could be achieved by decreasing feed and inclination angle. Increasing machining efficiency increases surface roughness, and decreasing the feed rate decreases the surface roughness. B. Jiang et al. using the algorithm (2.16.) found behavior sequences of characteristics and related factors in high-speed ball-end milling on hardened steel, such as surface roughness, cutting force, cutting temperature and the relative vibration of workpiece. X_0 is the systematic behavior characteristic sequence and X_i is the related factors sequence. The data treatment follows with these equations:

$$\boldsymbol{\overline{x_i(k)} = \frac{x_i(k)}{\bar{X}_i};} \qquad \boldsymbol{\bar{X}_i = \frac{1}{16}\sum_{k=1}^{16} x_i(k);} \qquad \boldsymbol{k=1,2,3..,16;} \tag{2.16}$$

Where x_i is the increment characteristic of cutting factor k, but $\bar{X}_i$ is the absolute incidence between cutting efficiency and high-speed milling characteristics.

From the analysis of all papers where the Taguchi method is used, B. Jiang concludes that for the most part, the L_{16} (4^4) orthogonal array was used. Improved exponential or polynomial coefficients of regression analysis show good results with less than 10% of error. But, again, this model can be applied only to improve the results of the empirical model based on the Response Surface function. Without experimental testing, industry cannot apply the knowledge of this model to realistic situations, except to make statements about the factors potentially impacting surface roughness.

To summarize:

A number of similar research projects have been conducted by different authors to develop and improve their prediction models. The structures of the proposed models are similar, the

results obtained in terms of accuracy are similar, but the obtained coefficients are valid only for specific cases, to calculate the rough value of surface parameters. There are some common assumptions in most of the aforementioned research. In more than 2 out of 3 of the described cases, the authors claim that the most influential parameter in surface formation process is the feed rate, followed by cutting speed. Furthermore, no matter what analysis method is used, the conclusions from the authors' results are similar in every case. Surface roughness increases with the increase in feed rate and decreases with the increase in spindle speed.

The developed model has to be tested before it is applied to industrial use. Of course, similar to previous cases, the authors mention feed rate as the most important parameter. As in other cases and, as mentioned previously, the feed rate is closely connected with other process parameters operating in the cutting process. But only the general feed rate parameter was considered. To create a more accurate model and to make the resulting feed rate model coefficient more accurate (variable with factors), it is necessary to extract factors that affect cutting feed or feed rate and cause model changes. These factors will be considered in the present author's research. But before this, we shall examine what kind of methods other authors have tried in order to improve their models.

Optimization

As mentioned in previous subsections, different types of algorithms are frequently used to optimize and improve the simple regression or artificial neural network models and their results. In the research of H. Oktem et al. [76] and P. Yongzhi et al. [77], the authors described the effect of the simple response surface model, improved with a genetic algorithm. In both cases, there were improvements in surface prediction accuracy. Therefore, in the paper by P. Yongzhi et.al., the model was used to optimize and select the best cutting tool geometry for the end-milling operation on 7050-T7451 aluminum alloy. Elsewhere, in ref. [53], the author B. Ozcelik et al. used a genetic algorithm to improve the result of an ANN. The obtained model was identified as reliable, to be able to select appropriate cutting parameters for a specific case on Inconel 718 material.

C. Prakasvudhisarn et al. in ref. [78] represented the surface propagation model based on Vector Support Vector Machines. Support vector machines (SVMs) represented a relatively new type of learning machine. SVMs were designed to minimize the structural risk by minimizing an upper limit of the generalization error rather than the training error [78]. They also used a new method, known as the Particle Swarm Optimization method (PSO) to optimize input parameters for better surface result.

$$\boldsymbol{Ra} = \frac{\mathbf{10}\boldsymbol{aR^bF^c}}{\boldsymbol{S^d}} \tag{2.17}$$

Where *R* is the radial depth of cut, *F* is the feed factor, and *S* is the spindle speed, coefficients *a, b, c,* and *d,* are unknown, to be determined by the PSO algorithm.

They concluded that high accuracy of this optimization was achieved, but they did not compare the results with and without optimization. In addition, they agreed that more

improvements were necessary, such as material type changes, tool geometry impact and other factors presence could improve the result of optimization.

Genetic programming

Genetic Programming (GP) is a similar problem-solving tool to the Artificial Neural Network. In GP, the structures subject to adaptation are the hierarchically organized computer programs, whose size and form dynamically change during simulated evolution. In order to compare it to the biological metaphor, the computer programs are called organisms or also chromosomes and this is described by Y. Yang et al. [79]. As said in this paper, the aim of genetic programming is to identify the computer program that solves the problem with the highest accuracy. These computer programs can be composed of a set of function genes:

$$\boldsymbol{F=[f_1,f_2,..,f_m]} \tag{2.18}$$

Where *m* is the number of function genes, and the set of terminal genes are:

$$\boldsymbol{T=[a_1,a_2,..,a_n]} \tag{2.19}$$

Where *n* is the number of terminal genes.

The appropriate number of arguments for function genes is determined with the list:

$$\boldsymbol{\{z(f1),\ z(f2),..z(fn)\}} \tag{2.20}$$

Examples of different programs are represented in Fig. 2.4.

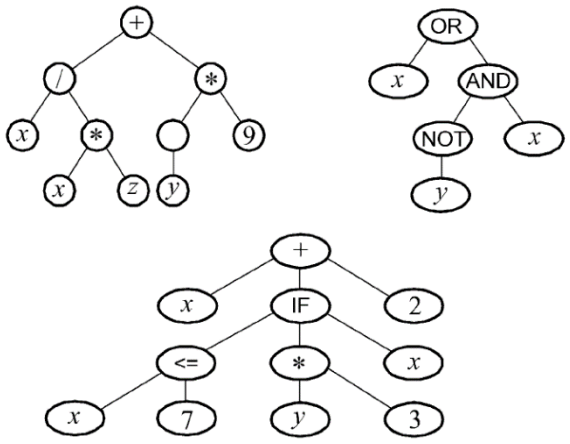

Fig. 2.4. Sample of different genetic computer programs [79]

In my conclusion about Genetic Programming and solving the surface prediction problem, the probability of successful solutions is the greatest if basic arithmetical functions are used in this specific case. Spindle speed and feed rate were the most important variables due to their existence in every program. Otherwise, unimportant parameters were automatically excluded from the program. We conclude that vibrations, as a dependent factor, has an important role in surface formation process. By increasing the number of input parameters, the model's accuracy can be increased. But, if there is no direct influence, the method excludes the parameters that can

be critical, such as tool deflection, vibrations, friction and cooling fluid influence on surface topography.

Similarly in the work of Y. Yang et al. [80], Genetic Expression Programming (GEP) was used. It is a combination of Genetic Algorithm and Genetic Programming. GEP is genotype/phenotype genetic algorithm that evolves computer programs of different sizes and shapes encoded in fixed-length linear chromosomes. The chromosomes are composed of multiple genes and each gene encodes a smaller subprogram. Y. Yang applied GEP for three-factor analysis. These factors are the most commonly used input cutting conditions. They claim that the highest surface roughness was achieved with their model using the higher feed-rate input parameter. The model is a powerful tool nowadays, when high-performance calculation machines are available. However, this model requires more input parameters to be more reliable and precise. A high number of measurements and measurement errors will decrease the accuracy of the result.

The same method model was used in ref. [81]. O. Colak applied the GEP method to analyze the same 3 parameter input domain. The authors observed the nonlinear behavior of input parameter influence on surface roughness parameters, but could not explain the reason for these nonlinearities. The accuracy of this model for a precise case was claimed to be around 91%.

Genetic algorithms are sometimes used together with artificial neural networks. H. Oktem et al. [54] described how GA was used to improve the result of optimization while using ANN. This combination enables improvements in the accuracy of the model developed by ANN. With this model, critical regions of machined part can be detected. Therefore this model helps to improve the quality of plastic molded parts that depend on the mold/die surface quality after machining. Cutting feed remains the most important parameter in this predicted model.

The same combination of models was used in the work of H. Oktem et al. [82], only in this case AISI 1040 Steel was used to make cutting experiments. The author performed validation experiments and measurements. The roughness error detected was 3.278%. They claimed that GA application, together with the ANN method, improves the accuracy and that the study was reliable and applicable to solve other kinds of problems related with cutting processes.

Also, a genetic algorithm was used in ref. [45]. A. M. Zain et al. considered tool angles as one of the most important input parameters to describe the surface roughness for Ti-6Al-4V (Ti-64). A regression model for each cutting tooth of the cutting tool was proposed. Different regression models were fitted to the RSM function to obtain the best fit. Subsequently, the genetic model was applied to improve the result. The authors found great differences between models, with and without optimization. In my opinion, high speed, low feed and maximum rake angle may slightly decrease the surface roughness values.

A very similar approach was taken by the author K. V. M. Krishnam Raju [83] et al. A multiple regression analysis using analysis of variance was conducted to determine the performance of experimental measurements and to show the effect of cutting parameters on the

surface roughness. A Genetic Algorithm (GA) supported by the regression equation was utilized to determine the best combinations of cutting parameters, providing roughness to the lower surface through the optimization process [83]. The author claims that the obtained model could be used by other cutting system environmental conditions, but at the same time, the model has to be improved by more input parameters. No confirmation tests were done, to prove the reliability of model. In their conclusions, feed rate was again the major input parameter that affects surface roughness.

A specific method applied by K. Kadirgama et al. [84] was the Response Surface Method combined with optimization using the Ant Colony Method. They applied ant colony optimization to improve the proposed roughness prediction model for milling AA6061-T6 Aluminum alloy. Typical RSM was used to determine the exponential roughness model coefficients.

$$\mathbf{P_{1(m+1)}} = \frac{(\mathbf{m_1+k})^{\mathbf{h}}}{(\mathbf{m_1+k})^{\mathbf{h}}+(\mathbf{m_2+k})^{\mathbf{h}}} \quad (2.21)$$

Where p = probability that ant m_1 chooses the first bridge and ant m_2 – the second bridge, parameters k and h are needed to fit the model to the experimental data. System pheromone values were updated by all the ants that had completed the tour. The pheromone update for τ_{ij}, that is, for edge joining cities i and j, is performed as follows:

$$\mathbf{Tij} \leftarrow (\mathbf{1-p}).\quad \mathbf{Tij} + \sum_{\mathbf{k=1}}^{\mathbf{m}} \mathbf{\Delta T_{ij}^{k}} \quad (2.22)$$

Where ρ is the evaporation rate, m is the number of ants, and Δ_{Tijk} is the quantity of pheromone per unit length laid on edge (i, j) by the k_{th} ant. Finally, the authors observed that the first-order model indicates that feed rate was the most significant factor affecting surface roughness.

To summarize:

Different combinations of non-traditional models have been used to predict or detect surface roughness, topography and quality parameters. These models show the relationship between changes of technological parameters and surface roughness parameters.

Even if the global results of analysis by different authors and different input parameters are comparable and their proposed conclusions are similar, it does not mean that the same model will generate correct roughness values for different systems, in which the tool, machine or material has been changed. This conclusion is often reached by the authors themselves. Why?

These models include factors taking into account only input parameters. Even if the artificial neural network system has been used, the machine type or tool, or even behavioral conditions will be additional factors to be considered. Polynomial or Exponential Regression models cannot physically include all the external behavior factors. ANN is theoretically able to include all the input factors, but, firstly, every factor should be separated by an additional value and secondly, none of the previously mentioned authors considered external factors in their analysis process.

An extensive amount of similar researches has been conducted to detect the most important parameters. Most of them repeat the same error, not including external or even internal factors that can vary not only because of cutting conditions, but also machine environment, tool type and material, etc. Without these particular factors, any model will be incomplete. But in the cutting process, other types of factors also contribute, related to the geometry and physics of the cutting process, which should not be neglected. We shall discuss these in the next subsection.

2.2. Theoretical models

Under the classification of theoretical models in this paper, the author refers to the models that use theory-based cutting process parameter variables that affect surface formation directly or indirectly. Geometry and its inaccuracies could affect the depth of marks left on material surface by every cutting edge. In general, this approach is based on machining theory principles. As this chapter will highlight, methods are described that are commonly used in surface prediction models. These models could be also called surface generation models, due to their importance for the surface generation process.

2.2.1. Geometrical models

In general, these are models that consider all the geometrics of the working system. It includes cutting tool angles, tool size, tool construction, tool inclination angle, tool rotation axis inclination angle and deflection, tool run-out and wear-out. In this subchapter, the author will review how other authors in the past have considered these effects.

Already in the mid-1980s, T.S. Babin et al. [85] started comprehensive research to analyze how the machining process parameter influenced surface topography formation in the end-milling process. In this and subsequent papers, the authors considered both cutter run-out and tool deflection errors and their influence on basic tool path equations. With these basic equations, they modelled the surface roughness of a laterally milled surface. This research was one of the first investigations into this topic, to identify tool deformations during the cutting process and their importance in topography formation. As it was observed, a considerable number of authors refer to this or other papers by these authors. In general, the model is a simple, geometrical approach to analyze how tool cutting-edge deformations leave an integrated effect on the laterally machined surface. At first, only tool run-out and deflection were considered. Later, the end-milled bottom surface was also considered [14]. W. Sutherland et al. developed an analytical model to describe the cutting edge trajectory and its influence on the machined surface profile height. The authors considered two types of run-out working in the process – parallel axis radial run-out and axis tilt run-out. From the results of the model verification, the authors concluded that the developed model was accurate and agreed with the measurement data. They discovered that the maximum surface height value (R_t) was more sensitive to factors that were not related to geometry. More importantly, they concluded that higher tool nose radius can reduce the negative result of concavity angle and decrease the surface R_a and R_t parameters.

After this, a great number of authors followed Babin and Sutherland's proposed model, or similar, to detect the same influence while machining different kinds of materials and with different applied cutting regimes. A similar approach was used by such authors as I. B. Corral [86], [87], M. Arizmedi, D. K. Baek and others.

The author K.Y. Lee et al. used exactly the same approach. [88]. They proposed this model as a signal acceleration model and provided the programming method to simulate the surface roughness in the high-speed milling process. The vibration effect was added. In this model, the authors consider only peak values of vibrations, in which the amplitudes were greater than half the amplitude of the second harmonics frequency of spindle vibrations, due to their higher effect. In general, the surface roughness profile is similar, but the resulting accuracy with different attempts was different. The authors provide only a simple conclusion, in which the result is good and the predicted roughness is similar to that which was measured.

Altintas et al. [15] proposed the mathematical cutting force model, based on the variable geometry of the cutting tool. In this model, the tool geometry was expressed with 7 different geometrical components. They describe the variable chip load and its direct effect on cutting force local constants on cutting edge. The general geometry of the cutting process by Altintas is represented in Fig. 2.5. This figure represents the tool cutting edge movement increment expressed from a geometrical point of view.

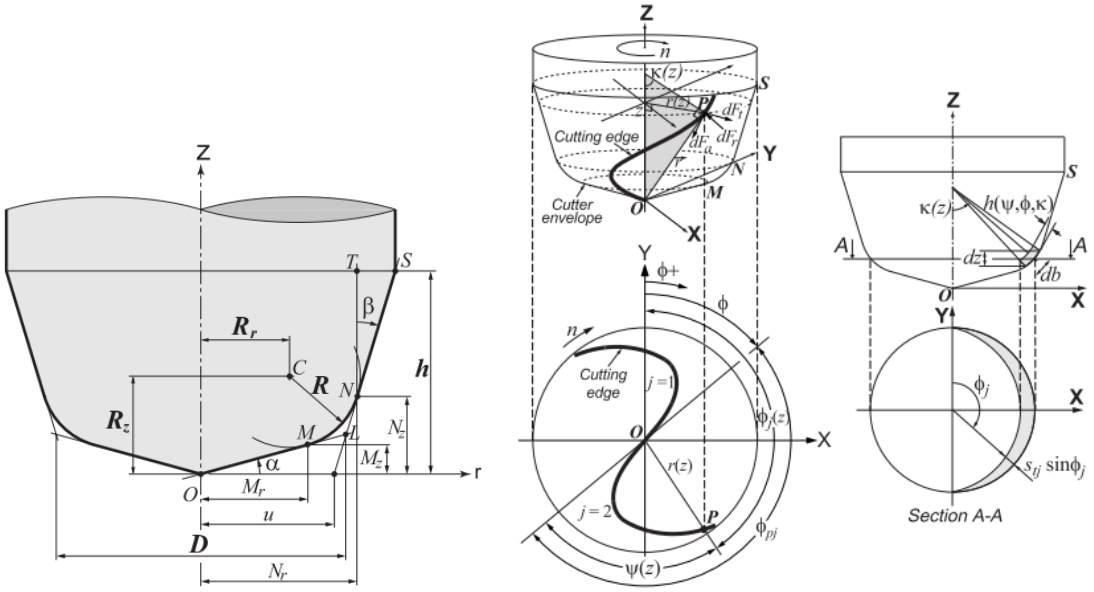

Fig. 2.5. General geometry of the cutting tool [15]

Where R is the radius of the cutter at elevation depth R_z , u is the distance between the cutter tip and the point at which the NS line intersects the XY plane and d*F*a, d*F*r, d*F*t are differential cutting forces at cutting points P along the cutting edge. Point *P* has an elevation *z*, radial distance *r*(*z*) on the *XY* plane, axial immersion angle (*z*) and radial lag angle y(*z*). The axial

immersion angle is defined as the angle between the cutter axis and the normal angle of the helical cutting edge at point *P*.

They describe different immersion angles due to the helix angle of the cutting tool. It follows that the uncut chip thickness is different and the total cutting force, due to the tool immersion, is different compared with the tool at different distances from the end of the cutting tool. Moreover, the dynamics of the system, more specifically the cutting tool vibration effect, was introduced in this research. Indeed, this factor will be analyzed in next subsection. The proposed model was tested on AL 7075 and Ti6Al4V alloys. Both of them have different cutting behaviour. Experiments with a tapered ball-end milling tool confirm that increased cutting depth affects the chatter and causes higher deviation of cutting forces. Unfortunately, the authors do not consider the effect on surface roughness or topography to be dependent on cutting forces.

The author D.K. Baek et al. [16] looked at how the cutters insert radial and axial run-out influence surface roughness. They used a geometrical relationship to describe the deviation from ideal tool tip point trajectory, taking into account that each cutting tool edge tip points may have deviations. This phenomenon is represented in Fig. 2.6 where every cutting tool edge deviation is represented and points *a, b* and *c* represent the surface roughness peaks of the machined surface. A methodology with three mathematical equations was used to calculate surface profile from each insert trajectory line. The authors also analyzed the feed ratio's influence on surface roughness and dimensional accuracy on the face-milling operation.

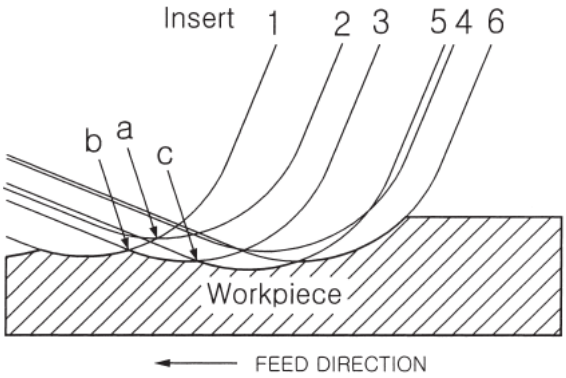

Fig. 2.6. Representation of surface roughness after one whole revolution of cutter [16]

Baek et al. concluded that the cutting feed rate was nonlinear in relation to the feed rate, and pre-measured tool run-out was introduced to find the real model. They proved that the proposed model was good enough to model the surface roughness of face milling operations.

P. Franco et al. [17] developed a surface prediction model for the face milling operation. They used a tool with 4 cutting edges and considered their run-out in combination with cutting parameters such as different feed speeds. The real tool run-out measurements were taken before the experiments. The model was verified with the experimental approach. The author P. Franco et al. concluded that a decrease in feed rate caused inaccuracies in the proposed model and elimination of them might increase the prediction accuracy. Of course, the theoretical model did

not include some local defects of the experimental surface. In cases similar to this, with high tool nose radius, these local deformations were not important. Furthermore, in the case of high Material Removal Rate, as in roughing operations, the accuracy of surface roughness was not decisive. But, this model works well enough for finishing operations or even high-speed milling operations. The most important conclusion made by the authors was that these run-out errors should be considered, if surface quality is important in machining operations.

Tool run-out has also been considered by S. H. Ryu et al. in their research [19] [89]. The authors took a clearly geometrical approach to analyze plain surface topography formation with end milling. For tool radial run-out, two point measurements were taken, to analyze tool run-out and inclination magnitude. They were the first who referred to such surface topography parameters as RMS, skewness and kurtosis parameters. The author S. H. Ryu et al. considered that surface generation with end cutting edges had not been studied in detail. They proposed a model which linked tool deflection caused by cutting forces, tool radial run-out and tool setup error with back cutting phenomena. Fig. 2.7 represents this behavior. The tool center point due to the axis inclination is redirected by distance Lsinτ. This distance depends on the tool mounting length l. Surface topography this time is generated with tool tip point F_i. In accordance with the authors, tool setup error was tool tilting over the cutting feed direction. The authors concluded that tool run-out and setup errors played a significant role in profile formation process and therefore, tool deflection affects surface form errors. [19]

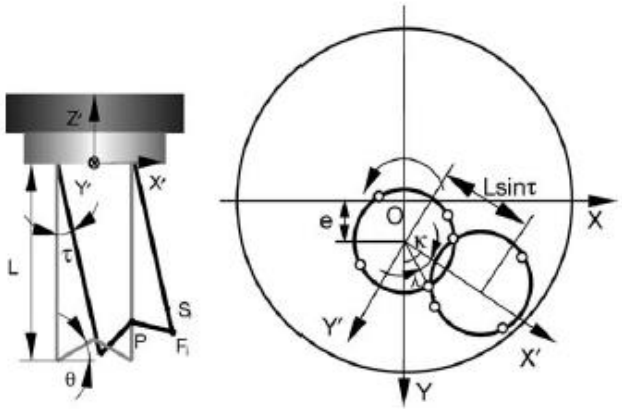

Fig. 2.7. Tool setup - inclination error [19]

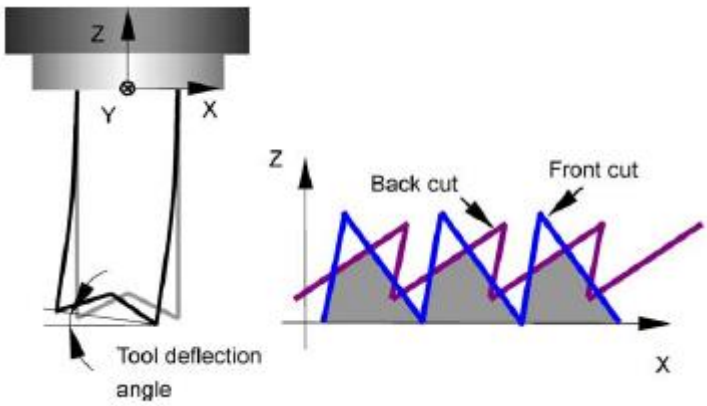

Fig. 2.8. Tool deflection due to cutting forces and increase of back cutting phenomenon [19]

Afterwards, the tool also has its own deformation-deflection. Deflection is represented in Fig. 2.8. The tool's front tip point generates the peaks and valleys on the surface topography, but the rear tip point cuts them off. Due to variations in tool deformation level, surface topography height changes according to the tool deflection. The magnitude of back cutting is influenced by tool deflection. In this work, the tool deflection angle is calculated using a cantilever beam theory under the assumption of quasi-static tool motion. Deformed tool cutting edge and tip point positions were expressed with $\boldsymbol{P}$, $\boldsymbol{F_i}$, $\boldsymbol{S_i}$ position vectors (Fig 2.7) [19] [89].

A group of authors used geometrical interpretation of cutting edge movement over the machined surface, such as the effect of vibrations, due to their frequent behaviour. Most of them consider these to be geometrical inaccuracies of the tool mounted into the chuck.

Geometrical considerations were used by H. Jiang et al. [21] in their work. The authors consider tool geometrical deformations and system vibrations to predict laterally machined surface height parameters. The main factors were tool mounting inaccuracies, which caused vibrations during the machining process. The proposed model was based on realistic measurements taken for the exact tested system. The authors regarded that it was necessary to measure the actual vibrational displacement to get an accurate prediction and reconstruction of the surface roughness and profile in milling. Vibrational effects were converted into geometrical tool cutting edge displacement to reconstruct the surface topography. The machined surface was the envelop surface of all the traces of the cutter's moving flutes relative to the workpiece, and the simulation was based on the numerical computation of height matrix.

The equation proposed by the authors to find the location of the displaced tool tip point is the following:

$$\boldsymbol{X = Ra * cos\theta} \tag{2.23}$$

$$\boldsymbol{Y = Ra * sin\theta} \tag{2.24}$$

$$\mathbf{Z = B'D' - CD' = } \boldsymbol{H - A'D' \times \cos(\varphi + \tau) = H - A''D' \times \cos(\varphi + \tau) =}$$

$$\mathbf{= H - \sqrt{(R * \sin\lambda)^2 + H^2 \times \cos(\varphi + \tau)}} \tag{2.25}$$

Where θ is the location angle of A'' in the new - inclined tool's reference coordinate system Os"U"V"W", represented in Fig. 2.9.

$$\boldsymbol{\theta = atan\frac{A''C}{CC} = atan\frac{\sqrt{(R*sin\lambda)^2+H^2\times sin(\varphi+\tau)}}{\rho+Rcos\lambda}} \quad (2.26)$$

Where H – tool length, R – tool radius, λ – tool immersion angle, ρ – radial run-out value, ϕ – tool internal complementary angle and τ – tool inclination angle. The other symbols are in accordance with Fig. 2.9. This figure represents the cutting tool initial coordinate system, referred to the cutting tool axis, inclination according to the tool deformation and vibration influence. Based on the geometrical approaches, this figure represents the tool tip point's deviation from its initial location.

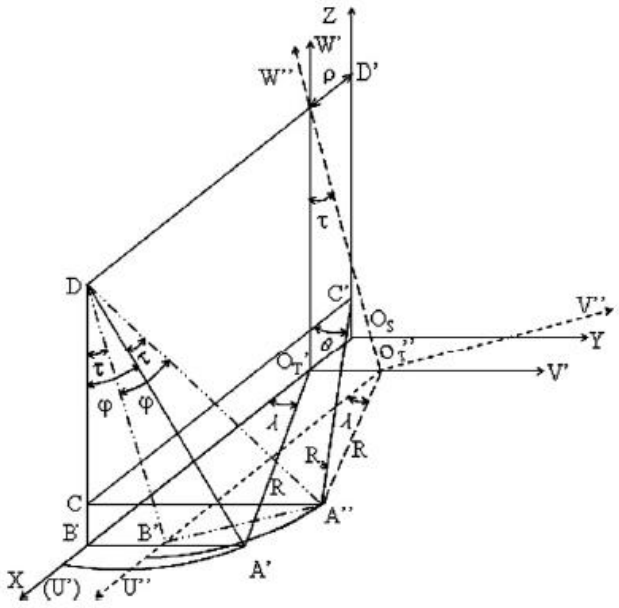

Fig. 2.9. Non-Ideal tool installation model [21]

The results of this simulation showed the obtained surface topography height parameter values were less than the measured values. Error values were 4.4% up to 6.8%, which satisfied the conclusions of the authors H. Jiang et al. From the results it is concluded that vibrations played a major role in the surface topography formation process. Their proposed model and conclusions were based on a lack of other important parameters influencing the cutting process. They also mentioned that effects of friction, tool wear, chip breakage and plastic deformation during the cutting process on the surface profile generation should not be ignored under other cutting parameters, but they were not considered at this stage. [21]

Authors including J. P. Costes et al. [90] started their work with the conclusion that, in previous research, the effect of tool deflection had been neglected. In their research, the authors considered tool axis and angular deflection and its impact on surface roughness, performed by bottom cutting edges.

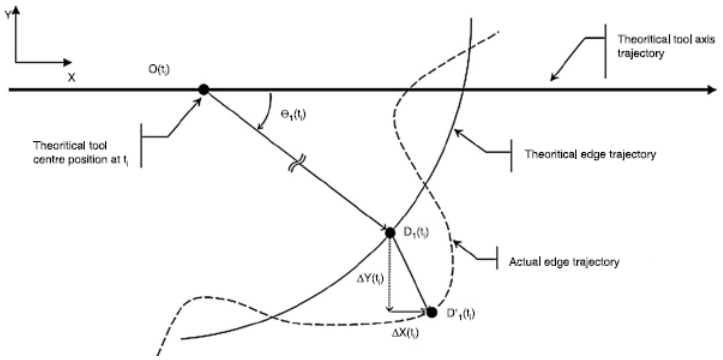

Fig. 2.10. Dynamical model of face milling operation [90]

Fig. 2.10 represents tool tip point movement due to deflection. The authors considered that tool deflection had a linear behaviour along the tool axis. Depending on tool dimensions and material behaviour, this could be an incorrect assumption. But in general, deflection cannot be neglected. In this case, the tool tip point position can be calculated by following:

$$\boldsymbol{OD'_1(t_i)} = \begin{pmatrix} \boldsymbol{R_{D1} \times \cos(\theta_1(t_i))} \\ \boldsymbol{R_{D1} \times \sin(\theta_1(t_i))} \end{pmatrix} + \begin{pmatrix} \boldsymbol{\Delta X(t_i)} \\ \boldsymbol{\Delta Y(t_i)} \end{pmatrix} \quad (2.27)$$

Where θ_1 – angular position of 1st cutting edge, t_i - time increment, R_{D1} – cutting tool radius and $\Delta X(t_i)$, $\Delta Y(t_i)$ is machining displacement [90].

They compared this vibration with a clamped beam first vibration mode. The obtained results showed more than 10% error, but the authors claimed that they were comparable with measured results.

M. Arizmedi et al. [91], in their research, developed a simple approximation model to predict the surface roughness of a laterally machined surface, based on the geometrical displacement and run-out of the tool cutting edges. They used a discretized geometrical model to describe tool cutting edge movement over the rotation, including tool vibration effect (Fig. 2.11). A procedure based on discrete positions along the feed direction was developed. Tool vibration effects were added to tool cutting edge path equations, which were transformed into equivalent polynomial equations. Edge paths were translated to the tool center point path, to describe tool movements. For experimental validation, tool vibration measurements were taken on the tool shank surface.

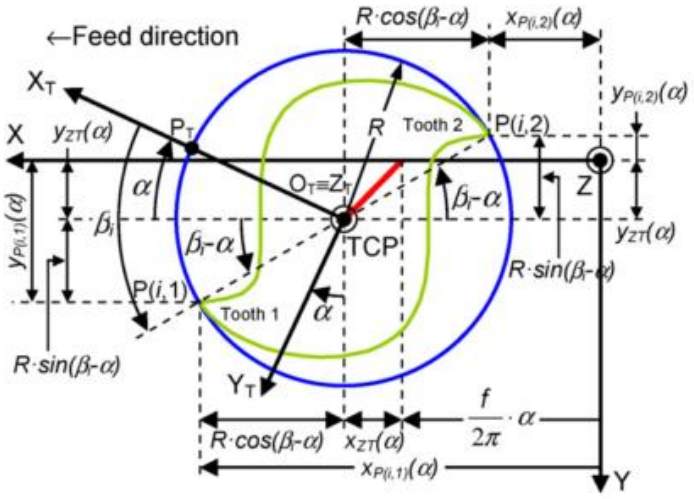

Fig. 2.11. Modelling tool cutting edge path with vibrational effect [91]

Where R – cutting tool radius, TCP – theoretical new center point position of the cutting tool, xZT(α) and yZT(α) define the TCP position as a function, P(i, k) are coordinates at angle α in the feed direction *X*, *Y* and perpendicular to the milled surface – axis *Z* for each cutting edge *k*.

The measured surface was compared with the proposed surface model and conclusions were drawn. With higher feed rate, the marks left on the material were more apparent. Measured surface images were similar to the proposed model and there was a reasonable comparability between modelled and measured surfaces. The authors refer to the arithmetic roughness height parameter, but they did not explain the exact difference between predicted and measured values. Subsequently, the same authors improved and described this model in more detail, ref. [92] Also the authors were considering a laterally machined surface, taking into account the run-out error variable.

The same approach made by M. Arizmendi et al. was used to describe the ball-end milling tool edge's path over the machined material [93]. The difference between models are in cutting edge dimensions from the tool axis, due to the tool spherical end and helix angle, while for flat-end milling, the difference between discrete parts are only due to the helix angle. The cutting edge path model is represented in Fig. 2.12, where $P_{(i,1)}$ and $P_{(i,2)}$ are selected points on the cutting edges accordingly in cutting depth, R_z – actual cutting radius, Z_s – actual cutting tool center point due to its run-out. O_S – intersection point of new coordinate system and R_Z – radius at height *Z*.

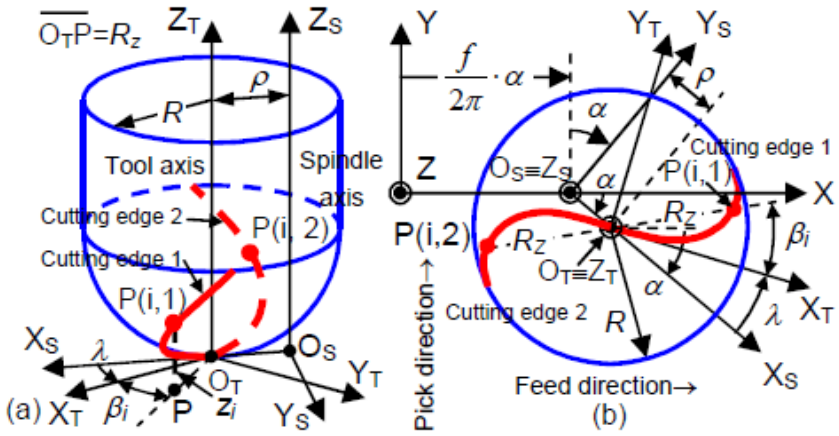

Fig. 2.12. Modeling ball end milling tool cutting edge path with vibrational effect [93]

. Arizmendi et al. developed this model to show how important the tool run-out values were for surface topography, due to the standard run-out of the tool chuck collet. It was assumed that the run-out is due to a parallel offset between the tool and the spindle axis. Cutting edge geometry in a ball-end mill was obtained by projecting a cylindrical helix on a spherical surface in the perpendicular tool axis direction. The authors determined cutting edge points by the following equations:

$$\boldsymbol{X_P(i,k)(\alpha) = \frac{f}{2\times\pi} \times \alpha + \rho \times \cos(\alpha) + Rz \times \cos(A-\alpha)} \quad (2.28)$$

$$\boldsymbol{Y_P(i,k)(\alpha) = -\rho \times \sin(\alpha) + Rz \times sin(A-\alpha)} \quad (2.29)$$

$$\boldsymbol{Z_P(i,k)(\alpha) = R \times \beta_i / \tan(\alpha_{hx})} \quad (2.30)$$

Where $X_P, Y_P, Z_P$are point coordinates by immersion angle α, R_z – distance from the discretized point $P_{(i,k)}$ to axis O_T, α_{hx}- tool helix angle, f – feed per tooth and β_i – location angle.

$$\boldsymbol{A = \lambda + \beta_i + (k-1) \times 2\pi / N_t} \quad (2.31)$$

Where N_t – number of cutting edges, λ – is the angular position of axis X_T with respect to axis X_S, β_i – location angle of cutting edge by tool deflection and ρ – parallel axis offset.

The authors compared topography results and considered the surface roughness parameter R_z. In this case, what was more important in our opinion was to analyze the distance between cusps and marks left on the surface. They concluded that the obtained results were reasonably good and the model was more simplified compared with other literature [93].

A similar approximation was used by I. Buj-Corral et al. [87]. They considered only static geometrical factors, such as feed per tooth and radial cutting depth. These two factors gave only a global view of the surface formation process and revealed that surface topography in general varies due to feed per tooth. The radial cutting depth even amplifies this behaviour.

Quinsat et al. [25] in their paper provided an analysis to find a 3D surface roughness parameter that formalizes the relative influence of both machining parameters and surface

requirements. This roughness parameter was deduced from simulations of the 3D surface topography obtained after three-axis machining using a ball-end cutter tool. They used a geometrical interpretation of tool cutting edge movement. With respect to other research with a flat form surface, they considered machining the free form surface with a known radius. They parameterized this surface to include its form into the analysis. They considered that the most representative cutting parameter in their case was S_Z – surface height deviation. However the authors did not consider tool errors, cutting vibrations, tool deflection, etc.

In paper [94] Quinsat et al. conducted a more detailed analysis to describe which topography parameter depends on cutting regimes. The prediction of the 3D surface topography according to the machining conditions was an important issue in 5-axis machining, to achieve correct process planning and to link the resulting surface patterns with part functionality. Their proposed model was based on discretized sampling point interpolation by the *N* buffer method. The sampled tool location along the elementary trajectory was calculated by:

$$\boldsymbol{X_P} *= \boldsymbol{{X_P}^i} + \left(\frac{{X_P}^{i+1} - {X_P}^i}{\Delta l^{i,i+1}}\right) \times \frac{{V_f}^* + {V_f}^i}{2} \boldsymbol{N} * \boldsymbol{dt} \qquad (2.32)$$

Where ${X_P}^i$ – coordinate of the tool tip point, *Vf* – feed speed, *N* – tool revolution, $\Delta l^{i,i+1}$ - displacement of the tooltip between two postures.

The authors concluded that the most significant cutting parameter was feed rate, which highly affected surface peak distribution. The tool tilting angle mostly affects the surface height deviation S_Z. Other surface parameters were also affected [94]. Again the authors considered an ideal machining process, without errors made by tool run-out, deflection or wear.

In their paper, I. Buj-Corral et al. [86] proposed a model to describe a laterally machined surface. Fig. 2.13 represents the behaviour of tool run-out and its influence on surface formation. It represents the geometrical calculation of tool center point deviation. Only static geometric factors, due to the workpiece–tool intersection, as well as tool grinding errors, eccentricity and helix angle, were taken into account. This approach does not consider vibrational effect.

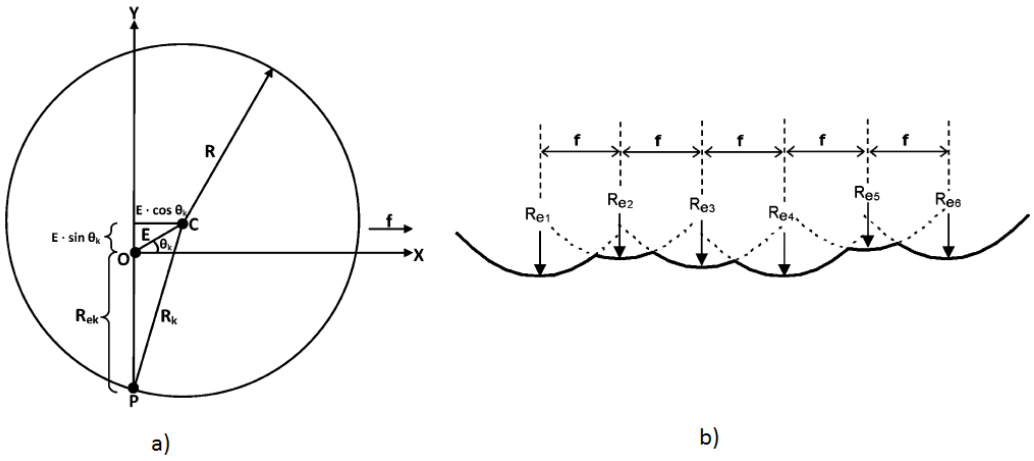

Fig. 2.13. Geometric representation of tool eccentricity (a) and this error's influence on a laterally machined surface (b) [86]

Where *C* - is the geometric center point of the milling tool, *O* - is the rotation centre and *P* the instantaneous position of tooth *k* end point, *f* represents the cutting feed rate and Re_i – represents rotation radius performed cutting depth made by each cutting edge. The results showed that increasing tool eccentricity or grinding errors leads to an increase in the effective radius in some cases. This could decrease the cutting marks left on the surface after one full tool rotation. Due to the helix angle, the surface profile changed along the tool height.

A geometrical approach without dynamics or system deformation was also used by A. A. Duroobi et al. [95]. Their approach was similar to previous authors, where scallop height was used as a descriptive parameter. They used three types of cutters to calculate scallop height – ball end, flat end and torus cutter. All types of cutters were used to calculate surface scallop height value by different cutter profile: flat, concave, inclined and convex plane. In this case, only the tool radial depth of cut parameter was used. In combination with tool geometry, it directly influences scallop height. In this case, it is not correct to talk about the surface topography, because compared methods were generally used for different machining stages – flat-end for rough milling of inclined surfaces, but ball-end milling for finishing operations. However, the ball-end milling model can be applied for surface topography analysis. Therefore, a torus type cutter provides the lowest surface scallop height due to its geometry. Combined with the correct inclination compared to the surface, the scallop height can be decreased to minimum. Otherwise, important dynamic factors and tool errors were not considered in this research due to the application, probably for rough machining stages. [95]

To summarize:

From the expertise of the researchers reviewed above, the author can conclude that cutting tool geometry has an important influence on the surface roughness and topography formation process. The bottom edge geometry, cutting tool run-out and tool axis inclination performs the basis of surface topography formation.

The different combinations of these parameters are well-known for a number of the authors reviewed. In general they use two kinds of geometrical approximations – with and without a dynamical effect. In a number of cases, with the ball-end milling tool, tool motion geometry was used to predict cusp formation. Tool static geometry errors, such as radial and axial run-out, were considered. In cases with laterally machined surfaces, the authors generally used tool run-out, tool axial mounting error and eccentricity.

The common aspect for all of these models is the importance of using the same cutting conditions, such as feed per tooth, cutting tool angles and tool run-out variables. But, another important factor in cutting process is lacking - dynamical system behaviour, which affects chatter formation.

As mentioned previously, a number of researchers included the dynamical properties of the cutting system. Excited vibrations due to cutting forces are one of most representative types of vibrations in the cutting process. Instead of these excited vibrations, other type of vibrations exist in the cutting process due to cutting system stability – chatter vibrations and natural frequency vibrations. The effect of these vibrations will be considered in papers described in the next section. Tool axial deformation, caused by tool natural frequency vibrations, will be introduced in the researchers' mathematical models, as well as important factors affecting the local surface topography height deformation.

2.2.2. Vibration model

As presented above, numerous authors have considered cutting system dynamics in their geometrical models. More specifically, tool displacement against material due to vibrations caused by irregular cutting forces and due to whole system vibration. In the milling process, there are forced and regenerative types of vibrations. Forced vibrations cause instant tool deflection. Regenerative vibrations appear when the cutting system cannot follow the system dynamics due to imposed cutting vibrations. These vibrations should be absolutely avoided, because of their influence on surface roughness [96]. A depth study of cutting dynamics was initiated by Y. Altintas et al. [97]. In their paper they analyzed the dynamical models of different authors. A dynamical model with two degrees of freedom is presented in Fig. 2.14. This figure represents the typical mass-spring-damper model in a 2-axis cutting system. Vibrations on both the *X* and *Y* axes affect the laterally machined surface topography mark formation.

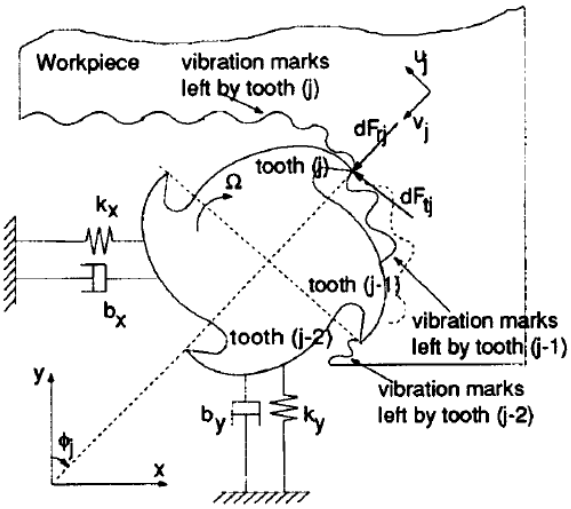

Fig. 2.14. Dynamical model of the cutting system with two degrees of freedom [97]

In this figure, k_X and k_Y are spring coefficients on *X* and *Y* axis accordingly, but b_X and b_Y are damping coefficients. Due to the dynamics acting on the cutting process, the chip load and cutting forces during tool radial depth of cut reveal dynamical behaviour. Dynamical tool displacement affects surface formation and cusp height on the laterally machined or ball-end milled surface. The same peak distribution is affected on a flat-end machined surface. Furthermore, dynamical cutting forces directly influence tool deflection.

$$\boldsymbol{h(\phi_j) = \left[s_t \sin(\phi_j) + (v_{j,0} - v_j)\right] g(\phi_j)} \quad (2.33)$$

Where $h(\phi_j)$ – chip load, s_t – feed per tooth, v_j, $v_{j,0}$ – dynamical displacement of the cutter at previous and present tooth period and $g(\phi_j)$ represents the contact of the tool with material $g(\phi_j)$ =(1/0).

Due to the change of the parameters over time and angular frequency, the dynamic cutting force is calculated by the following equation:

$$\{\boldsymbol{F(t)}\} = \frac{\mathbf{1}}{\mathbf{2}} \boldsymbol{a} \times \boldsymbol{K_t}[\boldsymbol{A_0}]\{\Delta(\boldsymbol{t})\} \quad (2.34)$$

Where A_0 - time invariant, but immersion dependent directional cutting coefficient matrix, K_T – tangential cutting coefficient and Δt – time increment. [97], [98]

Calculation of the dynamical displacement is based on the second-order differential motion equation:

$$\boldsymbol{m x''(t) + c_x x'(t) + k_x x(t) = \sum_{j=1}^{N} F_{xj}(t)} \quad (2.35)$$

Where *m* – mass of system, c_x – damping coefficient, k_x – spring coefficient and F_x - applied force.

This research mainly focuses on analyzing the process dynamics, but could it also be applied to the analysis of surface topography? Since it occurs when a machining process is unstable, it is important to select process parameters that promote stability [99].

D. K. Baek et al. [100] sought to develop a dynamic surface roughness model for face-milling by considering the static and dynamic characteristics of the cutting process. Cutting conditions were combined with geometric particularities, including each cutting edge run-out. Relative displacement from forced vibrations in feed direction may affect tool radial run-out error. This error affects the depth of cut in the axial direction. The authors did not consider forced displacement normal to the feed rate. They modelled the milling system as a system of one degree of freedom (Fig. 2.15)

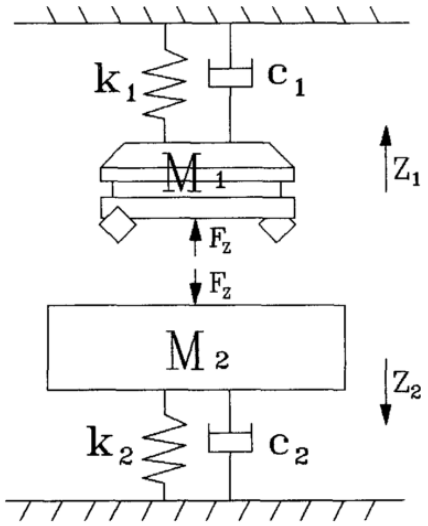

Fig. 2.15. Dynamical model of the face milling operation [100]

Where k_1 – spring coefficient of cutting tool, c_1 – damping coefficient of cutting tool, M_1 – mass of the cutting tool, F_z - cutting force, k_2 – spring coefficient of milling table, c_2 – damping coefficient of milling table and M_2 – mass of the milling table.

The results of this simple model provide basic conclusions that the dynamic model can be applied to predict more accurate surface roughness, and in combination with feed rate, is changing the topography point of view. However, the authors concluded that particular cutting edge run-out values affect surface formation more than the system's dynamic behaviour.

A similar approach, with a similar result, was taken by S. Zhenyu et al. [101]. But what happens if the system is not as rigid as in this case?

H. Paris et al [99] confirmed that in the case of end milling being used to machine a lateral surface, the dynamic behaviour of the same, one degree of freedom system, became more important. Their approach was similar to the previous one, only dynamical behaviour was considered in the tool, not in the workpiece. They concluded that chatter vibrations were one of the most important factors, when the machining system was not rigid enough. Therefore, it is

important to select appropriate cutting speeds, to beware of the tooth passing close to the natural frequency of the system.

H. Paris et al. [96] conducted a numerical and experimental study of the dynamics of flank milling operations at low cutting rates. It focused on both properties of the cutting vibratory phenomena and their impacts on the roughness of the machined surface. Forced vibrations were generated by the periodic excitement of cutting forces, and defined by a period equal to the teeth passing period. In this work, the modelling was based on an approximate calculation of the dynamic uncut chip thickness. A milling operation is stable when the vibrations period is equal to the tooth passing period. In such conditions, the configuration of material removal is the same for each tooth, giving equal cutting forces. The authors confirmed that forced vibrations had low influence on surface roughness, but regenerative vibrations due to instability had a large impact on the roughness [96].

As previously mentioned, three research groups used a rigid tool system where dynamical displacement was applied to the workpiece. S. J. Zhang et al. [102] applied dynamic analysis for micro machining to analyze the cutting process, where machining operated at the micro-scale level. Their model was based on the dynamical behaviour of the cutting tool, restricted to two degrees of freedom. In contrast to the above research, these authors concluded that both synchronous and asynchronous spindle vibrations were relevant for the excitation frequency of cutting forces.

In recent years, few authors have studied the vibrational effect on surface characterization. The same dynamical effect calculation has been used. A. Weremczuk et al. [103] sought to eliminate vibrations during machining process. To analyze the active vibrations, the same concept of dynamical system behaviour was used. Here, the dynamical behaviour is applied to both system parts: tool and workpiece (Fig. 2.16).

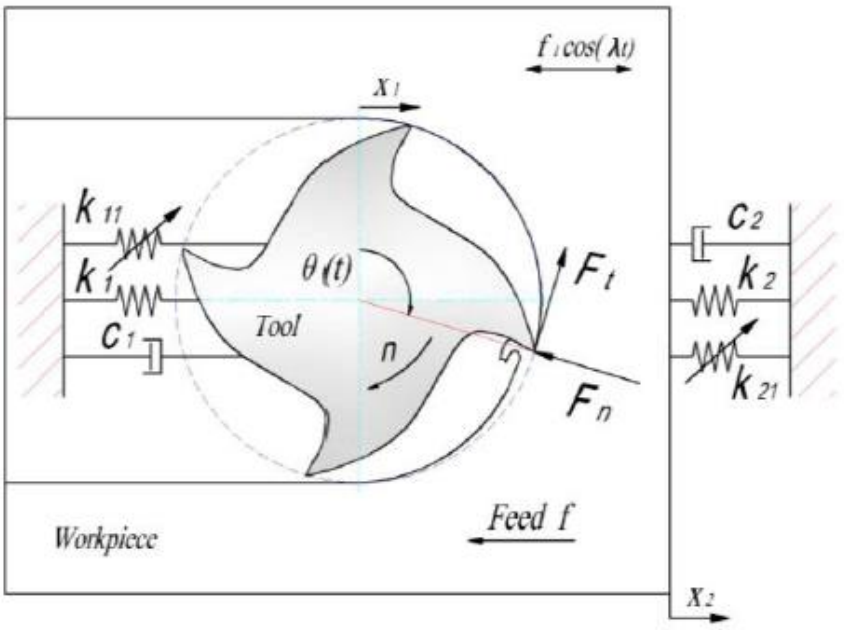

Fig. 2.16. Dynamical model with two degrees of freedom [103]

For the system, two nonlinear differential equations were used. With different damping and spring coefficients, different mass and opposite force vectors were applied. The difference from previous models is in chip load calculation, where uncut chip thickness was calculated by taking into account the dynamical behaviour of both the tool and the workpiece. In addition, harmonic motion was added to control the vibrations.

$$\boldsymbol{w_p(t)} = \begin{bmatrix} \boldsymbol{f + (x_1(t) - x_2(t))} \\ \boldsymbol{-\big(x_1(t-\tau) - x_2(t-\tau)\big) - f_1 \cos(\lambda t)} \end{bmatrix} \boldsymbol{\sin\theta_p(t)} \qquad (2.36)$$

Where f – feed per tooth, X_1 – tool dynamical displacement, X_2 – workpiece dynamical displacement, $\tau = 60/N*z$ – tooth passing period, N – rotation tool speed, z – tooth number, $f_1 cos(\lambda t)$ – active component of external signal, f_1 – amplitude and λ - amplitude. The authors concluded that small real-time vibration reduction could be reached with externally applied vibrations. Together with piezoelectric actuators, this model could be applied in industry. [103].

The latest model that includes the most significant kinematic-geometrical factors was proposed by S. Wojciechowski et al. [104] Research was introduced to combine the influence of cutting parameters, tool static radial run out and deflections induced by cutting forces. This model was presented as a reliable model to predict surface Ra and Rz values. Tool displacement combination by radial run-out and dynamical displacement provided a reasonable result, but the authors mentioned that error value was up to 20% for the Ra parameter and up to 39% for the Rz parameter. They indicated that the simultaneous impact of tool radial run-out and tool dynamical deflection strongly affects surface roughness.

To summarize:

Current theoretical models with dynamical behaviour provide a realistic view of surface topography prediction. At the same time, most of them have insufficient input parameters to provide a complete and accurate prediction of surface roughness. Secondly, most of them were looking at laterally machined surfaces that are easier to simulate due to geometrical particularities. However, even with the most complete simulations, other factors exist that may affect surface roughness formation. They generated differences between model predictions and measured surface topography and roughness parameters. In the majority of the research, the authors claim that more comprehensive research to improve the results has to be performed.

2.3. Conclusions and assumptions about the state of the art

This chapter provides a comprehensive investigation of the methodologies used to predict the surface topography parameters. Two, slightly different models of surface prediction were investigated – Empirical and Theoretical. In Empirical models, researchers apply their measured surface data to "learn" their functions and obtain reliable surface prediction models. Known input factors are coupled with measurements. Then, the surface roughness parameters are recovered. Otherwise, theoretical models were based on tool and cutting process geometry, cutting process parameters and the dynamical behaviour of the machine-workpiece–tool system. From the literature review, the following conclusions can be drawn:

1. Represented models in the literature review are comparable only under the same conditions of unknown process parameters. Obtained results are highly precise for exact cutting systems with selected equipment and its behaviour. In most cases, a model with the same coefficients does not work for another type of machining system, with a different machine, different tool size, etc. Therefore, cutting system behaviour affects the final result.
2. It is beneficial to improve artificial neural network models with data from other machines and systems, but it takes a huge amount of resources.
3. Predominantly these theoretical models are based on theoretical knowledge, physics of machining mechanics and geometry. Any additional research describes a particular cutting process result. Some authors combine process parameters with geometry and dynamical behaviour to predict surface roughness, mostly for laterally machined surfaces.
4. Analysis of previous works provides knowledge about the most important process parameters acting on the flat-end or ball-end milling process. These parameters are initial tool geometry, including tool run-out and tool mounting errors. Under tool mounting errors, the present author understands axial error of chuck and run-out component of chuck.
5. Tool alignment is affected by machine milling head alignment accuracy. It is important due to wear-out of linear guides and milling machine condition.
6. Tool initial geometry and helix angle affect the surface formation process directly and indirectly. Tool geometry errors, tool radial and also axial run-out have an important role in

the surface formation process. Indirect impact is due to the cutting forces on tool deflection and forced vibrations.

7. Cutting forces and system mass affect the system's dynamical behaviour. It is more important for smaller sized tools or less rigid cutting systems.
8. It is common to combine different approaches, to decrease the error between surface topography measurements and predicted surface roughness values. Anyway, error values in different approaches can be up to 30%. The author of this work concludes that this behaviour is due to the lack of all the most important process parameters in the general model.

There is a solid basis to conclude that the process parameters highlighted here play a major role in the surface formation process and the theoretical approach will maintain a similar accuracy for different cutting systems. Therefore, comprehensive research on a theoretical model with an improved number of input factors should be developed. This research will detect the influence of each of the cutting process parameters on the surface topography formation in the flat-end milling operation. The developed model will include the cutting process parameters reviewed in the literature, such as tool axial deflection, axial and radial run-out, dynamical behaviour, tool mounting geometrical particularities and others that may have an effect on the end milled surface. The same approach was proposed by other authors. Therefore, this methodology could be successfully applied for the more complex, ball-end milling process. To improve the model accuracy, process parameter influence on surface topography formation should be investigated first. It will improve the model accuracy and make it applicable for use with different cutting operations and environment. Simpler cutting conditions only contribute more generally to surface formation. They conceal cutting process parameters that affect the surface formation directly and are not taken into account. These parameters should be highlighted and used for further model development.

3. DESCRIPTION OF THE 3D SURFACE TOPOGRAPHY STANDARD

In the previous chapter, the present author introduced the discussion about term surface topography and surface topography parameters. What is the difference between surface roughness and topography parameters? Surface roughness measurements are defined by ISO 4287:1997 – Geometrical product specification standard. This standard defines 2D surface roughness parameters and measurement terms, usually measured with profilometers in one plane. It characterizes surface roughness only in profile. The obtained roughness image is represented in one plane and does not give researchers the full picture about the surface behaviour. Therefore, surface topography measurements described with ISO 25178:2012 represent surface peak and valley ratios from an area point of view, over the whole measurement area. ISO 25178:2012 - Geometrical product specifications (GPS) standard [105], [106] is the very first international standard to provide detailed specifications and measurement techniques for a 3D surface micro-topography. It covers spatial surface texture parameters, along with their measuring and processing rules. The first areal surface texture measuring instruments were made available around 1987 [106].

ISO 25178 part 2 defines symbols for surface texture parameters that have a prefix of a capital letter S or V, followed by one or several small letters for the suffix [106]. Profile parameters are defined based on either a sampling length or the evaluation length. If a parameter is defined on a sampling length, it is (by default) calculated on each sampling length (ISO 4288:1996) and a mean value is calculated also (the default number of sampling lengths is five). With surfaces and area parameters, the concepts of sampling and evaluation areas are still defined, but the default is one sampling area per evaluation area. This simply means that parameters are calculated on the measured surface without segmenting the surface into small sub-areas that depend on the sampling length [105], [106].

3.1. Height parameter group

These parameters are based on the statistical distribution of the height values along the z-axis over the surface [105], [106]. In surface texture parameter equations, the height function, z(x,y) must be centered. This means that the mean height calculated on the definition area is already subtracted from the heights. This leads to a simplified version of the parameter equations, as you can see in the equation used by F. Blateyron [106].

Root Mean Square Height, S_q

The root mean square height or S_q parameter is defined as the root mean square value of the surface departures, z(x,y), within the sampling area, A.

$$\boldsymbol{Sq} = \sqrt{\frac{\mathbf{1}}{\boldsymbol{A}} \iint_{\boldsymbol{A}} \boldsymbol{z}(\boldsymbol{x},\boldsymbol{y})\boldsymbol{dxdy}}, \boldsymbol{\mu m} \qquad (3.1)$$

Arithmetic Mean Height, S_a

The arithmetic mean height or S_a parameter is defined as the arithmetic mean of the absolute value of the height within a sampling area, A.

$$\boldsymbol{Sa = \frac{1}{A}\iint_A |z(x,y)|dxdy,\ \mu m} \quad (3.2)$$

Where: A – defined area of the reference surface in mm^2; z(x,y) –ordinate value height of the scale-limited surface at positions x and y.

Kurtosis, S_{ku}

The S_{ku} parameter is a measure of the sharpness of the surface height distribution and is the ratio of the mean of the fourth power of the height values and the fourth power of S_q within the sampling area, A. [105], [106].

$$\boldsymbol{Sku = \frac{1}{Sq^4}\frac{1}{A}\iint_A z^4(x,y)dxdy} \quad (3.3)$$

Kurtosis is strictly positive and unit-less, and characterizes the spread of the height distribution. A surface with a Gaussian height distribution has a kurtosis value of three. [106]

Maximum Height of the Surface

The S_p parameter represents the maximum peak height, that is to say the height of the highest point of the surface. The S_v parameter represents the maximum pit depth, i.e. the depth of the lowest point of the surface. As heights and depths are referred from the mean plane and are signed, S_p is always positive and S_v is always negative. [105], [106]. The S_Z parameter is the maximum height of the surface and is the sum of S_p and S_v:

$$\boldsymbol{Sz = Sp + |Sv| = Sp - Sv, \mu m} \quad (3.4)$$

3.2. Spatial parameter group

Texture Aspect Ratio, S_{tr}

The texture aspect ratio parameter, S_{tr} is an important parameter to characterize the isotropy of the surface [106]. S_{tr} is the texture aspect ratio of the surface. This parameter describes the ratio of the horizontal distance of *ACF(tx, ty)*, with the fastest decay to a specified value *s*, to the horizontal distance of *ACF(tx, ty)*, with the slowest decay to *s*, $0 \leq s < 1$ [105]:

$$\boldsymbol{Str = \frac{\underset{tx,ty \in R}{\mathbf{MAX}}\sqrt{tx^2+ty^2}}{\underset{tx,ty \in Q}{\mathbf{MIN}}\sqrt{tx^2+ty^2}}} \quad (3.5)$$

Where: $R = \{(tx, ty): ACF(tx, ty) \leq s\}$ and $Q = \{(tx, ty): ACF(tx, ty) \geq s\}$.

ACF(tx,ty) – autocorrelation function which describes the correlation between a surface and the same surface translated by *(tx, ty)*. It is calculated in the following manner [105]:

$$\boldsymbol{ACF(tx,ty) = \frac{\iint_A z(x,y)z(x-tx,y-ty)dxdy}{\iint_A z(x,y)z(x,y)dxdy}} \quad (3.6)$$

3.3. Functional parameter group

Parameters of this group characterize the surface zones involved in lubrication, wear and contact phenomena.

Valley fluid retention index, S_{vi}

V_v – void volume or volume of voids per unit at a given material ratio is calculated from the areal material ratio "***mr***" curve. The void volume is the volume of space bounded by the surface texture from a plane at a height corresponding to a chosen material ratio "*mr*" value to the lowest valley. "*mr*" may be set to any value from 0% to 100%. [105], [107]:

$$\boldsymbol{Vv(mr)} = \frac{\boldsymbol{K}}{\boldsymbol{100\%}} \int_{\boldsymbol{mr}}^{\boldsymbol{100\%}} [\boldsymbol{Sdc(mr)} - \boldsymbol{Sdc(q)dq}] \qquad (3.7)$$

Where K – a constant to convert to mm/m^2, $S_{dc}(mr)$ – inverse areal material ratio of the scale-limited surface [105], [107].

Summarizing:

In this chapter present author describes the theory of 3D surface topography standard. All of described 3D topography parameters have geometrical relation between others.

ISO 4287:1997 standard represent the surface profile in one plane, with low possibility to derivate areal representation of the measured surface. ISO 25178:2012 therefore represents the whole measured surface behaviour and roughness parameters related with ISO 4287:1997 can be derived from it.

ISO 4287:1997 is a well-known standard for mechanically machined surface quality description in industry. 3D surface topography parameters are selected as an innovative measurement development solution for application in industrial areas. It does not only generate visually easily perceptible representation about general surface formation, inaccuracies and local errors, but also provides information about the surface height in a measured area, represents surface direction and provides broad information about the surface to be analyzed. It could also provide a broader view about the mechanical processes acting at the sample or part machining process, instead of the 2D roughness standard options.

It is important to note that mechanical engineering, and manufacturing industry in general, is very slow and somehow reluctant to accept these standards in their manufacturing processes. Only pressure from the customer and obvious scientific and commercial benefits could speed up this process. This is one of the related objectives of this research.

4. OUTLINE OF THE PREVIOUS WORK AND BASIS OF THE RESEARCH

It is important to note that this research is a logical continuation of the author's Masters thesis [108], where statistical analysis of surface topography was introduced. As mentioned in the Introduction, an idea arose from the mold production industry, to analyze how to decrease surface topography height parameters and increase the quality of machined surfaces after application of HSM. Subsequently, this research was developed to significantly enhance this with the mathematical model of surface topography parameter value detection, considering environmental behaviour, and machining equipment and cutting conditions. Therefore it is important to outline the scope of the previous work, its objectives, methodology and relevant conclusions as well as its relevance to this research. The Masters thesis delivered the first results, which form a sound basis for this research. However, it is evident that comprehensive analysis of this previous work is required. This is explained in detail below.

4.1. Objective of the previous work

The quality of machined surfaces and the machining time are the most important qualities to emphasize the benefits of HSM. Injection mould surfaces are complex surfaces (sculptured surfaces), in which the cutting condition and cutting strategy can imply significant differences in the machining time. In the entire spectrum of high-speed machining, high-speed milling (HSM) is the leading and most widely used technological process in die and mold manufacturing technology [109]. It is important to note that HSM is envisaged by manufacturers as it leads to a significant reduction in total cutting time. It has been established that most benefits are achieved if this technology is prioritized for operations in which a major proportion of time is taken up by cutting. Non-cutting time and various other factors are nevertheless important considerations in the overall assessment of the benefits of HSM for a particular application [109], [110].

In order to quantify the quality of the machined surface, roughness measurements are needed. The main goal of previous work was to establish the relation between High Speed Milling technological parameters and surface topography measurements according to the ISO 21478:2012 standard.

4.2. Applied methodology of previous work

An experimental approach was used to detect the cutting condition influence on surface topography parameters. The set of experiments was defined: the most relevant cutting technology parameters were modified in order to establish their effect on surface roughness. Experiments were conducted and the machined surface was measured with a Taylor Hobson Intra 3D topography measurement device. ANOVA – Analysis of variance investigation provided the necessary information to decide which of these technological parameters to take into account for in-depth analysis [110], [111]. The result of this methodology is knowledge about the selection of cutting conditions in high-speed milling. [108], [112]

Cutting conditions were selected as input factors in this Masters thesis [108]. For die and mould manufacturing, applicable steel alloys and titanium were selected. Selected material types and their chemical and mechanical properties are represented in Table. 4.1.

Table 4.1. Experimentally selected sample material specifications [110]

Material	***DIN name***	***Chemical composition***	***Tensile strength - Yield strength - Elongation – Hardness***
Mould Steel 1.1730	C45	0,45C – 0,27Si – 0,7Mn	640N/mm2 – 340N/mm2 – 20% - 190HB
Mould Steel 1.2312	40 CrMnMo S 8-6	0,4C – 0,4Si – 1,5Mn – 0,03P – 0,08S – 1,9Cr – 0,2Mo	990N/mm2 – 860N/mm2 – 15% - 280-325HB
BT1-0 Grade 2	Unalloyed titanium	(maximums) 0,18Fe – 0,07C – 0,1Si – 0,04N – 98,61/99,7Ti – 0,12º - 0,01H – 0,3 impurities	400-450N/mm2 - 300-420N/mm2 – 30% - 210HB

Selected types of steel alloys have different chemical compositions and therefore, different machining behaviours. Additionally a third material, commercially pure titanium, was chosen to observe relevant tendencies, due to known difficulties with titanium machining and its chemical-mechanical properties.

Customized machining trials were prepared. Each material was divided into 16 sample parts. Each sample was machined with a specific combination of technological parameters, as listed below in Table 4.3. The chosen technological parameters and conditions are outlined below.

The high-speed milling machine GENTIGER GT-66V-T16B HSM was used to produce the samples. The milling machine's technological parameters, such as machine type, spindle speed r/min, motor power, machine dimensions and even chuck cone standard value are presented in Table 4.2. The machine was equipped with a Siemens 840D NC controller and BT-40 cone-type spindle.

Table 4.2. GENTIGER GT-66V T16B technical specification

Type	T16B
Spindle speed, r/min	16000
Motor power, kW	26
Axis movement (x,y,z), mm	1000*550*500
Rapid feed rate, m/min	30
Cutting feed rate, m/min	20
Spindle cone standard	BT-40

Fig. 4.1. GENTIGER GT-66V T16B milling machine

Ball-end milling tool – MITSUBISHI type VC2ESB made with ultra-micro-grain carbide; its ball nose radius is 4mm, coated with Al, Ti and N, it has two teeth and a 30º helix angle. The tool was operated with its axis at 90º to the work surface. This type of tool is a commonly applied cutting tool in mould manufacturing, where sculptured surfaces have to be machined. It is designed for hardened steel processing. The working radius of the cutting tool is suitable for machining tiny cavities on mold surfaces. It has a wide application in mould manufacturing.

Cutting speed and depth – Cutting depth was selected in accordance with finishing conditions and cutting speed. The recommended cutting speed for selected tool/material combination is 150 m/min. To ensure finishing conditions, a low cutting depth and high spindle speed should be maintained. The samples were machined with a 0.3 mm cutting depth. To maintain the defined cutting speed, the spindle speed at the selected cutting depth was set to 15,707 r/min.

Milling mode – UP and DOWN milling modes were used. In real mould machining situations, the cutting tool continuously follows the path of the CNC program and the milling mode is constantly changing. From conventional milling it is known that the milling mode affects surface formation and the dynamics of the cutting system. Therefore, both milling modes were selected for analysis during the sample execution.

Path or cutting strategy – in continuous mould manufacturing operations, cutting strategy is one of most important factors to save machining time. In continuous machining, the path changes frequently, sometimes overlapping an already machined area. This is why three different kinds of cutting strategies are selected to compare.

- Linear Path (LP), the tool cuts in one way and in one pass-direction – see Fig. 4.2(a);
- Circular Path (CP), the tool follows a spiral path from the centre to the outside – see Fig. 4.2(b);
- Two Linear Paths (TLP), combines two orthogonal Linear Paths. Fig. 4.2(c). One along the X axis and the other along the Y axis, without changing the step depth.

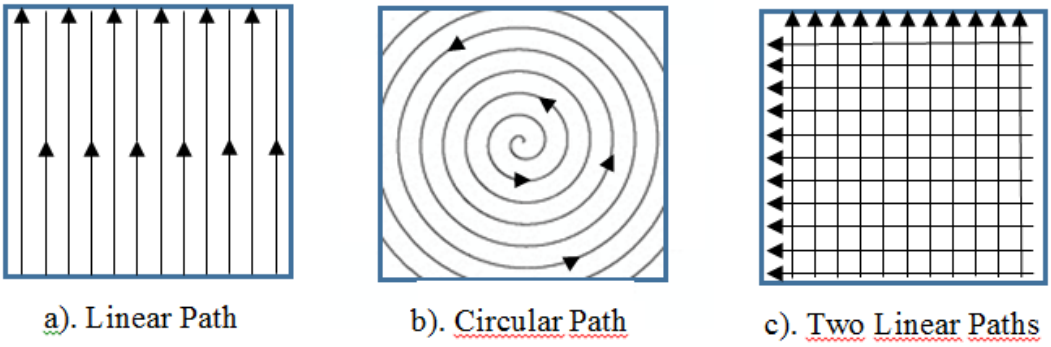

Fig. 4.2. Milling tool movement strategy over the sample surface

Feed rate – three different feed rates were selected – 0,08, 0,2 and 0,4 mm/tooth. When planning the experiment, the tool manufacturer's recommendations were followed, thus a constant three feeds per tooth were selected and maintained. From conventional cutting, cutting feed rate is directly related to cutting forces. If the surface topography formation has a direct geometrical influence on feed rate, these changes should be represented by the different feed rates.

Radial cutting depth is parameter that determines how much the cutting tool covers the width of the previous stroke. For current experiment were chosen following values of radial depth - 0,1mm and 0,05mm. Theoretically, like the feed rate, it has to be directly related to surface roughness (see Fig. 4.3). Cutting tool radius and radial cutting depth interaction forms the surface cusp heights. The smaller is tool radial cutting depth a_e, the lower the cusp height should be.

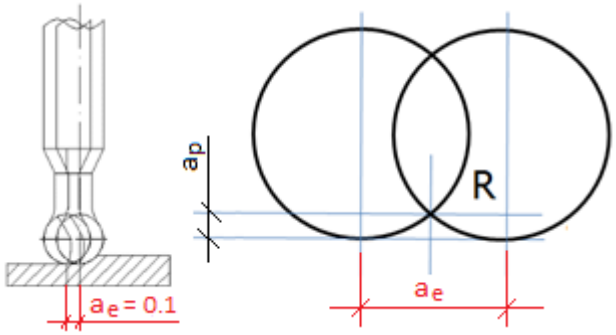

Fig. 4.3. Radial cutting depth performed by the milling tool

All the highlighted factors were used to develop 48 subsamples with different combinations of the selected cutting conditions. The experiment design is represented in Table 4.3.

Table 4.3. Cutting conditions used in the Masters thesis research [110]

#	Tool	Depth (mm)	Path	Radial depth of cut (mm)	Spindle (min^{-1})	Feed (mm/tooth)	Milling mode
1	3-VC2SB	0,3	LP	0,1	15707 – 3666 (Ti)	0,08	up
2	1-VC2SB	0,3	LP	0,1	15707 – 3666 (Ti)	0,2	up
3	2-VC2SB	0,3	LP	0,1	15707 – 3666 (Ti)	0,4	up
4	1-VC2SB	0,3	CP	0,1	15707 – 3666 (Ti)	0,2	down
5	2-VC2SB	0,3	CP	0,1	15707 – 3666 (Ti)	0,4	down
6	2-VC2SB	0,3	LP	0,05	15707 – 3666 (Ti)	0,4	down
7	3-VC2SB	0,3	LP	0,05	15707 – 3666 (Ti)	0,08	down
8	1-VC2SB	0,3	LP	0,05	15707 – 3666 (Ti)	0,2	down
9	3-VC2SB	0,3	CP	0,05	15707 – 3666 (Ti)	0,8	down
10	1-VC2SB	0,3	TLP	0,1	15707 – 3666 (Ti)	0,2	down-up
11	2-VC2SB	0,3	TLP	0,1	15707 – 3666 (Ti)	0,4	down-up
12	1-VC2SB	0,3	CP	0,05	15707 – 3666 (Ti)	0,2	down
13	2-VC2SB	0,3	CP	0,05	15707 – 3666 (Ti)	0,4	down
14	3-VC2SB	0,3	TLP	0,05	15707 – 3666 (Ti)	0,08	down-down
15	1-VC2SB	0,3	TLP	0,05	15707 – 3666 (Ti)	0,2	down-down
16	2-VC2SB	0,3	TLP	0,05	15707 – 3666 (Ti)	0,4	down-down

Three additional cutting tools were used in the experiment. Each of the tools was used for a separate level of cutting feed rate to machine the material. This tool selection ensured that the same chip flow speed was maintained against the cutting surface, as well as the same characteristics of tool wear during the cutting process. 1-VC2SB, 2-VC2SB and 3-VC2SB represent the tool order used for the milling experiments. The number represents the tool in order

of use. VC2SB – represent the tool coating type, as described above according to the manufacturer's product catalogue. The milling mode in the table above represents up-cutting (UP), or down-cutting (DOWN), or both milling modes used with the TLP cutting strategy type.

Statistical analysis of how the surface topography correlates with the technological cutting conditions was undertaken using IBM SPSS and Excel software. ANOVA analysis was performed with the Rcommander software tool.

4.3. Results of previous work with relevance to this research

Visual analysis of measurement images was undertaken, to detect the errors and particularities on it – Fig 4.4.

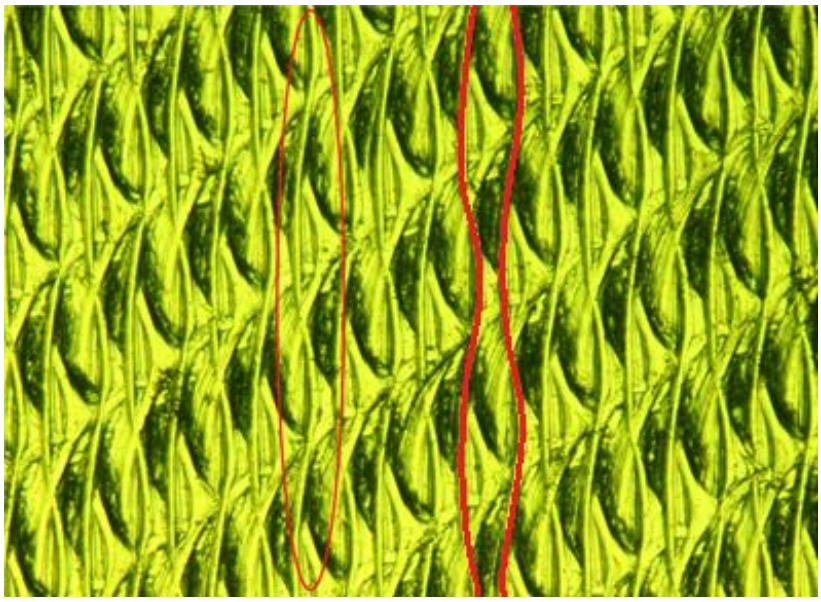

Fig. 4.4. Surface topography image – Sample #19.

With increased feed speed, the surface image reveals marks left from both cutting edges. With decreased feed rate, at a certain point the mark from a specific cutting edge tends to disappear due to the tool radial run-out component. At the same time, at the high feed rate an oscillating line can be observed (encircled in red in Fig. 4.4), to the left of the tool center point, due to possible tool deflection. As will be concluded later, deflection is one of the most important process parameters acting in high-speed milling. [113]

Surface topography measurements reveal a number of different topography parameters related with the ISO 25178:2012 standard. Each of them has its own application. For instance, leaks of the fluids between two mating surfaces can be described by the Texture spacing (Rsm) parameter. Surface texture parameters such as Summit Density (Sds) and Summit Curvature (Ssc) help quantify surface asperities. Peak Heights, Valley Depths, spacing and other bearing area related parameters (Spk, Sk, Svk) can be specified to control production processes and optimize friction characteristics [114]. However, there are parameters that best characterize the

machined surface in general. The surface topography parameters were chosen by selecting the most correlative topography parameters that may represent the surface topography from the measurements, represented in Table 4.4. Pearson's Correlation matrix analysis method was used [115]. This method compares the results of all the measurements between each other and represents the most significant correlation.

Table 4.4. Pearson's correlation matrix of surface topography parameter values

Parameter	Sa	Sq	Sku	Str	Svi	Sdr	S_z
Sa	1	,993**	-,566**	-,040	-,162	,636**	,818**
		,000	,000	,386	,116	,000	,000
Sq	,993**	1	-,538**	-,065	-,182	,637**	,816**
	,000		,000	,317	,090	,000	,000
Sku	-,566**	-,538**	1	,029	,098	-,261*	-,398**
	,000	,000		,417	,237	,026	,001
Str	-,040	-,065	,029	1	,922**	,141	-,036
	,386	,317	,417		,000	,150	,397
Svi	-,162	-,182	,098	,922**	1	,166	-,108
	,116	,090	,237	,000		,111	,215
Sdr	,636**	,637**	-,261*	,141	,166	1	,572**
	,000	,000	,026	,150	,111		,000
S_z	,818**	,816**	-,398**	-,036	-,108	,572**	1
	,000	,000	,001	,397	,215	,000	

**. Correlation is significant at the 0.01 level (1-tailed).

*. Correlation is significant at the 0.05 level (1-tailed).

Table 4.4 represented colors: 1st – Most correlative, 2nd – Second correlative parameter, 3rd – Third correlative parameter.

As represented in Table 4.4, the most correlative parameters, mostly used in the research methodology and scientific literature, are arithmetic mean height – Sa and root mean square height – Sq. They correlate with ¾ of the other parameters. Both of them describe surface height variability over the defined surface area. Geometrical formulation can be applied to express them. But S_z parameter is only one which directly represents the surface topography height parameter changes, not an approximation over the defined area. From this parameter, all other surface topography parameters could be derived. As represented in the correlation matrix, this parameter is the 3rd most correlative parameter calculated with Pearson's coefficient correlation matrix. This parameter represents the surface maximum height. The surface topography zero point – best fitting plane (or sphere) is the point from where the surface topography peak height and valley depth have been measured. This, together with the surface absolute height parameter,

will give the user the knowledge to calculate other, more widely applicable 3D surface topography parameters. In the earlier standard ISO 4287:1997 [27] knowledge referred to *Rz* as an average of the 10 highest to 10 lowest points and other variations. The ISO community agreed for the newer standard, ISO 25178-2 to establish S_Z as precisely the peak to valley height over an area measurement [110], [116]

More specifically, this research covered multifactorial analysis of the following factors: feed rate, manufacturing strategy, radial cutting depth and material influences on the most characteristic 3D surface parameters. The plot of means for the cutting feed factor's influence on the topography parameter S_Z on different material types is represented in Fig. 4.5.

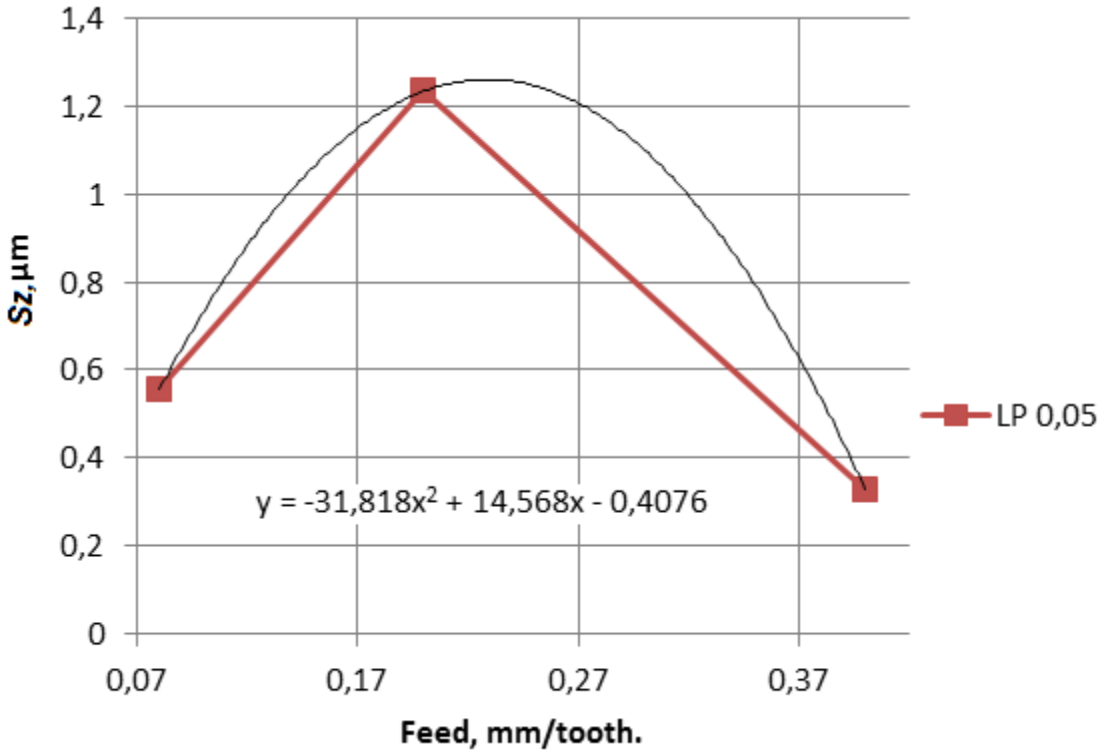

Fig. 4.5. Plot of means for parameter S_Z for feed rate and material influence [108]

The overall results were based on ANOVA – Analysis of Variance, where differences between different factor (e.g. material, path and feed rate) groups of means were analyzed using a range of statistical models (Fig. 4.6) [108]. Also, regression models were obtained, considering the input parameters and detecting empirical models of surface parameter dependence [110], [111], [113]. In the analysis, software numerical values of the cutting conditions were converted into factorial values. In the plot of means (Fig. 4.6), cutting conditions such as feed speed were converted into the levels: LOW (0,08 mm/tooth), MEDIUM (0,2 mm/tooth) and HIGH (0,4 mm/tooth) and analyzed with the ANOVA method. Results of this analysis represent the most

and less significant factors acting in the HSM cutting process with the ball-end milling tool on hard-to-cut materials.

```
> Anova(AnovaModel.122)
Anova Table (Type II tests)

Response: Sa
                          Sum Sq Df F value   Pr(>F)
Materials                 0.8020  2  2.0741 0.150658
Padeve                    0.1556  2  0.4024 0.673734
Strategija                3.1953  2  8.2632 0.002253 **
Materials:Padeve          1.6943  4  2.1907 0.105097
Materials:Strategija      0.3079  4  0.3982 0.807690
Padeve:Strategija         0.2050  4  0.2651 0.897073
Materials:Padeve:Strategija 0.2155  8  0.1393 0.996284
Residuals                 4.0603 21
---
Signif. codes:  0 '***' 0.001 '**' 0.01 '*' 0.05 '.' 0.1 ' ' 1

> tapply(PAMATDATI$Sa, list(Materials=PAMATDATI$Materials,
+    Padeve=PAMATDATI$Padeve, Strategija=PAMATDATI$Strategija), mean,
+    na.rm=TRUE) # means
, , Strategija = Lineara
```

Fig. 4.6. ANOVA analysis with Rcommander – Material, Feed and strategy factors [108]

4.4. Conclusions of previous work

After the visual analysis, correlation matrix and ANOVA analysis were performed, the following conclusions were drawn.

1. After visual analysis, it was concluded that milling mode (UP or DOWN) has the same importance as cutting feed rate.

2. ANOVA analysis demonstrates that the cutting strategy affects the surface topography formation in most cases, where the two-level cutting strategy (TLP) was applied. This behaviour appears due to insufficient cutting depth and the cutting tool geometry. The cutting edge radius is higher than the chip thickness, therefore the surface was more rolled-up than cut.

3. Material type affects the surface topography formation due to different mechanical properties. Results show that the behaviour between DIN 1.1730 and DIN 1.2312 is not so different. A difference appears when Titanium material was used in the cutting process. Cutting forces during the cutting process increases and surface topography parameters slightly increase also. Material type and feed factor, both affect cutting forces and have a direct effect on cutting process, so, these are impact cutting process parameters. Therefore material properties and cutting system properties are changing in

the cutting process due to vibrations, temperature etc. factors. These factors should be detailed and investigated.

4. Cutting feed and milling mode, as well as cutting tool radial cutting depth, are the next most important factors for surface topography height formation, especially for the parameter S_a. Furthermore, there appears to be an influence of insufficient cutting parameters, when the cutting process is masked with plastic deformation due to a low feed rate or radial cutting depth value.
5. Empirical analysis of simple input parameter influence was not sufficient to describe all of the factors at work in the machining process. The results of ANOVA analysis of various input parameter combinations provide different results. Another type of methodology based on a theoretical approach should be investigated to detect the process parameter influence on surface topography parameters.

Considering all of the above, it was decided to perform more complex analysis of cutting process parameters, working on the milling process. These parameters affect the surface topography formation directly or indirectly as a result of the applied cutting conditions. These parameters depend on the combination of cutting regimes, material type, tool and machining center conditions. In general, these parameters depend on the whole machining system. Furthermore, cutting with a ball-end milling tool, due to its geometry and behaviour in the cutting process, as used in the previous research, is too complex to be analyzed directly. It was decided to select a more conventional shaped cutting tool to develop the analytical model and afterwards transfer this model for application with ball-end milling tools.

In the next chapter, the author will start to divide up the most representative factors and combine them into groups, to develop a unified mathematical calculation model for the surface topography parameter S_Z value calculation.

5. RESEARCH METHODOLOGY

5.1. Introduction

The research methodology chapter briefly describes the methodology used to arrive at a reliable surface topography prediction model. In his Master's thesis the author set up a new task to perform a more complex analysis of cutting process parameters and to develop a unified mathematical calculation model for the surface topography parameter S_Z value calculation. The proposed surface topography model will be a combination of factors acting on the surface machining process. Correct drafting and the appropriate selection process of these factors play an important role on the whole model development. The research methodology chapter describes the methods used to develop and improve the prediction model. The research methodology consists of several development sections, where a separate goal for each has to be fulfilled. The research strategy describes the subject of the study, high-speed, flat-end milling surface topography measurements. The research method and approach contains a description of the necessary research work to be undertaken, following on from the results of the literature review, to the final conclusions of the study subject. This work contains an analysis of the literature, data collection and treatment methods, the selection of samples, research process description and type of analysis used for data treatment. Finally, the overall result of this methodology is the mathematical prediction model to describe the surface topography height value, for industrial use. Each of these steps is described below.

5.2. Research strategy

In this case study, the simplest procedure to perform the high-speed machining operation and do the reliable data analysis, based on the topography measurement results, is the high-speed flat-end milling operation. The surface topography measurements of flat-end milled surface topography measurements were selected as for study. They represent the cutting system behaviour in the best way, representing every change in the cutting system behaviour. The cutter is aligned perpendicular to the machining surface. Simple geometrical shapes must represent each of cutting tool deviations and cutting system inaccuracies, as well as the basic cutting tool geometry's influence on the surface topography formation. Each of these factors performs the surface topography. The result of this research aims to develop the mathematical surface topography prediction model with a high degree of accuracy, so that it can be applied to various milling procedures and processing phases. This model has to be translated to apply it for more complex shape cutting tools, used in die and mold manufacturing process.

5.3. Research method and approach

Several experiments with different process parameters were performed beforehand. The research method involves qualitatively and quantitatively analysing the collected data from the surface topography measurements. The methodology developed for this work is iterative and has

an incremental sequence. The incremental and cyclic approach is represented in flowchart below (Fig. 5.1).

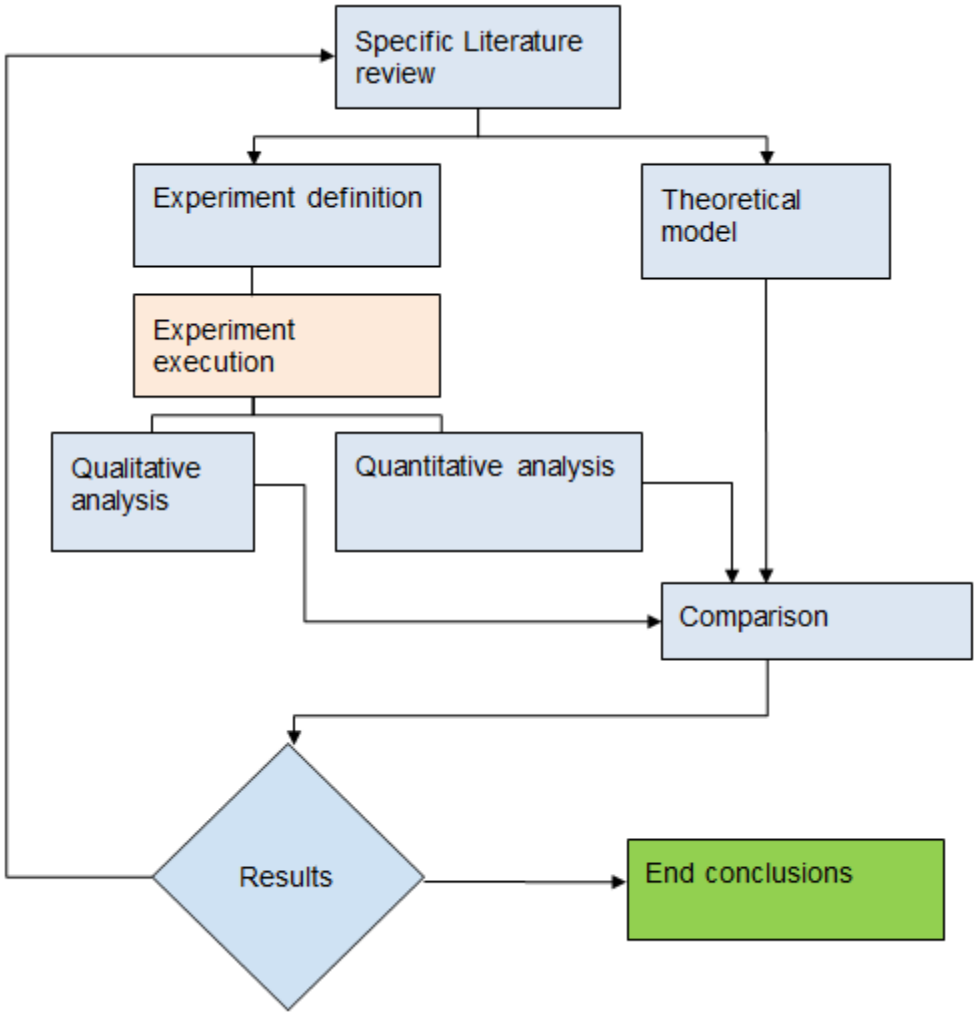

Fig. 5.1. Incremental and cyclical sequence research methodology flowchart

- The first step is a literature review specifically about the work and conclusions of other researchers. The results of this literature review helped us to understand the problems reported by other authors, the scientific challenges and achievements in this field of surface topography at HSM research;
- Theoretical prediction models are the logical outcome from this literature review. A number of theoretical surface topography and roughness prediction models have been developed by other authors, but each of them contains inaccuracies or disadvantages. A logical follow-up of this work is a new prediction model development, considering the most common methods reviewed in the specific literature and considering the geometrical interpretation of the cutting tool movement.

- From the literature review, the actual weak points of the proposed prediction model will be identified. Based on them, new experimental work will be defined. The most important cutting parameters, selected after the literature review, will be under scope. These parameters were selected for experimental execution and cover the main parameters required for general surface topography mathematical model calculation.
- The experiment is then carried out. The samples established in the experiment's definition are machined and measured, to obtain their 3D surface topography. The measured surface topography raw data is analyzed and filtered. The initial filters of raw data help to isolate random excessively high peaks and valleys, as well as to interpolate undetected data points.
- Qualitative and quantitative evaluation methods are acceptable for measurement data analysis. Qualitative analysis is undertaken in the form of visual data validation, such as the analysis of surface topography images, microscope images, tool wear, etc. Quantitative analysis can be applied to the 3D surface topography measurement data, to prove their reliability for the task. Both methods will be used in this research.
- The next step is to compare the experimental results (obtained from the analysis) and the theoretical model prediction, to identify the cutting system behaviour from experiments that is not included in the theoretical model. These unpredicted behaviours require updating the model, taking into account new inputs, not reviewed yet with the model.
- From this point, the cycle starts again with a new specific literature review about the analysis of new variables impacting the end-milling process. The theoretical model is refined, including the effect of additional inputs, and new experiments are designed. The designed experiments must allow controlling the new inputs. After the experiment is performed, further qualitative and quantitative analysis is carried out. The analysis results are once again compared with the theoretical model to detect the differences and cycle starts again.

Every new set of experiments has been based on the results of the previous analysis. Basically, this type of cycle is infinite, until 100% correlation is achieved.

5.4. Data collection and treatment methods

The basic quantitative method for collecting data from experiments has been 3D surface topography measurement. From the topography measurements, the surface roughness parameters for analysis are calculated and processed. In this subchapter, we will describe two methods available and widely used for surface topography measurement. Each of them has some flaws, but some can be enhanced with mathematical approximation capabilities. The surface topography measurement method and correct data treatment is a crucial part of the data collection procedure for this PhD.

5.4.1. Surface topography measurements

During the research process, two different types of 3D surface topography measurement methods were used. The first experimental sample measurements were conducted by means of the contact method. The equipment used was the Taylor Hobson Talysurf Infra 50 3D surface topography measurement device, see Fig. 5.2. This device uses a needle that crosses the surface on parallel paths, recording the peaks and valleys. The restrictions of this machine are the size of the needle and the minimum resolution of measurements. If the needle cone size is higher than the error or valley of the surface, the measurement cannot be carried out properly. A typical stylus measurement arm of the Talysurf Intra 50 3D measurement device is a 90° conisphere diamond with a 2 μm needle tip point radius. [116] Secondly, accurate measurements take a lot of time. Even up to 6 hours can be necessary for one measurement. Advantages and drawbacks of contact measurements method are collected in Table 5.1.

Table 5.1. Advantages and disadvantages of contact method

Advantages	Disadvantages
All measured points are recorded	Relatively low resolution
Stable and tested method	Slow measurements
Widely applied on industry	Wear parts of measuring device
Surfaces of non-reflective materials can be measured	High vibration influence on surface measurement

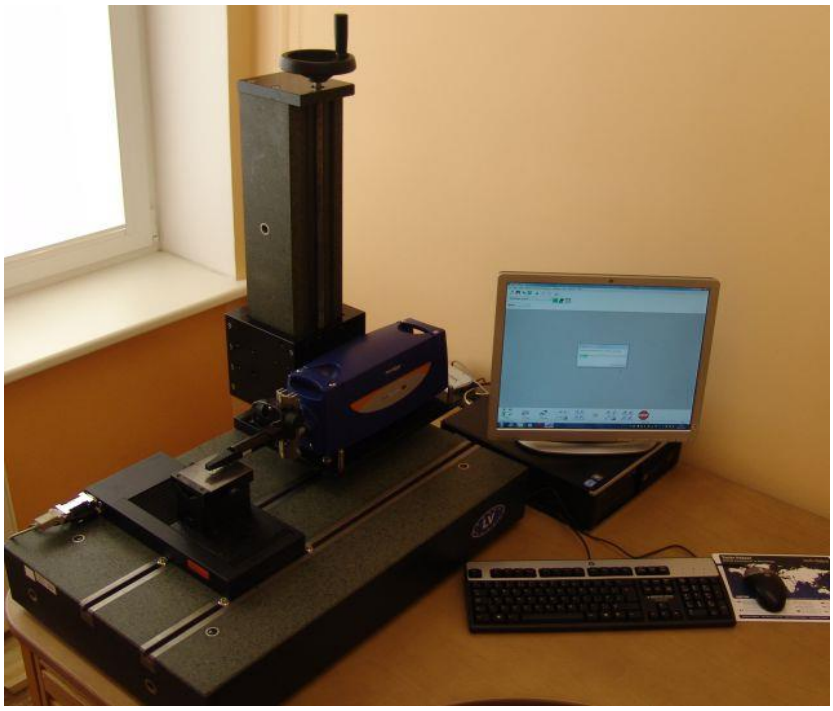

Fig. 5.2. 3D surface topography measurements with Talysurf Intra 50 contact measuring device

The other experimental samples' surfaces were measured with an optical surface topography measurement device (Fig. 5.3). In this type of measurement device, the measurements are based on light reflection from the base surface by calculating the distance between the light source and the surface. Measurement devices based on this technique are quicker than contact devices, and so the time taken for measurement process is shorter. The measurement time is up to 200 times faster than the contact one.

However, some problems may appear, due to absorption or incorrect reflection of the measurement light. Some sample points could not be measured because: a) the light is not reflected against the camera matrix; b) the light is absorbed on the surface and not reflected; c) the reflection intensity is too high and the camera matrix cannot distinguish each data point separately. In these cases, unmeasured points in the data file were generated as NA points, where data is not available. The advantages and drawbacks of the optical measurement method are summarised in Table 5.2.

Table 5.2. Advantages and drawbacks of the optical method

Advantages	Disadvantages
Fast measurements	Inside surfaces cannot be measured within standard equipment
High resolution of measurement	High error possibility of non-reflected light from surface
Low environmental influence	Possibility of representation errors

FIG. 5.3. 3D surface topography measurements on the Bruker Contour 3D optical measuring device

3D surface topography measurement methodology with Optical and Contact measurement techniques:

The topography measurement methodology describes 7 points that have to be considered when taking the surface topography measurements with the optical measurement device. All 3D topography measurements have been taken using the available measuring equipment in the Tallinn University of Technology, Estonia. Before measuring them, all the samples had to be cleaned with paper and alcohol and dust had to be removed with compressed air. The measurement process involves following steps:

1) Preparing the device for 3D surface topography measurements, taking into account the environmental conditions, and calibrating the measurement device;

2) Placing the measurement sample on the measurement table and adjusting its level;

3) Adjusting the measurement device settings for the type of material and surface reflection;

4) Adjusting the cutting direction in accordance with the machine, to ensure the same measurement alignment for all samples;

5) Taking a control measurement, applying the filters and checking the obtained surface parameters;

6) If the control measurement is successful, taking the main measurements. If not, adjusting the machine;

7) Recording all the results in line with the measurement protocol. Saving the obtained data file with the sample numbering, measurement and location numbering.

5.4.2. Surface microscope imaging

After measuring the surface topography, additional surface identification was performed with microscope images, to compare the digital surface interpretation with the real surface topography. The pictures were taken either at Riga Technical University or at the Universitat Politècnica of València. The photos had to be taken with different scales – 50x, 100x and 200x, to analyze the different areas of the machined surface and to measure the distances between the marks left from the tool. The Canon EOS camera and Meiji Techno IM 7200 Trinocular inverted microscope were the tools available for this process. The equipment is illustrated in Fig. 5.4.

Microscope photography is an important tool to support the surface topography measurements, to compare the marks and lines on the surface. It helps to justify the results taken by the topography measurements. The surface topography height cannot be measured from the photos, but the intensity of the surface areas represents and justifies the same surface behaviour as the measurements.

Fig. 5.4. Microscope used to take the surface topography photos

5.4.3. Obtained data management

The surface topography measurement equipment software generates surface topography measurement raw data files. These files contain the measurement area coordinates and height data values. In simple terms, these are pixel coordinates with a surface height value. Measurement data from the measurement device has to be collected in the measurement files and spreadsheets for representative and analytical purposes. Surface topography analysis software converts these raw data files into the surface topography parameters and surface topography images that will be used for the analysis.

The measured surface topography parameters were compared and analyzed using statistical analysis methods. Statistical analysis was performed to detect the influence of technological regimes on surface topography parameters, to approve the measurement accuracy and to confirm compliance of the results from the developed mathematical model. A descriptive statistics correlation matrix, regression coefficient detection and ANOVA analysis are appropriate tools for this analysis.

Descriptive Statistics involves the presentation of numerical facts, or data, in either tables or graphs, and the methodology for analyzing the data. Together with simple graphical analysis, they form the basis of statistical data to describe the reliability of the measurement data. [117 - 118]

Regression analysis provides an objective and systematic way to analyze data. As a result, decisions based on regression are less likely to be subject to bias, they are consistent and the basis for the decisions can be fully explained – and they are generally useful. [118] Regression analysis was used in this research to create a simple regression model for surface topography prediction. It is the most commonly used data approximation model among the various authors in this research field, where data are reliable and there is a fixed, known number of input factors.

To test the hypothesis of the topography parameter influence, the ANOVA method was used. Analysis of Variance (ANOVA) is a statistical method used to test variance of means from the measurements and to test the hypothesis. [119], [109] Initially, multi-way ANOVA data analysis was used to study the most relevant parameters in the results. Values for the parameters to be analyzed (e.g. cutting feed and tool radial cutting depth) were replaced by factors with two or three levels. The series of ANOVA analyses were performed using different combinations of two or three factors. In this analysis, each of the roughness parameters selected were taken as a response variable.

5.5. Selection of significant samples

The machined samples for surface topography analysis were designed to include all the influence factors that potentially affect surface topography formation. A lack of influence factors may affect the result of the mathematical model's accuracy and conclusions of this research project. Therefore, the selected specimen type has to represent these factors. Specimens with opposite cutting directions are the most suitable form of sample design. This sample design includes four cutting directions, different cutting speeds, cutting direction changes, behaviour of milling equipment and radial cutting depth that is equal to the cutting tool diameter.

The systematic probability sampling method [120] was used for surface topography measurement. Surface topography parameters in different cutting tool interaction areas may be different. Surface form errors may differ from sample to sample. It is therefore important to select the same area for measurements from sample to sample. The measurement area and the milling process behaviour should be the same or similar, even if the exact point is not the same.

5.6. Research process description

The results from the statistical analysis of the author's Master's thesis project provided a challenge to investigate surface topography more extensively. The most representative cutting parameters influencing surface roughness are known (feed, speed, etc.). However, using only these parameters, precise roughness predictions cannot be made. Each of the new process parameters added to the topography model had to be tested with the overall model. Some of these parameters could not be measured directly, so the new set of experiments had to be performed to test the newly-developed model and its accuracy. Therefore, it was proposed to build this research process in an incremental and cyclical sequence. The first cycle had to set the basic model of the surface topography prediction. Simple, basic process parameters, such as

cutting speed, cutting depth, feed rate tool and specimen material were selected. It gave us a basic comprehension about the surface prediction model and its structure. The second and following cycles had to improve this developed model with additional process parameters and factors. But the last cycle had to confirm the results and serve as a validation model for research results. Each new cycle continued the previous cycle's work, improving the general mathematical model until 100% accuracy had been achieved. The first of these cycles, the flat-end milling case study, will be discussed in the next chapter.

6. EXPERIMENTAL PLANNING OF THE HSM MODEL: a case study of flat end milling

Researchers nowadays are looking for more detailed analysis on how surface topography is generated with HSM technology. As shown in the literature review, most researchers are looking for statistical methods to define an accurate prediction model. As concluded in Chapter 2., none of these models are satisfactory for use with different machining equipment, where different behavioural properties can be observed. Thus, a more detailed analysis is necessary into the mechanisms participating in surface topography generation, in order to include them in surface roughness prediction models.

Furthermore, to provide this detailed analysis, the information collected using ball-end milling is not the most appropriate, because of difficulties to distinguish cutting marks left on the machined surface one from passage to the next. Visual analysis revealed marks that did not correspond either to machining tool rotation or movement direction. The author could not visually relate topography marks with the cutting-tool edge and its movement. Material spread over the surface reflected the tool movement (marks presented in Fig. 4.4), but hid the real cutting process and its parameters that affect the surface topography height. At this point it was decided to switch to a more conventional milling method – flat-end milling. The flat-end milling model more clearly reflects the surface topography formation lines and marks and helps to identify the process effects on surface generation.

End-milling tools are mostly used to do the rough or final flat surface machining operations in die and mold manufacturing. In theory, an ideal flat-end milling operation would perform equal surface topography over the entire machined surface. Therefore, every inaccuracy and every disturbance of the machining process should leave a mark on the machined surface. Is it the case? The first investigation was focused on the simplest milling operation to sweep an area using overlapped straight tool paths at a constant depth.

At this point, analysis began with the decision to prepare simple, straight, flat-end milling cutting paths on only one selected material specimen. The development of the experiment design started with the selection of material. In the paragraphs below, the measurement results are compared with the developed mathematical model results. Cutting tool kinematics, geometry and

material mechanical properties have been considered as the main mathematical model components.

6.1. Material selection for the experiment

This research is based on machining considerations to develop and improve die and mold manufacturing for plastics industry. In previous work (Chapter 4), a selection was made for die and mold application materials [108]. Therefore, the material used in the following experiment will be the same DIN 1.1730 or C45U/ 1045 carbon steel, widely used for injection mould production. Its hardness in a hardened state can be up to 58 HRC. This alloy is a representative sample of the range of materials used by the dies and molds industry internationally. The basic material composition and properties are represented in Table 4.1 in Chapter 4.

6.2. Machining equipment selection

To perform flat surface machining using a flat-end tool with a linear sweep strategy, it is not necessary to search for complex machining centres. A simple, 3-axis milling machine, even without digital control, can be used. From the available resources, the 3-axis KONDIA B500 CNC milling machine (Fig. 6.1.) was selected for the experiment. The machine's specifications are included in Table 6.1. All the machining operations in this part of the research were performed at Universitat Politècnica de València, Spain.

Table 6.1. KONDIA B500 series specification

TYPE	B500
Spindle speed, r/min	6000
Motor power, kW	15
Axis movement (x,y,z), mm	600*550*400
Rapid feed rate, m/min	25
Cutting feed rate, m/min	20
Spindle cone standard	BT-40

Fig. 6.1. KONDIA B500 CNC milling machine

The selected tool to machine the samples was a MITSUBISHI 2-flute cylindrical-end milling tool. In particular, the MITSUBISHI flat-end milling tool MS2MSD1000 (Fig. 6.2) with a cutting diameter (D) of 10 mm and a total length of 60 mm was used. It is a tungsten carbide (WC) cutting tool with two cutting flutes and the MITSUBISHI UWC - TiAlN miracle coating to decrease the friction, protect the tool surface from high temperatures and increase the tool's lifetime. [121–123]

Information about certain cutting angles not provided by manufacturer were measured directly from the actual cutting tool using a 10x electronic magnifying system. Primary and secondary cutting edges are represented and the cutting tool flute nose angle is 88°. The tool helix angle (β) is 30° and the concavity angle (κ) - 2°. Measured angles are presented in Fig. 6.2.

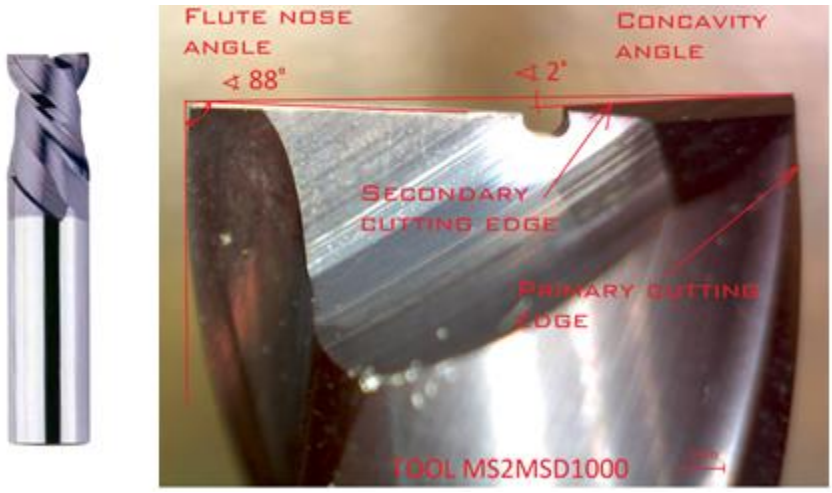

Fig. 6.2. MITSUBISHI MS2MSD1000 cutting tool geometry.

6.3. Selection of cutting conditions

For studying how surface topography is generated in this type of milling operation, three variable input parameters were selected: feed (feed rate), radial cutting depth and cutting direction. The cutting conditions selected in this research project came from the recommendations of the tool manufacturer [122] as appropriate for the selected workpiece material.

One of the cutting parameters with a direct impact on the machining operation is the feed rate. Furthermore, feed changes the chip section, affecting the cutting forces. It was decided to use three feed levels: Feed #1 (F1) = 0,04 mm/tooth, Feed #2 (F2) = 0,1 mm/tooth, Feed #3 (F3) = 0,2 mm/tooth.

Another selected parameter is the radial cutting depth. The selected radial cutting depth first value is a_{e1} = 5 mm and the second value: a_{e2} = 10 mm. This means either ½ tool or whole tool diameter area is involved in cutting process. This value is the gap between the tool center points of consecutive straight cuts. The cutting speed has to be maintained at 150 m/min. The cutting depth has been maintained at 0.3 mm. It was decided to develop samples, where different radial cutting depth values and feed rates will be used on the same specimen to save machining time and material consumption. Every specimen has been machined with both radial cutting depth values. The sample design is presented in Fig. 6.3., which shows cutting tool rotation and feed directions. The dashed lines represent the trajectory of the tool center point. No sample adjustments have been made between radial cutting depth value changes. Each specimen was machined with a separate cutting feed value.

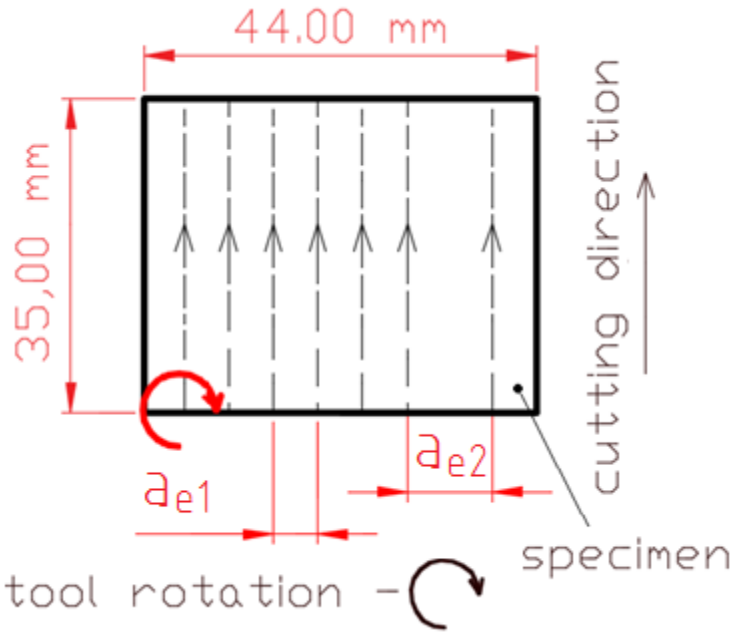

Fig. 6.3. Straight movement flat end milling sample design.

6.4. Design of Experiment

Design of experiment is a task to describe the variation of the selected cutting conditions and their arrangement on the sample specimens. For our case, 6 different experiments were planned, combining the selected values for each factor. The exact selected cutting parameter values for each experiment are shown in Table 6.2. As deflections can significantly affect the surface topography, for all samples the tool was set in a tool holder with the same cantilever length, as indicated in the table.

Fig. 6.4 presents the selected Material type – DIN 1.1730. The NORTH direction symbol represents the same cutting tool direction as the machine coordinate system used in the cutting experiment– NORTH cutting direction, looking at the milling table from above. The radial cutting depth and feed rate represent the selected variable cutting regimes. These cutting conditions were used to execute the developed design of experiment. The goal of this experiment is to observe and analyze effect from different feed rates, their influence on the surface topography, its errors and inaccuracies. From this it will be easy to understand, is there behavioral relation between surface topography values and selected cutting conditions. The specified design of experiment requires a minimum number of 6 samples.

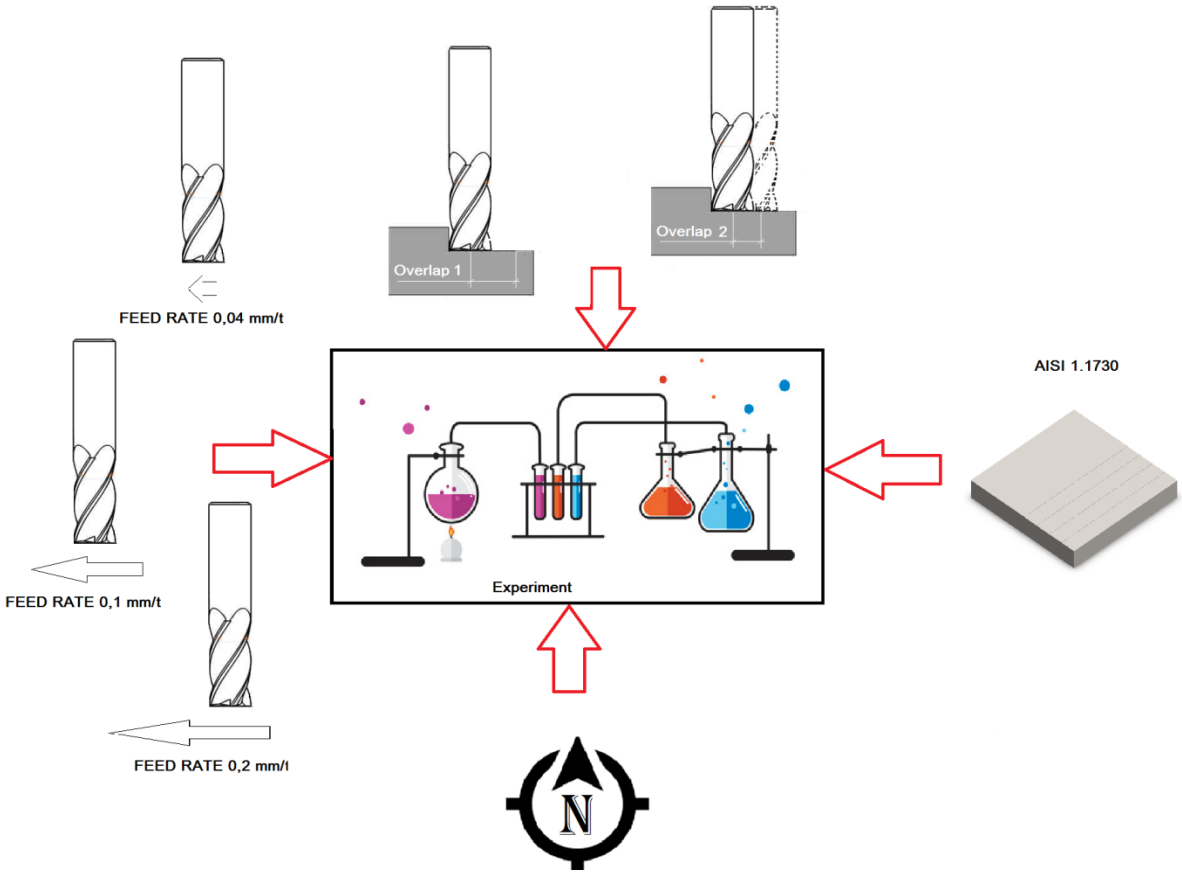

Fig. 6.4. Design of experiments - 1st cycle

Table 6.2. Experiment design

Conditions	Samples Nº.		
	2. and 5.	3. and 6.	4. and 7.
Feed rate, mm/tooth	0,04	0,1	0,2
Feed speed, mm/min	382	954,9	1909,9
Radial cutting depth, mm	5 / 10	5 / 10	5 / 10
Cutting mode,	Up	Up	Up
Milling Machine	KONDIA B500	KONDIA B500	KONDIA B500
Tool length, mm	34,8 mm	34,8 mm	34,8 mm

6.5. Experimental execution and measurements

When performing simple machining operations with a flat-end milling tool, it is common to analyze the surface roughness, irrespective of differences between the cutting behaviour in different directions on the machining center.

At this point, all the factors and cutting conditions have been identified and selected material samples prepared for the experiments. Wear of the cutting tools was not considered, as the cutting length and number of samples prepared is sufficiently low. For each selected feed rate, a new cutting tool was used, to avoid the influence of excessive wear and tool failure with different speeds and to monitor the behaviour of cutting tool wear at a constant cutting speed, radial and axial depth parameters. Experimental sample Data sheet example is represented in Appendix B.

The execution process of experiment consists of several parts.

a) Cutting program preparation:

To do the machining in an automatic cycle, the author writes a CNC numerical code. The milling machine executes the prepared CNC code and performs the machining process. NC Programs are written according to the ISO 6983-1:1982 NUMERICAL CONTROL OF MACHINES -- PROGRAM FORMAT AND DEFINITION OF ADDRESS WORDS standard [124]. The CNC cutting program codes for all the samples are included in Appendix B - Design of experiments.

b) Specimen preparation:

The specimen was fixed onto the milling machine workbench using a precision vice clamping tool. Before experimental execution, the specimen was flattened with an indexable shoulder milling cutter. The preparation procedure ensures uniform surface height and roughness over the entire specimen area.

c) Machine setup and machining execution:

The prepared CNC execution program was loaded into the milling equipment computer and post-processing was performed manually, as the program was prepared by the author and not loaded from CAM software. With respect to the workpiece surface and corner of the specimen, the machine spindle coordinates were set to zero. This is the reference point for the CNC program. The selected specimen zero point is the lower right corner of the machining area. Milling execution was started and the automatic program execution cycle was launched. After execution, the sample was cleaned with dried, compressed air and covered with protection grease, to avoid humidity and oxidation before taking measurements.

Measurement execution:

Measurements were taken with the BRUKER CONTOUR 3D topography measurement equipment presented in sub-section 5.4.1. (Fig. 5.3). Data files contain the data-point coordinates and height values with no filters applied. Visual representation of commercial software applies filters for waviness and surface errors. During the measurement process, the surface topography data files with error data points (NaN – not a number) were found. Error data points appear when using the optical surface measurement device. These points are non-reflected data points at certain coordinates, where the device cannot detect the surface height or surface Z coordinate value. For this point, there are only X and Y coordinates. This is a common error in surface topography measurements due to highly inclined surface peak slope, a high light reflection from surface, etc. Commercial software has an integrated function to interpolate NaN data points with surrounding point average values. Measurements are acceptable, if NaN data points are less than 1% of the total image resolution. Below, is an example of the MATLAB script for interpolating NaN data points. This part of the program is included in the author's Python script to solve the error points of surface data files and complete the surface coordinates with Z coordinate values. This is important, owing to the result differences between the surface topography parameter values with and without NaN data points.

Interpolation program sample:

```
A = data(:,1);
B = data(:,2);
C = data(:,3);
A1 = reshape((data (:,1)),2295,1687);
B1 = reshape((data (:,2)),2295,1687);
C1 = reshape((data (:,3)),2295,1687); %// this is my matrix with surface points
%// identify indices valid for the 3 matrix
idxgood=~(isnan(A1) | isnan(B1) | isnan(C1)); %// re-interpolate scattered data
(only valid indices) over the "uniform" grid
SURF = griddata( A1(idxgood),B1(idxgood),C1(idxgood), A1, B1 ); %// Indices
of NaNs
NAN = find(isnan(SURF));
Z = reshape(SURF,3871665,1);
FINAL = [A B Z];
save SURFACE.txt FINAL -ASCII; %// save to TXT text format
```

Visual analysis reveals some other behaviour of machined surfaces, such as form errors, waviness, etc. These shape errors are important when striving for more accurate surface topography analysis and will be discussed in the next section.

6.6. Analysis of the flat-end milling model

This section deals with the analysis of the observed data (qualitative and quantitative) collected from sample measurement. Data analysis is performed with different methods. Descriptive statistical and visual analyses have been applied to analyze machined surface topography. Different types of analysis may reveal particular errors on the surface, during the

measurement process or due to the inaccuracies when machining. The sample measurements are compiled in Appendix C – Surface topography measurements.

6.6.1. Numerical analysis

Numerical analysis results show the reliability of the measured data. In Chapter 4, it was decided to investigate the surface topography parameter S_Z. This parameter represents the total surface topography height and is a representative parameter to describe cutting process factors and their influence on topography formation. Descriptive statistics is a method used to compare numerical results and describe the main features of the data set with simple summaries. Graphical representation of data features is the most common representation of statistical summaries and will be used in this research. Fig. 6.5 presents the Box-Whisker diagrams which shows the influence of radial cutting depth and cutting feed values on S_Z. From the Boxplot for radial cutting depth, the overall results for two selected values are similar. From the Boxplot for feed factor, it can be concluded that feed values have a higher impact on the S_Z values, because there is a major S_Z difference between the low and high cutting feed rates used. Also, medium feed rate produces higher variability compared with other feed rates. Accordingly, from Boxplots we can draw some conclusions: a) the radial cutting depth does not have a significant influence on S_Z in the machined surface; and b) conversely, the feed rate factor has a significant influence on the surface topography parameter S_Z. This statement will be used in further calculations.

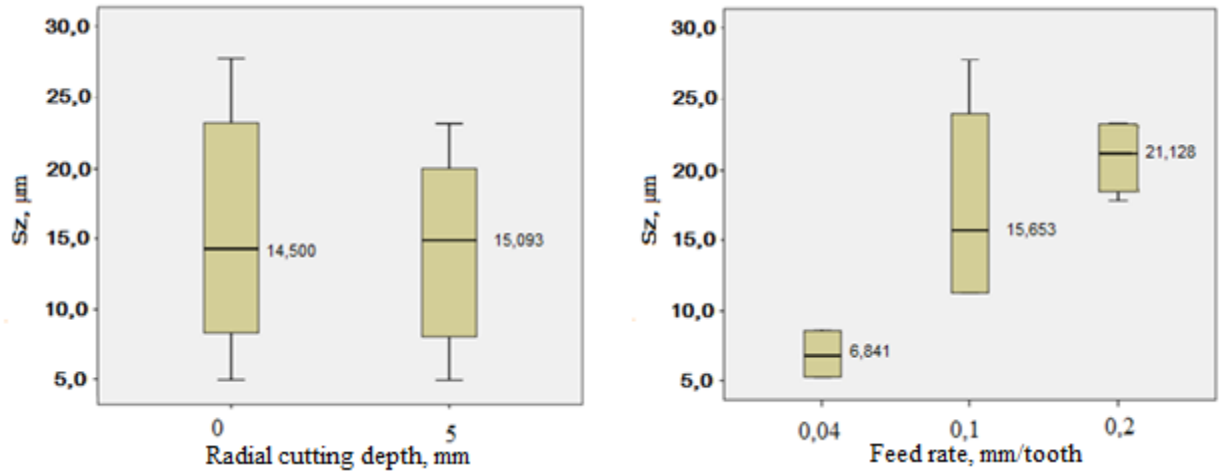

Fig. 6.5. Box-Whisker diagram for radial cutting depth and feed rate factors.

To confirm the previous effects, an Analysis of Variance (ANOVA) study was conducted. The ANOVA results are shown in Table 6.3. Each stage of this model and the whole model has been tested for its ability to account for variation in the dependent variables. The source column presents the dependent variables, in this case, Feed rate, radial cutting depth and interaction of feed and radial cutting depth. The columns, Type III Sum of Squares, df, Mean Square and F are ANOVA analysis default options and calculations to obtain significance coefficients of each dependent variable. The last column (Sig.) represents the statistical significance of each source.

This is the main column that represents which dependent variable is significant and which is not. The CORRECTED MODEL is the sum of squares that can be attributed to the set of all the between-subject effects, excluding the INTERCEPT, i.e. all the fixed and random factors and covariates and their interactions that are listed in the Between-Subjects table, [125-126]. TOTAL represent values related to the Statistical Package for the Social Sciences SPSS internal model used to calculate ANOVA.

TOTAL refers to values related to the Statistical Package for the Social Sciences SPSS internal model used to calculate ANOVA.

In this case, only the significance coefficient of FEED is less than 0.05, such that Feed is the only statistically significant factor. All the other factors (radial cutting depth by itself and the interaction between feed rate and radial cutting depth) are not statistically significant, since their significance coefficient is higher than 0.05.

Table 6.3. Tests of Between-Subjects Effects – Feed rate (FEED) and Radial cutting depth (RCD)

Source	Type III Sum of Squares	df	Mean Square	F	Sig.
Corrected Model	440,036[a]	5	88,007	2,494	,148
Intercept	2738,204	1	2738,204	77,604	,000
FEED RATE	424,838	2	212,419	6,020	,037
RCD	3,889	1	3,889	,110	,751
FEED RATE * RCD	11,310	2	5,655	,160	,855
Error	211,705	6	35,284		
Total	3389,946	12			
Corrected Total	651,741	11			

The significance coefficient value of the FEED factor is more than 20 times lower than the value of the RCD factor. This means that the feed rate influence is 20x higher than the radial cutting depth and that this factor is not significant for further calculations.

6.6.2. Visual analysis

After the statistical analysis, a visual analysis was made. This visual analysis was carried out studying the surface topography images and microscope photographs. Each of the surface topography images represents different behaviour of the surface appearance, peaks and valleys orientation, peaks slope and other surface characteristics that may be described with parameters specified by the ISO 25178: 2012 standard. These parameters help to distinguish other influential cutting process factors. Topography images revealed significant marks on the material's surface,

which clearly shows the tool travel and rotation direction. In flat-end milling, the lowest surface pattern is dependent on the tool feed direction. Fig. 6.6 and Fig. 6.7 represent the cutting marks left on the machined surface by the cutting edges of the flat-end cutting tool.

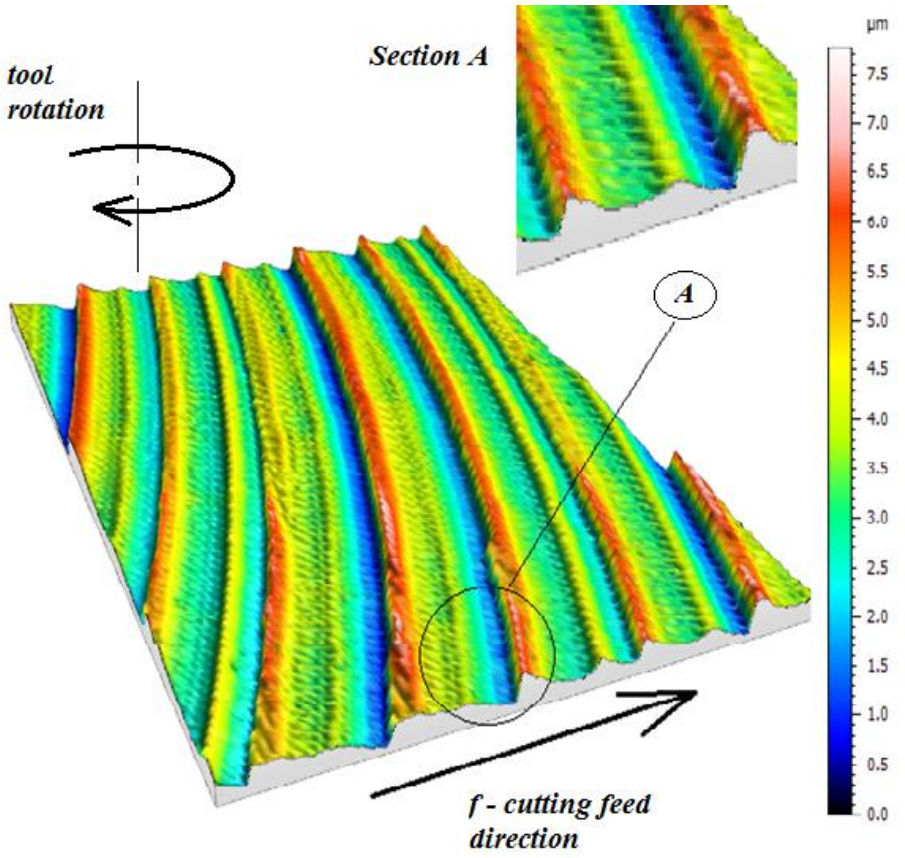

Fig. 6.6. Surface topography measurements. Sample #3. Section A – area near to the highest uncut chip thickness.

The sample illustrated is sample #3 – machined in the NORTH direction of machine coordinate system with a feed rate of 0,1 mm/tooth. The characteristics of sample #3 are presented in Table 6.4. This table presents the material type and equipment used to machine the sample, Cutting direction, feed rate and measured surface topography height, S_Z.

Table 6.4. Cutting conditions and S_Z parameters of the illustrated samples

Sample	Material	Machine	DIRECTION	Feed/tooth	S_Z, µm
#3	1.1730	KONDIA	NORTH	0,1	8,0833
#5	1.1730	KONDIA	NORTH	0,1	7,2276
#7	1.1730	KONDIA	NORTH	0,1	10,48263
#12	1.1730	KONDIA	NORTH	0,04	6,2028
#13	1.1730	KONDIA	NORTH	0,04	9,2633
#14	1.1730	KONDIA	NORTH	0,2	12,1256

#15	1.1730	KONDIA	NORTH	0,2	16,5226

Fig. 6.6 presents the cutting feed direction and tool rotation. Section A presents the topography pattern more closely – the deepest part of the surface valley is represented by a dark blue color, but the highest surface peak is shown in red on the color map. Surface mark curvature follows the cutting tool rotational movement. Surface markings reveal that both slopes have a different inclination. Followed by the cutting direction, the surface mark has the lowest slope. This slope results from the cutter's concavity angle facing the tool center. The second slope pattern is faster – formed with peripheral cutting edge. Fig. 6.7 represent this description for sample #14.

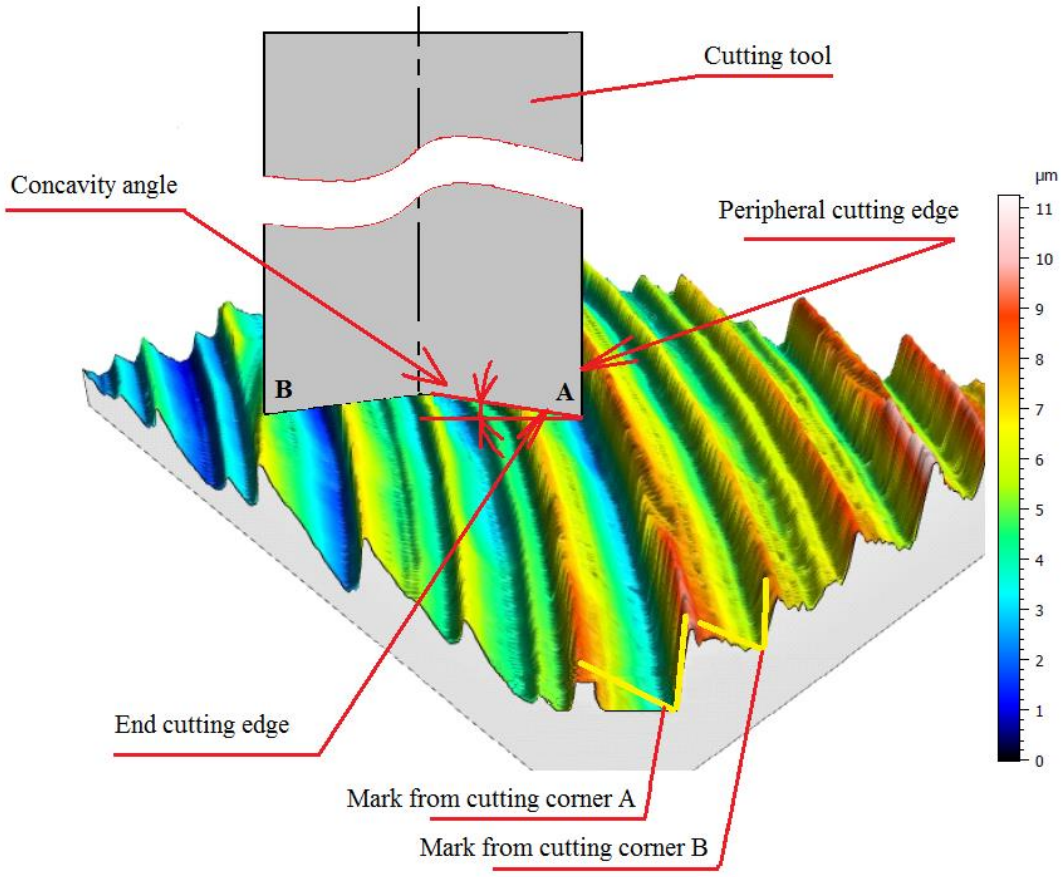

Fig. 6.7. Cutting tool geometry interaction with surface - Sample #14.

Sample #14 cutting conditions and surface topography height parameter S_Z value is represented in Table 6.4. This time, surface topography image has been supplemented with sketch of cutting tool. This sketch represents how surface has been affected by each of cutting edge. Cutting tool run-out or vibrations affect the surface height performed by each of cutting edges. If one of the cutting edges is located higher than other, the surface height will be uneven

and will cause the vibrations that may affect run-out phenomenon even more. The same behavior has been observed in all of material C45 (1.1730) samples machined with flat end milling mode.

Analysis of the other sub-samples reveals other marks left from back cutting edge – cutting edge that is not involved in instant cutting process. In Fig. 6.8 cutting marks on material surface in two different positions of the same cutting sample can be observed. In the middle of the picture cutting tool projection with its rotation direction (CW) and feed direction is represented. In left side of cut, accordingly to feed direction, author can observe the back cutting effect. This effect may become from machine milling head inclination error in some specific direction. We suppose that milling head (tool axis normal to the sheet) has been slightly tilted to the left and backwards direction simultaneously. Therefore, at the right side of the sample, cutting tool back cutting edge cannot touch the surface anymore.

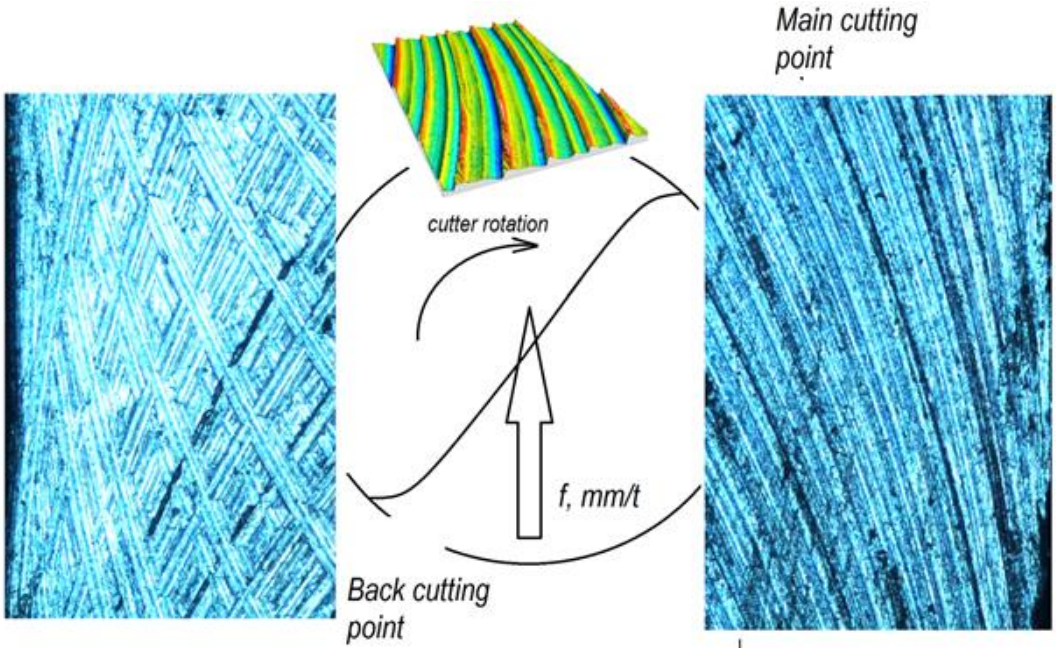

Fig. 6.8. Surface topography photos: Sample's #3 left and right region, according to feed direction.

Behaviour of surface topography formation process is represented in Fig. 6.9. It collects the representation of surface topography based on roughness measurements, and in Table 6.4 the corresponding S_Z parameter is indicated. These four cases are collected here to show, what kind of surface topography deviations, marks and errors were observed on machined surface from all the surface topography measurements.

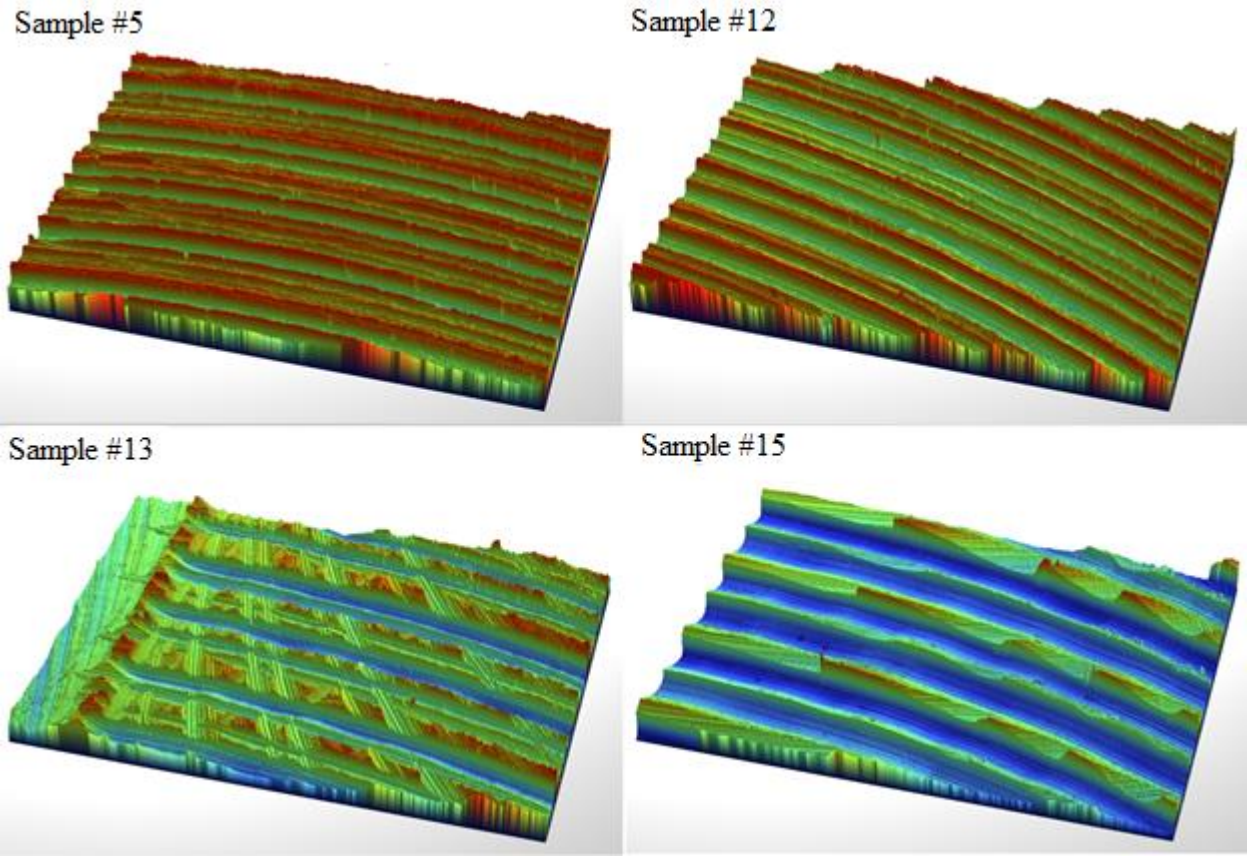

Fig. 6.9. Compilation of different sample surface topography measurement device images

Area of surface covered by one tool path may be divided in three parts. In left part UP cutting mode is performed. Middle area is where maximum uncutted chip thickness has been achieved and transition from UP to DOWN cutting modes becomes in action. Right part of path is area, where only DOWN milling mode is performed.

Sample #5 in Fig. 6.9 represents middle area of cutting tool path. This surface represents marks left from the corner of end cutting edges and peripheral cutting edge intersection. No additional marks appear on the machined surface and this surface may be claimed as a perfectly machined surface, easy to predict. The same clear cutting is represented in image of sample #12. Both samples are machined with LOW (0,04 mm/tooth) and MEDIUM (0,1 mm/tooth) feed rates accordingly.

However, samples #13 and #15represent surface topography errors made by the cutting tool. Fig. 6.10 represent the section from sample #13 and sample #15.

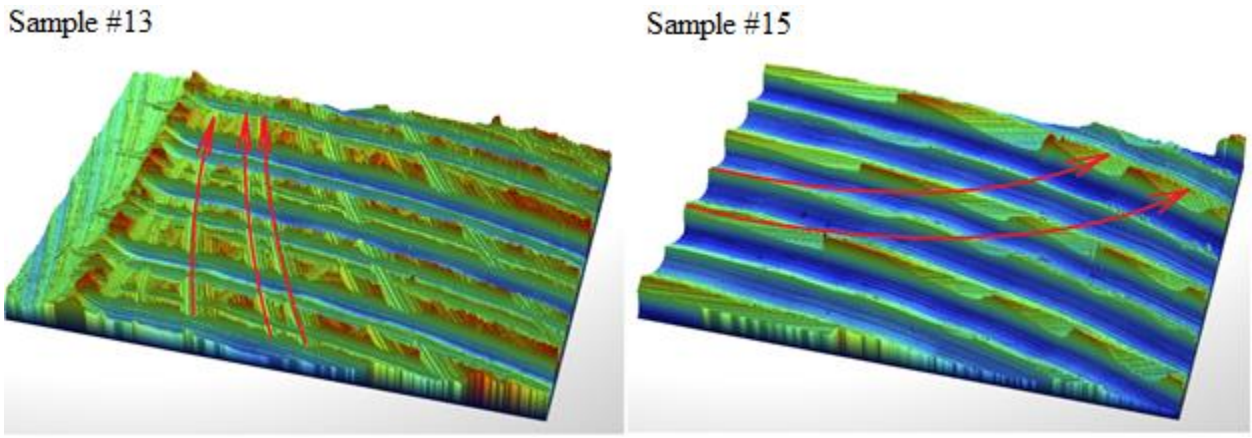

Fig. 6.10. Back cutting marks on surface topography - Sample #13 and Sample #15

In normal cutting process, where no cutting tool deflection is in progress, back cutting process should be observed in whole tool back cutting edge travel length. In surface topography images (FIG. 6.10) it is observed that cutting process is not so even and back cutting marks appear only on some of tool path areas. Back cutting marks in sample #15 are light, tiny and may be attributed to normal cutting tool orientation against the specimen. Close to the tool path center line, they disappear due to the tool inclination in cutting feed direction. However, back cutting marks on Sample #15 are represented along all the back cutting edge travel distance. They become shallower at the middle of tool path area, and left side of sample. While at the right side of area they are deep enough. We suppose that these marks represents high machine cutting tool inclination in NORTH-EAST direction, while back cutting edge retires from surface at the SOUTH-WEST corner of specimen. These surface heights dramatically change the surface topography parameter S_Z height values. But, on the machined surface, other more interesting marks have been observed. We explain them at the next subchapter.

6.6.3. Oscillation marks at surface topography

Visual analysis and color map plots of the measured surfaces reveal some other behaviour that should be investigated. As we can see from the color change along the cutting edge rotational movement on sample #3 (Fig. 6.11), there are differences in height of surface. To improve the visualization on color change, light intensity should be changed continuously. These color changes means that additional marks left from the cutter edges over the surface are deeper in some places and shallow at other, compared with typical cutting area. The above mentioned information leads to consider the involvement of the vibration generators acting in the cutting process. Number on the blue background in Fig. 6.11 is the length of valley, where color is darker.

Furthermore, tangential distances between the highest peaks approximately coincide with defined cutting feed per tooth, but the magnitude between adjacent highest peaks is different. This phenomenon is represented the best in surface topography image of sample #7 (Fig. 6.12)

Between them exists non-linear forms that are not constant in every step. Numbers on the blue background in and Fig. 6.12 are the distances between cuts on the sample #7.

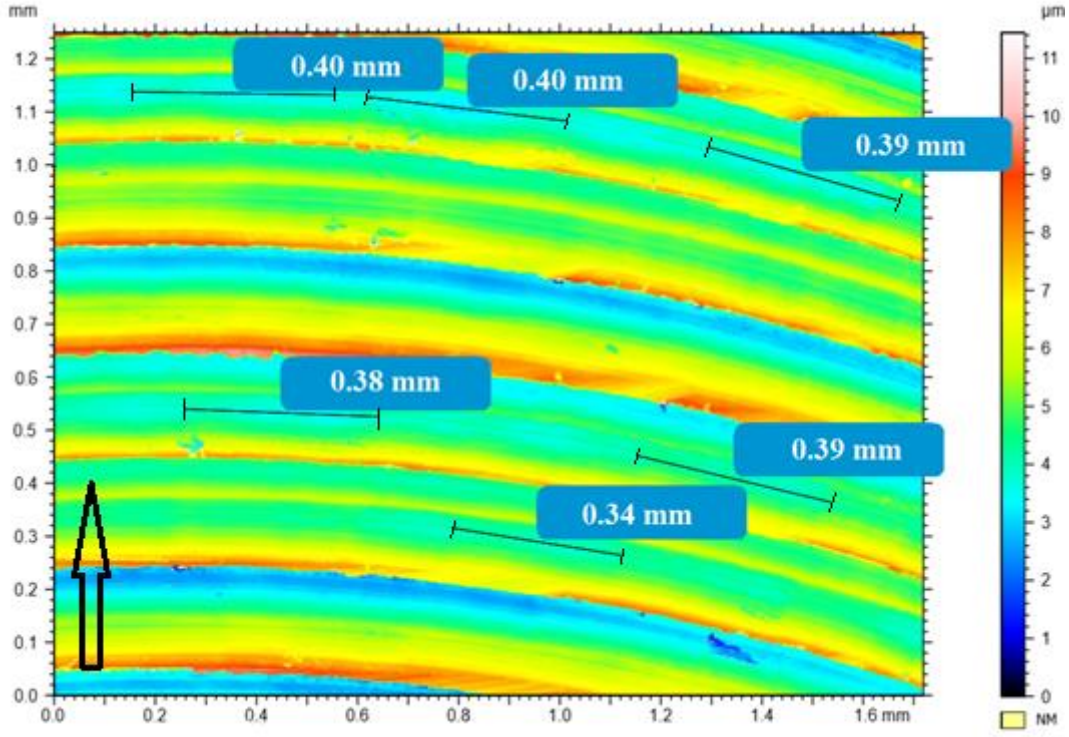

Fig. 6.11. Surface topography height deviation over one tool overlap.

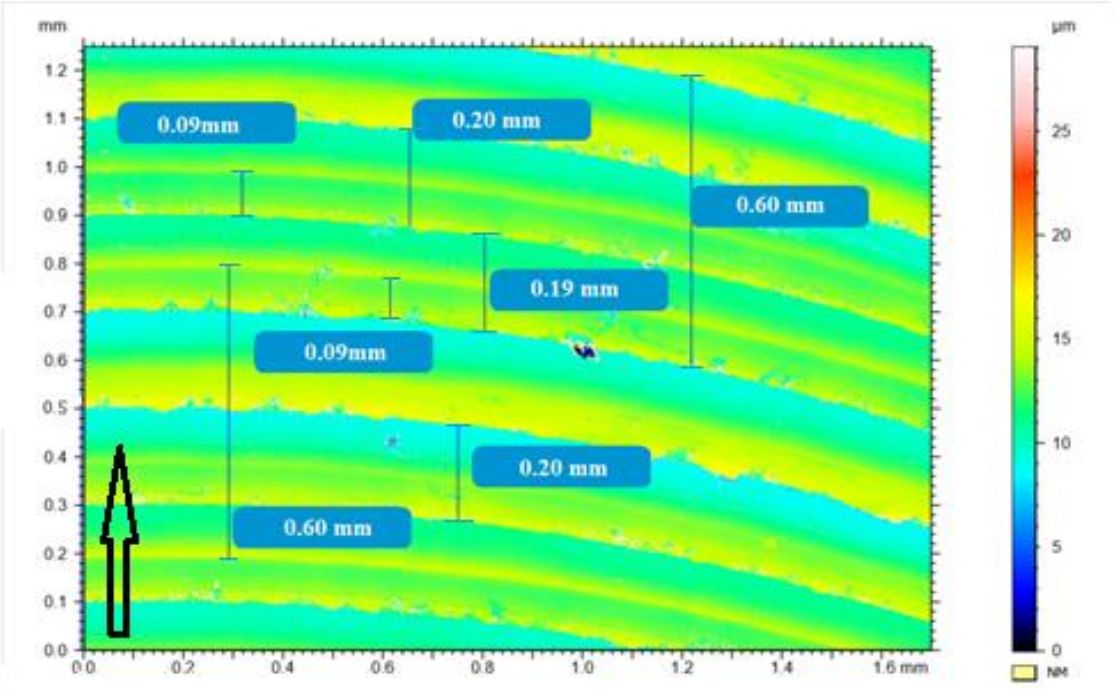

Fig. 6.12. Surface topography mark distance deviation

6.7. Theoretical model: discussion of the results

Cutting tool geometry is a constant component that doesn't change a lot during the cutting process. Tool wear-out and breakage will affect the surface topography formation changes only. The same tool with the same tool geometrical particularities, described in previous chapter, has been used to develop the samples. The basic cutting tool geometry was represented in Fig. 6.2. Basic cutting tool angles have been represented to make it clear, what performs the minimum surface topography height, represented in Fig. 6.13. This is called also as a Theoretical surface topography formation model. It depends only on the cutting tool angles and the set of cutting parameters.

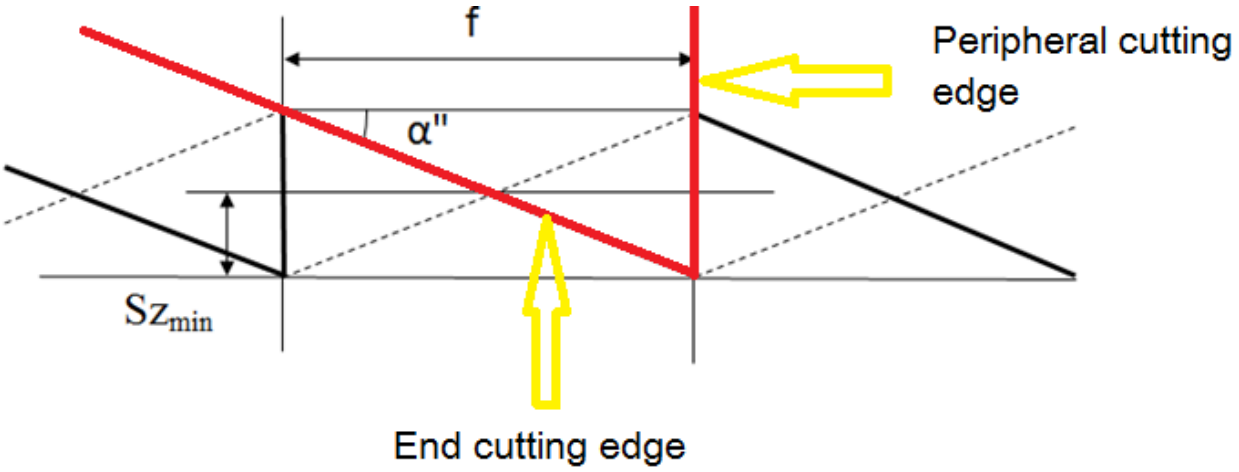

Fig. 6.13. Surface topography Sz parameter formation by interaction of tool cutting edges.

At this point a simple geometrical model for surface topography formation is proposed. This model is represented in Fig 6.13. This model is based on the assumption that machined surface micro-geometry is equal to the cutting edges geometry generating it. As shown in previous chapter, surface topography is formed by cutting tool end cutting edge and concavity angle, and they are not perpendicular to the tool axis. In the Fig. 6.13, tool edges are represented using thick lines and tool is moving from left to right, so the marks on the surface corresponding to the main cutting edges are displaced by the feed value (f). The bottom lines are the marks from the tool tip edges (secondary tool edges) and they are oriented according to the tool concavity angle (α") measured with respect to the horizontal direction (normal to the tool axis). The dashed lines are the prints of cutting edges (back cutting) at the rotation movement to the active cutting zone. Then, if only the theoretical tool geometry is considered, neglecting other process effects and disturbances, the Sz for the generated surface is calculated as:

$$\boldsymbol{Sz(min)} = \frac{\mathbf{1}}{\mathbf{2}} * \mathbf{tan}(\boldsymbol{\alpha}) * \boldsymbol{f} \qquad (6.1.)$$

Considering the selected flat end milling tool concavity angle, that was measured, and feed values used in the machined samples (F1 – 0,04 mm/tooth, F2- 0,1 mm/tooth and F3 - 0,2

mm/tooth), the following minimal surface topography height parameter S_Z values can be obtained:

$$\mathbf{S_{Z\ minF1} = 0{,}69842\ \mu m;}$$

$$\mathbf{S_{Z\ minF2} = 1{,}74604\ \mu m;}$$

$$\mathbf{S_{Z\ minF3} = 3{,}492077\ \mu m.}$$

This component fills in the first part of mathematical model. Theoretical model is only a model, which represent the surface topography formation in ideal conditions – without other possible errors related with tool inclination, deflection or milling machine errors. The calculation results and topography parameter S_Z measurements are compiled in Table 6.5 below. Measurements for each direction on specimen were done at two points to confirm the first measurement credibility and surface topography behaviour at multiple machined surface points (sample #5 and #6 are from the same specimen).

Table 6.5. Comparison between measured and predicted results

Sample	Feed, mm/tooth	Measurements, µm	Predicted value, µm	Difference, %
#3	0,1	8,0833	1,74604	463 %
#5	0,04	7,22759	0,69842	1034 %
#6	0,04	7,49193	0,69842	1072 %
#7	0,1	10,48263	1,74604	600 %
#8	0,1	9,77934	1,74604	560 %
#9	0,2	30,32363	3,49208	868 %
#10	0,2	15,39734	3,49208	442 %
#11	0,04	5,61196	0,69842	804 %
#12	0,04	6,20284	0,69842	888 %
#13	0,1	9,2633	1,74604	530 %
#14	0,1	12,12557	1,74604	694 %
#15	0,2	16,52264	3,49208	474%
#16	0,2	19,17729	3,49208	550%

As it is possible to observe from the comparison Table 6.5, differences between actual measurements and the theoretical model predicted topography values are large, from 221% up to 536%. It is 2,3 up to 5,3 times difference for LOW and MIDDLE cutting feed rate and 2,2 up to 4,3 times difference for the HIGH cutting feed rate. Basically, the theoretical model claims that between 1/6 and 1/3 of the surface topography is created by the geometry of the cutting tool. This is a serious application to conduct more extensive research and identify other process

factors that affect the surface topography formation in flat-end milling operations performed with cutting regimes according to High-Speed Milling functions.

But, in surface topography images, taken in middle area of the cut, we cannot observe any marks, left from the back cutting phenomenon. This means, either cutting tool inclination is higher than concavity angle and eliminate the effect of back cutting edge, either other factor, like tool deflection is high enough and cutting tool back cutting edge is retracted from the machines surface. Fig. 6.9. represent the statement that near to the side area of the cut, back cutting phenomenon in observed, but more closer to the middle area of the cut it disappears.

As mentioned at the start of this chapter, some marks observed might be caused by tool alignment errors, tool run-out issues and cutter deflection during the cutting process, under the influence of cutting forces. These components may contribute to other significant parts of the surface topography formation. They can have a direct influence on topography parameter formation, especially on height parameters. To prove it, a further cycle of experiments should be performed.

6.8. Conclusions

At the start of this chapter, the author stated the objective to develop the experiment with samples, where it is easy to observe the factors influencing the surface topography formation. Flat-end milling was selected as an appropriate surface milling operation from where to start the analysis.

Based on the visual and statistical analysis carried out for machined samples, the author can draw certain relevant conclusions. These conclusions will conduct the objective for subsequent research.

1. In general, the analysis of surface topography images shows the behaviour of the milling system on the surface machining process. Local deformations and disturbances appear on the surface topography. These disturbances have been related with late chip removal of the machining area, cutting tool inclination and deformations, or with cutting process vibrations.

2. In some areas of the machined sample surfaces, marks left from the back cutting edge have been observed. These marks do not appear in every sample. Usually, samples with increased feed rate reveal these marks. This behaviour suggests that during the cutting process, the cutting tool has high deformations along its axis. These deformations should be investigated and the prediction model must include them.

3. Surface topography in all samples is formed with the tool tip point (the intersection of the main - end and secondary – peripheral cutting edges). The primary and secondary

cutting-edge marks that each tool rotation marks on the surface can be observed in Fig. 6.8. Every tool rotation leaves 2 marks on the surface topography, performed with each of the cutter's teeth. Visual analysis is used to identify the differences in height between marks formed with the two cutting edges. This suggests that tool geometry errors caused by sharpening deviations and other effects like vibrations, has a significant influence on surface topography formation.

4. The distance measured between the consecutive cutting-edge marks differs according to the feed rate applied in the machining process. Low feed rate generates small distances between surface pattern marks, whilst a high feed rate increases the distances. Furthermore, the distances between cutting marks within the same sample are not equal. We suppose that these distances differ due to tool deformations, run-out, milling tool and machining equipment vibrations and other effects acting during the process.

5. A highly deformed surface pattern has been observed in some areas, where two sequential and parallel tool paths have been used with radial cutting depth of whole cutter diameter, with a tiny radial cutting depth or with half-tool radial cutting depth. To avoid surface measurement errors, topography parameters should not be measured close to the border of two sequential tool paths. If surface sample should be measured in this area, surfaces with some radial cutting depth value will have lower surface topography parameters. But samples where radial cutting depth covers whole cutting tool diameter will have high surface uncut chip leftovers close to the path changing area.

6. The use of the geometric model proposed leads to a huge difference between the predicted and the measured values. We assume that differences are due to process inaccuracies, vibrations, tool errors and cutting-force influence on the cutting process. Each of these factors should be investigated more extensively to improve the prediction model.

To further this research, the next statement is supposed: Cutting tool deflection and inclination drive the surface topography and influence the 3D surface topography parameters. To prove this statement, a new set of experiments should be designed. This new experiment should enable changes to be introduced in the cutting deflections and inclinations. At the same time, a new mathematical model is needed. This model must include the tool axis inclination and tool deformations during the cutting process.

7. ANALYSIS OF THE FLAT END MILLING MODEL – SAMPLES WITH CONTRARY AIMED CUTTING DIRECTIONS

The conclusion of previous chapter suggests that in addition to feed, radial cutting depth, etc., other factors (tool deflection, tool axis inclination) influence the surface roughness. So the question is, how does the feed direction affect roughness? In this chapter, a new type of experiment is proposed with the aim of studying these factors and including them in the mathematical model. Moreover, a refined and more complex mathematical model to predict and analyze the possible errors and deviations has been introduced. This model is compared with the results to assess its appropriateness.

7.1. Design of the Experiment

7.1.1. Selection of the cutting tool movement strategy

It is common to do simple machining operations with a flat- end milling tool to analyze the surface roughness, without considering that there are differences between cutting behaviours on different directions of the machining center. To analyze the impact of cutting feed direction on the surface topography parameter S_Z, it is also important to consider machine alignment inaccuracies.

During the sample preparation process in the previous experiment, a new, additional experiment was introduced, whereby a 4-direction cutting model was used. The introduction of the 4-direction experiment was decided to perform the surface topography analysis for the measurements, taken from each separate cutting direction. Deviation in surface height should indicate if there are differences in surface height between opposite cutting directions for the given equipment. The results, in turn, will characterize the alignment precision of the milling axis compared with the milling table. This analysis is intended to ascertain if there is really a difference between cutting directions, and whether it is worth extending the analysis of the cutting direction's influence on the surface topography S_Z parameter formation.

The selected cutting conditions for this experiment were based on the same selection made in section 6.3. The only factor with variable changing (in 4 levels) was the cutting direction. By cutting direction, we understand the NORTH/SOUTH (Y axis) and the EAST/WEST (X axis) when looking at the milling table from the top of the machine.

The feed rate, radial cutting depth, axial cutting depth, material factor, equipment and cutting tool factors are fixed did not change during this experiment. In total, all the factors gave a $1^1 \times 1^1 \times 1^1 \times 1^1 \times 4^1$ design of experiment. In this case, the design of experiment represents the minimum amount of 4 samples to be prepared for this experiment. Examples of sample design and machining parameters are included in Appendix B – Design of experiments.

Named experimental parameters are compiled in Table 7.1.

Table 7.1 Design of experiment for additional specimen with a 4- direction sample

Material 1			
F1 D1 O1	***F1 D2 O1***	***F1 D3 O1***	***F1 D4 O1***

Abbreviations in Table 7.1: F – cutting feed level (F1 = 382 mm/min), O1 – radial cutting depth factor and D – cutting direction level (D1 – South, D2 – West, D3 – North and D4 – East).

It was decided to perform cutting procedures using a rounded rectangular tool movement strategy, to ensure a straight tool movement in the four cutting feed directions, to determine machine milling head alignment inaccuracies and their influence on surface topography height. A sample with a rectangular cutting strategy (Fig. 7.1) was located on the same specimen with a previously developed straight strategy and flat-end machined samples. Fig. 7.1 illustrates the developed sample-processing scheme, the numbers relate to the measurement order and the four direction machining areas (1. = South, 2. = West, 3. = North, 4. = East) where a slot cutting procedure will be performed.

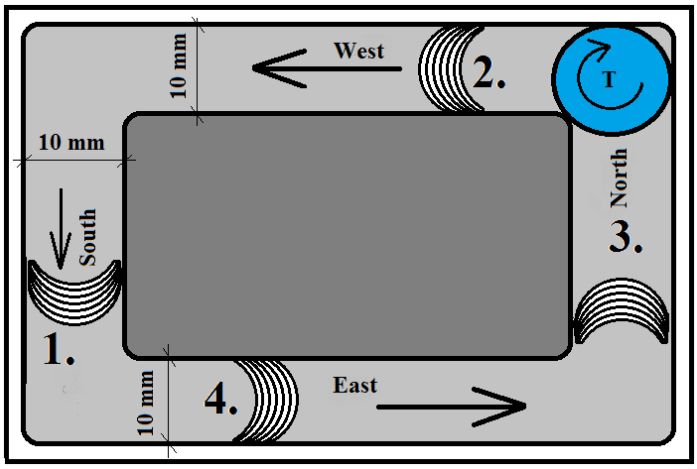

Fig. 7.1 Cutting strategy of machined samples

The ordered numbers in Fig. 7.1 represent the surface topography measurement order used later. The blue circle in the upper-right corner represents the cutting tool and its rotational movement in the CW direction. The light grey area is the machined tooth path over the sample with a general representation of the surface pattern. This is the first variable in this part of the research, with 4 direction levels. The SOUTH, WEST, NORTH and EAST cutting direction variables were selected as factor levels for statistical analysis.

Topography measurements were taken using the BRUKER CONTOUR 3D topography measurement equipment as previously, to ensure uniform measurement conditions. Every

direction was measured in two points. The measurement results are compiled in Table 7.2. The graph in Fig. 7.2 represents the mean values of S_Z. We interpret our assumptions about the milling machine axis inclination with these topography measurements, which represent the milling tool axis inclination over the specimen surface.

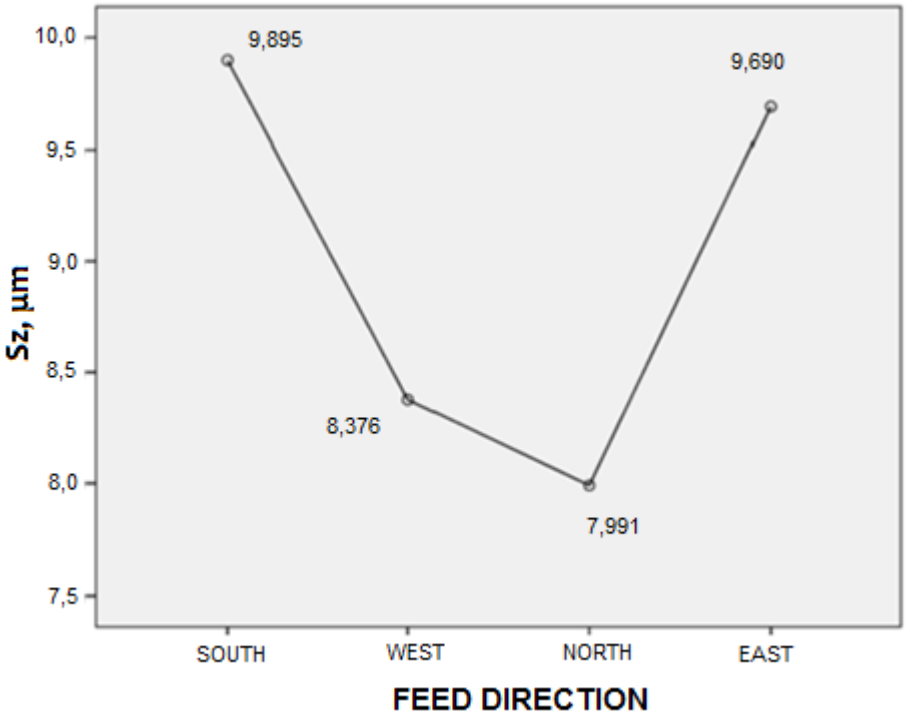

Fig. 7.2. S_Z parameter dependence on machining feed direction (first 4 samples)

Table 7.2 represents the measured mean values and their difference. This graph basically represents the inclination of the milling machine axis in relation to the milling table. Mean value differences between contrary aimed cutting directions are 16% and 24% on the respective milling machine X and Y axes.

Table 7.2 Measured mean values for the specimen with 4 orthogonal cutting directions

Feed direction	S_Z value measured, µm	Difference between directions, %
1. SOUTH	10,60445	**24%**
	9,19131	
3. NORTH	8,0833	
	7,89854	
2. WEST	8,29217	**16%**
	8,46029	
4. EAST	9,33774	
	10,04144	

Results indicate a high S_Z parameter deviation between contrary aimed cutting directions SOUTH-NORTH – the difference between opposite direction measurements are up to 24%. At the same time, measurements between opposite EAST-WEST directions represent a surface topography difference of up to 16%. If the surface topography change between opposite directions is almost ¼ of the whole topography height, it offers significant evidence to question the milling axis or machine milling table inclination accuracy.

At this point it was decided to develop broader analysis and investigate how variable cutting parameters affect the surface topography height S_Z formation in contrary aimed cutting directions. Next, the material selection and machining equipment and cutting conditions will be selected and design of experiments developed.

7.1.2. Cutting conditions and Design of Experiment

In the previous analysis (Chapter 6.) radial cutting depth was recognized as a low influence parameter on surface topography formation within end milling operations. Therefore, only one variable was left for further experiments – cutting direction. But this is not a goal, to analyze only cutting direction factor for one milling machine again and again. It was decided to add additional milling equipment – other milling machine factors, with different milling axis alignment behaviour. These factors are represented graphically in Fig. 7.3.

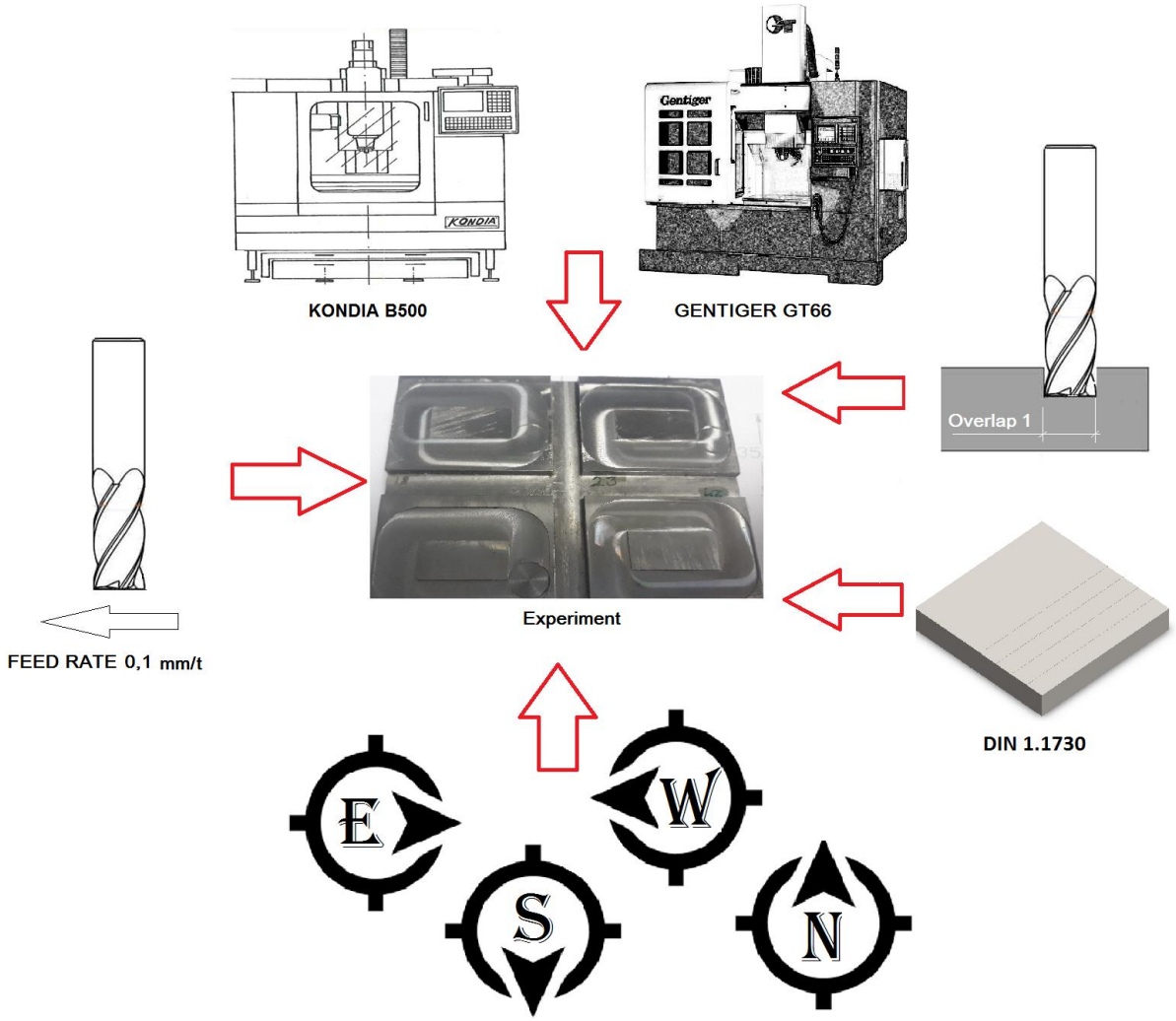

Fig. 7.3. 2nd cycle Design of experiments

In this illustration, the symbols NORTH, SOUTH, EAST and WEST represent the cutting tool direction with respect to the machine coordinate system, if one looks at the milling table from the top of the machine. The other symbols represent the machine, feed and radial cutting depth that have a single value. Other factors like cutting depth, material factor and cutting tool factors are fixed and remain constant during this experiment. In total, all the factors will give a 1^1 x 1^1 x 1^1 x 2^1 x 4^1 experiment design and will be performed on 8 samples. The experiment design serves as the basis for expert sample and processing program preparation, as well as experimental execution. These processes will be described in next sections.

7.1.3. Material and machining equipment selection

This section continues the preliminary investigation in Chapter 6 into the flat-end milling model. It was planned to develop an orthogonal sampling model to detect the cutting direction's influence on the surface topography formation parameter. This is a further exploration of the

study, so the selected material type and cutting equipment are exactly the same as in the previous chapter.

Hardened state C45U/AISI 1045 carbon steel (DIN 1.1730) was selected throughout this study. It was chosen because this material is widely used by die and mold industries all over the world. The same specimen of the material was flattened to make the same initial surface height across the sample. To ensure the same cutting system behaviour, the previously selected cutting equipment was used in this part of the research project. This allows previous results with newly obtained data to be compared. One of the milling machines used for experiment was the KONDIA B500 CNC 3-axis milling machine with a maximum spindle speed of 6000 r/min. The machine's technical specifications are presented in Table 6.3 in the previous chapter.

As mentioned above, it is important to change the cutting environment for the developed surface model testing. A good way to change the environment is to select other milling equipment – another milling machine. The GENTIGER GT-66V T16B High-Speed Milling machine (Fig. 7.4) (as described in Chapter 4.) is available and is an appropriate machine for our task. Compared with the KONDIA B500 milling machine, this machine construction is more rigid and the table is heavier (168.2 kg compared with 112.68 kg for the KONDIA B500). The machine's properties are presented in Table 7.3. The selected milling machine was available in the milling workshop for experiments and it meets the requirements for HSM milling equipment.

Table 7.3. GENTIGER GT-66V T16B technical specifications and features

Type	T16B
Spindle speed, r/min	16000
Motor power, kW	26
Axis movement (x,y,z), mm	1000*550*500
Rapid feed rate, m/min	30
Cutting feed rate, m/min	20
Milling table weight, kg	168.2

Fig. 7.4. GENTIGER GT-66V-T16B High-speed milling machine

For the GENTIGER GT-66, another spindle chuck was used, as the fixation and tool exchange mechanisms are different for both milling machines, even if the cone angle and cone standard is the same. Both machines have different tool fixtures with the same cone type but with different automatic tool feeding mechanics, therefore the different chuck designs cannot be substituted. Accordingly, the same type of cutting tool was used (described in Chapter 6.2). This was the MITSUBISHI MS2MSD1000 two-flute flat-end milling tool selected for experimental execution. The tool setup in the tools chuck was maintained as previously – 34.8 mm.

7.2. Experimental execution

Once the necessary factors were selected for experimental execution, it was time to prepare the appropriate cutting programs. Experimental executions were performed in the laboratory where previous samples were machined, applying the same type of cutting tools. The cutting depth is low, so the tool wear was not considered. The experiment consists of multiple parts:

a) Specimen preparation:

A precision vice clamp was used to fix the material specimen on the milling machine workbench and flattened with an indexable shoulder milling cutter, to ensure uniform surface height before the experiment was conducted. In this way, we obtain equal initial surface conditions for sample processing.

b) Cutting program preparation:

To avoid having several sample setups on the milling equipment workbench, a unique experimental sample was developed, where 4 orthogonal cutting directions were included in one continuous sample. The CNC program code was prepared before the experimental setup. A small part of this code, used to machine the represented sample, appears as follows:

```
N10     G71 G90 G94 G97
N20     G53
N30     T4.4
N40     M6
N50     G0 X-6 Y11 S4775 M3
N60     G0Z1
N70     G1 Z-0.3 F50
N80     G1 Y20 F954,9
N90     G3 X-11 Y25 R5
N100    G1 X-33 F954,9
N110    G3 X-39 Y20R5
N120    G1 Y11 F954,9
N130    G3 X-33 Y6R5
N140    G1 X-11 F954,9
N150    G3 X-6 Y11R5
N160    G0 Z100
N170    M30
```

The G3 code was used to avoid extra vibrations caused by starting/stoping the tool movement at the corners. The use of the G97 code is necessary to keep a constant surface speed and revolutions per minute in the spindle. CNC programs for other samples processed in this study are included in Appendix B, at the end of this document. The inevitable start/end point can be seen in the lower right corner of Fig. 7.5. This leaves a completely different mark than in the rest of the path.

c) Machine setup and machining execution:

The CNC execution program was loaded into the PC of the milling machine. Post processing execution was performed manually and the test run of the machine was launched to confirm the accuracy of the prepared CNC program. After successful testing, the end-milling process was

launched in automatic mode. After milling, the specimen was cleaned and lubricated with grease, to avoid oxidation.

d) Measurement execution:

To ensure uniform measurement conditions, the measurements were taken with the same BRUKER CONTOUR 3D topography measurement device, as previously. In general, one sampling area on each sample was selected (Fig.7.5) at the diagonal center point of the machined path. Two measurements were taken at the sampling area. Thus it is possible to see an analysis of two measurement results in further sections. The same filters were used to obtain the filtered surface topography images. The collected data will be used for further analysis, as described in next section.

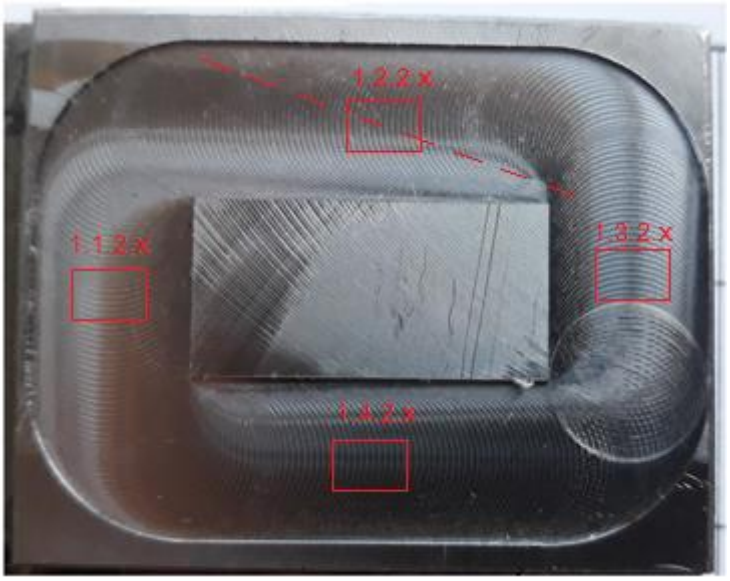

Fig. 7.5 Location of sampling areas for measurements on the specimen

7.3. Analysis of experimental results

This section deals with the qualitative and quantitative analysis of result data from the performed experiments. The same analysis procedure as described in Section 6.5 was applied. Results of the sample measurements are compiled in Appendix C – Surface topography measurements.

7.3.1. Numerical analysis

Numerical analysis starts with descriptive statistics. This method is used to describe the basic features of the technological parameter (factors) and measured data in a study. They provide simple summaries about samples and their measurements. Together with simple graphical analysis, they form the basis of virtually every quantitative analysis of data [117 - 118]. Descriptive statistics have been prepared for measured values obtained on the specimen

diagonal, at a distance between the center and specimen corner point (Fig. 7.5 – sampling areas 1.1.2.x (#3 - #4) –1.4.2.x (#21 - #22)) For the measurements, the author used the BRUKER contour GT3 optical surface topography measurement device. A Gaussian filter was applied for every sample before saving the measured values. Measurement results were processed with the MountainsMap Premium software tool. From the measurements, the author obtained numerical values of surface roughness, in μm, and other values as ratios.

Statistics of measurements are represented in Table 7.4. It represents a number of valid and missing data from the measurement, along with other statistical averages like Mode, Median, Mean, etc. It shows 16 measurements taken for the analysis (DoE represented 8 samples with 2 measures from each of them). The Represented Mean value - is the central value of a discrete set of numbers. Median is the central value of the entire data set, but if there is an even number of samples, then the median is the average value of the two central samples. This value separates higher values from the lower values of the data set. The mode of a distribution with a discrete random variable is the value of the term that occurs the most often. Std. deviation is a measurement that represents dispersion of a set of data values. Skewness represents symmetry of the data set value distribution, but kurtosis represents whether the data are heavy-tailed or light-tailed relative to a normal distribution. Std. error of kurtosis and Std. error of skewness represents the normality of the data distribution. The standard error of Skewness and Kurtosis suggest that the data is likely to be relatively normally distributed. [126][127]

Table 7.4. Statistics of S_Z measurements

N	**Valid**	16
	Missing	0
Mean		13.1509
Median		12.3785
Mode		7.654
Std. Deviation		2.8106431
Skewness		0,244
Std. Error of Skewness		0,564
Kurtosis		1,63
Std. Error of Kurtosis		1,091

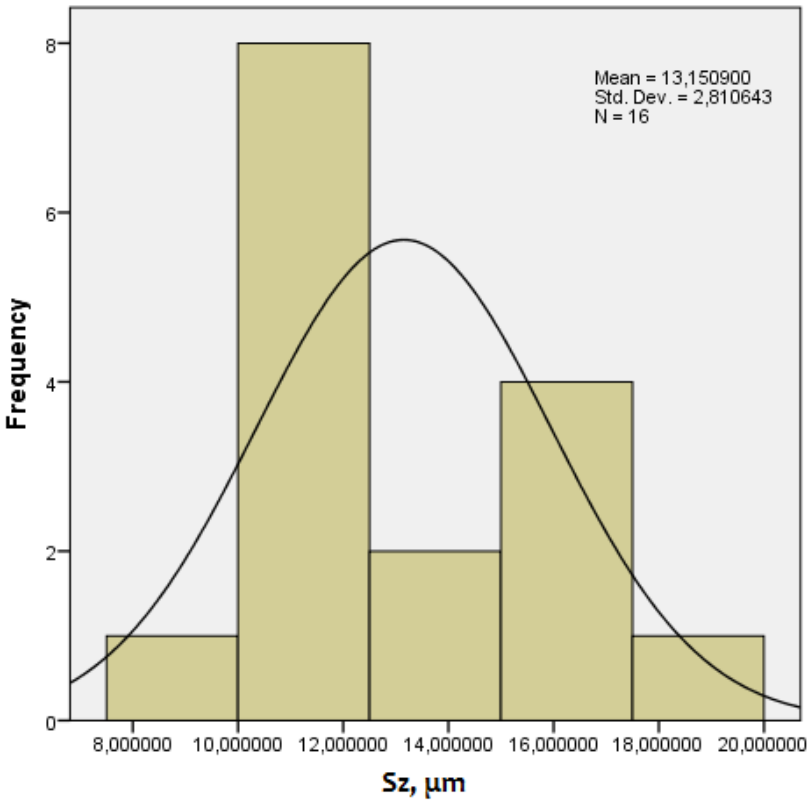

Fig.7.6 Parameter S_Z frequency distribution histogram #1

The frequency histogram is shown in (Fig. 7.6). The histogram of measured data confirms the statistics fixed in Table 7.4. The skewness value is positive: 0,244 (positive skewness), which means that the histogram distribution curve is moved to the left of the median and the curve is fairly symmetrical. Skewness indicates that data is located around the Median and is not skewed. Kurtosis is also positive: 1,63. This shows that the average level of parameter distribution is lower than normal distribution.

The Box-Whisker plot of means represents a median value for every factor that the author has selected – the milling machine is variable in our experiment (Fig. 7.7). The Box-Whisker diagram analysis reveals an even surface topography height distribution for the selected equipment around the Median value of dataset and no excessive surface height deformations were detected by the topography measurements. This indicates that measurement accuracy is acceptable.

Surface topography, on average, is higher for the KONDIA B500 milling machine, while the GENTIGER GT66 milling machine generates samples with lower surface topography height parameter S_Z values. Topography height values for the KONDIA milling machine are scattered further from the median value than for the GENTIGER machine. This leads us to conclude that the GENTIGER milling machine is more accurate than the KONDIA.

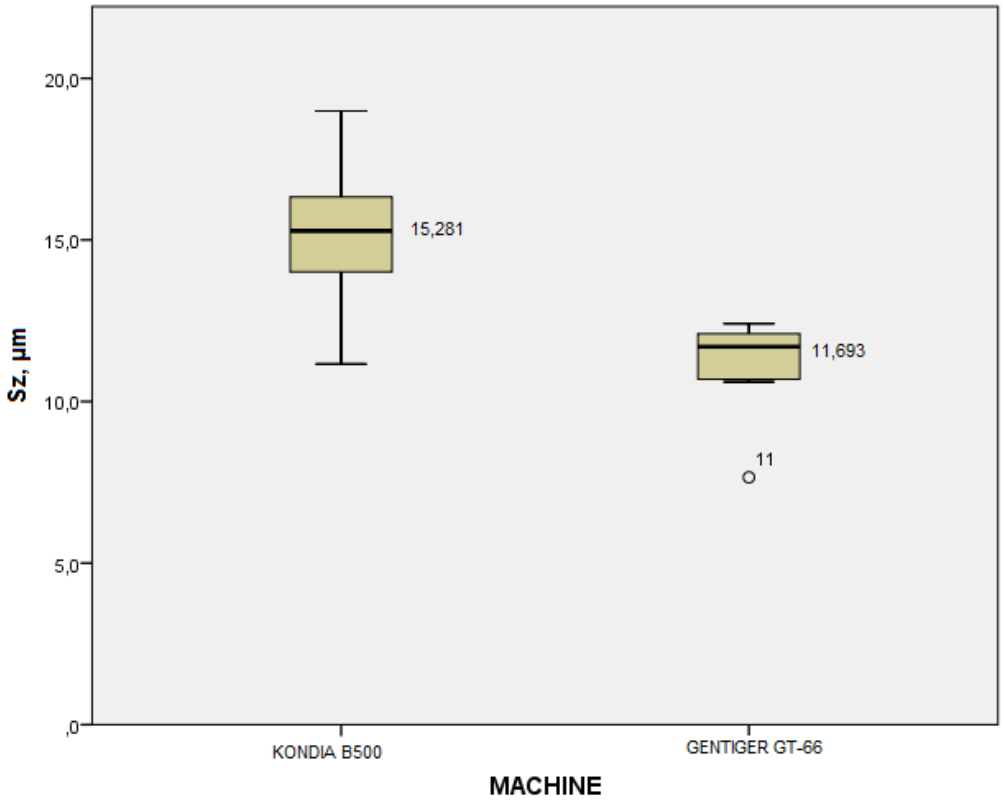

Fig. 7.7. Box-Whisker diagram for milling machine influence analysis

The same boxplot analysis has been undertaken with the Cutting-Direction factor - Fig. 7.8. In this case, all the measured points belong to the data array, except sample #11. No abnormal surface deformations were observed for the KONDIA B500 milling machine that may create extremely high topography measurement values. The GENTIGER GT-66 milling machine sample with order number #11 represents an abnormally low value. This result may arise from interpretation samples, where surface topography is slightly higher, with some excessive topography peak points, but sample #11 is the only sample where no excessive deviation is observed, only the clear cutting process.

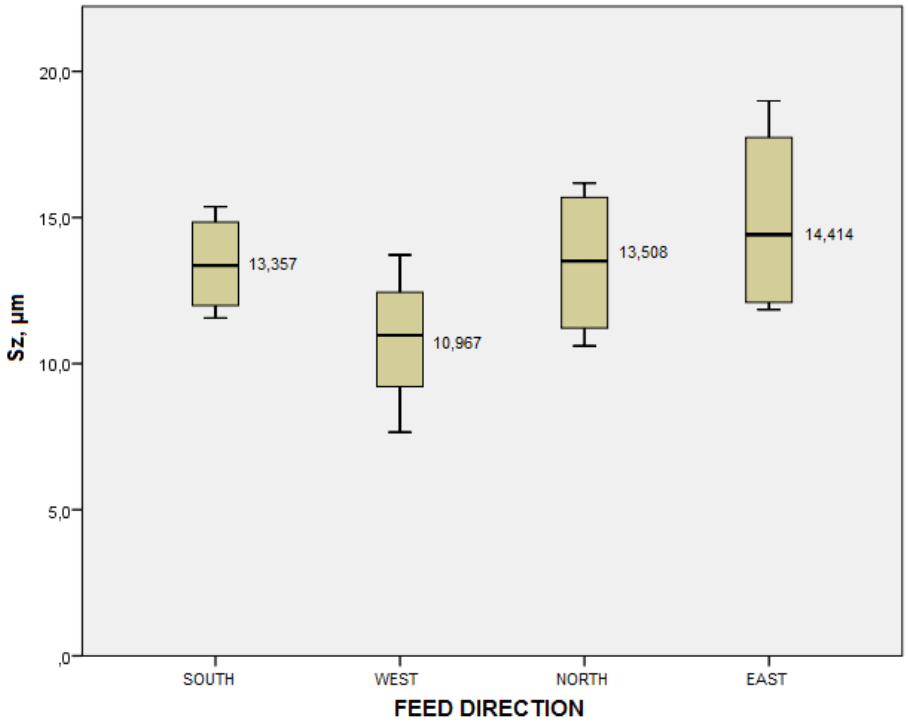

Fig.7.8. Box-Whisker diagram for cutting direction factor influence analysis.

Boxplot represents the surface topography measurement data distribution in orthogonal cutting directions. It also shows that there are differences between median values in these directions. The SOUTH and NORTH direction median values are similar, while in the WEST cutting direction topography, the height is slightly lower than in the EAST direction. But are these differences significant enough for surface topography formation? The next chapter will provide an answer.

7.3.2. ANOVA analysis of the influence of cutting feed rate, radial cutting depth and cutting direction on S_Z formation

Descriptive statistics calculated in the previous section describe the selected data reliability. At this point, the factor influence must be checked by verifying the null hypothesis for each of them. To this end, One-way ANOVA or univariate analysis has been used.

The hypothesis to analyze is:

$H_{0\text{-}1}$ – Milling machine has no significant influence on the surface topography parameter S_Z.

$H_{0\text{-}2}$ – Cutting direction has no significant influence on the surface topography parameter S_Z.

The ANOVA results for machine factor are represented in Table 7.5. The CORRECTED MODEL is the sum of squares that can be attributed to the set of all between-subject effects, excluding the INTERCEPT [128]. TOTAL and ERROR represent values related to the SPSS

internal model used to calculate ANOVA. The CORRECTED TOTAL is the squared deviation of the dependent (S_Z) variable without mean value of data set.

Calculation generates F-value = 17,284. Sig. coefficient is lower than 0,05 which is the lowest value of significance to reject the H_0 hypothesis. Sig.=0,001 < 0,05. The result reject Null hypothesis $H_{0\text{-}1}$. Hence, selected milling machines have significant influence on the surface height formation.

Table 7.5. Tests of Between-Subjects Effects – milling machine

Dependent Variable: S_Z

Source	Type III Sum of Squares	df	Mean Square	F	Sig.
Corrected Model	65,468	1	65,468	17,284	0,001
Intercept	2767,139	1	2767,139	730,554	0,000
MACHINE	65,468	1	65,468	17,284	0,001
Error	53,028	14	3,788		
Total	2885,634	16			
Corrected Total	118,496	15			

Where df – degrees of freedom, F – F-value from descriptive statistics, represent the significance of the model dependent variable, Sig. – significance coefficient P value.

In the same way, the ANOVA results for the cutting direction factor have been represented in Table 7.6. This time, the significance coefficient *P* (Sig.) value is 0,229. P (Sig.) > 0,05, thereby the null hypothesis H_0 has been approved. We conclude that the cutting direction factor alone, has no significant influence on the surface texture parameter S_Z. As analysis will show later, this is nevertheless an important factor, together with the feed factor, on the surface topography formation, even if the descriptive statistics reject this hypothesis.

Table 7.6. Tests of Between-Subjects Effects – Cutting Direction

Dependent Variable: S_Z

Source	Type III Sum of Squares	df	Mean Square	F	Sig.
Corrected Model	34,686	3	11,565	0,361	0,229
Intercept	2767,139	1	2767,139	123,314	0,000
DIRECTION	34,686	3	11,565	0,361	0,229
Error	83,809	12	6,984		
Total	2885,634	16			
Corrected Total	118,496	15			

As mentioned previously, 2 sampling points were selected for each specimen cutting direction, designated as separate samples. Arithmetical means of measurements represent the different surface height behaviour at each plotted machining direction point. Fig. 7.9 represents the plots of the cutting direction influence. Numerical analysis shows a low significance for cutting direction influence. However, significant differences are found when comparing both directions on samples machined with the KONDIA machine: NORTH-SOUTH and EAST-WEST.

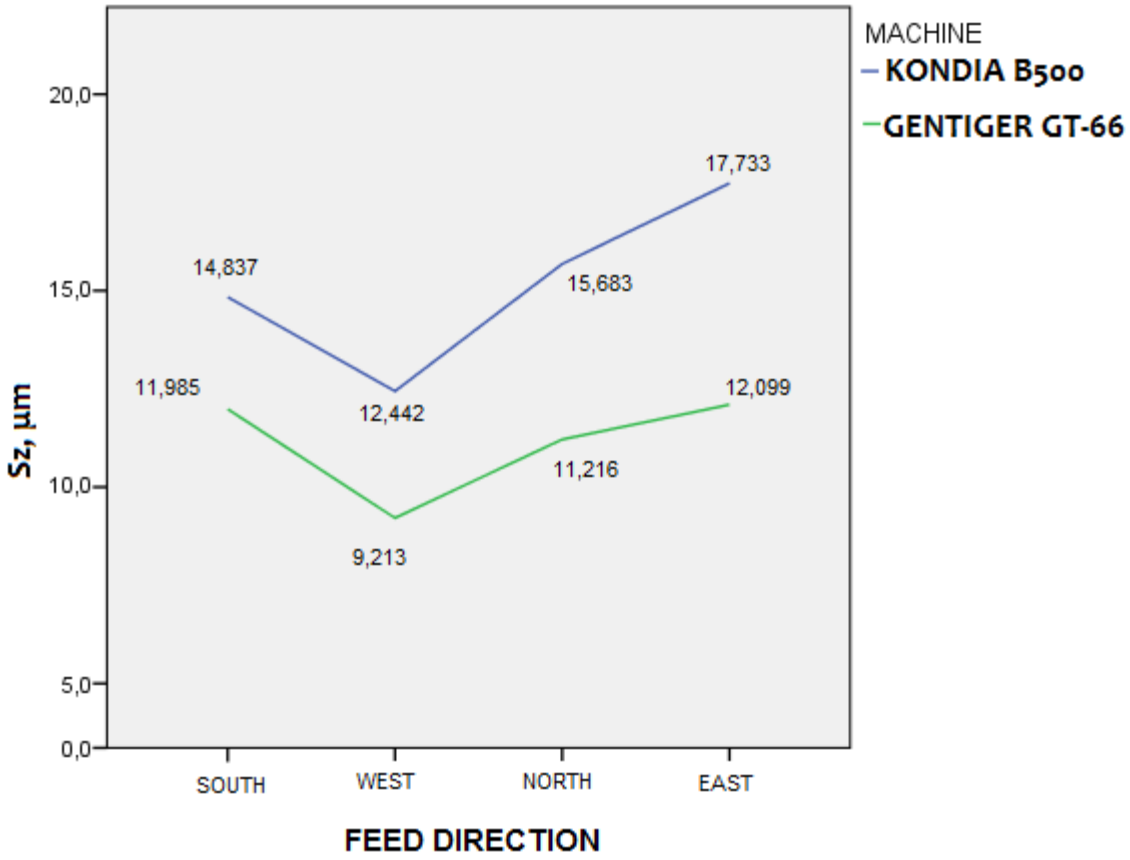

Fig. 7.9. Sz parameter dependence on machining feed direction (both machines)

As we can see, the difference between values in the SOUTH-NORTH (S/N) direction (Y axis of the machine) for GENTIGER is negligible, but values in the EAST-WEST (E/W) direction (X axis of the machine) are higher and can have a significant influence on the surface topography height. Surface height behaviour for both machines is similar and may be just luck in the measurements. However with the KONDIA machined sample, the difference between each two opposite directions is significantly higher. The difference is up to 5µm in the WEST-EAST direction and up to 3µm in the SOUTH-NORTH direction. Next, we will see how the ANOVA Test between subject analysis will respond to both feed factor and cutting direction interaction.

The Between-Subjects test is a good tool to test several subject factor interactions. Combinations of factors show to the author why some additional factors cannot be simply excluded from further analysis. Milling machine and cutting direction factors have been tested together, to see the influence of their interaction on surface topography formation.

Table 7.7 shows that the interaction between milling machine and cutting direction factors is not significant. The F value for both factor interaction is 0,944 (Sig. =0,464 respectively), which means that the direction factor is not significant either alone or in interaction with the milling machine factor. But, as the plot of means reveals, and the between-subjects test confirms, the direction factor becomes statistically significant, if the conditions of differences in milling equipment is analysed. The plot of means (Fig. 7.9) represents the deviation between directions that should not be overlooked.

Table 7.7. Tests of Between-Subjects Effects – milling machine and direction

Dependent Variable: Sz

Source	Type III Sum of Squares	df	Mean Square	F	Sig.
Corrected Model	104,950	7	14,993	8,855	0,003
Intercept	2767,139	1	2767,139	1634,229	0,000
DIRECTION	34,686	3	11,562	6,828	0,013
MACHINE	65,468	1	65,468	38,664	0,000
DIRECTION * MACHINE	4,796	3	1,599	0,944	0,464
Error	13,546	8	1,693		
Total	2885,634	16			
Corrected Total	118,496	15			

Cutting direction measurements (WEST direction) reveal the same low value, similar to previous samples. Otherwise, SOUTH direction measurements are lower than in the NORTH and even in EAST cutting directions. The topography behaviour of other directions reveals a difference, but it is more random than certain difference, and is not caused by the milling axis inclination. In general, we can assume that these results indicate a milling axis inclination in NORTH and EAST directions for the KONDIA B500 milling machine and milling axis inclination in SOUTH and EAST cutting directions for GENTIGER GT-66 milling machine.

Summary:

Statistical analysis has been applied to the measured values to detect the reliability of the measurements taken. It also offers an understanding of how the selected factorial variables influence the surface topography formation. According to the analysis, all measured values belong to the normal distribution. The test of Between-Subjects analysis shows that the influence

of selected input factor is not always certain for a selected dependent variable. Some factors are not representative when they are used alone. However, in combination with other factors, their importance grows. Die and mold manufacturing processes are complicated due to different cutting regimes combinations, such as tool movement direction and variation of feed rate. The combination of them is more important than additional factor influence. Statistical analysis represents these statements with reliable numbers. In Table 7.7 the influence of the DIRECTION factor is represented. Cutting direction as a separate factor becomes significant, if different milling equipment is used for sample development. If we consider only one individual milling machine, the DIRECTION factor is not significant at all. Meanwhile, MACHINE and DIRECTION factor interaction shows a lower F value, which means that the DIRECTION factor, for both of machines, makes a tiny change on surface topography formation, albeit not significant. In general this statement confirms hypothesis $H_{0\text{-}2}$ – Cutting direction has no significant influence on the surface topography parameter S_Z. However only one specimen per machine was prepared. Hence, the comparison of cutting direction influence on both machines will always reject the null hypothesis due to the low number of specimens prepared. To make statistical results more reliable, the number of specimens must be increased.

Previous analysis led the author to think about different indirect factors involved in the formation of the 3D surface topography parameters. For this reason, statistical analysis methods are not always reliable in practice to predict 3D surface topography parameters. Differences in machine types, behaviour of cutting tools and machined materials and even workpiece size may have an effect on surface parameter formation. To obtain the same effect with statistical analysis, the number of samples has to be increased. There is no defined number of samples that will produce a reliable result in terms of statistical analysis; therefore another type of surface topography prediction tool has to be in the event of a low number of samples.

Many authors of different publications, reviewed in Chapter 2, wrote about the mathematical description of surface topography and roughness prediction. A mathematical model could be the most accurate tool to predict the surface formation. But, most models consider only general cutting conditions and prediction issues; they do not consider particularities that may affect the overall result of predicted surface topography parameters. For this reason, particular indirect influence properties have to be extracted for mathematical surface topography formation model development. As topography measurement results represent different topography levels in every cutting direction and the same behaviour repeated with different samples, there is reason to believe that milling equipment has some particular inaccuracy on the milling head or column of the machine. An inaccuracy error value can be derived from the topography measurements and used for further calculations..

At this point it was decided to improve the mathematical model for surface maximum height parameter S_Z calculation, considering cutting tool inclination and deflection values.

7.3.3. Visual analysis

Numerical analysis is insufficient without visual analysis to validate scientific justifications and vice versa. To claim the behaviour of surface topography formation changes, these changes have to be justified with numbers. At the same time, numbers cannot be explained without visual representation. An orthogonal cutting sample and generated surface topography images are no exception. Different cutting directions result in different topography patterns. Firstly, as shown in Fig. 7.10, the surface topography reflects the cutting edges paths during the machining. In this figure, fine arrows indicate cutting feed direction and thick arrows indicate back cutting edges marks, in the movement to engage a new material section.

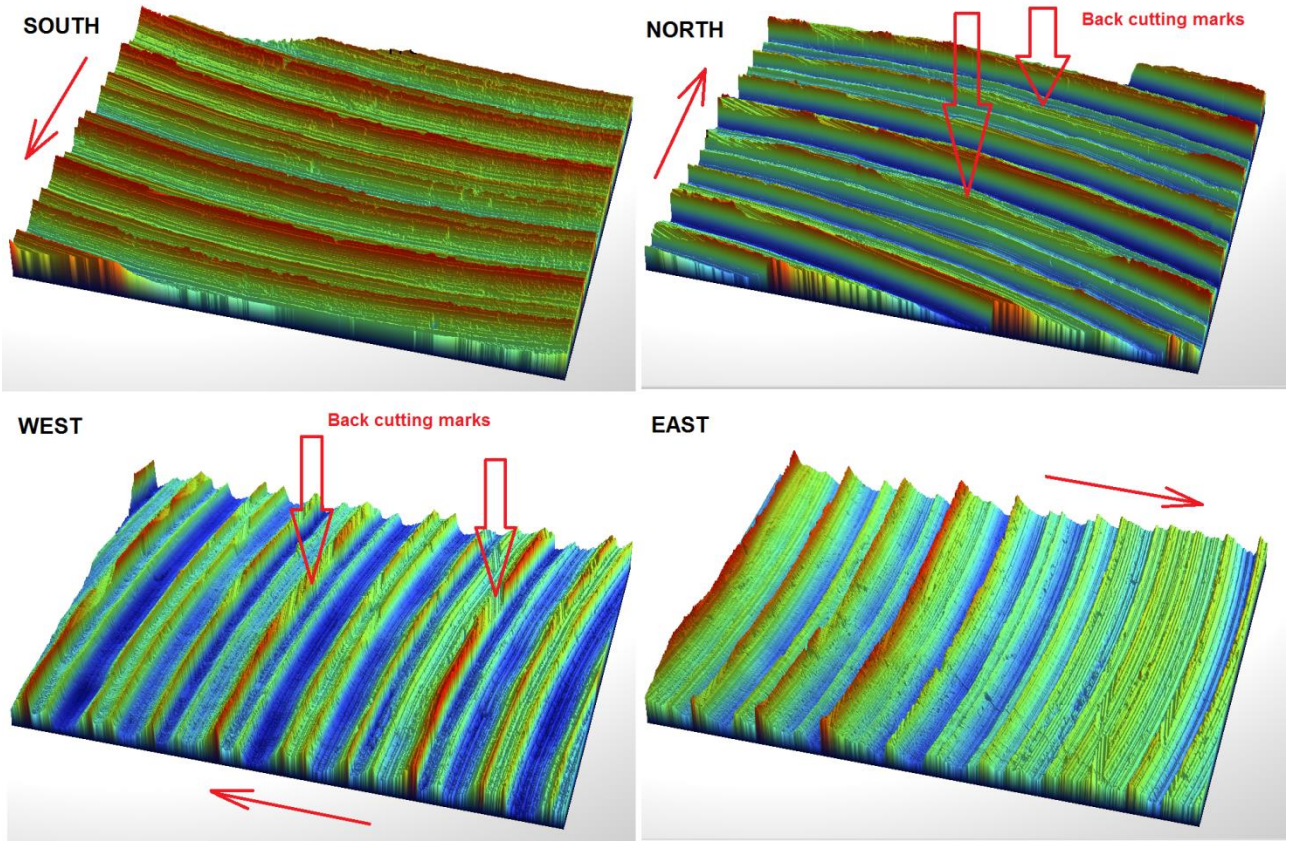

Fig. 7.10. Samples #1 - #2, Feed = 0,1 mm/tooth, material 1.1730 – Machined with KONDIA milling machine

From the surface topography images it is possible to clearly identify the cutting direction. The flattest surface peak slope decreases in the cutting feed direction. This slope results from the cutter's clearance side of the cutting edge. Distances between the highest peaks coincide with the cutting feed per tooth. This phenomenon appears due to the cutting tools geometrical behaviour. Concavity angle always perform minimum surface topography pattern and this pattern is clearly represented on machined surface. Why doesn't back-cutting edge leave its effect on surface

topography formation? Surface topography measurements are taken on the area with the highest uncut chip thickness. This causes high tool deflection and back-cutting edge is moved away from the machined surface. Back cutting is often observed in areas where uncut chip thickness is small. In some directions it is still possible to observe the back-cutting phenomenon at the highest uncut chip thickness area. Why?

The samples also represent cutting tool and milling equipment accuracy behaviour. In some of the sample surface topography, back cutting marks can be observed, but not all. The first specimen sample #1 in the SOUTH direction and Feed rate of 0,1 mm/tooth does not contain any traces of back cutting at the sampling point, Fig. 7.10. Considering mean values from Fig. 7.9 and observations from surface topography images, we can assume that the milling head is strongly tilted in the South direction. This means that the cutting tool inclination/deflection is high enough to cover the tool concavity angle performed back cutting phenomenon.

The tool inclination and cutting force caused a deflection, increasing the surface topography parameter S_Z value in the SOUTH direction. Accordingly, the surface topography in the opposite cutting direction should decrease. Numerical and visual analysis of samples with WEST cutting direction identifies low surface topography parameter S_Z values. However the SOUTH cutting direction does not represent a high tool inclination. The back cutting marks appear in both directions. These marks are more likely to be caused by tool deflection rather than milling head alignment inaccuracy. Some local deformations appear on every sample, and this can be related with chip extraction failure, cutting tool and material surface failure or vibration, causing tool deviations. The difference between the surface height parameter S_Z in opposite directions can be calculated as a combination of the inclination of the milling equipment axis and tool deflection.

From visual analysis, it can be concluded that the cutting direction influences the surface topography formation. It reflects both the machine and tool behaviour during machining. The statements of this section will be considered in the mathematical model development in the next sections.

7.4. Theoretical model of contrary cutting directions

Visual analysis and descriptive statistics in the previous section reveals two cutting equipment properties acting on the cutting process. One of them is the milling axis inclination, which influences the cutting direction; the other is the influence of tool deflection, caused by the cutting force. In this section, these two factors are included in the theoretical prediction model.

7.4.1. Cutting force model influence on cutting tool deflection

This section describes the cutting tool deflection, caused by cutting force changes during the cutting process. Cutting force directly affects cutting tool deflection, so a cutting force model is crucial for prescribing the instantaneous tool deflection during the cutting process. This section

contains two aspects of the analysis – force model development and cutting force influence on tool deflection.

a) Cutting force model development

The cutting tool tends to deflect as the cutting force increases against its cutting flute. The cutting force consists of the tangential cutting force (Ft), normal cutting force (Fn) and axial cutting force (Fa) components, represented in Fig. 7.11. In this illustration, λ is the angular tool location, known as the tool immersion angle.

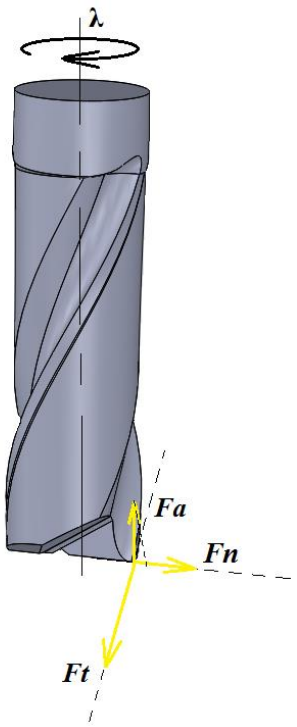

Fig. 7.11. Cutting tool and respective cutting forces Ft, Fn and Fa in the cutting tool coordinate system

No direct cutting force measurements were taken during the cutting process. Nowadays, the Finite Element Method (FEM) has become a reliable tool for engineering calculations and has been widely used for the kinds of statistical and dynamic process calculation. Accordingly, simulation was selected as the appropriate tool to estimate the cutting forces. A Finite Element model was developed with the AdvantEdge^{TM} commercial software tool. A realistic tool-workpiece interface was developed. FEM simulation was performed taking into account all cutting tool geometrical parameters obtained from tool geometrical measurements and material properties from the tool manufacturer.

Experimental cutting parameters (represented in Table 6.2) were applied to the FEM simulation, to simulate the same cutting conditions. For FEM simulation we used three different cutting feed rates – 0,04, 0,1 and 0,2 mm/tooth. Radial cutting depth parameter was selected 5

and 10 mm and spindle speed was set to 4774 r/min according to the design of experiments. Other process parameters like cutters length, in this case, were not considered, but all the cutting tool angles were defined according to the cutting tool measurements: Rake angle - 10°, concavity angle – 2°, helix angle - 30°, primary relief angle - 13°. Measured cutting tool helix spiral length is 29 mm, length of primary clearance land is 0,9 mm, but cutting tool core diameter is 6,71 mm. Cutting tool material defined as carbide-general with TiAlN coating layer, similar as used for real cutting tool used in experiments. AdvantEDGE^{TM} software has its own material library with C45 material available, therefore material properties were defined with software resources. Workpiece dimensions were defined to cover whole cutting tool radial cutting depth and leave enough material for chip formation to every side. Finite element meshing was improved for workpiece model with definition of minimum element size – 0,01 mm. Smaller definition of element size was not possible due to computational resources and not necessary as minimum feed rate is 0,04 mm/tooth. Other FEM model mesh definitions were standard, suggested by software. Adaptive re-meshing mesh refinement factor value was set to 2, but mesh coarsening factor value was set to 4. Meanwhile, chip refinement factor value was set to 2 – medium value and grading value was set to 7. Otherwise, cutting tool mesh factors were improved, to improve the accuracy. Minimum tool element size was decreased from its standard value 0,1mm down to 0,05 mm, as this was the lowest value to execute FEM calculation within transparent period. However, mesh grading was set to 0,1 as cutting tool is un-deformable for this simulation. Model execution was performed without run out parameters active for FEM simulation. All the rest unnamed parameters over the FEM simulation were default. AdvantEDGE software automatically defines workpiece constrains and cutting tool movement trajectories and paths.

Simulated cutting forces are represented in Fig. 7.12. The plotted simulated cutting forces represent cutting force deviation as the uncut chip thickness increases. The simulation results are cutting forces in the X, Y and Z directions. X direction corresponds to cutting tool feed direction, consequently the cutting force Fx will be used to calculate cutting tool deflection and consequent Sz parameter deviation. With FEM simulation authors obtain cutting forces that are numerically graduated in relation to the immersion angle λ of the cutting tool.

Cutting forces in the machine coordinate system consist of the local tool cutting force components Ft, Fn and Fz.

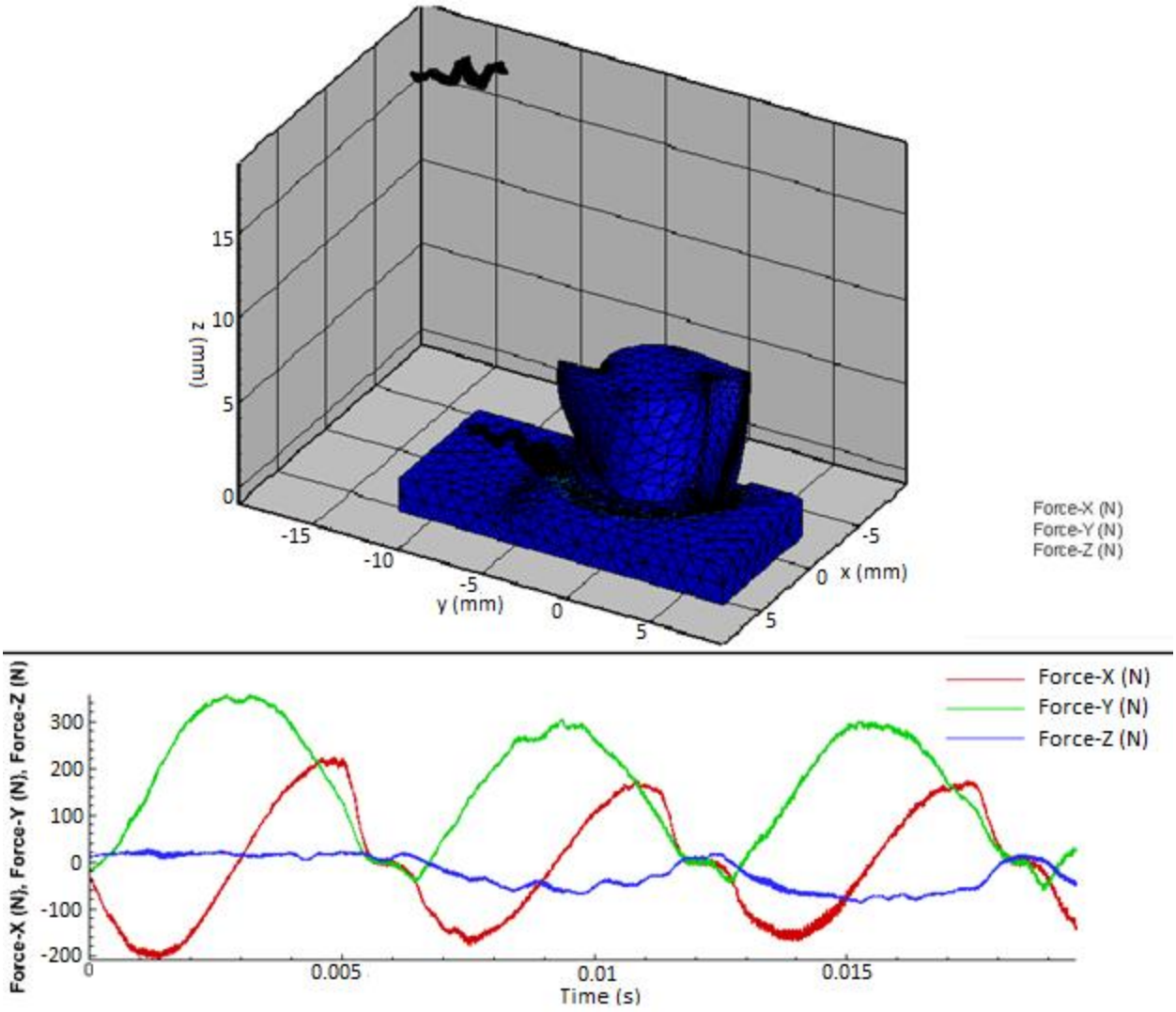

Fig. 7.12. Results of simulated cutting forces at extra high feed rate – 0,4 mm/ tooth.

With FEM simulation, numerically graduated cutting forces in relation to the immersion angle λ of the cutting tool were obtained. Results from the FEM software were exported directly into Excel tables. Simulated cutting forces were used to determine cutting coefficients for the DIN 1.1730 material. To mathematically calculate the numerical values of cutting coefficients, the local coordinate system cutting force equations substituted (7.1 – 7.3) into the machine coordinate system cutting force equations (7.5. - 7.7) and express coefficients as a result of cutting forces and immersion angle interaction. The Excel Solver tool was applied to fit the simulated data with the mathematical model and to propose the material's cutting coefficients Kt, Kn and Ka. The data fitting method applies the data from FEM analysis and extracts the cutting force coefficients to determine the machined material properties to be used in the analytical model. The determined cutting coefficients for DIN 1.1730 are: Kt = 2563 N/mm^2, Kn = 0,0089 N/mm^2 and Ka = -0,269 N/mm^2. After fit model development, the calculated cutting forces were

graphically compared with simulated ones. Cutting coefficients was fitted several times to obtain the most accurate simulated cutting force match with simulated cutting forces. The plot of the cutting forces (Fig. 7.13) represents this match:

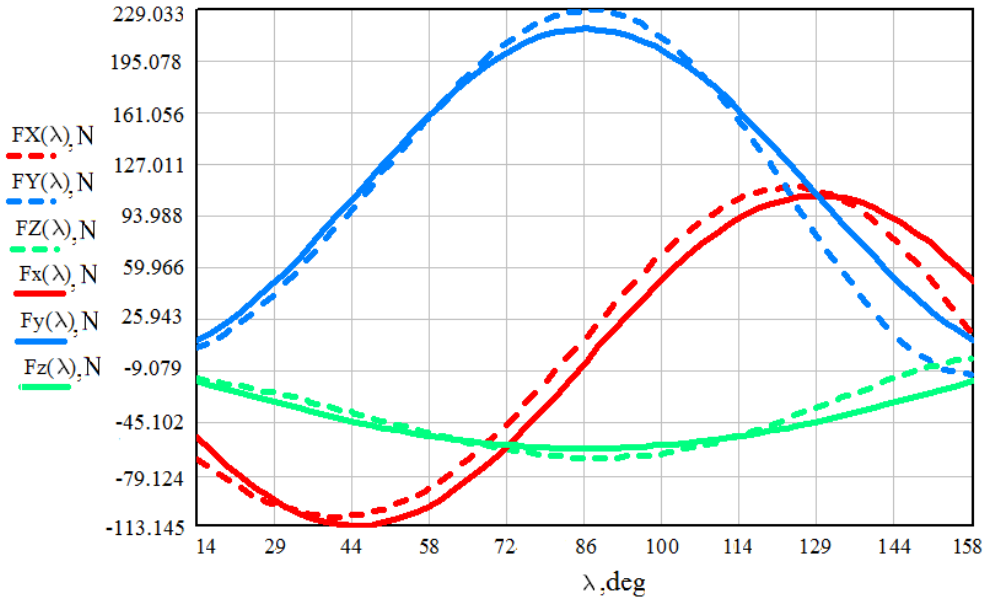

Fig. 7.13. Plot of cutting forces *Fx*, *Fy* and *Fz* (in Newtons) along the tool immersion angle λ (in degrees)

In the cutting force plot above, a discontinuous line represent the cutting forces simulated by FEM and a continuous line represents the analytically predicted cutting forces, by using predicted material cutting coefficients. The X axis (abscissa) of the plot represents Cutting tool immersion angle λ in degrees and the Y axis (ordinate) represents Cutting force graduation in N (Newton's). As can be seen, the model is not perfect. There are some mismatches in designated areas, but improvements of force Fx (fitted coefficient accuracy) reduce the accuracy of forces Fy and Fz. Therefore, this model is the best possible solution for exact calculation. Table 7.8 below represents the simulated cutting forces for the appropriate cutting feed value.

Table 7.8 Machine coordinate system cutting force peak values according to the selected feed rate

FEED RATE *f*, mm/ tooth	**Fx, N**	**Fy, N**	**Fz, N**
0,04	15,2	30,8	8,3
0,1	38,7	76,9	20,7
0,2	76,2	153,8	41,4

The given cutting coefficients allow to calculate cutting forces in any cutting tool position. With knowledge of the cutting forces, real-time cutting tool deflection could be calculated during one tool rotational movement.

Cutting force components can be determined by a general, well known, model that uses three cutting pressure coefficients Kt, Kn and Ka, where Kt is the cutting pressure for tangential force, and Kn and Ka are the cutting pressure for normal and axial forces. Kn and Ka are expressed as a function of Kt. Using these cutting pressure coefficients and the instantaneous uncutt chip cross section tc, the cutting forces components in a local coordinate system of the tool are [18]:

$$\mathbf{Ft}(\boldsymbol{\lambda}) = \mathbf{Kt} \times \mathbf{tc}(\boldsymbol{\lambda}) \tag{7.1}$$

$$\mathbf{Fn}(\boldsymbol{\lambda}) = \mathbf{Kn} \times (\mathbf{Kt} \times \mathbf{tc}(\boldsymbol{\lambda})) \tag{7.2}$$

$$\mathbf{Fa}(\boldsymbol{\lambda}) = \mathbf{Ka} \times (\mathbf{Kt} \times \mathbf{tc}(\boldsymbol{\lambda})) \tag{7.3}$$

The uncut chip cross section tc, depends on the feed, f, cut depth, ap and tool immersion angle, λ, and is expressed as:

$$\mathbf{tc}(\boldsymbol{\lambda}) = (\mathbf{f} \times \mathbf{sin}(\boldsymbol{\lambda})) \times \mathbf{ap} \tag{7.4}$$

The cutting force components, Fx, Fy and Fz, in the machine coordinate system [18][24] are:

$$\mathbf{Fx}(\boldsymbol{\lambda}) = -\mathbf{Ft}(\boldsymbol{\lambda}) \times \mathbf{cos}(\boldsymbol{\lambda}) - \mathbf{Fn}(\boldsymbol{\lambda}) \times \mathbf{sin}(\boldsymbol{\lambda}) \tag{7.5}$$

$$\mathbf{Fy}(\boldsymbol{\lambda}) = \mathbf{Ft}(\boldsymbol{\lambda}) \times \boldsymbol{sin}(\boldsymbol{\lambda}) - \mathbf{Fn}(\boldsymbol{\lambda}) \times \mathbf{cos}(\boldsymbol{\lambda}) \tag{7.6}$$

$$\mathbf{Fz}(\boldsymbol{\lambda}) = \mathbf{Fa}(\boldsymbol{\lambda}) \times \mathbf{sin}(\boldsymbol{\lambda}) \tag{7.7}$$

Fig. 7.14 represents the two cutting systems – machine and tool. The *S1* coordinate system relates to the cutting tool. Cutting force normal component vector Fn – force vector is pointing in normal towards the cutting edge, the tangential component Ft – is pointing parallel to the cutting surface, while the axial component Fa – is parallel to the cutting tool axis. *S2* represents the machine coordinate system that is fixed to the machine basis and doesn't change with the tool rotation or cutting direction. Forces Fx, Fy and Fz are related with cutting force coefficients Fn,

Ft and Fa combined with the cutting tool immersion angle λ. Tool immersion starts at a 0° angle, where uncut chip thickness is 0 mm, it increases until it reaches the theoretical maximum uncut chip thickness at a 90 degree angle and cutting continues until it reaches the 180 degree angle, when the uncut chip thickness becomes 0 mm again. Cutting force coefficients change in relation to the uncut chip thickness and its interaction with the cutting tool main cutting edge.

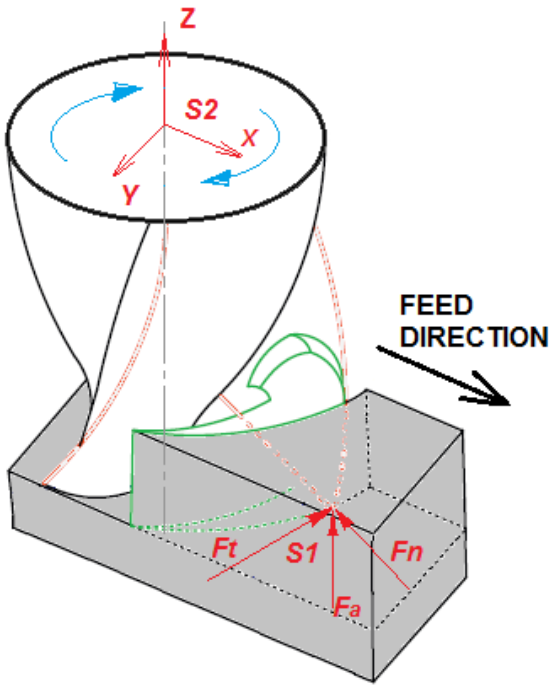

Fig. 7.14. Cutting forces – local tool coordinate system S1 and machine coordinate system *S2*

b) Cutting tool deflection model

Cutting tool deflection has two important components. One is tool deflection on the Z axis, to detect the cutting tool deflective variation within one cut in the axial direction. This component affects the surface geometry errors in general. The other is the tool deflection component in the cutting feed direction. This component affects the surface topography parameter group formation, along with the spatial and height parameters. In further analysis we will use both of these components to develop the most reliable surface topography prediction model.

To analyze the impact of cutting force on tool deflection we used FEM software for deflection analysis. With FEM software we can determine the tool rigidity coefficients and use them later to calculate tool deflection amplitude. For this FEM simulation, Abaqus™ software was used. Abaqus™ is known and widely used FEM software for developers, scientists and industrial manufacturers. To perform a precise simulation, a realistic cutting tool CAD model was developed with SolidWorks software, considering all the measured cutting tool dimensions, tool length out of chuck and its material. First, the CAD model was integrated in FEM software (Fig. 7.15). Material and coating properties were provided by the cutting tool manufacturer –

Carbide standard tool with TiAlN coating layer on the work surface. Material properties were selected by software tool available resources for Tungsten Carbide (WC) material. Defined Young's modulus was 580 GPa, but density – 14,45 mg/m^3. Length of the cutting tool for simulation was set to 34,8 mm, since this is the tool length out of the chuck. We do not consider the effect of the chuck deflection, so this was assumed as basis of cutting tool. In this zone, constraints of fixed position in the Abaqus™ software were defined. Single load was defined against the cutting tool tip point, simulating the effect of cutting force on the curvature of cutting tool, along its length out of the chuck. Defined mesh type in software was 10-node quadratic tetrahedron elements from standard element library. This type of elements fits to the shape of cutting tool and do not create errors in meshing cycle. 11568 elements were created with element minimal element size of 0,059039 mm, Min/Max angle: 14,10 / 131,.66 and Aspect ratio of 2,14, but geometric deviation factor is 2,20e-006. These are standard values proposed by software automatic meshing tool, if there is selected appropriate element type that fits to the tool CAD model.

Graduated cutting forces of 0, 100, 300 and 500 N were applied against the cutting tip point in the 3 axes and FEM simulations were performed. Selected force values represent the incremental distribution of the expected cutting forces in a real cutting process. From each simulation, the tool tip point displacement from its initial position (when no force is applied) was measured. The tool stiffness coefficients were computed from measured data. Cutting coefficients are computed as an inverse function of tool tip point displacement data. The tip point deviation (mm) is divided by the applied force. The tip point displacement is divided by the corresponding applied force value. The calculated multipliers for each applied force have close numerical values, representing stable deflection behaviour. The inverse function of the average values of the obtained multipliers provides the cutting tool geometry and material dependent stiffness coefficients. These coefficients are represented in Table 7.9.

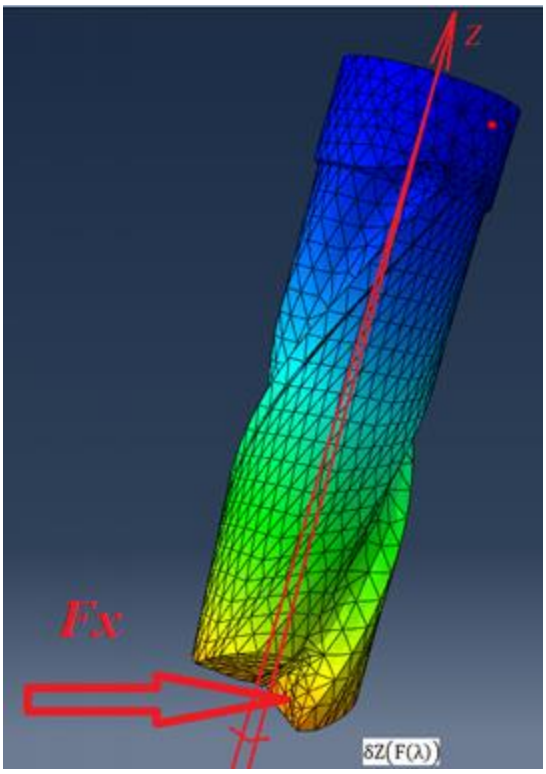

Fig. 7.15. Cutting force interaction on the flat-end milling tool and tool deflection

Table 7.9. Cutting tool MS2MSD1000 material (WC) stiffness coefficients (depends on tools geometry)

Force applied direction	**Deformation direction**	**Stiffness coefficient, N/mm**
Tangential	Tangential	Mt = 8146,374
Normal	Normal	Mn = 11334,784
Axial	Tangential	Mz(t) = 40150,968
	Normal	Mz(n) = 57703,738
	Axial	Mz(a) = 15885,716

Where Mn is tool stiffness in the normal force direction, Mt is tool stiffness in the tangential force direction, Mz(t) is tool stiffness in the axial direction under tangential force influence, Mz(n) is tool rigidity in the axial direction by normal force influence, Mz(a) is tool rigidity in the axial direction under axial force influence. The lower stiffness coefficients correspond to the tangential and normal directions. However, when force is applied in the axial direction, due to the twisted geometry, the tool is deformed in tangential, normal and axial directions. So, a force in a tangential direction produces a tangential deformation, a force in a normal direction produces a normal deformation, but a force in an axial direction produces tangential, normal and axial deformations.

Considering these cutting tool material and geometry stiffness coefficients, we can calculate tool deflection models in accordance with the global machine coordinate system. To do this, stiffness coefficients (Mz(t), Mz(n) and Mz(a)) are substituted into the force model (Eq. 7.5., 7.6. and 7.7.):

$$\boldsymbol{\delta X\big(Fx(\lambda)\big) = -Ft(\lambda) * \frac{1}{Mt} * \cos(\lambda) - Fn(\lambda) * \frac{1}{Mn} * \sin(\lambda)} \quad (7.8)$$

$$\boldsymbol{\delta Y\big(Fy(\lambda)\big) = Ft(\lambda) * \frac{1}{Mt} * \sin(\lambda) - Fn(\lambda) * \frac{1}{Mn} * \cos(\lambda)} \quad (7.9)$$

$$\boldsymbol{\delta Z\big(F(\lambda)\big) = \left(-Ft(\lambda) * \frac{1}{Mz(t)} * \cos(\lambda) - Fn(\lambda) * \frac{1}{Mz(n)} * \sin(\lambda)\right) +}$$

$$\boldsymbol{+ \left(Ft(\lambda) * \frac{1}{Mz(t)} * \sin(\lambda) - Fn(\lambda) * \frac{1}{Mz(n)} * \cos(\lambda)\right) +} \quad (7.10)$$

$$\boldsymbol{+\left(Fa(\lambda) * \frac{1}{Mz(a)}\right)}$$

In the last model, tool deflection along the Z axis was selected as a corresponding equation for the surface height prediction model. This equation combines the interactions of cutting force and tool stiffness in tangential, normal and axial directions. Substituting cutting force coefficients and tool material stiffness coefficients into Eq. 7.10, tool tip point deviation in the Z axis were obtained. Results were plotted with MATHCAD software (Fig. 7.16). The plot represents tool tip point deviation in μm. The calculation results are represented in Table 7.10 below.

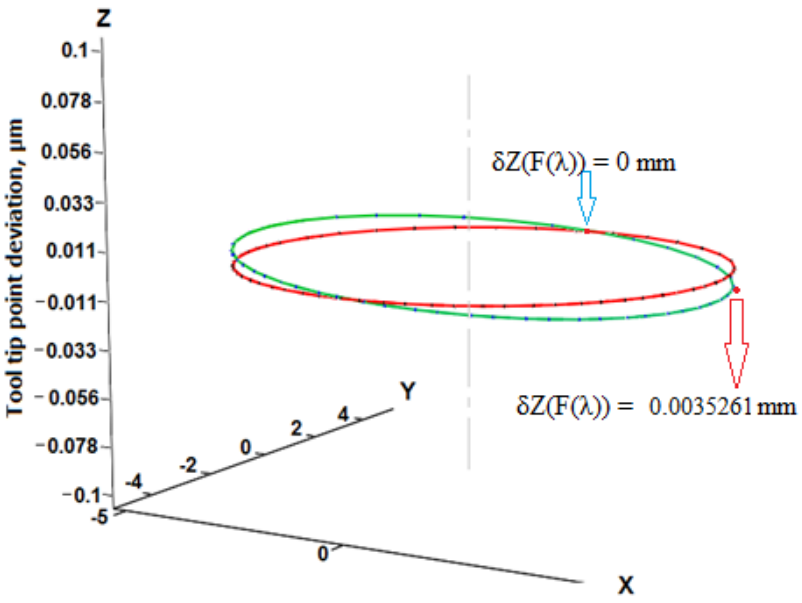

Fig. 7.16. Cutting tool tip point deflection due to cutting forces (Mitsubishi MS2MSD1000, West cutting direction)

The red circle in the diagram represents ideal tool tip point trajectory with ideal tool stiffness, where no tool deformations exist. The applied cutting force causes cutting tool axis deflection and tools tip point deviation from its ideal trajectory. The represented plot of the tool deflection model (green circle) provides a complete view of how the cutting force influences the travel of the tool tip point over one tool revolution. The tool tip point is displaced over the X, Y and Z axes. Deflection along the Z axis is a component of tangential, normal and axial deformations, assuming that there are no local deformations of the tool body. We are more interested in axial displacement of the tool tip point, because it determines the differences in surface height.

Table 7.10. Cutting tool deflection along the axial – Z direction according to applied cutting force in the feed direction

FEED RATE *f*, mm/ tooth	**CUTTING FORCE *Fx*, N**	**TOOL's AXIAL DEFLECTION, mm**
0,04	15,2	0,0014105
0,1	38,7	0,0035261
0,2	76,2	0,0070517

The tool tip point deviation affects the surface formation process directly, as surface pattern depends on tool geometry and tip point alignment against the surface. Tool deformation along the Z axis can be linked directly to the surface topography height parameter determination. These values are components of the surface topography height parameter Sz formation model.

7.4.2. Cutting tool axis inclination model

The first part of the cutting tool alignment error component—tool deflection—was described in the previous section. This section deals with second alignment component: describing the influence of the cutting tool axis or milling head inclination on surface topography formation. Cutting tool axis inclination model represents the tool component and consists of milling machine alignment, adjustment and wear inaccuracies. There are a couple of methods to detect the milling head inclination angle. In real life, it is possible to determine the machine milling head inclination angle in relation to a calibrated bar indicator, while the machine head is moving in the Z direction. It was assumed that surface topography should be the same level in any cutting direction. All the differences between directions are caused by milling head/cutting tool inclination errors.

Regular use of milling equipment tends to cause wear. Also, milling machine base alignment accuracy affects the milling head inclination in relation to the milling table. Topography measurements represent surface height deviation in opposite cutting directions (Table 7.2). This deviation occurs in other specimens, with similar behaviour. This behaviour may result from tools axis inclination. Cutting tool axis inclination is represented in Fig. 7.17 and shows the cutting tool axis inclination from its theoretical perpendicular position. The cutting tool concavity angle σ [43], as described in previous subchapters, is one of the sources of surface topography height parameter S_Z formation. θ_T represents the milling spindle or cutting tool axis inclination angle. Both of these angles together ($\theta_T+\sigma$) result in the minimum surface topography height S_Z value. Surface height depends on the machined surface slope length - *a*. This in turn depends on the feed rate – *f*. If we consider tool inclination, slope length *a* is the actual cutting depth in the axial direction.

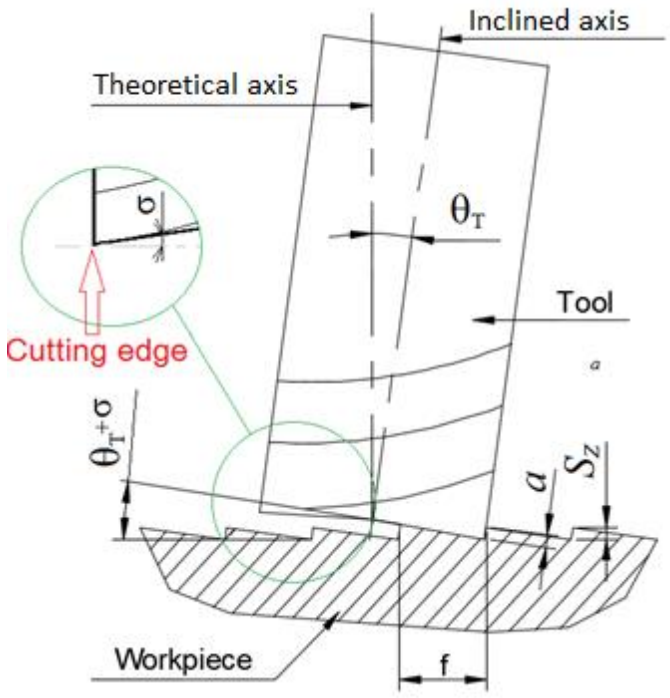

Fig. 7.17. Representation of milling machine spindle axis inclination

As the cutting tool inclination increases, the main cutting edge axial cutting depth also increases, while the cutting tool's concavity angle machined surface slope length decreases. With increased feed rate, the slope length and minimum surface height also increase. Furthermore, the created slope of the surface is increased (faster) in the inclination direction and is decreased (slower) in the opposite direction. Considering this tool inclination in the feed direction, accordingly, it decreases in the opposite direction. The difference in measured surface topography height between two opposite cutting directions, in the same conditions, may be derived as a tool axis inclination. Therefore, this difference may lead us to consider tool axis inclination in this model calculation as it has a high S_Z deviation between opposite cutting directions. Development of the tool inclination influence model and its implementation in the surface topography prediction model should improve the general model and make results more accurate.

The basis for the surface topography prediction model is taken from the cutting tool geometry and its interaction with the surface. If we assume that the tool's concavity angle, cutting feed rate and cutting depth are known values, it is possible to calculate minimum surface depth, how deep a path the cutting tool edges make on the machined material. Cutting tool inclination may increase the influence or decrease it. Tool axis inclination always works together with a tool's concavity angle. When the cutting tool axis is inclined towards the tool's movement direction, the assumed concavity angle, between the end cutting edge and specimen surface, increases (represented in Fig. 7.16). Therefore, the depth of cut increases and surface height

increases accordingly. The relation between cutting tool geometry and surface topography height is represented in Eq. 7.11.

$$\mathbf{Sz_T(\lambda)} = \frac{\mathbf{t(\lambda)} * \mathbf{\tan(\theta_T + \sigma)}}{\mathbf{1 + \tan(\theta_T + \sigma) * \tan(\theta)}} \quad (7.11)$$

$S_{ZT}(\lambda)$ – is proposed surface topography height, considering cutting axis inclination angle θ and minimum surface topography height. This calculation does not contain cutting tool deflection. σ is the end cutting edge radial relief angle, also called the concavity angle. $t(\lambda)$ represents uncut chip thickness with the immersion angle λ, which depends on the tool's rotation against the cutting direction. The sum of the concavity angle and tool axis inclination angle, $\theta_T+\sigma$, is the main machine alignment component that affects surface topography formation.

If the cutting tool is inclined in the cutting feed direction, the surface topography increases, if the tool is inclined away from the cutting feed direction – the surface topography parameter S_Z decreases. The question represents the geometrical interpretation of the surface formation. With every tool rotation, the tool nose and bottom cutting edge result in a minimal surface topography height. In this case, the bottom cutting edges have a concavity angle $\sigma = 2°$ which forms the tool complementary angle (flute nose angle) of 88°. The cutting tool axis inclination angle can be reconstructed from the surface measurements using the same equation. A second order differential equation was applied to solve the routes of Eq. (7.11) and obtain the tool inclination angle. If the tool is inclined in one direction by angle "x", in the opposite direction of the same axis, it will also be declined by magnitude "x". Using this angle we can represent the tool tip point deviations from the ideal trajectory, over the tool rotational movement.

7.5. Complete surface topography height prediction model

The main surface topography formation components have been described above. Now, it is time to compile them in a general model and use it to predict the surface topography parameter S_Z values. Each of the previously described model components generates additional influences on the surface topography height. A general model compiles them in simple equation that sum up all these component values. Some terms are dependent on the tool rotation angle and, accordingly the final proposal, is a function of the tool rotation angles. The result of the general model is total tool tip point milling variations $S_Z(\lambda)$ along the machine's *Z* axis, taking into account the cutting tool rotation and feed factor interaction on the specimen material.

$$\mathbf{Sz(\lambda)} = \mathbf{Sz_{min}} + \mathbf{\delta Z\big(F(\lambda)\big)} + \mathbf{Sz_T(\lambda)} \quad (7.12)$$

The terms in this expression are:

- Sz_{min} - minimum surface height performed by the cutter's geometrical behaviour. As calculated in the previous chapter, the cutting tool's concavity angle performs minimum surface topography height with every tool rotation;

- $\delta Z(F(\lambda))$ – tool deflection caused by cutting forces is a component formed by cutting forces and described in start of this Chapter. Depending on the feed rate, this component is one of the most important components and may be the main factor on the overall surface topography parameter S_Z height. Delta, δ, describes the maximum and minimum surface height difference, when the cutting tool is rotating;

- $Sz_T(\lambda)$ - cutting tool axis inclination component due to machine inaccuracies.

Samples were machined with the KONDIA milling machine in four orthogonal cutting directions. The corresponding milling axis inclination angles in the various directions, the real concavity angle value, feed rate and according cutting force were used. These cutting process parameters selected for the prediction model are represented in Table 7.11.

Table 7.11. Cutting process parameters for Sz prediction models

CUTTING DIRECTION, *DIR*	**FEED RATE *f*, mm/ tooth**	**INCLINATION ANGLE θ_T, degrees (KONDIA)**	**INCLINATION ANGLE θ_T, degrees (GENTIGER)**
SOUTH	0,1	-0,242255	0,22043240
NORTH	0,1	0,242255	-0,22043240
WEST	0,1	-1,515311	-0,82634761
EAST	0,1	1,515311	0,82634761

The determined output data was substituted in the equations (6.1), (7.8) – (7.11) to predict the minimum angle, tool deflection and tool inclination components. Predicted surface topography values by different components were represented in Table 7.12. In this table, components with the measured surface topography height value Sz were compared.

Table 7.12. Sz prediction model component results - KONDIA

DIRECTION	TOOL DEFLECTION, mm	TOOL INCLINATION, mm	MIN SURFACE HEIGTH, mm	Sz, µm
SOUTH	0,0035261	-0,000221806	0,00349208	6,796374
NORTH	0,0035261	0,000221806	0,00349208	7,239986
WEST	0,0035261	-0,001327009	0,00349208	5,691171
EAST	0,0035261	0,001327009	0,00349208	8,345189

The results of SOUTH/NORTH and WEST/EAST cutting direction calculations were selected to plot the cutting tool tip point height deviation (Fig. 7.18). The plot represents the sum of tool tip point performed surface topography height that depends on tool angular position. Whereas the table represents only the maximum obtained topography height, the plot, therefore, represents the topography height changes over half a tool revolution. The plots of tool tip point deviations show that an increase in the tool immersion angle λ (abscissa), leads to surface topography increases until the maximum uncut chip thickness has been reached (ordinate). As the immersion angle continues to increase, the surface height decreases again, because the uncut chip thickness decreases along with the cutting forces. In the same way, the roughness prediction was executed for each of the four cutting directions.

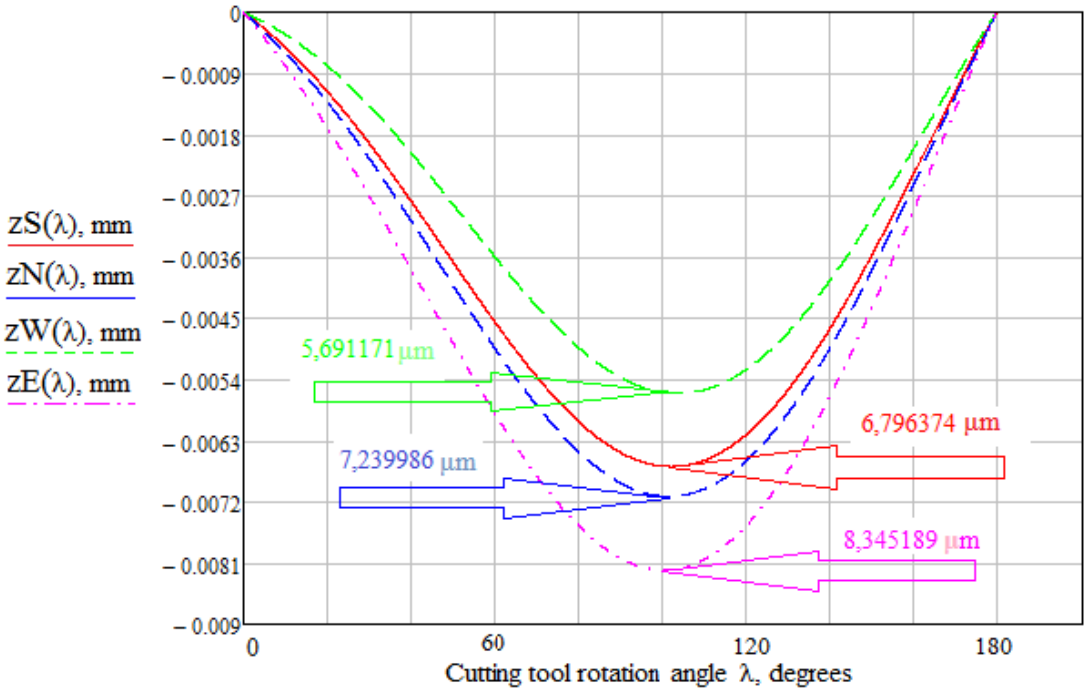

Fig. 7.18. Plots of the differential Z coordinate values depending on immersion angle λ in South, North, West and East directions.

A comparison of the mathematically estimated values and average means of the measurement results are represented in Table 7.13. The cutting feed direction column represents the cutting tool movement direction compared with the milling table, looking down onto the machine. The measured Sz values are mean values from 2 measurements from the same area to avoid measurement errors. The difference between measured and predicted values represents numerical value and % of difference between the measured and predicted surface height Sz parameter. The last columns show the difference between opposite directions for both measurements and predicted results. This helps us to compare the surface topography behaviour in the measurements and the prediction model.

The measured data corresponds to one specimen, which was milled in four directions. In the mathematical approach, the same surface formation behaviour appears, i.e. in the NORTH direction, the predicted S_Z value is greater than in the SOUTH direction, as well in the measured values. The same was observed in the comparison of the EAST and WEST direction measurements and calculated values. Two measurements were taken from the central area of the specimen (Fig. 7.5), therefore 2 values were observed and mean surface topography parameter S_Z value was extracted for comparison with the simulated value.

Table 7.13. Table of measured and predicted surface topography parameter S_Z values for the KONDIA B500 milling machine

Cutting feed direction	**S_Z measured value, µm**	**S_Z mean value, µm**	**S_Z predicted value, µm**	**Difference between measured average and predicted, µm & %**	**Difference between contrary directions, %**	
					Measured	**Predicted**
1. SOUTH	14,3043	14,837155	6,796374	8,040781 54,2 %	5,7 %	6,5 %
	15,3700					
3. NORTH	16,1740	15,68290	7,239986	8,442914 53,8 %		
	15,1918					
2. WEST	13,7202	12,44145	5,691171	6,750279 54,2 %	87,4 %	46,6 %
	11,1627					
4. EAST	16,4806	23,32125	8,345189	14,976061 64,2 %		
	30,1619					

The difference between directions presents the percentage difference for the predicted and measured values for the opposite directions. This comparison allows to judge whether the behaviour of the tool inclination influence is the same in measurements and predicted results. We use % to eliminate the effect of absolute values. Table 7.13 shows whether the predicted surface

topography parameter S_Z has the same behaviour as measured values. Its value is higher in the NORTH and EAST directions, according to the Fig. 7.9, but lower in the SOUTH and WEST directions, for both measurements and the prediction model. The difference between measurements and predicted results is 53,8 % up to 64,2 %. The differences in orthogonal directions between measured values are 5,7 % in SOUTH-NORTH directions and 87,4 % in EAST-WEST cutting direction. The differences between predicted Sz values are 6,5 % in SOUTH-NORTH direction and 46,6 % in WEST-EAST directions. Accuracy in the SOUTH-NORTH direction is acceptable, while WEST-EAST cutting directions create doubts about the cutting process stability. This kind of difference (87,4 % for surface topography measurements) may be caused by the insufficient stability of milling process. Further investigation is required here. Meanwhile, the same model has been simulated with milling axis alignment accuracy parameters from another milling machine – the GENTIGER GT-66 (Table 7.14).

Table 7.14. Table of measured and predicted surface topography parameter S_Z values for the GENTIGER GT-66 milling machine

Cutting feed direction	**S_Z measured value, µm**	**S_Z mean value, µm**	**S_Z predicted value, µm**	**Difference between measured average and predicted, µm & %**	**Difference between contrary directions, %**	
					Measured	**Predicted**
1. SOUTH	11,5615	11,98525	7,256872	4,728378 39,5 %	6,86 %	7,04 %
	12,4090					
3. NORTH	11,8250	11,2157	6,77948	4,43622 39,6 %		
	10,6064					
2. WEST	7,6540	9,21295	5,970961	3,241989 35,2 %	31,3 %	35,08 %
	10,7719					
4. EAST	12,3480	12,0985	8,065392	4,033108 33,3 %		
	11,8490					

The results in Table 7.14 show that the predicted model accuracy is more stable. Differences between the measured and predicted parameter Sz values from 33,3 % up to 39,6 % and reflect stable behavior. Measured difference between SOUTH-NORTH directions is 6,86 % while predicted value difference is 7,04%. In WEST-EAST direction measured difference is 31,3 %, while predicted value difference is 35,1 %. Here, the predicted results are more similar and show more stable behavior. Nevertheless, the accuracy needs to be improved, including other cutting process factors.

Simulated values represent the worst cutting scenario with selected cutting process factors so far. This means that in simulation milling, the head axis has been maximally tilted and the cutting tool maximally deflected. In reality, these errors have a high threshold and the measured surface topography may be lower than simulated. The same applies to topography measurements. Measured topography contains a number of errors that increase the Sz parameter amplitude, such as local surface areas, where valleys have deep wells or extremely high peaks. These errors make a direct influence and cannot be predicted in geometrical models as we can see here. The difference between measured and predicted results is too high here to be able to talk about a reliable prediction model. Clearly, either this model should be improved or serious improvements are required in the measurement process related to surface measurement filtration, to improve the coincidence between measured topography parameters and prediction model results.

7.6. Conclusions

The objective of this chapter was to prove the importance of cutting tool deflection and milling axis inclination on surface topography parameters formation.This has been achieved. Cutting tool deflection is the main factor in surface topography formation, as well as the geometry of the cutting tool (or concavity angle, to be more precise). The objective was reached for the development of a mathematical model to represent tool cutting edge movement. This movement includes high tool deformations along the tool's *z* axis and cutting edge deviations from the initial trajectory. With regard to the measured topology width, this model represents the surface's greatest height differences, but considering the area of full tool overlap, it reflects surface geometrical errors, such as machined surface inclination, waviness, etc. This model will help to predict the machined surface topography, without experiments, taking into account the behaviour of the milling machine (measured before), the cutting conditions and workpiece material. A prediction model was developed as a useful tool for industrial needs.

In this chapter, a mathematical model were developed to predict surface topography parameter S_Z values for one specific material type – DIN 1.1730, machined with two different milling machines and the specific cutting conditions of Feed rate, F2= 0,1 mm/tooth, spindle speed, n= 4774 r/min and axial cutting depth, a_e= 0,3mm.

The following conclusions were reached by visual analysis and from the results of the developed model:

1) Cutting tool deflection is the most significant parameter affecting the surface topography parameter S_Z formation. FEM simulation results show that cutting force directly affect the tool deflection angle. Furthermore, deflections have the highest influence on the surface formation and can account for up to 38,3 % of the total measured surface topography height.

2) Cutting tool geometry directly affects the surface formation and there is a geometrical relation between cutting tool angles and topography height parameter formation. This is the second most important factor in the surface topography S_z parameter formation process, so far. It can account for up to 37.9 % of the total measured surface topography height.
3) Milling head inclination plays a significant role in surface topography formation, even if statistical analysis rejects this statement. Back-cutting marks confirm the influence of milling head inclination and tool deflection on the surface formation process. Also, milling head inclination increases or decreases the effect of back cutting phenomena, by retracting or bringing the back cutting edge closer to the machined surface. As a result, in combination with cutting tool deflection it exaggerates or diminishes the minimum surface topography height.

4) Mathematically obtained inclination values, extracted from topography measurements shows that in all end-milling operations, milling head inclination is in action and affects the surface topography. This factor increases the total measured surface topography height by 8,67 % or decreases it by 11,4 %. Its influence accounts for more than 1/5 of total measured surface topography height and should be considered as an important factor.

5) The overall sum of the influences of cutting tool geometry, the minimum surface height component, and the milling axis inclination and cutting force component varies from 36% up to 77 % in some cases and this cannot be considered a well-developed model, and still needs to be improved.

6) We conclude that discrepancies between measurements and the predicted model result from the influence of other factors at work in the cutting process that is not considered in this cycle. They are not caused by the inaccuracy of the developed mathematical model.
7) To obtain more accurate fit with model results, the data processing measurement procedure should be reconsidered. Additional filters should be used to filter surface errors that can pollute the overall surface topography measurement values and, consequently, affect the prediction model coincidence accuracy.

As has been concluded, there is still a difference of up to 77% between predicted and measured values. Visual analysis of previously developed samples revealed cutting marks repeating with some frequency. It also represented true marks, difficult to observe due to their light appearance. It was possible to observe them due to their frequent occurrence. Do they affect the surface topography formation? The vibration of the cutting system has been investigated by many authors [96]–[100], [102]–[104]. This leads us to think they have important influence in surface topography formation. Vibration in the flat-end milling operation will be investigated in the following chapter.

8. ANALYSIS OF THE FLAT-END MILLING MODEL – VIBRATION COMPONENT

Results from the previous chapter suggest that there are still some flaws in the mathematical model developed so far. Literature analysis, covered in Chapter 2, shows that one of the factors that cannot be omitted in the milling process is the vibration effect of the cutting system and cutting tool's natural vibration frequency, the tool-chuck interface and the actual milling machine stiffness.

Furthermore, a great deal of analysis by other researchers has been conducted into the behaviour of milling process vibrations and dynamics, and their influence on laterally machined surface roughness parameters, or cutting force [98], [129], [130]. But only some of them were focused on end-milled surfaces. The end-milling technique, as mentioned before, is the most commonly used application for die and mold manufacturing. The resulting high quality mold surface is directly related to the machining technique, surface topography and shape errors during the machining process. End milling is one of the last steps in the automatic treatment of the mold surface. The remaining work has to be done manually.

As mentioned at the end of the previous chapter, some frequent marks were observed on the machined surface. Is it possible to relate them to cutting system vibrations? The aim of this chapter is to relate the cutting vibrations on the milling process with surface topography formation. It is common knowledge that there is vibration during the cutting process (here, milling), when cutter edges enter or exit the un-machined material. With a defined frequency, these vibrations increase or decrease the movements of the milling system. Depending on cutter stiffness and milling system rigidity these vibrations are dampened.

In this chapter we will detect and analyze how much vibrations affect the surface topography parameter S_Z formation. This section is a continuation of the work in Chapter 7. Therefore, we are not going to describe the material, machining conditions and equipment selection again. Instead, we will switch directly to the questions related with vibrations at cutting process.

Vibrational factors will be analyzed in this chapter and some of them applied to develop the mathematical surface topography parameter S_Z prediction model.

8.1. Experimental execution and measurements

Firstly, to discuss the influence of vibration, it is important to detect the behaviour of the selected equipment and the milling system as a whole unit. The way milling equipment stability can be characterized is by detecting the natural frequency of the equipment assembly. This can be done with experimental natural frequency measurements for the equipment parts.

From physics, we know the higher the mass of an object, the higher its damping coefficient will be on vibrations and the higher its natural frequency. Milling machine have large lateral surface areas, where it is easy to fix the measurement sensors. The same measurements can be taken for the clamp fixture. It is more complicated for the cutting tool. With its round shaped geometry, measurement devices cannot be attached to its surface correctly to perform natural frequency measurements. Again, FEM software is a good tool to perform the vibration analysis on the cutting tool. Considering the twisted shape geometrical configuration of the tool, and characterizing the cutting system behavior, FEM software generates several vibration types and their associated vibration magnitudes. Therefore, the two objects were selected for general, natural frequency measurement calculations – cutting tool and milling machine table, described in the next two subchapters.

8.1.1 Performance of FEM analysis to detect the cutting tool's natural frequency of cutting tool

As introduced before, the selected end-milling cutting tool geometry does not permit natural frequency measurement directly on the cutting tool. Therefore, a good way to detect the natural frequency is FEM software. A realistic CAD model of the cutting tool was introduced into the ABAQUS^{TM} software. This CAE software analyzes the natural frequency of the CAD model and proposes the results.

Firstly, the cutting tool was measured and a real tool model was developed considering the smallest detail of its geometry. Basically, this is the same model used to detect cutting tool deflection, only instead of applied cutting force as a load conditions, this time we use frequency output tests to detect the vibration modes, frequency and amplitude that belongs to the selected cutting tool geometry. The CAD model was developed using the available SolidWorks^{TM} software, including the same tool length as used in the experiments. Measured cutting tool concavity angle is 2°, rake angle is 10°, primary relief angle is 13° and helix angle is 30°, while tool's core diameter is 6,71 mm, length of the helix spiral is 29 mm and length of primary clearance land is 0,9 mm. To simulate realistic conditions, the CAE model had to be updated with material properties, constraints (degrees of freedom – DoF) restrictions and loading conditions. We defined Frequency output tests, to detect the natural frequencies at different modes and fixed constrains of the cutting tool according to the cutting tool length out of the chuck. The software library enabled us to select previously prepared material properties. Cutting tool material we defined as carbide-general with TiAlN coating layer. The size of mesh were created with 11568 of elements with element minimal element size 0,059039 mm, like this was done for deflection simulation.

Execution of the FEM simulation calculates the possible variations of different deformation modes. Mode 1, for example, represents cutting tool deformation in X axis, but Mode 2 represents tool deformation in Y axis. Mode 3, in turn, represents torsional deformations of the

tool. The most common and most frequently observed natural frequency mode is Axial Deflection (Fig. 8.1).

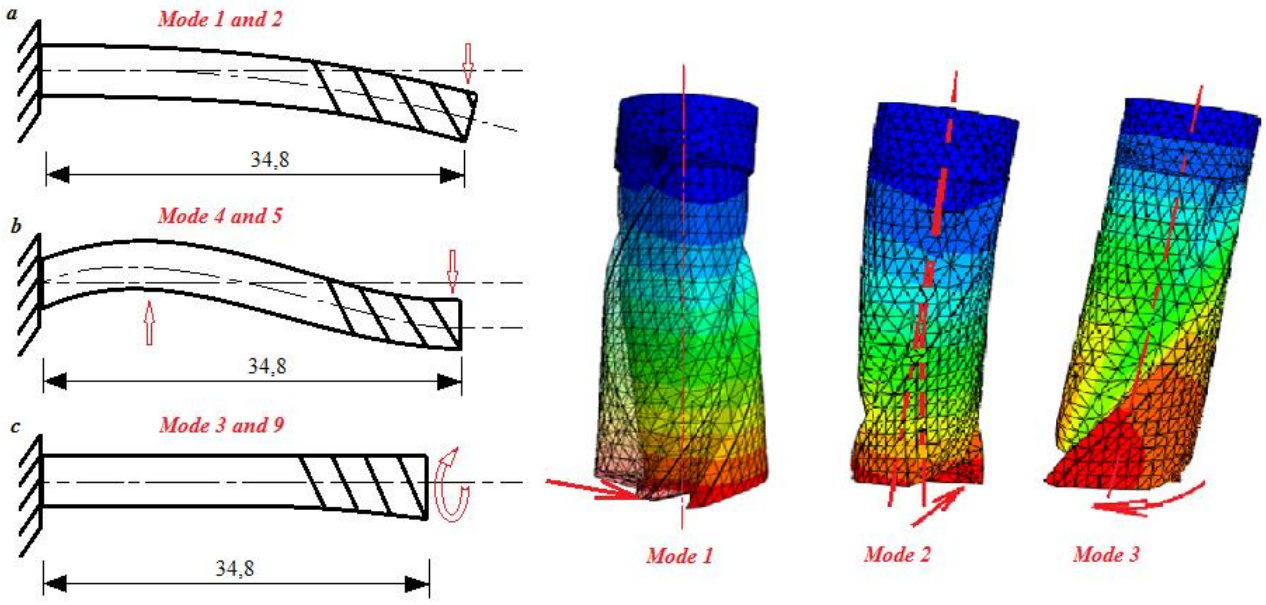

Fig. 8.1. Flat-end mill deflection modes from ABAQUS^{TM} simulation: a) 1st axial deflection MODE 1, b) axial deflection MODE 2, c) Torsional deflection MODE 3.

Table 8.1. Natural frequency simulation results

Index	Increment	Type	Cycles/second (Hz)
1	MODE 1	Axial Deflection	6907,7
2	MODE 2	Axial Deflection	7590,7
3	MODE 3	Torsional Deformation	30024
4	MODE 4	Axial Deflection 2 DoF	34831
5	MODE 5	Axial Deflection 2 DoF	38046
6	MODE 6	Extensional Deformation	47654
7	MODE 7	Axial Deflection 3 DoF	81370
8	MODE 8	Axial Deflection 3 DoF	85480
9	MODE 9	Torsional deformation 2 DoF	88876

Table 8.1 represent tool axial deflection along the rotational axis, where all the other tool DoF are restricted in one point, fixed into the tool chuck. Both of them have the lowest natural frequency; therefore, they should be analyzed to detect their influence on the surface topography parameter Sz formation. Fig. 8.1 shows the tool deflection amplitude (magnified). This picture represents the 1st natural frequency mode, where the tool deflects from the point where it is fixed. Axial deflection affects the tool tip point deviation in the radial and axial directions.

The frequencies for the 1st and 2nd modes are similar due to deflection deformation along the orthogonal planes. It depends only on tool geometry. Due to the units used for material properties and model dimensions, the simulated frequency units are in *Hz*. MODE 3 describes tool torsional deformation with the same conditions as previously. MODE 4 and 5 represent tool deflection along the orthogonal planes, when one more degree of freedom is restricted perpendicular to the deflection plane. MODE 6 represents tool extension deformation, with only one point of tool fixation, the tool chuck. MODE 7 and 8 represent tool deflection along the orthogonal planes, similar to MODE 1, 2, 4 and 5, but one more degree of freedom is restricted at two tool points. MODE 9 represents tool torsional deformation around the tool's rotational axis, with one more fixed degree of freedom.

The other modes reported by the application are not representative, as they repeat the same behavior, except that the restrictions by degrees of freedom are located in multiple points on the tools axis. For further analysis and model development is sufficient to select the lowest natural frequency that may have the highest influence on surface topography formation. In this case, the first two modes are the most representative and may give the highest influence on surface topography formation.

8.1.2 Measurements of the milling table's Natural Frequencies

As mentioned above, the milling table and machining center frame are straightforward objects for taking the direct vibration measurements to determine their natural frequencies. For the analysis of the vibrations in the machine-tool-workpiece system, the natural frequency measurements of the machining center were taken on the milling table, where the fixture for the workpiece is attached. Fig. 8.2 is a photograph and establishment plan for taking the measurements. A Dactron Photon+ vibration measurement device was used for measuring the cutting vibrations. To measure the milling machine vibrations, three accelerometers were attached to the workpiece milling table, clamped in each of the machine traveling axis directions. Vibration measurements were recorded at every working stage, including the machine's idling state. Idling state measurements allow us to isolate certain external vibrations, which were unrelated to machine errors or cutting process errors. Results of vibration measurements and the detected natural frequency of the machine parts or general machine assembly were used to calculate dimensional deviation between the tool tip point and material surface. This deviation may affect the surface height deviation between surface areas located near to each other.

Vibrations cannot occur without external force. Natural frequency measurements were taken by applying the external force of a hammer. The hammer was connected to the Dactron Photon+

vibration measurement device, to exactly identify the force applied to the milling machine structure.

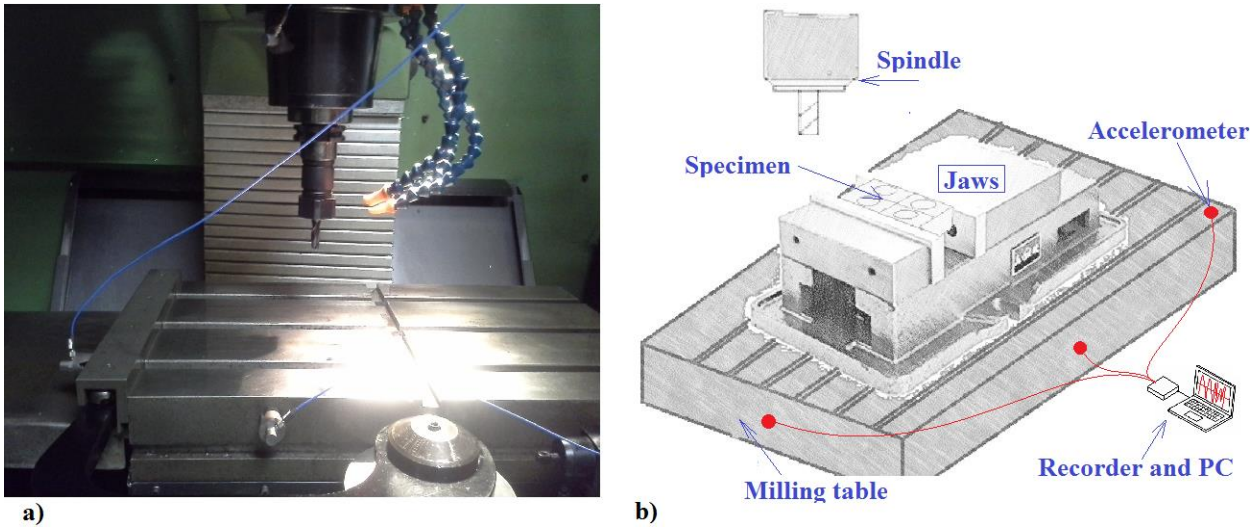

Fig. 8.2. a) Sensor arrangement on machine milling table; b) established plan for vibration measurement experimental execution.

The measurement device records the applied force and acceleration in all three axes of the milling equipment table. Vibration calculation software uses the Frequency Response Function (FRF) to calculate the natural frequency of the milling table. FRF is the system's output spectrum response function and is measured in $m/s^2/N$. Fig. 8.3 represents FRF (ordinate) with respect to the increase in the vibration frequency. The X axis represents the frequency and the highest level of response corresponds to 76 Hz of vibration frequency. These frequencies correspond to the milling equipment natural vibration frequencies in the selected axis.

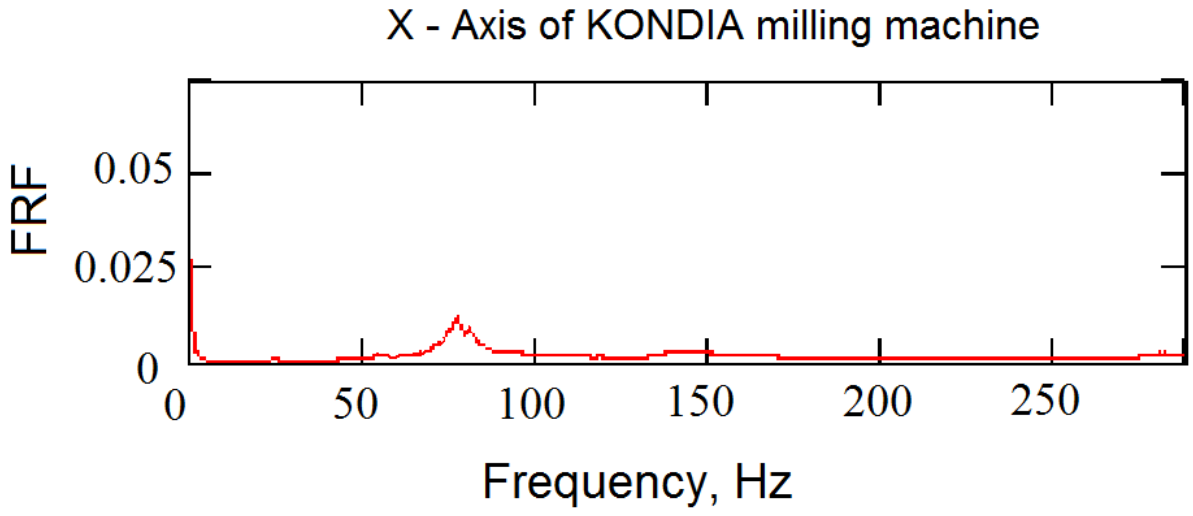

Fig. 8.3. Frequency response function analysis of KONDIA CNC milling table X axis

Each accelerometer may generate its own result. Fig. 8.3 represents the lowest and most powerful frequency in which the machine table oscillates around the X axis. The overall result from machine table frequency measurements in X and Y axis are represented in Table 8.2.

Table 8.2. KONDIA B500 natural frequency measurements.

Axis	Type	Cycles/second (Hz)
X	Oscillations	76
Y	Oscillations	78

In general, milling machine table natural frequency has been defined at level of 76 Hz and 78 Hz. These values will be used for further calculations and for developing mathematical S_Z prediction model.

8.2. Visual analysis

Observations of unevenly distributed marks, on the contrary aimed sample surfaces, suggest that we should consider the vibration effect as an additional important factor in the surface topography height formation process. Importantly, even in the same cutting tool travel direction, the depth and distance between these marks deviates. This section will make it clear where and why there are differences observed on the machined surface.

Firstly, visual analysis of machined surface photography identified an important aspect (Fig. 8.4). Stopping and starting at the sample's corners, where the tool's center path is changing direction, generates surface roughness damage. In a part of the samples, this damage is continuous for a whole cut, until the next stop. In this area, distances between topography peaks are not equal and no longer correspond to the feed rate. They are influenced by extra vibrations from the machine's stops and starts. In samples with a higher cutting feed rate, the vibration is higher and generates higher damage to the machined surface. This damage can be observed even with the naked eyes. No damage at all was observed on the samples machined without any stopping during the machining cycle (different CNC program).

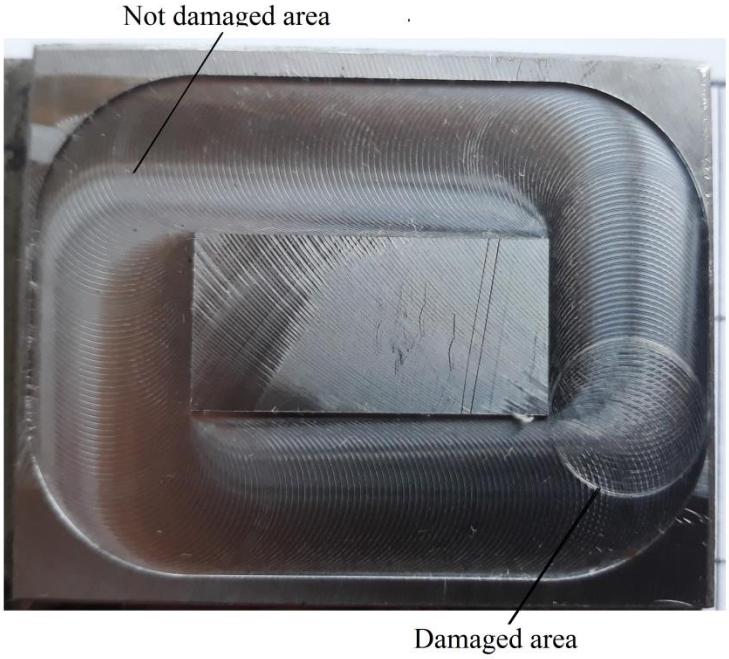

Fig. 8.4. Machined sample with and without stops at the corners.

Another type of visual analysis was undertaken on the surface topography images, taken from the optical or from the contact topography measurement device and generated with commercial and self-developed software. Images represent different colors and distances between two, apparently identical cuts. Furthermore, if looking at the margins of one cut, or one tool stroke, there are additional kinds of changes in color that represent changes in depth. By changing the light intensity in Fig. 8.5, it is possible to observe these marks on the machined surface. These marks seem to be a local deformation in depth, performed by tool deformations due to natural frequency vibrations. If we look carefully, we can see that this behaviour is repeated in every sample, at any cutting feed speed.

Measured distances in Fig. 8.5 represent the length of color change. Measurements of surface height deviations along one tooth path were taken using commercial software for 2-dimensional image distance measurements. By changing the brightness and color contrast of measurement image, the variation is highlighted. With the naked eye it is almost impossible to see this change. It appears as waves of cooler mapped under the tooth path. In Fig. 8.5 there are 3 almost equal line segments on one tool path. The number of waves along one whole tool rotation was estimated from the distance measurements between two subsequent waves.

To relate these vibrations with cutting equipment, their frequency needs to be calculated. To do this, measurements on the topography image plot were taken with measurement software. Accuracy of the measurements was checked against the general dimensions of the image, indicated by the size scale alongside it. Further calculations describe the approximate length of each color change and number of changes per revolution.

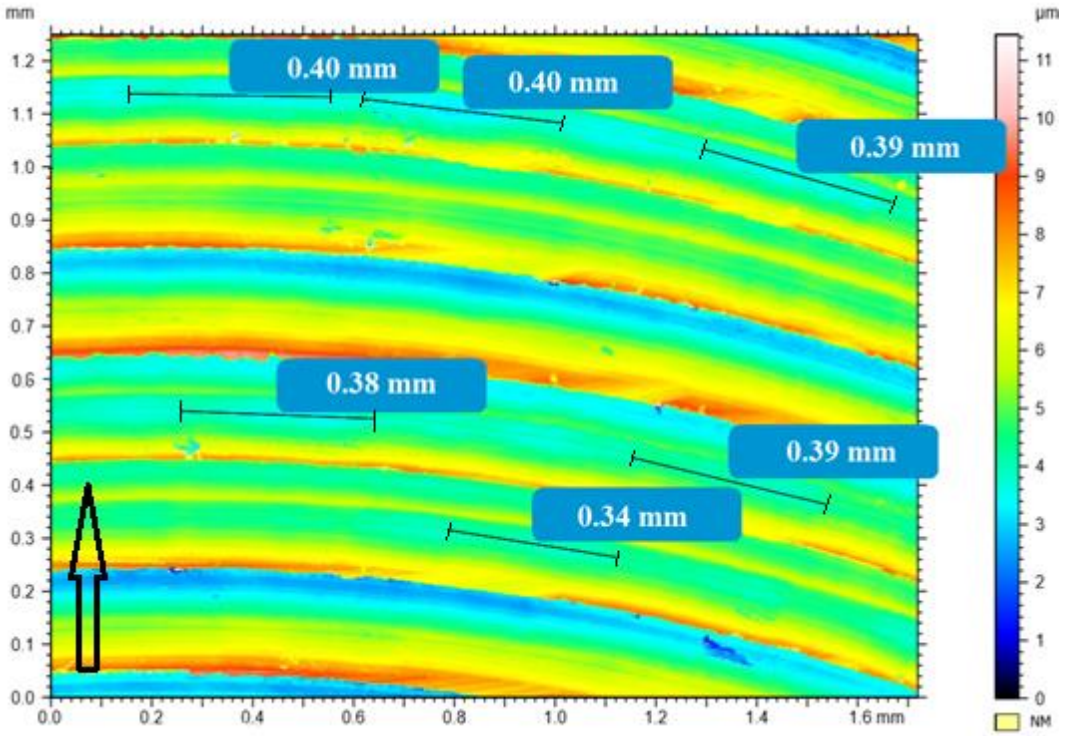

Fig. 8.5. Frequent surface height changes in depth – Sample #13

The distance between the marks is 0,34 – 0,4 mm. At the same time, the spindle rotation frequency is 4775 r/min. Therefore, the tool rotation frequency period is:

$$T = 60/4775 = 0{,}012 \text{ sec/rev}, \quad (8.1)$$

The tool tip radius, R = 5mm, length of the circle line of the tool tip point travel is:

$$C = 3{,}14 \times R \times 2 = 31{,}4159 \text{ mm} \quad (8.2)$$

The mark repetition frequency for one tool revolution:

$$f_m = 31{,}4159 / 0{,}36 = 87{,}2 \text{ times/rev} \quad (8.3)$$

$$f_t = 87.27/0{,}012 = 7272{,}21 \text{ Hz (times per second)} \quad (8.4)$$

Where, T - rotation period, C – tool tip point travel distance per one revolution, f_m – mark repetition frequency per one revolution and f_t - mark repetition frequency on the machined surface.

The frequency calculated for the frequent marks in Fig. 8.5 is similar to the natural frequency of the first two deformation modes of the tool – 6907 and 7590 Hz, respectively. We suspect that these marks are left due to the natural frequency vibrations of the cutting tool. The height of these marks changes with this frequency. Color change in these areas is between light blue up to slightly light green color. This means, surface topography height is changing approximately up to half micrometer (as color map indicates).

8.3. Theoretical model of milling table vibrations

Other types of deviations, observed on the surface color plot images are between subsequent cutting marks. Visual analysis of the machined surface 3D topography images, Fig. 8.6 for example, shows marks repeated with an irregular frequency. Between some marks, the distances are equal to the tool feed distance, formed by one tooth path. Between other similar marks, this distance increases or decreases in the feed direction. The same behavior was observed with surface height changes between subsequent cuts. Theoretically, these marks should be equal. The color plot of the surface image in Fig. 8.6 represents how surface height varies between the tooth passage marks. In one tooth cut, the maximum depth of cut reaches 3µm with second cut it reaches only 5µm from the set zero point of measurements. It can be related to tool run-out or wear-out, if surface height changes repeatedly. But this time, a cut results a different surface height than the previous one. If cutting tool vibrations during the cutting process affect the surface topography during the same cut, then these marking deviations are affected by other vibrational behaviour. Could these marks be related to the milling equipment natural frequency measured in section 8.1.2? The cutting tool has a vibrational deviation along the X axis, so it changes its tool tip point position on Z axis too, but by how much?

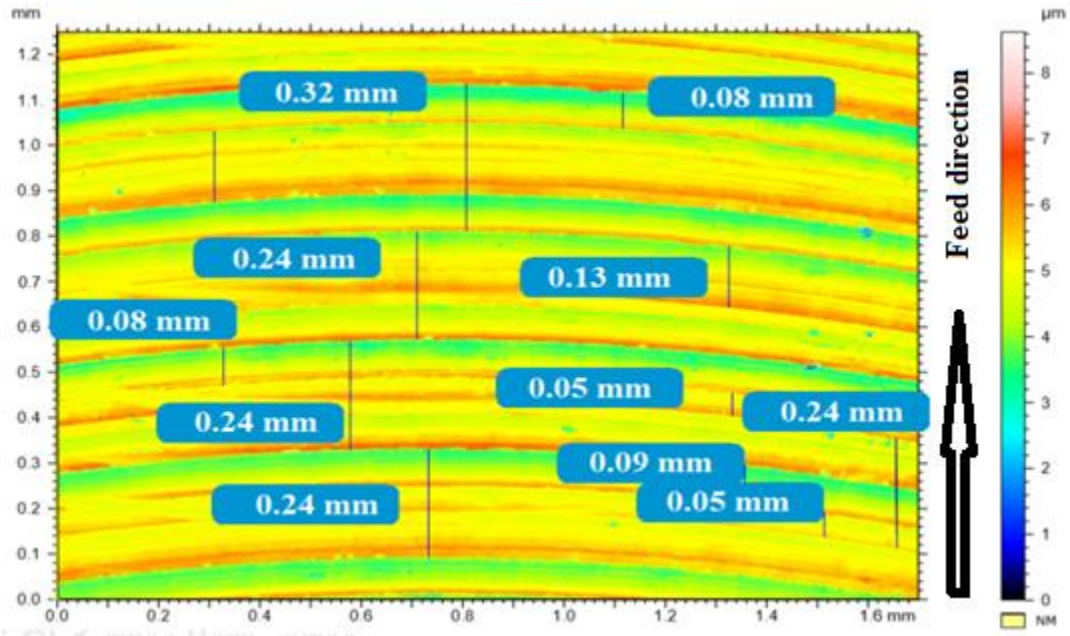

Fig. 8.6. Distribution of cutting marks over the material surface after the end-milling process of DIN 1.1730 material. (Sample #5 – North cutting direction, 0,04 mm/tooth)

To prove this statement and check vibrational behavior, it is necessary to calculate, the vibration amplitude of the milling equipment. As a reminder, natural frequency measurements for milling tables were taken in section 8.1.2. The measured natural frequency value in the Z direction is too high to be considered a significant factor affecting the surface roughness directly. The measured natural frequency value for the KONDIA B500 milling machine is 76 Hz in the X

direction and 78 Hz in Y direction. But what is the relation between the natural frequencies of the milling table and the surface topography parameter S_Z value?

A second order differential equation is used to solve the force vibration system function in dynamic system calculations. The results of the solved equation are vibration amplitude in desired direction, where excited force is applied. The vibration differential equation (8.5) is a function that relates the mass, damping and rigidity coefficients, and external applied force with vibrational displacement amplitude.

The result of the solved function is the dynamic displacement [132]–[134]. In an ideal situation, if no continuous exciting forces have been applied to the object, the system damping coefficient and mass are high enough to dampen the vibration up to standstill. Otherwise, the continuously applied cutting force excites vibrations and continuously generates material or cutting tool tip point vibration displacement. In this calculation, the milling table displacement amplitude is the solution for the vibration differential function. The MathCAD™ solving tool with the ODE (ordinary differential equation) solver function was used to make final calculations, and to detect the chuck fixed workpiece displacement. The variables used for calculations are milling table mass and cutting force value. The damping and spring mass coefficients have been adjusted to fulfill the deviation amplitude in the feed direction, observed on surface topography between two subsequent cuts. Important variables are cutting force and its frequency, obtained from the spindle rotation frequency. All of them are given variables for ODE solver in MathCAD™ software tool. The results were obtained by solving the following differential equation.

$$\boldsymbol{M} \times \left(\frac{\boldsymbol{d^2}}{\boldsymbol{dt^2}}\boldsymbol{y(t)}\right) + \boldsymbol{C} \times \left(\frac{\boldsymbol{d}}{\boldsymbol{dt}}\boldsymbol{y(t)}\right) + \boldsymbol{K} \times \boldsymbol{y(t)} = \boldsymbol{f(t)} \tag{8.5}$$

$$\boldsymbol{f(t)} = -\boldsymbol{Ft}\big(\boldsymbol{\lambda(t)}\big) * \boldsymbol{cos}\big(\boldsymbol{\lambda(t)}\big) - \boldsymbol{Fn}(\boldsymbol{\lambda(t)}) * \boldsymbol{sin}(\boldsymbol{\lambda(t)}) \tag{8.6}$$

Where M – mass of the table, C – damping coefficient, K – spring coefficient, $f(t)$ – cutting force functions that depend on time and $y(t)$ is displacement, $\lambda(t)$, is the tool immersion angle, as a function of time.

Cutting vibration amplitude was calculated, considering the natural frequency measurements on machine elements, estimated machine table weight and exciting cutting force during the cutting process. Cutting forces were not measured, but simulated with the AdvantEdge™ FEM simulation tool. The simulation model was prepared considering the cutting process conditions and specimen material mechanical properties. The cutting tool CAD model was developed taking into account realistic cutting tool geometry from measurements and material properties from the tool manufacturer. A realistic tool-workpiece interface was developed with the FEM software tool. With FEM software tool settings it was possible to determine the conditions of interaction. With these conditions we understand cutting regimes, mechanical properties, environmental properties and thermal properties. All selected conditions were taken from the experimental part of the research. Constraints and degrees of freedom were determined to define the conditions of

the simulation. Simulation results represent 3 cutting forces in X, Y and Z directions. Fx cutting force magnitude represents the most representative cutting force in Feed directions in our case. The simulated feed direction cutting force Fx values at different feed rates are presented in Table 8.3.

Table 8.3. Cutting force Fx values at different feed rate for DIN 1.1730 material.

MATERIAL TYPE	***F1 = 0,04 mm/tooth***	***F1 = 0,1mm/tooth***	***F1 = 0,2 mm/tooth***
DIN 1.1730	15,2 N	38,7 N	76,2 N

The best way to represent the results of dynamic displacement is a graph. Dynamic displacement is a variable and can change hundreds of times per second. The graph represents displacement values over time that can be transformed into revolutions or tooth passes. It can be used to follow up the dynamics of the cutting process and draw the surface topography, affected by the dynamics of the milling system. As discussed in a previous section, the natural frequency of the KONDIA B500 milling machine table was measured at 76 Hz and 78 Hz. Considering dimensions of milling table and density of tool steel, it was estimated the mass, M, of its milling table:

Density of milling table material: $\delta_{table} = 8138\ kg/m^3$

Volume of Milling table (calculated with SOLIDWORKS from CAD drawing):

$V_{table} = 0.0138\ m^3$

$$\boldsymbol{M = \delta_{table} \times V_{table}} \tag{8.7}$$

The result of this calculation is the mass of the KONDIA B500 machine milling table:

$m_1 = 112{,}68 kg.$

The measured natural frequency, milling table mass and cutting force magnitude Fx was substituted in Eq. 8.5. and solved with the MathCAD™ software tool. Fig. 8.7 represents the results – KONDIA B500 milling machine and cutting feed F2=0,1 mm/tooth interaction caused milling table vibrational displacement in the cutting feed direction. Vibration amplitude changes over time, so is different for every tool revolution. For samples #1 – #24 vibration amplitude increases up to 0,005864 mm in feed direction.

The solved function is represented as a plot of milling table vibrational behaviour. The dampening coefficient has an assumed value, customized for the deviation in marks in the feed direction observed in Fig. 8.6. This plot of vibrations represents the vibrational amplitude magnitude (in meters) for milling table axial displacement on the *X* axis. This function is used in all further calculations to detect the vibrational behaviour of the milling table. The most representative value of calculated vibration amplitude is maximum magnitude of the vibration

plot and it is selected for mathematical surface topography Sz parameter formation calculations in this research.

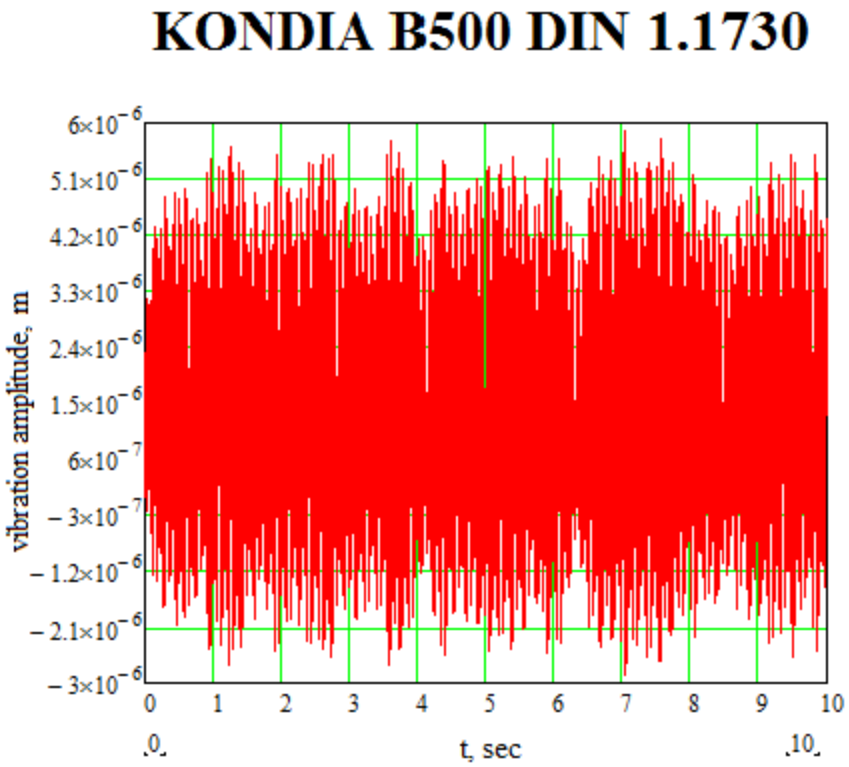

Fig. 8.7. Plot of the solved second order vibration system equation (KONDIA B500 machine, feed F2 = 0,1 mm/tooth.)

Where δz_{vib} – vibration amplitude is in meters and "t" - time in seconds. The graph represents dynamic displacement along the Z axis of the milling table due to natural frequency and excited cutting force F_X, in time. Time can be substituted by revolutions, since we know the rotation frequency and period. Simulated vibration amplitudes according to feed rate for DIN 1.1730 material machined with KONDIA B500 milling machine are represented in Table 8.4.

Table 8.4. KONDIA B500 milling machine vibration amplitude along the *X* axis due to cutting force Fx

MATERIAL TYPE	FEED 1, 0,04 mm/t	FEED 2, 0,1 mm/t	FEED 3, 0,2 mm/t
DIN 1.1730	0,005159 mm	0,005864 mm	0,007126 mm

Predicted values represent the worst scenario due to vibrational influence. With increased feed rate, vibration amplitude increases. Mathcad software calculation shows that cutting force Fx in feed direction always perform high milling table deviations that affect the distances

between cuts and surface roughness indirectly. The higher is milling table deviation, the higher is surface topography parameter S_Z value and bigger deviations can be observed between subsequent cutting marks. Therefore, we can observe increase of surface topography with increase of feed rate. Real deviation between cuts may be lower and may not coincide with deflection of tool axis. Accordingly, tool deflection importance could be decreased. But, if cutting tool inclination, angular displacement and vibration, have influence together to cause deflection in one phase, this may result in greater surface roughness.

8.4. Theoretical model: discussion of results

The analytical model of all previously detected deviation components was plotted, to obtain the total tool tip point deviation from its ideal condition trajectory. Tip point deviation is not constant over the contact area of the material. It is affected by tool axis deflection and inclination, milling machine alignment and cutting forces of the milling process. The previously developed model, as it was concluded, still had some flaws. In this chapter, the prediction model was supplemented with a vibration component to improve its accuracy. As a result, we compared mathematical results with measured ones. The estimated analytical model presents tool point deviation in a situation of slot milling, when whole diameter radial cutting depth is in contact with the workpiece. 3D topography measurement regions were rectangular zones of 1,7mm x 1,25mm. The plotted result is divided by the same interval, to see the appropriate surface height in a specific area.

Total surface height variation in the Z axis direction, $\delta S_Z(\lambda)$, is calculated as the sum of each calculated component. The model has been improved by including the machine-tool-workpiece system's natural frequency, causing milling table deviation in feed direction that affects the radial cutting depth. This, in turn, affects the cutting forces and cutting tool deflection value, influencing variations in depth of machined surface marks. The addition of this will give a more accurate surface maximum height in the scale-limited surface area parameter Sz, Eq. (8.8).

$$\boldsymbol{\delta Sz(\lambda) = Sz_{min} + \delta Sz\big(F(\lambda)\big) + \delta Sz_T(\lambda) + \delta z_{vib}} \qquad (8.8)$$

Where the basis of this formula is taken from the result of previous chapter: $\delta Sz(\lambda)$ – is calculated surface topography height value which is made up of Sz_{min} – minimum surface height performed by cutters geometrical behavior, as calculated in previous Chapter 7.5. $\delta Sz(F(\lambda))$ – tool deflection caused by cutting forces is the component formed by cutting forces. $\delta Sz_T(\lambda)$ – is the cutting tool axis inclination component due to machine inaccuracies. The last variable added – δz_{vib} – Vibration component resulting from the Mathcad vibration solver analysis. The following variables from the previous experimental part were used: the same cutting tool and its length outside of chuck, H = 34,8 mm, feed rate F2 = 0,1 mm/tooth, milling head inclination around machine X axis τ_X–1,5153107°, around machine Y axis τ_Y – 0,2422552°, cutting force component according to feed rate F2 and natural frequency of KONDIA B500 milling table is 76 Hz.

The results of the mathematical model components and their comparison with averages of measurement results are represented in Table 8.5. Sz value without the vibration component are results from previous chapter of Table 7.13. Sz value including the vibration component is the amplitude of Sz change due to vibration in feed direction. Total predicted Sz represents the sum of total predicted value of surface topography height parameter Sz. Differences between the measured average and predicted value represent the percentage between the measured and simulated surface topography heights. The ddifferences between directions represented as a percentage between calculated surface height discrepancies of opposite cutting directions.

Table 8.5. Table of measured and predicted surface topography parameters for KONDIA milling machine

Feed direction	**Measured S_Z mean value, µm**	**S_Z value without vibration component, µm**	**S_Z value from vibration and deflection in feed dir., µm**	**Total predicted S_Z value, µm**	**Difference between measured average and predicted, µm, %**	**Difference between directions, %**	
						Measured	**Predicted**
1. SOUTH	14,837155	6,796374	0,0003721	7,168471	7,668684 51,7 %	5,4 %	6,2 %
3. NORTH	15,682900	7,239986	0,0003721	7,612084	8,070816 51,5 %		
3. WEST	12,441450	5,691171	0,0003591	6,050268	6,391182 51,4 %	46,6 %	43,9 %
4. EAST	23,321250	8,345189	0,0003591	8,704286	14,616964 62,7 %		

We can now compare the results from Table 8.5 with previously simulated results from Table 7.13. The calculation show higher surface topography parameter Sz values in all directions. The highest tool inclination was observed in the EAST direction, as previously, with the lowest value – in WEST direction. We can see that the difference between measured and predicted value due to impact of deflection and vibration component decreased by 2,3 % (from 53,8 % (Table 7.13) down to 51,5 % in latest analysis). The differences between orthogonal directions decreased from 6,5 % down to 6,2 % in SOUTH-NORTH and from 46,6 % down to 43,9 % in WEST-EAST directions. These results represent improvements of developed model accuracy, but still do not demonstrate the reliability of the developed prediction model. There are still differences in some samples between predicted and measured values up to 62,7 %, which may result from other factors not considered in this research.

Summarizing:

The “Analysis of the Flat-end Milling Model – Vibration Component” chapter deals with improvements to the previously developed surface topography prediction model including the vibration component. Vibrations generate surface topography deviation during the cutting process. This deviation was added to the surface topography parameter S_Z prediction model, developed in previous chapters. General observations from this analysis and the results of the mathematical model lead us to the following conclusions:

1. The natural frequency of the cutting tool causes a visible but not significant influence of surface topography parameter Sz formation. Marks on the machined surface images along one tooth pass-by correspond to the cutting tool vibration frequency. These marks affect the local surface deformation and don’t affect the total surface topography parameter S_Z deviation.

2. The natural frequency of the milling table directly affects milling table vibrations, excited by cutting forces. The vibration component is one of the most important factors for machines with low stability, low mass and low natural frequency. When included in the developed mathematical model, the vibration component represents changes in surface topography height due to the dynamic change of axial and radial cutting depth. With the change in radial cutting depth, the feed rate changes constantly, affecting cutting forces, tool deflection and uncut chip thickness. This, in turn, affects the machined surface topography.

3. Every redundant stop and start of the cutting feed during the milling process generates high amplitude excited vibrations. The consequences of these stops and starts are surface damage and a higher surface topography parameter S_Z value.

4. One of the reasons why the prediction results differ from measurements so widely is the error in measured data treatment. The data threshold for surface measured data must be applied at last 2 % from minimum and maximum value, to avoid disturbances in real topography height representation. Therefore, measured data for further analysis must be treated more carefully, excluding the unreliable data points from calculations and faulty interpretation of measurements.

Dynamic behavior is an important factor and must be considered in further topography simulation for all milling equipment used in flat-end milling operations. The developed mathematical model for surface topography parameter S_Z is an accurate, useful tool to predict the surface topography when considering technological and process parameters. It provides high accuracy and includes all the most important factors that have a major impact on the surface topography height. There is still space for some more minor improvements in future, that may change the cutting system behavior and affect the surface topography. But is this model

applicable for different milling environment, different milling machine and others metallic materials? The next chapter will confirm or refute this statement.

9. DATA VALIDATION MODEL AND RESEARCH RESULTS

In previous chapters we were working on the mathematical model development, to calculate the surface topography height parameter S_Z. All the listed effects, including tool alignment error, tool deflection, tool concavity angle and its subsequent minimal surface roughness performed sharpening errors, etc. provide a prediction result with a high error value. The mathematically obtained results are not comparable (difference is more than 10%) with the outcome of surface topography measurements. Discrepancies between predicted and measured values are from 51% up to 62%. To make results comparable and achieve an error difference of less than 10%, measured surface topography, from where we take important data for further model development must be treated carefully. The new treatment function will be introduced in this chapter for surface topography analysis.

Also, to be sure about the reliability of the previously developed mathematical surface topography calculation model, these calculations should be tested and checked with other environments involved in the experiments. What would have happened if we had selected different machining conditions, a different machined material type or tool? Is this model applicable also for another machining system environment? This is the main question to be answered in this chapter. The question arose from analysis of other authors' related literature in Chapter 2. Another type of workpiece material will be introduced, to extend the factors and analyze their influence on surface topography formation. Both milling machines will be used to diversify the cutting process factors.

In this chapter, the same calculations and analysis will be performed once again, with an improved number of technological parameters, to validate the model accuracy and make statements about the material mechanical property, technological factor and cutting environment influence on 3D surface topography parameter values.

9.1. Material and milling equipment selection

As mentioned in the introduction, an additional milling environment has to be selected to test the developed model with different cutting environment. In this section we will select a second type of mold steel material and technological environment, to use it for mechanical treatment of steel samples.

In line with the work conducted during the Master's thesis and prior to the PhD, we decided to select the mould steel DIN 1.2312. Its mechanical properties are represented in Table 4.1 of Chapter 4.

The milling equipment selected for the experiment is the same, used before – KONDIA B500 and GENTIGER GT-66 High-speed Milling machine. Both machines have known vibrational behavior (described in Chapter 8.) and they are acceptable for the requirements of this research project. Laboratories and sample fixture environmental conditions are the same in both cases. The same clamp system "FORZA" was used for both machines and for both experimental cases (Fig. 9.1).

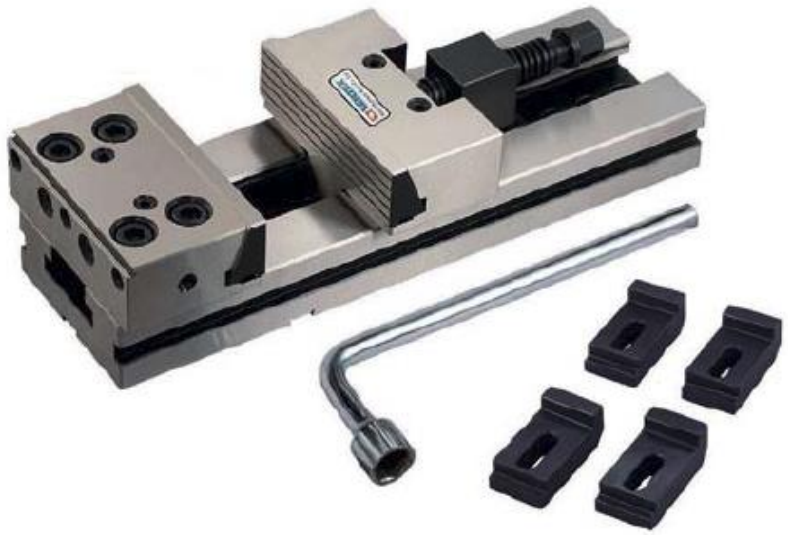

Fig. 9.1. "FORZA" fixture for milling machine workpiece setup [135]

The selected sample clamping system from FORZA meets the HSM requirements and is suitable for selected sample setup. The same clamp was used in sample preparation for the Master's thesis (Chapter 4.) and previous samples in Chapter 6 and 7. Therefore, it is a logical step to apply the same clamping tool for further analysis, if equipment vibrations are to be analyzed. Now that the additional milling equipment and material have been selected, we shall turn to the development of new experiment designs.

9.2. Cutting conditions and Design of Experiments

The previously developed four-directional cutting strategy samples (Fig. 7.1) was recognized as a good general tool to take into account different milling equipment behavior, according to the four basic directions. It was used to analyze differences in the milling head alignment against the milling table. The same four-directional sample strategy was selected for this part of the analysis.

In total, this part of the experiment involves 4 different variables (machine, material, feed speed and cutting direction). Machine and Material Factor is changing in 2 levels, feed speed – in 3 levels and cutting direction – in 4 levels. In total, we obtain a 2^2x 3^1x 4^1 design of experiment

and 48 samples to be performed. Table 9.1 compiles the values of the factors for each sample to machine.

Table 9.1 Design of experiment

Machine KONDIA B500			**Machine GENTIGER GT66V**		
F1 D1 M1	F2 D1 M1	F3 D1 M1	F1 D1 M2	F2 D1 M2	F3 D1 M2
F1 D2 M1	F2 D2 M1	F3 D2 M1	F1 D2 M2	F2 D2 M2	F3 D2 M2
F1 D3 M1	F2 D3 M1	F3 D3 M1	F1 D3 M2	F2 D3 M2	F3 D3 M2
F1 D4 M1	F2 D4 M1	F3 D4 M1	F1 D4 M2	F2 D4 M2	F3 D4 M2
F1 D1 M2	F2 D1 M2	F3 D1 M2	F1 D1 M1	F2 D1 M1	F3 D1 M1
F1 D2 M2	F2 D2 M2	F3 D2 M2	F1 D2 M1	F2 D2 M1	F3 D2 M1
F1 D3 M2	F2 D3 M2	F3 D3 M2	F1 D3 M1	F2 D3 M1	F3 D3 M1
F1 D4 M2	F2 D4 M2	F3 D4 M2	F1 D4 M1	F2 D4 M1	F3 D4 M1

Where F – cutting feed level (F1 = 764 mm/min, F2 = 1910 mm/min and F3 = 3820 mm/min); M – material factor (M1 = DIN 1.1730, M2 – DIN 1.2312) and D – cutting direction level (D1 – South, D2 – West, D3 – North and D4 – East).

This time we increase each cutting feed rate 2 times, to better distinguish the marks left on the material surface. For the remaining cutting parameters, we selected the same values as previously, to make these models comparable.

1) Spindle speed: n = 4775 r/min, equivalent to cutting speed V_c = 150 mm/min;
2) Axial cutting depth – 0,3 mm;
3) Radial cutting depth – a_e = 10 mm;

As mentioned with reference to Table 9.1, feed speed is increased 2 times, comparable to the speed used in experiments performed for our Master's thesis. All presented factors are included in Fig. 9.2 for a clearer view. The images represent the aforementioned cutting parameters with their numerical values.

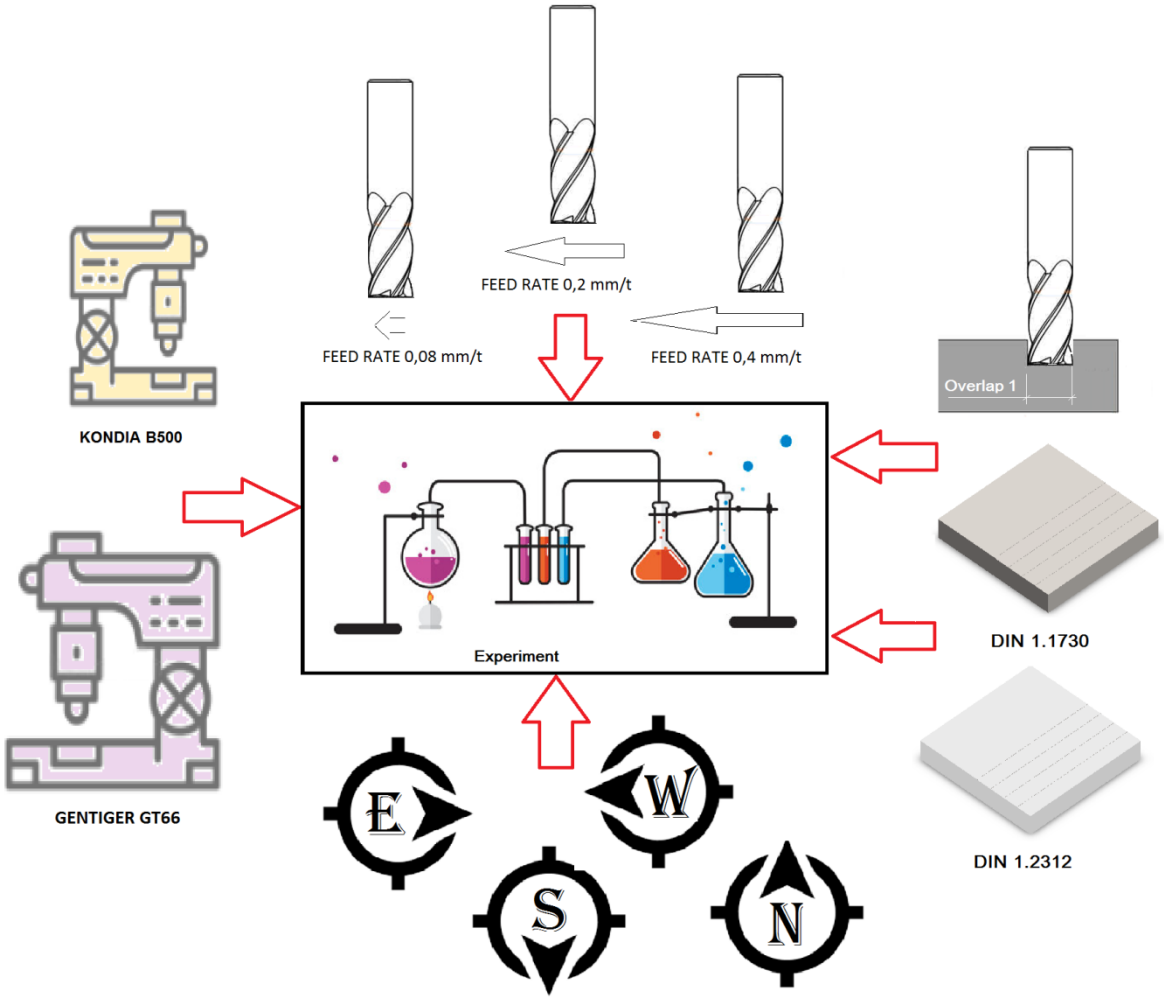

Fig. 9.2. Design of Experiments for research validation model

The sample arrangement on the specimen is an easy task. Each material has 6 specimens which have been machined with 3 different feeds on both milling machines. As one machining operation contains all 4 cutting directions, no additional specimen is necessary for cuts in other directions. Now that all the necessary machining factors have been determined, we can turn to the experimental itself.

9.3. Experiment execution, surface topography and natural frequency measurements

The experiments were undertaken in the same laboratory, using the same cutting tools as for the first two cycles of experiments. Wear of the cutting tools was not considered, for the same reasons as previously. 6 specimens of each sampling material were flattened after clamping them, to ensure the same cutting depth all over the sample surface - three for each machine. CNC machine code was prepared before experimental execution, to hold the execution cycle automatic and without interruptions that may affect the surface topography formation. Number of each sample was fixed in the processing protocol.

After surface preparation, roughness and topography measurements were taken. The same measurement equipment as previously was used to maintain uniformity of measurements – the BRUKER CONTOUR 3D optical measurement device. The main equipment properties were described in Subchapter 6.2.

Previously, direct surface topography measurement values for Sz parameter were used. These values contain measurement device errors and machining errors. This time a new studiable – Threshold option has been introduced to make the measurement results more reliable. Threshold filters 2 percent of minimum and maximum values, where measured values are not reliable, faulty or disturbed. Correctly treated surface topography images gives more reliable results, where exactly the milling equipment and workpiece material effect can be precisely observed in the machined surface topography.

Topography measurement results are represented numerically and visually. Numerical results are easy to use for statistical and mathematical analysis; they were used to compare means of the calculated and measured surface topography. Visual representation reveals local surface topography changes and provides a clue for investigating the influence of local deformation and inaccuracy on surface topography formation. The color plot helps to compare every single pass of the tooth. Differences in the colors represent the differences in surface height for every tooth pass, as represented in Fig. 9.3, where the DIN 1.2312 material specimen, machined with KONDIA milling machine at NORTH cutting direction (#43) has been selected for representative purposes without any filter applied after topography measurements. In this figure, color changes represent variations in surface heights by each of the cutting tooth passes. We can observe machining errors like rapid color changes at the cutting tool path and sometimes, we can observe points as spikes, spread over the measured surface. Also, some areas of the measured image may reveal different color plots of the measured surface, which indicate drastic changes in the surface topography level. The measured area is only 1,7 x 1,25 mm and fast slope of whole machined surface may indicate measurement errors. Measurements and predicted surface topography compared in previous chapter revealed significant differences and suggest that the prediction model was not applicable for this surface machining type. However, a general and more accurate filtration diminishes the effect of a distorted surface due to measurement and machining inaccuracies. Optical surface topography measurement equipment enables fast topography measurements by reflection of light on the machined surface

First of all, a sample with a machined surface must be leveled against the surface capture matrix very carefully. Otherwise, measuring equipment recognize sample inclination as surface inclination and may give us incorrect measurements. Secondly, raw measurements contain multiple data points, where reflected light demonstrates incredibly high or incredibly low surface point value, or sometimes do not record this data point due to non-reflected light. These high and low data points are not machining errors and must be filtered with the threshold function of the analysis software.

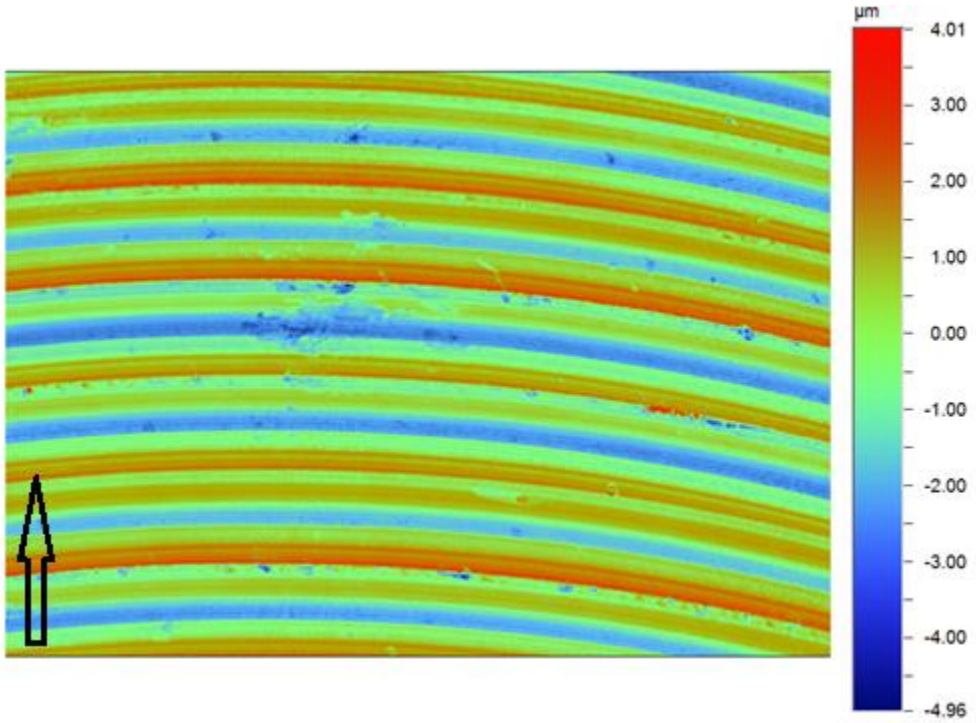

Fig. 9.3. Surface topography image: KONDIA B500 and DIN 1.2312 specimen – 0,1 mm/tooth – NORTH cutting direction.

To understand how the threshold function is used, below we include two images with and without threshold (Fig. 9.4). The level of 2% from minimum and maximum surface topography is the average level, where the most of measurement and machining errors were observed. Consequently, 2% of threshold is an average value that filters the most part of unreliable data points, can be applied for all the machined samples without additional adjustments and this does not affect the real surface topography. Increasing this number increased deformation of the measured surface, while decreasing this number increased the level of measurement error and number of total surface height value Sz. As seen from the 3D topography image, the maximum measurement height is decreased by the level of grey area (h) below the lowest point where cutting tool edge can touch the material. The same is with the highest points of measurements. At the same time, the surface topography image is not altered overall.

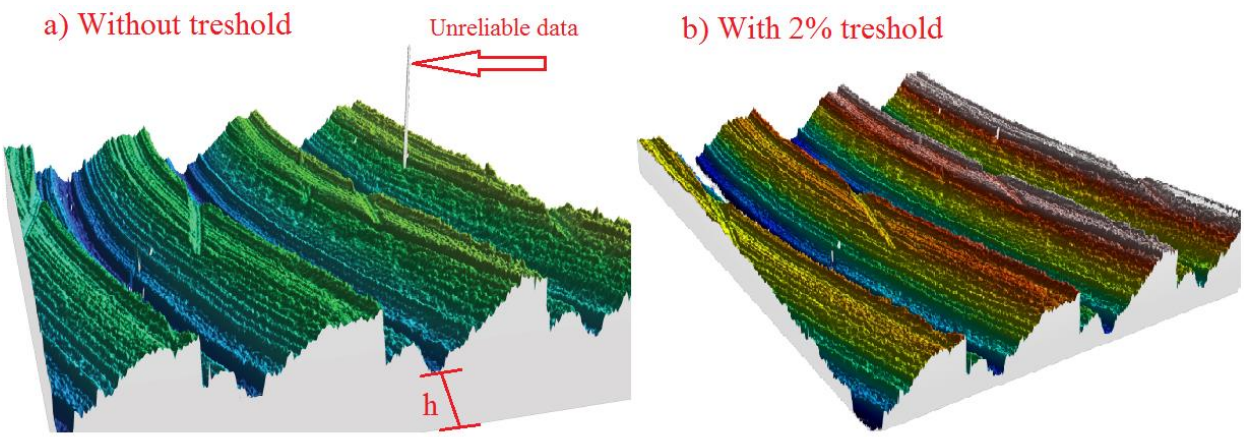

Fig. 9.4. a) Surface 3D topography without applied threshold function, b) surface with applied threshold of 2% from min and max surface height.

From this point, only such measurements with the data threshold applied are available for surface topography analysis model development. Raw data usage from files provided by the measurement device may give incorrect results and make a distortion in result representation.

The next step is to measure the vibration. Milling machine vibration measurements were taken with the Dactron Photon+ vibration measurement device. Accelerometers were attached to the milling table and spindle with a magnet. 3 accelerometers were used to measure vibration in 3 directional axes of a Cartesian coordinate system. Machine table and spindle natural frequency was measured. Natural frequency represents the behaviour of the milling machine structural influence. Dynamic measurements were performed to check for any additional noise on the cutting process from the spindle motor or feed motors.

Cutting forces act as exciting forces that produce vibrations and resonances. Mass and machine geometry affect excited vibration amplitude. Naturally, these resonances may affect the milling material and tool movement interaction and may affect the surface topography formation. Fig. 9.5 represents the vibration measurement process for the KONDIA B500 milling machine.

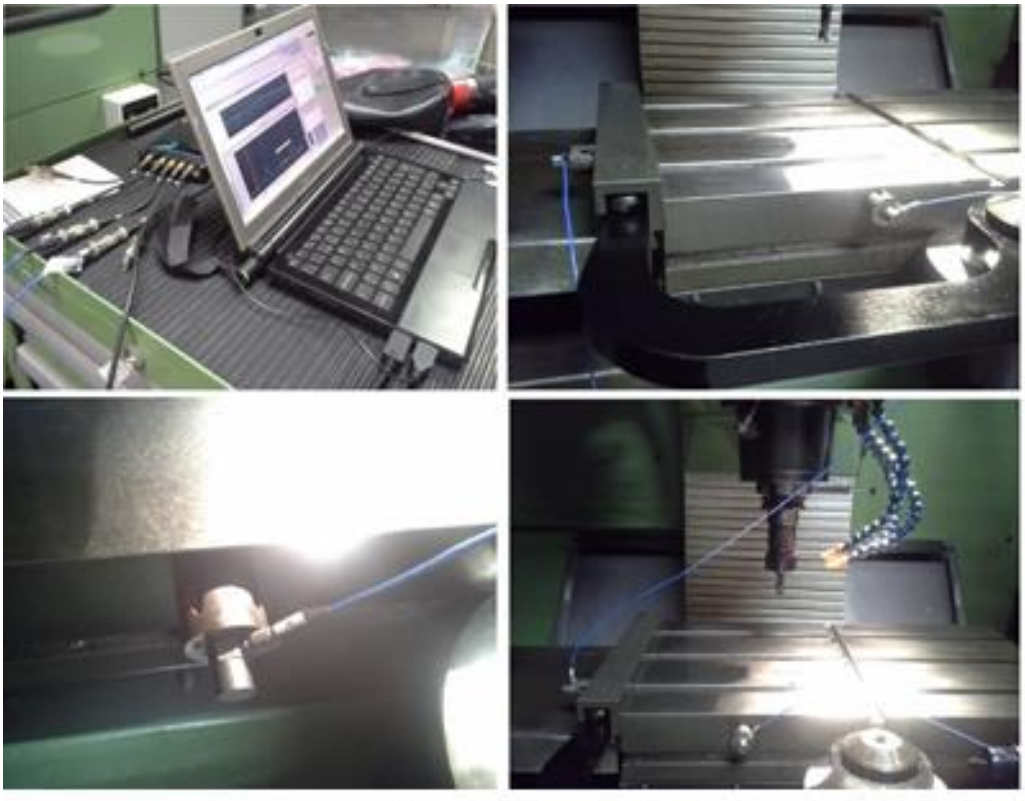

Fig. 9.5. Vibration measurements on KONDIA B500 milling machine table

Dynamic vibration measurements during the specimen preparation procedure were taken during the cutting process. Cutting vibrations were recorded with the measurement device while performing the sample cutting process. The same measurement points selected for natural frequency measurements were used.

9.4. Analysis of vibration data and result validation

9.4.1. Descriptive statistics of measurement data

Surface topography measurements result in a plot of numerical surface point height data values. Descriptive statistics were analysed in a similar way as previously. Results should confirm whether the machining process and surface measurements were performed correctly. Numerical analysis allows us to discuss the surface behaviour and dependence on milling equipment conditions.

Statistical data of all the measured surface topography parameter S_Z values are represented in Table 9.2. This table represents the key values that describe the reliability of the measurement dataset. The mean value is the central value of a discrete set of numbers (7,264278). The median is central value of all data set, if there is even number of samples, that median is the average of both central samples – 6,785 in this case. The mode is the variable of the term that occurs the

most often – 1,841. Std. deviation is a measure that represents dispersion of a set of data values. Skewness represents symmetry of the data set value distribution, while kurtosis – represents whether the data are heavy-tailed or light-tailed relative to a normal distribution. In this case it is 0,717 and 0,343 accordingly. Both values are redirected from normal distribution. Std. error of kurtosis and Std. error of skewness represent the normality of data distribution. Table 9.2 represents the results of statistical analysis. It shows that data are highly skewed and not grouped around the medium value. Also Kurtosis is a high number and represents the wide data distribution.

Table 9.2. Descriptive statistics

N	**Valid**	48
	Missing	0
Mean		7,264278
Median		6,785
Mode		1,841
Std. Deviation		3,50454
Skewness		0,717
Std. Error of Skewness		0,343
Kurtosis		0,343
Std. Error of Kurtosis		0,674

The histogram in Fig. 9.6 represents the numerical result of descriptive analysis from Table 9.2 in a visually more prominent way. The most important parameters to analyze at this stage of work are skewness and kurtosis. Both of them represent the data set match or otherwise with the normal distribution law. If the data set doesn't match the normal distribution law, some selected data is not representative, false or inaccurately measured.

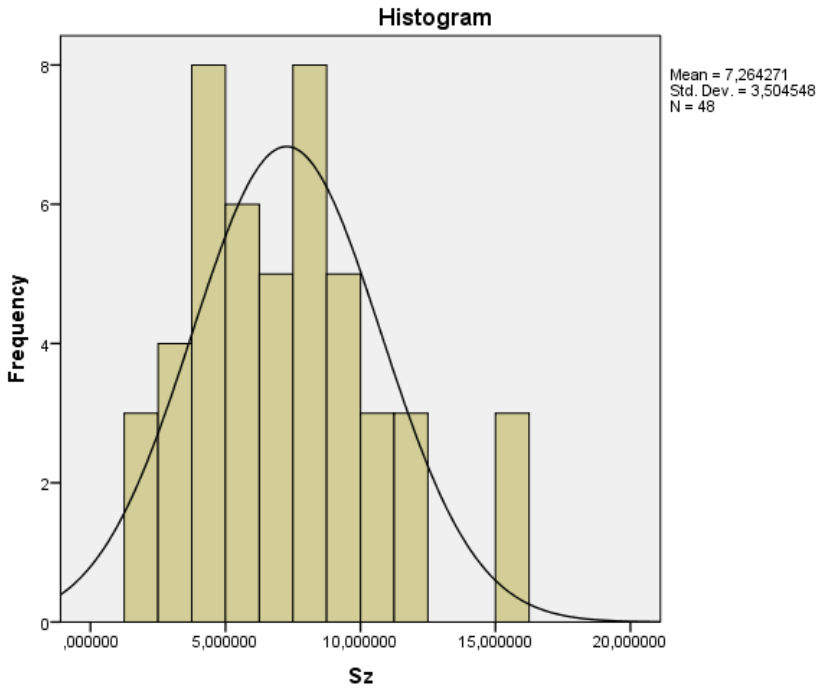

Fig. 9.6. Parameter S_Z frequency distribution histogram.

The skewness value is less than 1: 0,717 (negative skewness), which mean the histogram curve is highly moved to right side from normal distribution. This means most of S_Z values are higher than average. Kurtosis value is also less than 1: 0,343. This represents, that average level of parameter distribution is lower than normal distribution. Values are out of skewness and kurtosis range for normal distribution law (out of range between ±1). If the data set does not match with normal distribution law, some of selected data are not representative, are extremely distorted, or are false or incorrectly measured. Here the skewness and kurtosis coefficients are very high. This means the data distribution doesn't agree with normal distribution law. High feed rate increase has an effect on surface topography measurements, such that Skewness and Kurtosis are distorted from the normal distribution level. Samples which distort the data set can be detected with help of the Box-Whiskers diagram.

The Box-Whiskers diagram shows any unreliable data in the selected data set. It is necessary to separate topography parameters by common input factors like cutting feed rate, cutting direction, etc. Thus the Box-Whiskers diagram represents the deviation of each variable value. Deviation represents how selected measurement data are distributed around Median value and if there are any values outside the distribution boundaries. In Fig. 9.7, the plot represents the deviation of all data, based on 3 feed factors. Y-axis (ordered) represents the surface topography height parameter S_Z, while X-axis (abscissa) represents the selected cutting feed value for machining. The diagram Box represents the upper and lower quartiles of the measurement values. The line that divides the box is median value. The Box Plot shows that the values for LOW and MEDIUM cutting feed are not expanded, while the values for HIGH cutting feed are

expanded to the positive side. Value is highly deviated away from the upper quartile and median value. This is due to sample #46. It has an increased value, but the surface topography is not damaged. Also, its value agrees with the normal data distribution law, as the data point still belongs to the data set – connected with the line in the Box-Whiskers diagram. Therefore, the results should be used in further analysis.

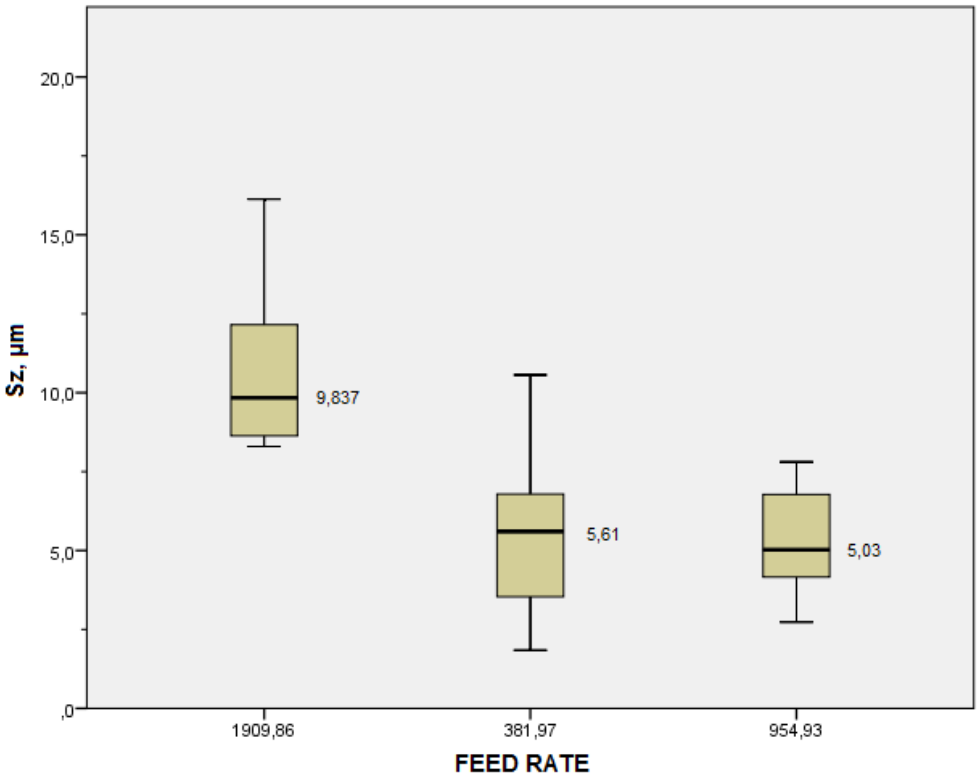

Fig. 9.7. Box-Whisker diagram for feed factor influence analysis

The next selected parameter for statistical analysis is cutting direction. 4 variables – SOUTH, EAST, WEST and NORTH were selected for analysis. In Fig. 9.8, the Y-axis represents the surface topography height parameter S_Z, while X-axis represents the selected cutting direction. One separate point in the West cutting direction bar indicates a sample where values are out of the normal distribution range. This data point belongs to material 1.2312 with HIGH feed rate – sample 17. Moreover, visual analysis will prove that there is no damage or measurement error, It is just a surface topography increased for this sample. Why? This should be analyzed in a visual analysis chapter.

Some of the measurement values do not correspond to the normal distribution law. Sample #34 shows that the measurement values are highly redirected from the median value for the WEST cutting direction. The extraneous measurement is very close to the set of all other measurements. So this time data won't be excluded from further analysis, to make the results

more reliable for a realistic situation. This sample has the highest measured value at the high cutting feed rate and will be considered in further analysis.

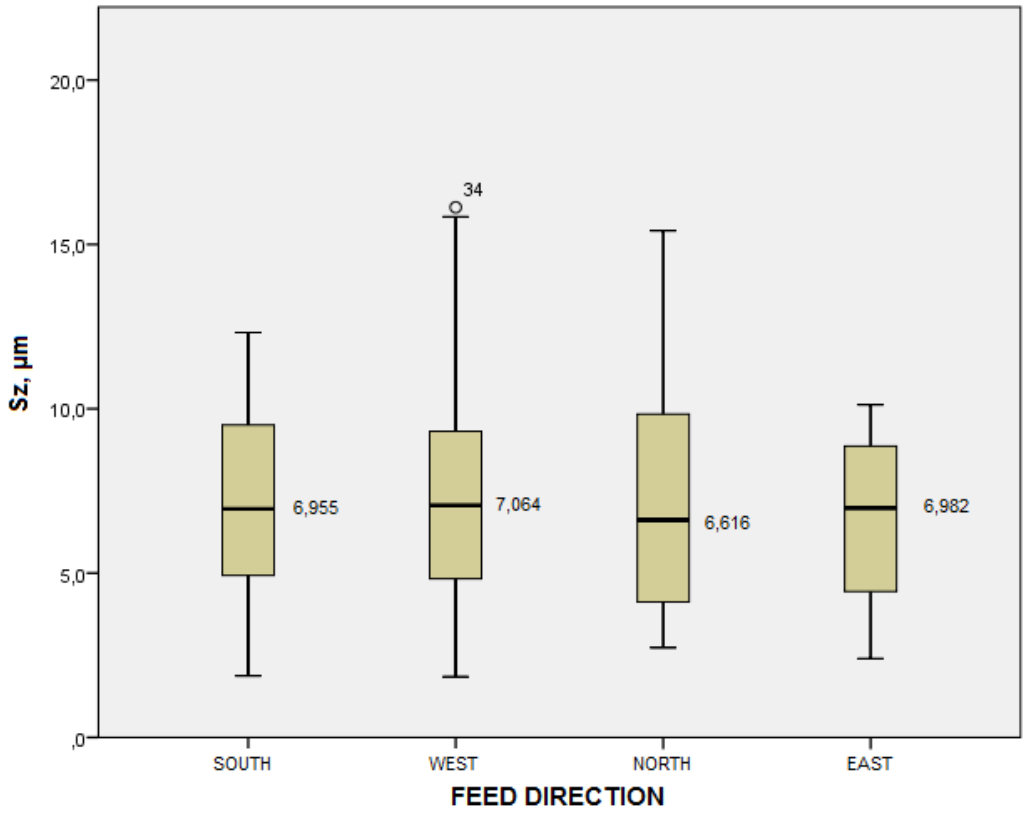

Fig. 9.8. Box-Whisker diagram for analysing teh influence of cutting direction

The next logical step is to understand which of the cutting technological parameters have the highest influence on surface topography formation. For this, ANOVA analysis will be used.

9.4.2. ANOVA analysis of the influence of cutting feed rate, radial cutting depth and cutting direction influence on S_Z formation

ANOVA analysis or Analysis of Variance is a powerful tool to detect selected input factor significance in surface topography parameter formation. One-way ANOVA and Multi-Way ANOVA analysis are main analysis tools, used by a number of authors in the literature review in Chapter 2. In this chapter we analyze each of the input factors with ANOVA to detect their influence on surface topography parameter S_Z formation in the measured samples. Univariate or One-way ANOVA analysis will be performed with statistical computing software IBM SPS.

Feed factor

To analyze only FEED factor influence on the surface topography parameter S_Z, we decided to conduct univariate ANOVA analysis. Feed factor was identified as the input factor, but S_Z

measurements are set as dependent variables. Software computes the results and represents them in result Table 9.3.

The table represents several designations, explained in previous chapters. The F value is the variance of group means, divided by the mean of the variances within the group. The F value in ANOVA also determines the P value (Sig.). The P value (Sig.) is the probability of getting a result at least as extreme as the one that was actually observed, given that the null hypothesis is true [136]. The higher ratio of the F value results in a lower significance P level (Sig.), thus indicating the selected factor's high significance on surface topography S_Z formation. This time, for feed factor software generates F value = 26,480. Respectively, Sig.=0,000 is lower than 0,05 which is the lowest value of significance to reject the H_0 hypothesis (Sig.=0,000 < 0,05). The result reject null hypothesis $H_{0\text{-}1}$. The feed rates used have a significant influence on the measured results (Table 9.3).

Table 9.3. Tests of Between-Subjects Effects – Feed effect

Source	Type III Sum of Squares	df	Mean Square	F	Sig.
Corrected Model	312,076	2	156,038	26,480	0,000
Intercept	2532,942	1	2532,942	429,844	0,000
FEED	312,076	2	156,083	26,480	0,000
Error	265,171	45	5,893		
Total	3110,190	48			
Corrected Total	577,247	47			

Where df – degrees of freedom, F – F-value from descriptive statistics, represent the significance of the model dependent variable, Sig. – significance coefficient P value.

The Corrected Model (in the column 'Source' on Table 9.3) is the sum of squares that can be attributed to the set of all the between-subjects effects, excluding the *Intercept* [128]. Error and Total represent values related to the SPSS internal model used to calculate ANOVA. Corrected Total is the squared deviation of the Dependent variable without grand mean value of data set. All these variables are significant only for final P-value significance Sig. detection. The same designations will be used for further numerical analysis tables.

Direction factor

As explained above, we then conducted ANOVA analysis for another factor - the Cutting direction. The results are represented in Table 9.4. The higher ratio of F value gives lower significance P level (Sig.), thus indicating the selected factor's high significance. This time the significance coefficient value (Sig. = 0,846) is higher than 0,05, which means this factor is also not significant. We accept the H_0 hypothesis and conclude that the cutting direction factor is not

a significant influence on the surface texture parameter S_Z value. Why? The topography height difference between opposite or adjacent directions is not so great and furthermore, the difference between other factors counteract the Direction factor significance. Nevertheless, it still affects the surface topography.

Table 9.4. Tests of Between-Subjects Effects – Cutting direction effect

Source	Type III Sum of Squares	df	Mean Square	F	Sig.
Corrected Model	10,460	3	3,487	0,271	0,846
Intercept	2532,942	1	2532,942	196,634	0,000
DIRECTION	10,460	3	3,487	0,271	0,846
Error	566,788	44	12,882		
Total	3110,190	48			
Corrected Total	577,247	47			

Machine factor

Machine factor analysis represents the result significance according to the type of machine used in experiments and their influence on the surface topography parameter S_Z formation. The results from two types of machines as described earlier were used in this analysis.

The higher ratio of F value gives lower significance P level (Sig.), thus indicating the selected factor's high significance. ANOVA analysis shows that the P-value is greater than the minimum value to reject the H_0 hypothesis (Sig.=0,240 > 0,05). This means that the surface topography parameter S_Z has not been significantly influenced by the selected type of milling equipment. The results of the ANOVA analysis are presented in Table 9.5.

Table 9.5. Tests of Between-Subjects Effects – Machine type effect

Source	Type III Sum of Squares	df	Mean Square	F	Sig.
Corrected Model	17,255	1	17,255	1,417	0,240
Intercept	2532,942	1	2532,942	208,066	0,000
MACHINE	17,255	1	17,255	1,417	0,240
Error	559,992	46	12,174		
Total	3110,190	48			
Corrected Total	577,247	47			

As described later, the second type of machine has no significant alignment particularities that affect the surface topography formation. In this case the difference may arise from the

dynamic behaviour of the milling equipment. For this reason, in addition to analyzing the alignment accuracy of the milling machine, it is also necessary to perform dynamic analysis of milling equipment and include it in the model development. In general, milling equipment has no significant influence on surface topography formation, based on the latest surface topography measurements.

Material Factor

For the material factor, in Table 9.6 we see a significant influence on surface topography formation. The higher ratio of F value gives lower significance P level (Sig.), thus indicating the selected factor's high significance. The F-value ratio is high – this time more than 9 times. It determines the P-value and in this case it is Sig.= 0,000 < 0,05. The other results are represented in Table 9.6. ANOVA rejects the null hypothesis and we can conclude – the Material factor is important for surface topography parameter S_Z formation.

Table 9.6. Tests of Between-Subjects Effects – Material effect

Source	Type III Sum of Squares	df	Mean Square	F	Sig.
Corrected Model	148,154	1	148,154	15,882	0,000
Intercept	2532,942	1	2532,942	271,538	0,000
MATERIAL	148,154	1	148,154	15,882	0,000
Error	429,094	46	9,328		
Total	3110,190	48			
Corrected Total	577,247	47			

Hence, all the factors have been analyzed separately. Now it is time to do the complete Multi-way analysis to detect, which factors are actually significant, in combination with all the others.

Comparison of multiple factors

Table 9.7 below represents the ANOVA results of the surface topography parameter S_Z dependence on all selected and previously described factors.

Table 9.7. Tests of Between-Subjects Effects

Source	Type III Sum of Squares	df	Mean Square	F	Sig.
Corrected Model	510,793	11	46,436	25,155	0,000
Intercept	2532,942	1	2532,942	1372,16	0,000
MATERIAL	148,154	1	148,154	80,259	0,000
FEED	312,076	2	312,076	84,530	0,000
MACHINE	17,255	1	17,255	9,347	0,004
MATERIAL * FEED	2,744	2	1,372	0,743	0,483
MATERIAL * MACHINE	0,004	1	0,004	0,002	0,963
FEED * MACHINE	26,856	2	13,428	7,274	0,002
MATERIAL * FEED * MACHINE	3,704	2	1,852	1,003	0,377
Error	66,454	36	1,846		
Total	3110,190	48			
Corrected Total	577,245	47			

Test of Between – Subject effects represent the real situation of the measurement results.

A combination of different factors may have less or even more effect on the surface topography formation. It depends on the combination. Comparing means by the Sum of Squares, the cutting FEED factor and MACHINE type, as well as MATERIAL, have the most influence on surface topography parameter S_Z. As indicated through F-value ratios and accordingly determined P-values (Sig.). the MACHINE and FEED factors return a Sig.=0,002 value. Other combinations of input factors are not significant.

This section revealed information about the most significant factors acting on surface topography formation. Previously, one-way ANOVA analysis proposed that MACHINE had no significant influence. But, as we observed in results in Table 9.7, MACHINE factor interacting with the FEED factor has a significant influence and may affect the surface formation more than separately.

Nevertheless, the cutting DIRECTION factor in different combinations has no significant influence on the surface topography parameter S_Z, according to the ANOVA analysis. These findings don't tell us whether tool axis inclination is an important contributor to the topography parameter value. The result has been suspended by machine factor in general and it is difficult to distinguish milling axis inclination factor from the topography measurements. As ANOVA shows, machine factor is more significant than direction alone. It involves both alignment accuracy and vibrational behaviour together, and multivariate ANOVA cannot separate these

factors to extract their individual influence. The measurement results plotted in the data chart, Fig. 9.9, present the difference between measurements for different feed directions and material influence on them. Both lines present the difference in surface topography height by used milling equipment. As a validation for ANOVA analysis, figure Fig. 9.9 shows that there are random differences between different directions of cutting tool travel. The highest increase of the S_Z value with both material types was observed in the WEST direction for both machines, while the lowest values are in the EAST direction. The difference between minimum and maximum values is less than 1 micron and it shows that really, the direction effect is not as important as previously considered. The lowest surface topography parameter Sz, this time was achieved in the EAST and SOUTH cutting directions. Therefore, the cutting direction factor will be used in the surface topography prediction model, but it is not significant.

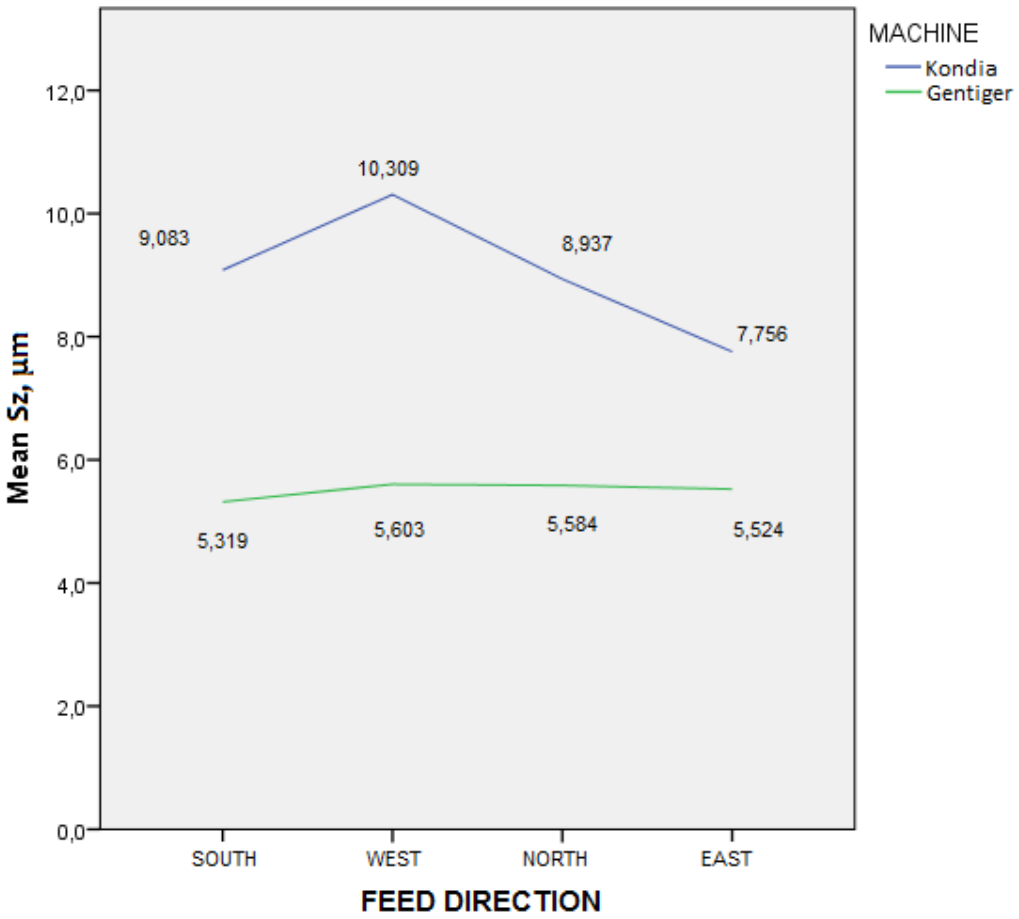

Fig. 9.9. Surface topography height values in different cutting directions by applied milling equipment.

On the other hand, the FEED and MATERIAL factors are the most significant factors affect ingthe surface topography parameter S_Z formation. Fig. 9.10 represents this statement and results of the ANOVA analysis.

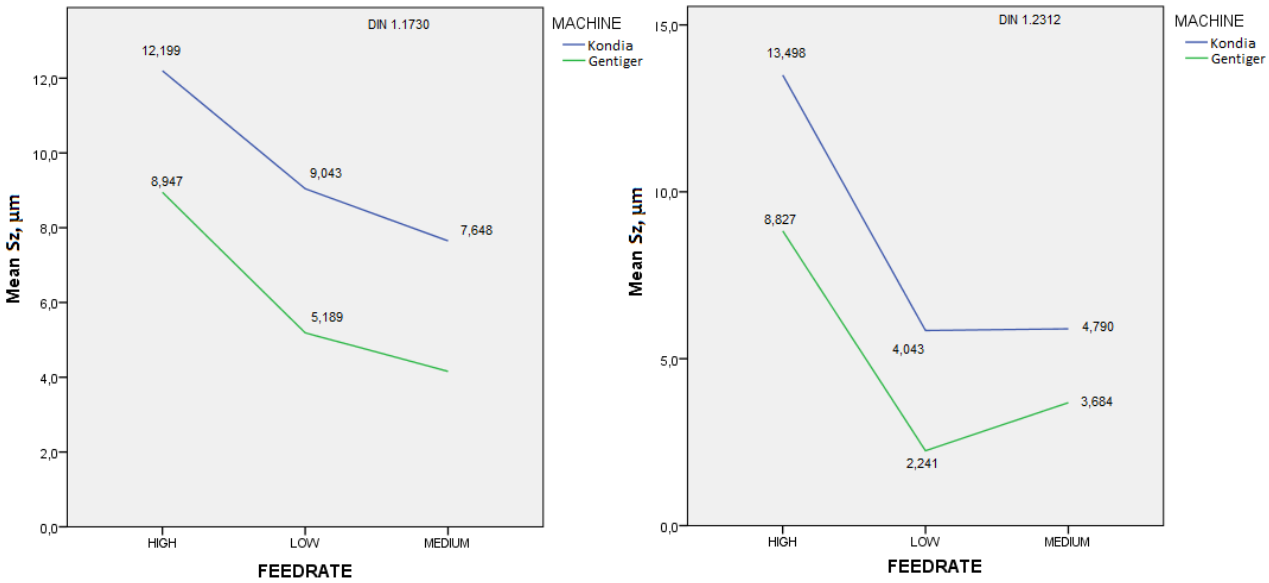

Fig. 9.10. Plot of means for S_Z value by feed rate of both material types (MATERIAL 1 - DIN 1.1730 and MATERIAL 2 - DIN 1.2312.)

In Fig. 9.10, on the left, the DIN 1.1730 material Plot of Means for S_Z parameter by FEED rate is presented. On the right is the same type of representation for the DIN 1.2312 material. In both cases, the plot of Means for the KONDIA B500 (Machine 1) has higher topography values overall than the GENTIGER GT66 (Machine 2). Behaviour of the topography value distribution by feed rate is similar in every case. The lower feed rate generates low or medium topography values, while the higher feed rate producers a surface with slightly increased S_Z parameter values. Distinctions between different feed rate performed S_Z values cannot be overlooked therefore, which confirms the previously developed statement about the MACHINE and FEED rate influence.

It is now clear which factors have the highest influence on the surface topography parameter S_Z. These are machining feed rate, the actual machine itself and the machined material, in order of importance. Cutting direction, as discussed before, is recognized as a less important factor. How it does affect the sample surface, as we see in the next section.

9.4.3. Visual analysis

Measurements of machined samples are crucial to be able to validate the developed model and prove the results. Based on measurement data, surface topography analysis software generates the surface image. Visual analysis of these images may reveal more significant

information about the processes acting on the cutting process. Furthermore, topography parameters should be reflected on surface topography image.

Visual analysis of the measurements reveals highlighted lines of the cutting tool trajectory and movement direction (Fig. 9.11 and Fig. 9.12). General marks that repeat frequently are left from the cutting tool main cutting concavity. Warmer colors represent the highest points in the plot, and cold colors the lowest. In a normal situation, without any disturbances, transition from one color to another should be homogenous. In some samples there were some marks observed from the back cutting edge, where tool deflection and axis inclination together were not high enough to hide these marks. For example, in the NORTH and EAST directions of Fig. 9.11, it is possible to see some interruptions in the transition process. Also, other oppositely performed marks between the highest, red colored points, represent the behaviour of tool deflection, inclination and vibrations, when back cutting edges affect the surface topography formation. Tool inclination is lower than the minimum surface topography height performed with the back cutting edge.

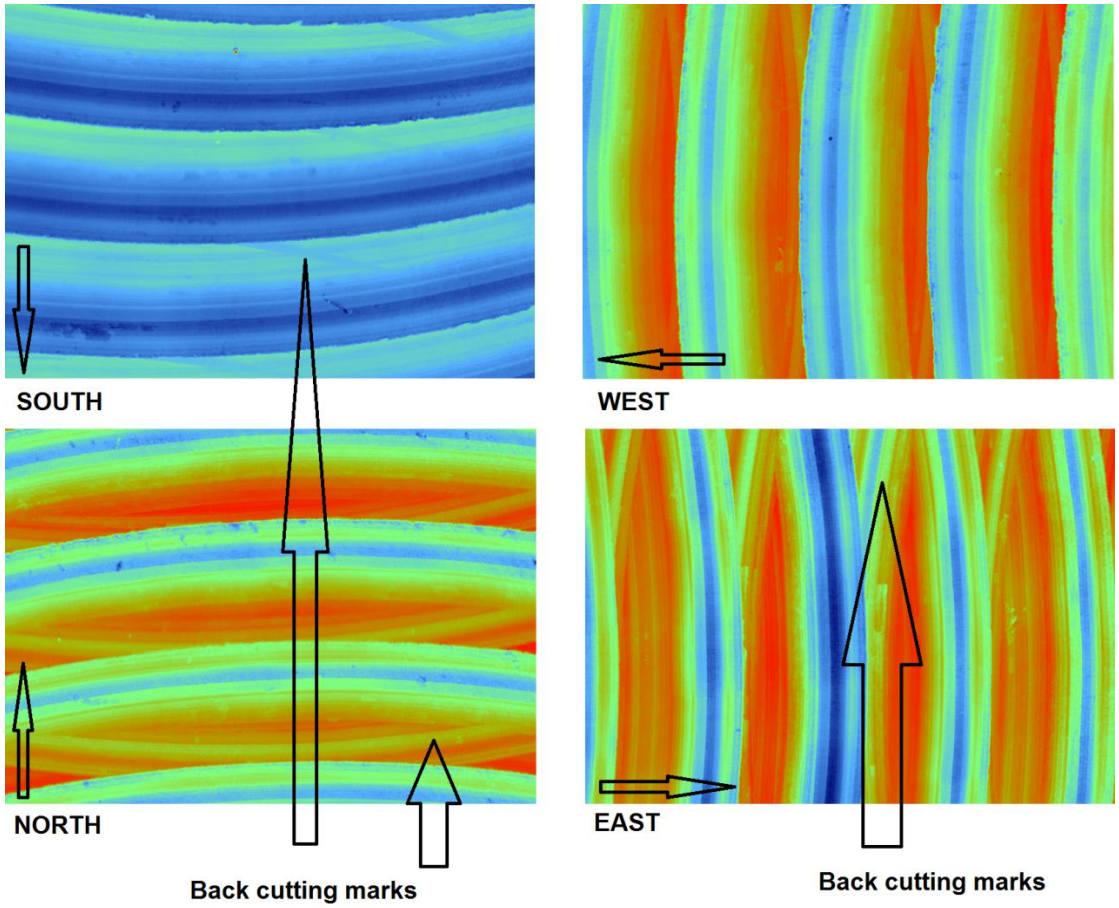

Fig. 9.11. Sample #33 - #36, Feed = 0,4 mm/tooth, material 1.1730 – Machined with KONDIA milling machine

KONDIA milling machine reveals greater differences between cutting directions than the GENTIGER milling machine (Fig. 9.12).

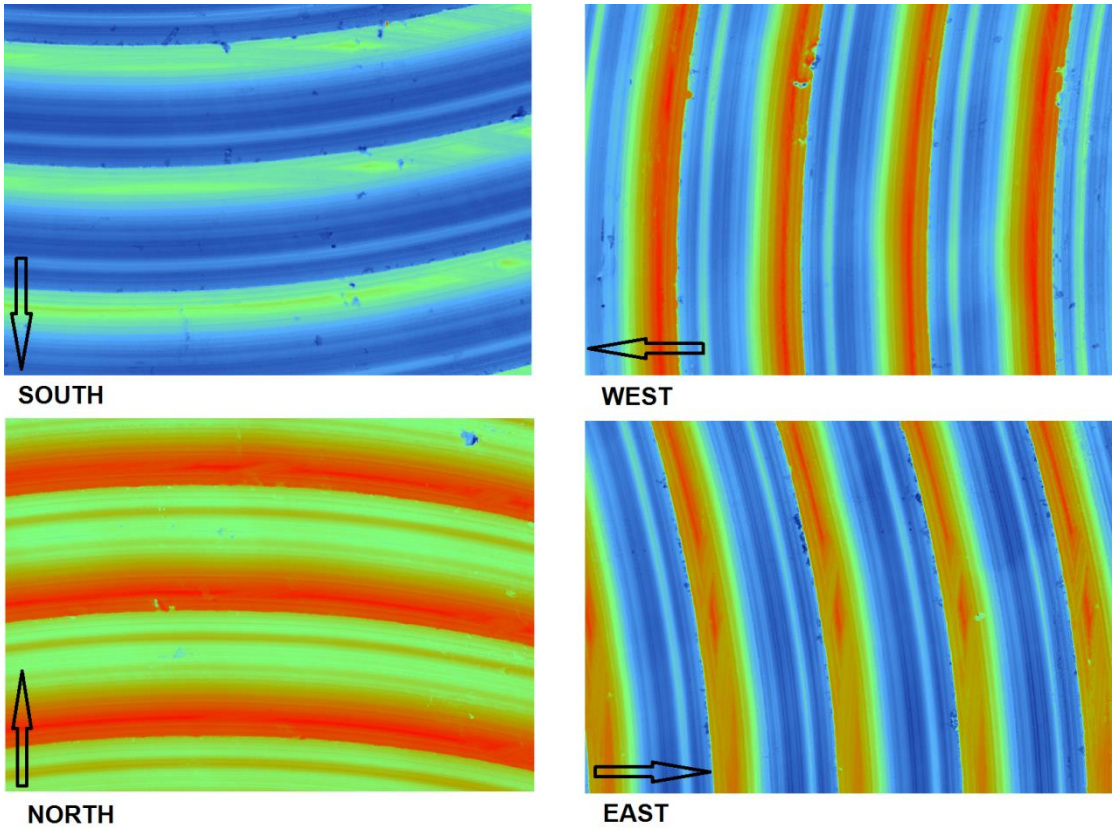

Fig. 9.12. Sample #31, Feed = 0,4 mm/tooth, material 1.2312 – Machined with GENTIGER milling machine

Differences between cutting directions on the sample surface images performed with the GENTIGER milling machine shows lower alignment accuracy error. Also, the transition is more homogeneous and the surface has been less affected by the back cutting edge. Therefore, the surface topography height is more even between all 4 directions.

This time, it is more complicated to conclude anything further from the visual analysis alone. With the KONDIA B500 milling machine the same behaviour was observed as previously. But with the GENTIGER GT-66 milling machine, surface topography is more even and homogeneous. Therefore, it is more difficult to detect unambiguous spindle inclination angle. To do this, we have to make calculations and test the developed theoretical model, as described in the next section.

9.5. Theoretical model: discussion of results

The title of Chapter 9 already indicates that this is a validation chapter. As such, the previously developed mathematical model (Eq. 8.8) will be used to test the reliability of the model with a different machining environment and additional process factors. A new set of experiments have been prepared and executed, and topography measurements have been used to validate the accuracy of the previously developed surface topography model equation.

The main surface topography S_Z prediction model consists of the minimum surface height achieved by the cutter's geometrical behavior S_{Zmin}, cutting tool deflection $\delta Sz(F(\lambda))$, the cutting tool axis inclination component $\delta Sz_T(\lambda)$ and the vibration component δ_{Zvib}. Experimentally applied machines and material types affect these components differently. The results of all mathematical calculations will be described in the next paragraphs of this section. Furthermore, topography measurements of the samples from 3rd research part will be used to confirm the mathematical results.

9.5.1. Cutting force and cutting tool deflection component

In the previous part of this research work, cutting force as a factor of feed rate was recognized as one of most important factors that influence surface topography formation. As visual analysis reveals, with increased cutting feed rate, uncut chip thickness increases along with the cutting force. As the simulation in section 7.5.1 presents, cutting force directly affects the cutting tool deflection along its Z axis. Therefore, the cutting force model component should be considered as one of the main model components, in this case also. Similar to our previous work, cutting forces were not measured but simulated with the AdvantEdge™ software tool.

Cutting force FEM simulation was performed to calculate forces for both types of materials used in this research. A realistic cutting tool-material interface was prepared, with the same approach as in Chapter 7, to ensure realistic simulation conditions. Cutting Force Fx magnitudes, obtained from cutting force simulations for both types of materials used are presented in Table 9.8.

Table 9.8. Cutting force Fx values at different feed rate from FEM simulation with AdvantEDGE software

MATERIAL TYPE	***F1 = 0,08 mm/tooth***	***F2 = 0,2 mm/tooth***	***F3 = 0,4 mm/tooth***
DIN 1.1730	30,5 N	76,2 N	155,15 N
DIN 1.2312	30,2 N	75,4 N	113,4 N

Simulated cutting forces represent the overall picture of the cutting process. By increasing the cutting feed, the cutting force increases proportionally. Similar to previously, the cutting force coefficients for developing the tool deflection component were calculated with the Excel solver tool. It fits the graduated cutting force values to the cutting force equation by least squares, to obtain three values of constants. The solved cutting coefficients are presented in Table 9.9. Coefficient Kt represents tangential forces, Kn – normal forces and Ka – axial forces against the cutting tool local force system.

Table 9.9 Solved system cutting coefficients for both types of materials and 3 cutting feeds

Material Types	**Cutting force coefficients**
C45 – 1.1730	Kt = 2563
	Kn = 0,00889
	Ka = -0,269
40CrMnMoS8-6 – 1.2312	Kt = 2180
	Kn = -0,143
	Ka = -0,293

Considering feed factor correlative cutting coefficients, and substituting the coefficients into equations 7.1 – 7.7 from Chapter 7, the appropriate cutting force components can be detected.

Cutting forces more than double with higher cutting feed, in the *Y* direction, and double in the *X* direction with increased feed rate. In general, calculated cutting forces are proportional. Similar behaviour has been observed also in the *Z* direction. With an increased cutting feed rate, the cutting force F_Z tends to increase proportionally due to the selected calculation method and calculated cutting force coefficients. Thus, the different material DIN 1.2312 has different cutting coefficients, presented in Table 9.9. Cutting forces are represented in Fig. 9.13. The X axis represents the cutting tool immersion angle in degrees, while the Y axis represents the mathematically calculated cutting force, in Newtons (N). The left column represents cutting forces against the tool cutting edge. The right column represents cutting forces in the global machine coordinate system. Both of these plots represent cutting force changes during the cutting tool 180° rotation movement. As it is possible to observe from the force calculation, differences in cutting coefficients lead to differences in force magnitudes. These plots represented in Fig. 9.13 and 9.14 suggest that there are differences between the mechanical properties of both

selected materials (represented in Table 9.10.). The differences are not high, but they affect the cutting process in terms of performed surface topography height. This confirms the ANOVA analysis, that selected material type has a significant influence on S_z and its behaviour should not be ignored in further analysis and may give us sound conclusions about the surface topography formation process during high-speed machining.

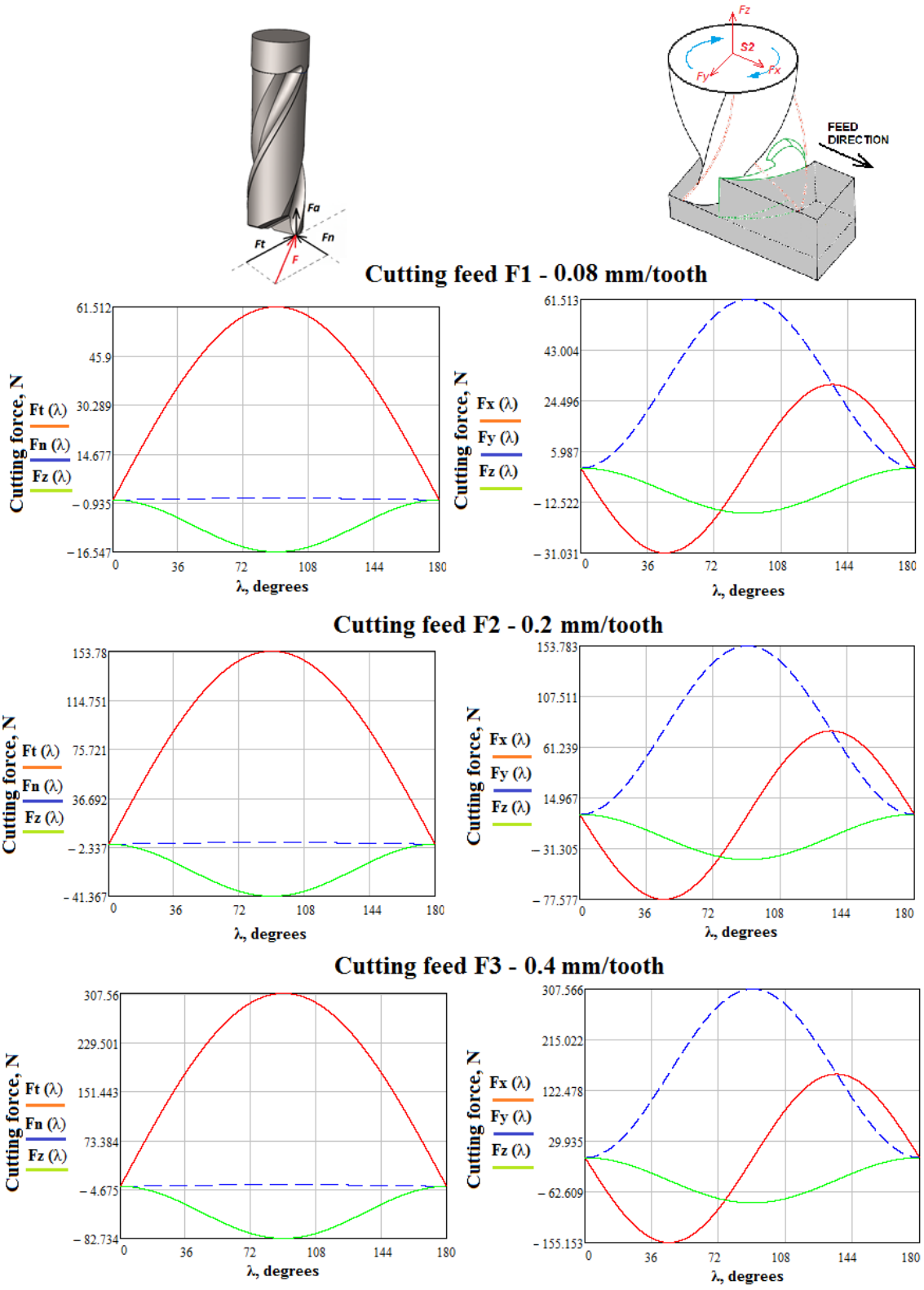

Fig. 9.13. Results of the cutting force model for C45 – DIN 1.1730 material type.

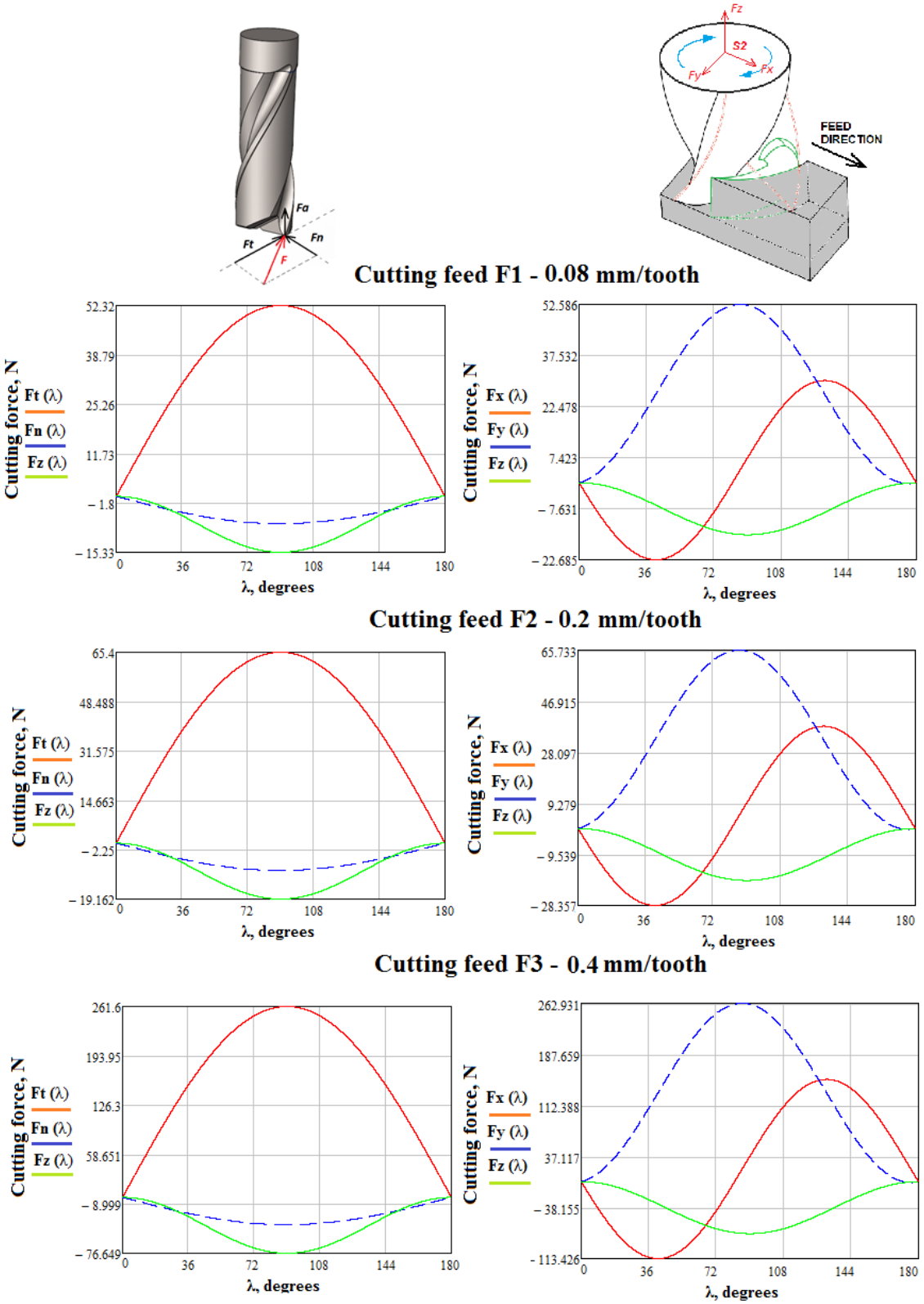

Fig. 9.14. - Results of the cutting force model 40CrMnMoS8-6 – DIN 1.2312 material type.

Table 9.10. Cutting force Fx values at different feed rates modelled in Mathcad with cutting force coefficients.

MATERIAL TYPE	*F1 = 0,08 mm/tooth*	*F2 = 0,2 mm/tooth*	*F3 = 0,4 mm/tooth*
DIN 1.1730	31,031	77,577	155,153
DIN 1.2312	22,685	28,357	113,426

In general, cutting force calculations are used to reach two goals. All three cutting force components affect the sum vector and make a total component of force that may affect the total cutting tool deflection, and accordingly the tool tip point deviation from its initial position. This observation will be discussed in the next section. Secondly, it is used to detect the material mechanical property behaviour which consequently affect the cutting forces and ultimately the cutting tool deflection. As outlined above, it can be concluded that the cutting tool deflection causing tool tip point deviation affected surface topography formation. Cutting tool material and rigidity coefficients, due to the tool geometry, are the basis for the tool deflection model calculation. In the next section we analyze how both selected workpiece material types affect the cutting tool deflection magnitude.

9.5.2. Tool deflection

Different cutting resistances of machined materials affect the cutting forces at work during the cutting process. Cutting forces directly influence the tool deflection and affect the surface topography height accordingly. How great is this effect? We shall find this out below.

Cutting process conditions and tool type have been used as in previous essays. Also, the same tool length setup was applied for each machining operation – 34,8 mm. As previously, we focus on the axial tool deflection. Tool material and geometry-dependent stiffness coefficients were also used, as calculated in Chapter 7. The deflection component is obtained by multiplication of material rigidity coefficients with cutting forces (Eq. 7.10). For the simulation, we use previously simulated cutting force F_Z values and material rigidity coefficients, presented in Table 9.9. The deflection results of DIN 1.1730 were compared with DIN 1.2312. The graph represents cutting tool deflection component value by cutting tool ½ revolution. Where $\delta zFt(\lambda)$ – deflection caused by tangential force, $\delta zFn(\lambda)$ – deflection caused by normal force, $\delta zFa(\lambda)$ – deflection caused by axial force.

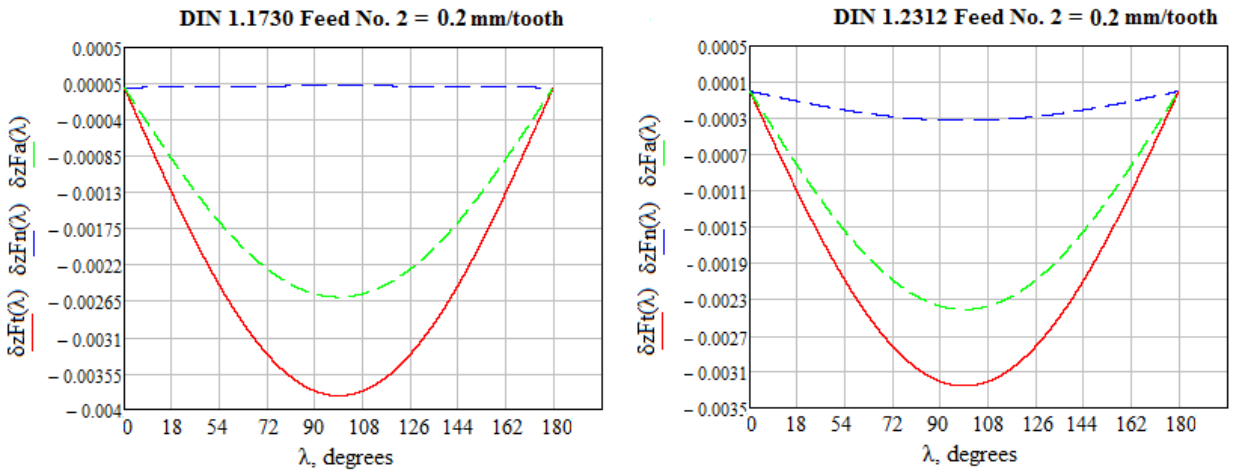

Fig. 9.15. Cutting Tool Mitsubishi MS2MS1000 deflection affected by DIN 1.1730 material and feed factor F2

Tool deflection represented in Fig. 9.15 for both types of materials are similar, as cutting force values for both materials are similar. Displacement differs by tool rotational alignment against the feed direction, as cutting forces depend on uncut chip thickness. Maximum deflection was reached with highest uncut chip thickness, at the half-way point of cutting edge travel from immersion until leaving the uncut material. Therefore, maximum displacement from the tool tip point's initial location could be accepted as a maximum displacement during the whole revolution, and it generates the surface topography height parameter S_Z deviation within one cutting tool revolution.

The sum of the tool deflection component $\delta Z(F(\lambda))$, from Eq.7.10, and cutting tool geometrical component $S_{ZT}(\lambda)$, obtained by Eq. 7.11, forms the minimum surface topography parameter S_Z used for the prediction model. The results of cutting tool deflection caused surface topography formations that are represented in Table 9.11. Surface topography measurements were selected to compare the predicted result accuracy.

Table 9.11 Maximum predicted S_Z parameter value performed by tool deflection for DIN 1.1730 (M1) and DIN 1.2312 materials (M2), compared for samples machined with the KONDIA B500 milling machine

Feed direction	Cutting force, N	S_Z value - measured, µm	Predicted deflection S_Z value, µm	Difference between measured and predicted, µm %
M1 F1 KONDIA	30,5	9,0425	2,4384408	-6,6040592 73 %
M1 F2 KONDIA	76,2	7,6475	6,0960770	-1,551423 20,3 %
M1 F3 KONDIA	155,15	12,19975	12,1921539	0,0075961 0,06 %
M2 F1 KONDIA	30,2	5,844	2,3618238	-3,4821762 59,6 %
M2 F2 KONDIA	75,4	5,8955	5,9044770	0,008977 0,15 %
M2 F3 KONDIA	113,4	13,4975	11,8091539	-1,6883461 12,5 %

Cutting force, or more precisely – the cutting feed rate, affects the surface topography indirectly. With increased feed rate, the cutting forces increase. Consequently, it affects cutting tool deflection. The deflection, together with minimum surface topography height performed by cutting tool geometrical properties performs the main part of whole surface topography parameter Sz value. Predicted results becomes more significant – from 27% even up to 99,94 % of measured topography values, that is an excellent result. Of course, the effect of plastic deformation increases this difference dramatically, if there are uncutted particles left on the machined surface.

The highest differences between measured and predicted values are with a low feed rate. Low value feed rate and plasticity of the work-piece material increase the surface topography values. The cutting process leaves a plastically deformed surface after machining at a low feed rate. Insufficient radial depth of cut, performed in samples with low feed rate, generate higher surface topography parameter Sz values than in samples with double the feed rate. Increased surface height is due to the plastically deformed base material, not being removed by the normal

cutting process. As tool deflection depends on cutting forces rather than equipment behaviour, the difference between predicted values is higher, due to the higher topography measurement values. With increased feed rate, the cutting tool deflection value increases and the importance of the deflection component increases also. We can assume that cutting tool deflection as a direct reflector of the cutting feed influence is one of the most important factors, as the descriptive statistics reported. It directly affects the machined surface topography height value Sz and is the basis of the entire developed mathematical prediction model.

An example with cutting force and tool deflection model calculations is compiled in Appendix D – Mathematical calculation of minimum surface, cutting forces and tool deflection, cutting tool inclination and vibration model.

9.5.3. Milling head inclination

As shown in previous chapters, surface topography, with the same cutting condition, depends on cutting direction. As calculated in the first part of this research project, milling head inclination may account for more than 23% of the surface topography, and together with tool geometry initially be responsible for more than 42% of the surface topography height.

From the visual analysis of samples machined with the GENTIGER GT-66 milling machine, it becomes clear that this machine doesn’t have high inaccuracy related with the column alignment or the milling head alignment to the basis of the machine - Fig. 9.16. This figure represents surface topography images in the 4 cutting directions. The GENTIGER GT-66 milling machine has no certain inclination error in any of the cutting directions. Descriptive statistics and Fig. 9.9 in previous subchapters represent the same behaviour. As we can see from the results of statistical analysis, topography behaviour, distribution and even height level changes between valleys and peaks are similar in every cutting direction.

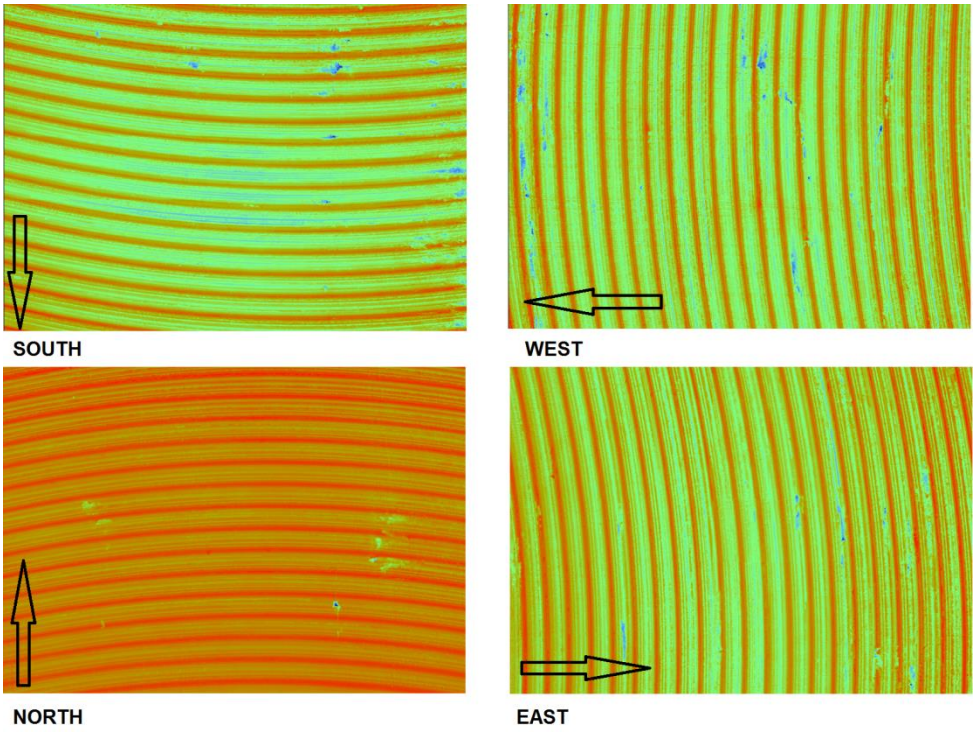

Fig. 9.16. Picture with one sample 4 directions prepared with GENTIGER GT-66 HS milling machine – no major difference in surface height has been observed.

As topography images without filters present, some materials have isolated and separated particles left on the machined surface, with high peaks, see blue circles in Fig. 9.17. These particles are scattered all over the surface and it is difficult to measure only rough surface height without considering material errors. Therefore, with the increased feed rate, these particles become scattered less frequently and other areas, no material errors can be observed. Therefore, it is easier to filter rough topography data of the cutting process, thereby eliminating the effects of a damaged surface or uncut material on surface topography measurements.

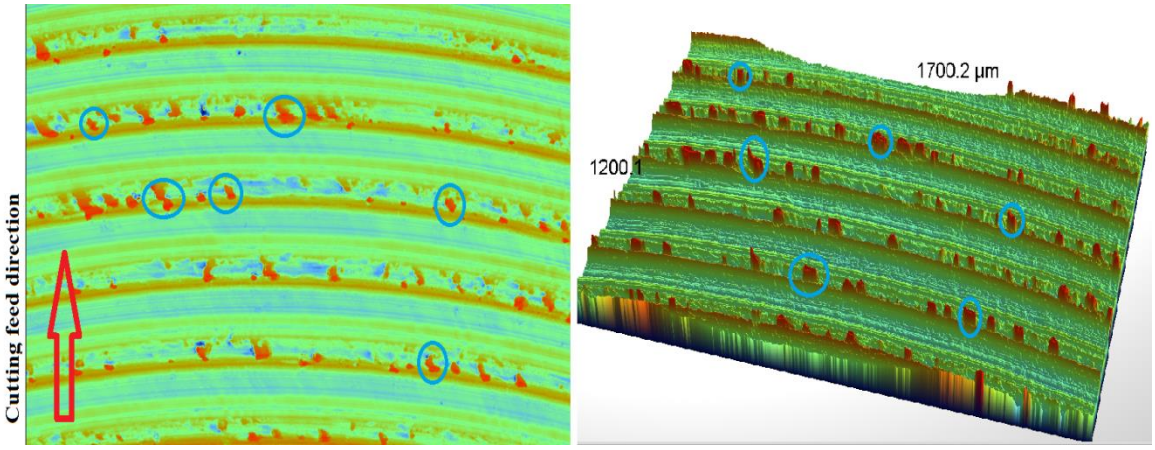

Fig. 9.17. Uncut particles left on machined surface

As discussed previously, the inclination angle of the GENTIGER GT-66 and KONDIA B500 milling machine spindle has no direct important influence on the topography height parameter in general. In particular, it changes the topography value and causes a difference in value magnitude between opposite cutting directions. Even if it is difficult to distinguish direction errors on opposite cutting directions, the GENTIGER GT66 milling machine has differences between contrary aimed directions up to 1,635 μm in SOUTH - NORTH direction that is derived from measurements with high cutting feed rate. How does it affect the surface topography formation in general? Data in Table 9.12 is obtained from surface topography measurements and prediction model inclination component. Predicted results in Table 9.12 are simulated with the Eq. 7.11. Factors selected to predict the Sz parameter are: Feed rate F2 = 0,4 mm/tooth and DIN 1.2312 material. Representative surface topography measurements were selected to compare the predicted result's accuracy.

From the values in Table 9.12 we can see that the cutting tool inclination factor is not significant for the GENTIGER milling machine and leaves a tiny effect on surface topography formation. The maximum tool inclination value in the SOUTH – NORTH direction is 0,298219 μm - only 3,5% of the surface topography parameter S_Z value. If we compare this result with other components, this is minimal and does not affect surface formation significantly. In EAST – WEST cutting direction, the influence is even less – 2,17%.

Table 9.12. Sz maximum simulated parameter value performed only by cutting tool maximum inclination for the GENTIGER GT-66 milling machine

Feed direction	**S_Z value - measured, µm**	**S_Z value by tool inclination, µm**
1. SOUTH	8,400	-0,298219
3. NORTH	9,018	0,2982190
2. WEST	9,593	0,180739
4. EAST	8,295	-0,180739

From the topography measurements, the detected GENTIGER GT-66 machine milling head inclination is 0,08 degrees in the NORTH direction and 0,05 degrees in the WEST direction. The detected inclination angle results in a surface topography increase or decrease in the relevant cutting direction. GENTIGER GT-66 surface topography is increased in NORTH and WEST cutting directions, as presented in Table 9.12. As discussed previously, the inclination angle of the GENTIGER GT-66 spindle has no direct, important influence on the topography height parameter in general, but in particular, it changes the topography value and causes a difference of value magnitude between opposite cutting directions.

It is different for the KONDIA B500 milling machine. Each of the cutting directions has a quite distinct surface height, compared with the previous part of this research, as described in chapter 7. This behaviour is maintained in almost all of the developed research samples. Table 9.13 represents the results of the KONDIA B500 milling machine alignment accuracy influence on surface topography.

Table 9.13. Maximum predicted S_Z parameter value performed by cutting tool inclination in the KONDIA B500 milling machine

Feed direction	**S_Z value - measured, µm**	**S_Z value by tool inclination, µm**
1. SOUTH	11,99000	0,07499804
3. NORTH	15,84000	-0,07499804
2. WEST	11,84000	3,35157163
4. EAST	9,12900	-3,35157163

We can now compare the GENTIGER GT66 alignment accuracy with that of the KONDIA B500. Results in column "**S_Z value by tool inclination**" in Table 9.13 are modeled with equation 7.11. The factors selected to predict the surface topography are: Feed rate F3 = 0,4 mm/tooth, DIN 1.1730 material and Cutting force F_X = 155.15 N. From the topography measurements, detected KONDIA B500 head inclination is 0,96 degrees in WEST direction and 0,02 degrees in SOUTH direction. The detected inclination angle causes a surface topography increase or decrease in the relevant direction of cut. In the KONDIA B500 milling machine, surface topography is increased in the SOUTH and WEST cutting directions, as represented in Table 9.13. Consequently, this behavior is considered in the prediction model and in its results. Here, the inclination component accounts for 36,7% in EAST direction of the total measured surface height Sz.

The most important conclusion here is that on the samples prepared on an accurate milling machine with a low number of working hours, we may have problems to distinguish milling head alignment inaccuracy directly from the topography measurements. Calculating an average surface topography height value on every cutting direction, we identified an average error value that can be related with alignment error. This inaccuracy for the GENTIGER GT-66 milling machine is very small – less than half a degree in each direction. Therefore, results from the KONDIA reveal that conditions still exist for directional influence. An example of the calculation and results of the tool axis inclination model are compiled in Appendix D – Prediction model calculation and analysis. From this point it is clear that the highest influences on the surface topography parameter Sz are feed factor and cutting tool geometry. Results from

the tool deflection component indicate deflection as the second most important factor. The sum of predicted surface topography components do not account for the entire measured surface topography parameter value, and predicted values are lower than measured ones. In the next section we add an additional factor, equipment vibrations, which were considered an important factor in the previous chapter.

9.5.4. Vibration component

In Chapter 8 it was concluded that sample measurements reveal unevenly distributed marks over the surface topography and these deviations are related with system's dynamic behavior. It was also concluded that the vibrational model has an important role in topography formation and it should be included in a general mathematical surface topography prediction model. Milling machine manufacturers tend to build machines with a solid structure to avoid vibrations in the cutting process. As presented in the visual analysis, the GENTIGER milling machine has less deviations in surface topography between peaks and valleys. But is it true that this machine's dynamic behaviour does not affect surface topography formation?

Dynamic behavior was measured only for the KONDIA B500. Now it is time to do the same measurements on the GENTIGER GT-66 milling machine and to compare the results. Similar to Chapter 8, vibration amplitude of the milling machine table can be calculated by considering exciting cutting forces. If we know the values of the cutting equipment natural vibration frequency, it is easy to calculate the vibration amplitude of the vibrations acting on the cutting process. To calculate vibration influence, identifying certain factors such as exciting forces, mass of the table and natural frequency of the milling table is mandatory.

During vibration measurements, auxiliary force was applied with a measurement hammer on the machine table and spindle. Natural frequency is an important value to calculate vibrations and their amplitude during the cutting process. The most representative measured natural vibration frequency of the machine milling table was 139 Hz on the Y axis For the GENTIGER GT66 and 76 Hz for the KONDIA B500 (taken from the previous chapter). Other significant natural frequency amplitudes at our spindle speed range were not observed. Below, Fig. 9.18 and Fig. 9.19 represent the GENTIGER GT66 milling table resonance frequency. Resonance measurement results for the KONDIA B500 milling table are presented in Fig. 8.3 of the previous chapter. The graph's Y axis represents FRF – Frequency Response Function, while the X axis represents the frequency.

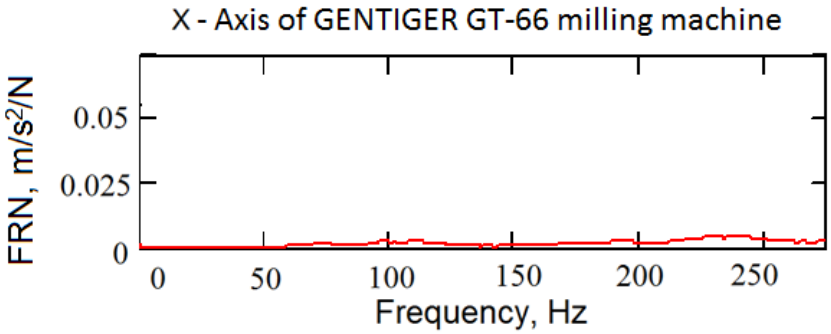

Fig. 9.18. Frequency response function analysis of the GENTIGER GT66 milling table X axis.

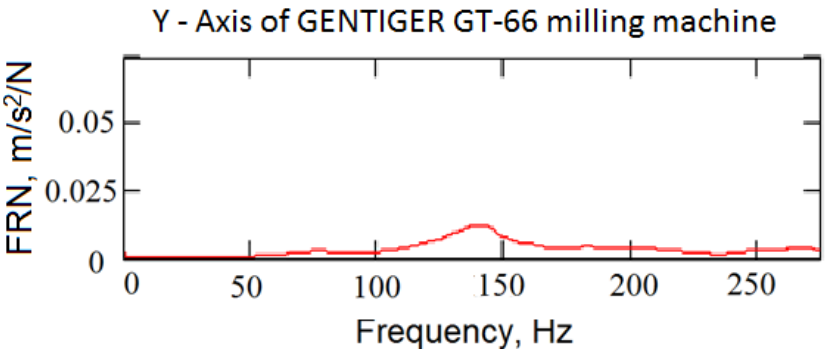

Fig. 9.19. Frequency response function analysis of GENTIGER GT66 milling table Y axis.

Results for the GENTIGER GT-66 milling machine natural frequency (resonance) are represented in Table 9.14. The same resonance results for the KONDIA B500 were presented earlier, in Table 8.2. Measurements and an example of vibration amplitude calculation are compiled in Appendix E - Vibration analysis of the KONDIA B500 and GENTIGER GT-66 High-speed milling machines. Calculated milling table mass for the GENTIGER GT-66 is higher than for the KONDIA B500, as shown in Table 9.15.

Table 9.14. GENTIGER GT66V natural frequency measurements

Axis	Type	Cycles/second (Hz)
X	Oscillations	139
Y	Oscillations	141

Table 9.15. GENTIGER GT66V and KONDIA B500 milling table mass

Machine	Equipment	Mass, Kg
B500	Milling table without chuck	112.65
GT66V	Milling table without chuck	168.2

Selected variables were used in the Mathcad™ solving tool to calculate and plot the vibration amplitude of the milling table. The Mathcad™ solving tool was applied to Eq. 8.5. Results of the solved system are presented in Fig. 9.20, Fig. 9.21 and Fig. 9.22 for the KONDIA B500 and GENTIGER milling machines at different feed rates. Graphs in the figures represent vibration amplitude δz_{vib} in meters (m) on the Y axis, while cutting time is represented on the X axis. The left column in both figures represents milling table vibration amplitude while machining DIN 1.1730 material, while the right column represents the same for the DIN 1.2312 material. Every row represents the milling machine accordingly.

Simulated milling table vibration amplitude with F1, F2 and F3 cutting feed levels on DIN 1.1730 material, calculated with Eq. 8.5 for the KONDIA B500, are 5,337 μm, 7,126 μm and 11,92 μm respeectively. Simulated milling table vibration amplitude with the same feed levels for the GENTIGER GT-66 are 2,719 μm, 3,005 μm and 4,035 μm respectively. Comparison of the results shows that the KONDIA B500 with every feed rate performs higher vibration amplitude than GENTIGER GT-66. KONDIA B500 has low table mass and low natural vibration frequency, which increase the vibration amplitude up to 2 times. Amplitude is slightly affected by the selected workpiece material and cutting forces. The low mass of the milling table, low natural vibration frequency and increased the cutting force combined increase the milling table vibration amplitude along the *Z* axis.

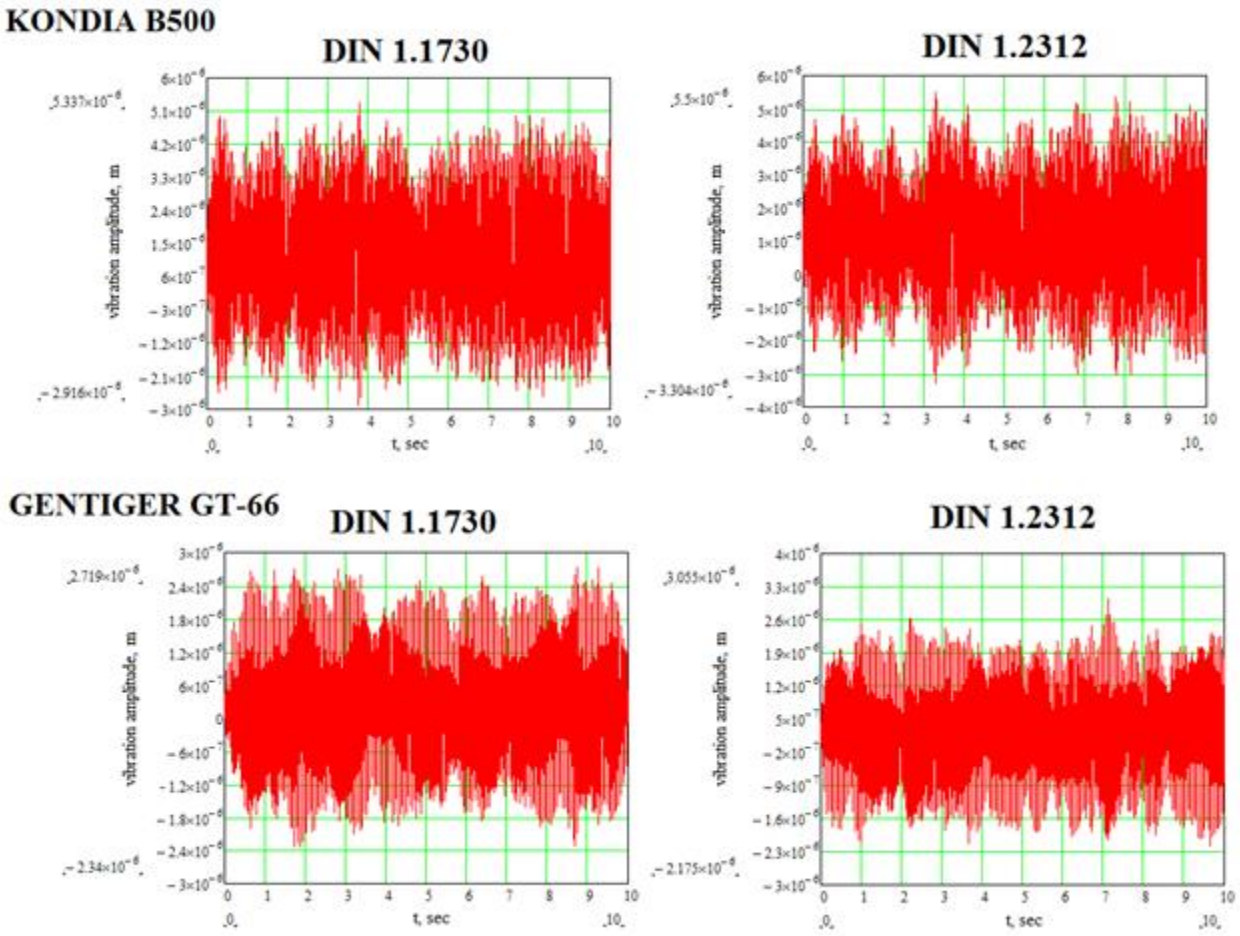

Fig. 9.20. Milling table vibration amplitude for the KONDIA B500 and GENTIGER GT-66 milling tables with feed rate F1 = 0,08 mm/tooth

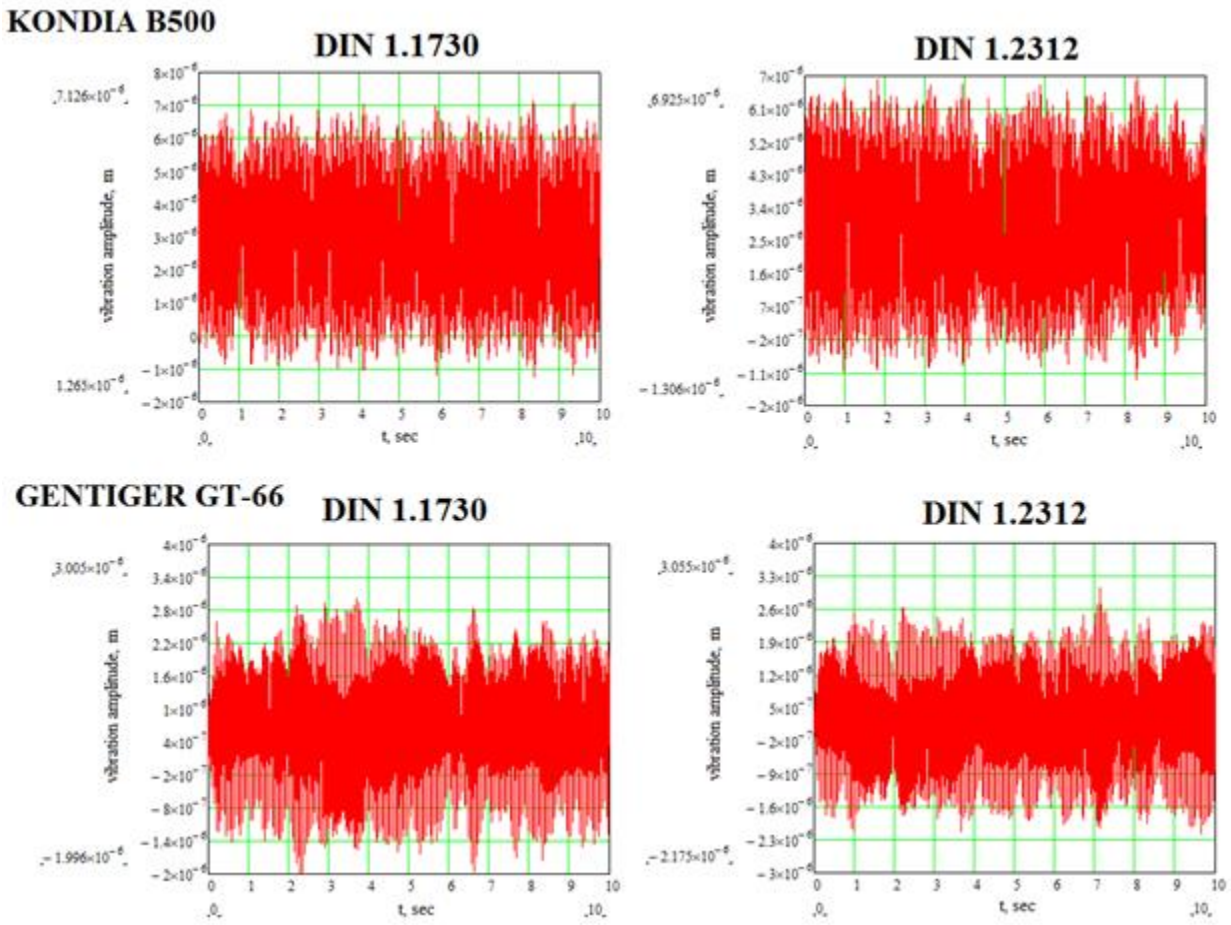

Fig. 9.21. Milling table vibration amplitude for the KONDIA B500 and GENTIGER GT-66 milling tables with feed rate F2 = 0,2 mm/tooth

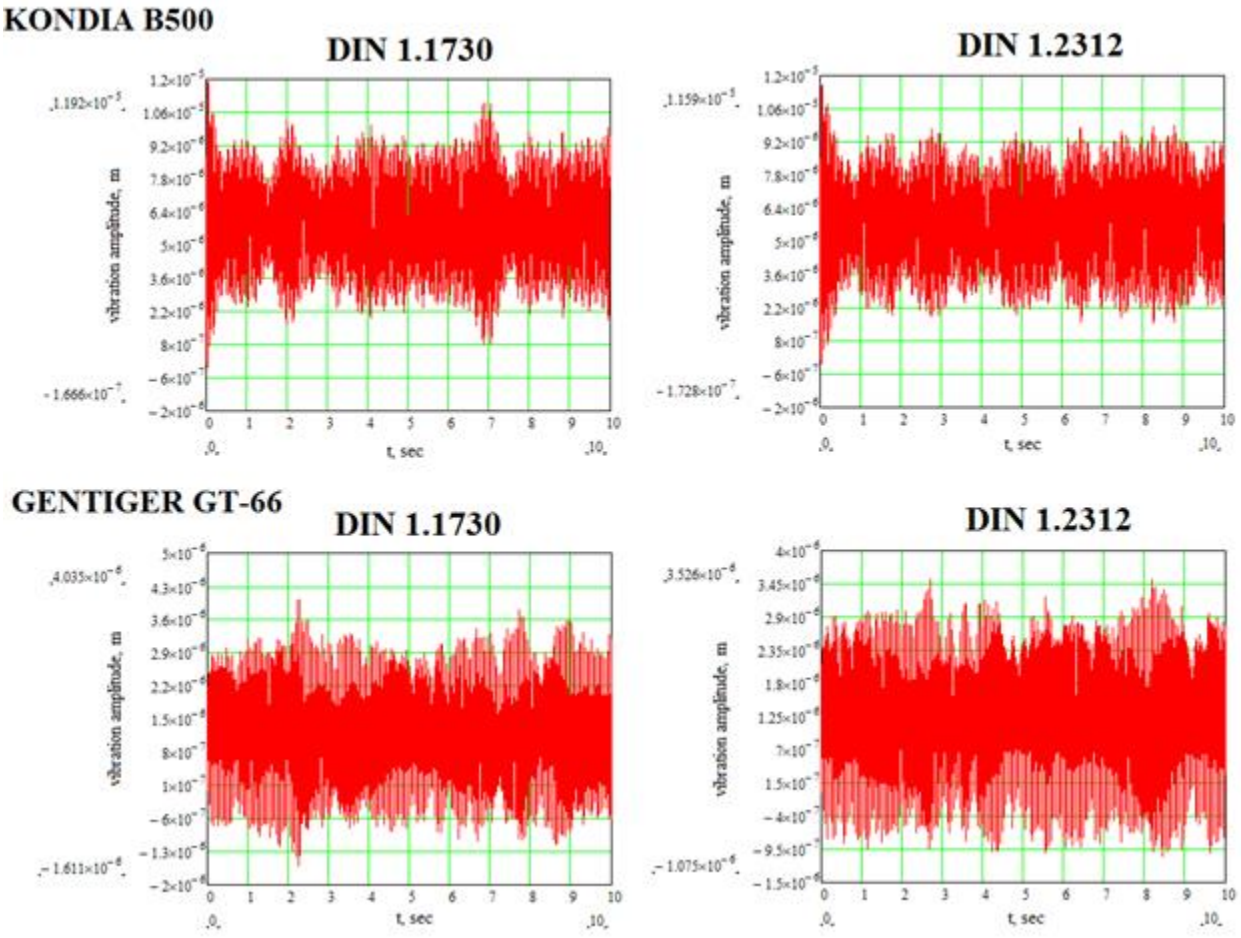

Fig. 9.22. Milling table vibration amplitude for the KONDIA B500 and GENTIGER GT-66 milling tables with feed rate F3 = 0,4 mm/tooth

From the vibration measurements, we can conclude that the GENTIGER GT66, with more mass and solid construction, heavier milling table and, probably, a better bearing system, has higher natural frequency and generates lower amplitude of vibrations at *Z* axis that affect the surface topography formation. At the same time, the KONDIA B500 has low natural frequency and it directly affects to vibration amplitude, caused by the same excited forces than in the GENTIGER GT66. Changes between different feed values show that the excited force value has a high influence on vibration amplitude. It directly affects the value of the predicted model and with increased feed rate, excited force increases and, consequently, the surface topography parameter S_Z vibration component increases. Vibration amplitude may account for up to 3/8 times higher topography values, if milling equipment is not resistant enough. In the next section we will add a vibration model to the previously confirmed topography prediction model to complete it.

9.6. Validation of predicted surface topography

This is the last section of calculations in this part of the research. We substitute all previously named factors, and their levels, into the Eq. 8.7. The results of the solved equation are surface topography height parameter S_Z values. S_Z values are directly affected by technological parameters such as feed rate, cutting speed, cutting depth, radial cutting depth and number of other important factors. S_Z values are also affected by cutting tool geometry and process parameters according to the selected machining equipment, including vibration and machine alignment errors.

Comparative analysis was undertaken to evaluate the difference between predicted results and measured topography S_Z values. The difference value (see last column in Table 9.16) is calculated as a proportion of measured values, expressed in microns and percentages. General calculation results are compiled in Tables 9.16 and 9.17 for the GENTIGER GT66V and KONDIA B500 respectively. These tables represent measured and predicted S_Z values, the difference between measured and predicted results, represented as a proportion of measured value, expressed as micrometers and percentages and difference error between opposite directions.

Table 9.16. Average result comparison – predicted and measured results with properties of the GENTIGER GT66 milling machine

Feed direction	Cutting force, N	S_Z value - measured, µm	Predicted deflection S_Z value, µm	Difference between measured and predicted, µm %
M1 F1 GENTIGER	30,5	5,1885	2,48371078	-2,70478922 52,1 %
M1 F2 GENTIGER	76,2	4,1575	6,159777	2,002277 48,2 %
M1 F3 GENTIGER	155,15	8,94725	12,2941539	3,3469039 37,4 %
M2 F1 GENTIGER	30,2	2,24125	4,06590878	1,82465878 81,4 %
M2 F2 GENTIGER	75,4	3,6835	5,969377	2,285877 62,1 %
M2 F3 GENTIGER	113,4	8,8265	11,8950539	3,0685539 34,8 %

Results in Table 9.16 still show high deviation between predicted and measured topography parameter values. The situation is absolutely different with the KONDIA B500 milling machine. Here, all the factors significantly affect the surface topography formation, and even the cutting direction factor has a high importance. The results are represented in Table 9.17.

Table 9.17. Average result comparison – predicted and measured results with properties of the KONDIA B500 milling machine

Feed direction	Cutting force, N	S_Z value - measured, µm	Predicted deflection S_Z value, µm	Difference between measured and predicted, µm %
M1 F1 KONDIA	30,5	9,0425	2,51832078	-6,52417922 72,2 %
M1 F2 KONDIA	76,2	7,6475	6,213677	-1,433823 18,7 %
M1 F3 KONDIA	155,15	12,19975	12,3938539	0,1941039 1,59 %
M2 F1 KONDIA	30,2	5,844	2,42946878	-3,41453122 58,4 %
M2 F2 KONDIA	75,4	5,8955	5,999477	0,103977 1,76 %
M2 F3 KONDIA	113,4	13,4975	11,9606539	-1,5368461 11,4 %

Summarizing:

The complete developed prediction model represents the advantages and flaws of surface topography prediction and proves or refutes the statements made in the first part of the analysis about the process parameter influence on topography formation. In the last part we tested the validation model with 2 well-known mold manufacturing materials and 2 milling machines. The differences between milling machines represent different structural behavior, applicable to cutting process analysis – milling head alignment accuracy and equipment dynamics. An increase and change in experimental factors help improve the amount of data and broaden the calculation to prove the accuracy of developed surface topography prediction model.

Careful surface topography filtration is one of the most important stages in surface topography analysis. Unfortunately, the optical surface topography measurement method contains multiple flaws, i.e. extremely high and low data points. These points in the

measurement topography image give an overall value of surface height, up to 4-5 times higher than the realistic surface topography. To diminish the measuring equipment errors, non-measured data points were approximated and substituted by values taken from surrounding data points, while surface errors were filtered with 2% of threshold from max and min values of measured data points. Filtered data was used for comparison with predicted results. Use of correctly filtered data maddest possible to reduce the inaccuracy error between predicted and measured parameter Sz values down to 1,59% for DIN 1.2312 material, machined with the KONDIA B500 milling machine with a high feed rate.

The predicted results for behavioural factors of the KONDIA B500 represent higher predicted parameter Sz values than the model with behavioural factors of the GENTIGER GT66 milling machine. Equipment natural frequency affected vibration amplitude of the milling table in Z direction is higher for the KONDIA due to lower natural frequency and lower milling table mass. Conversely, due to the higher GENTIGER GT66 stiffness, mass and vibrational behaviour, the prediction accuracy for this equipment is higher. In general, high vibrational amplitude and lower mass and alignment accuracy of the milling machine result in lower accuracy in the prediction model, and increases the difference between predicted and measured values.

Finally, the overall results of the developed mathematical model represent the common mathematical model accuracy picture. Of all the previously counted and described cutting process factors, such as cutting tool geometry, cutting regimes, material type, milling machine type and their accuracy, cutting process parameters play a significant role in surface topography formation and representation of 3D surface height parameters. Moreover, prediction model accuracy is higher with samples where factors like feed rate and cutting tool geometry play a higher role. Afterwards, a minor effect is noted for such factors as milling equipment accuracy and stability of cutting process. In turn, measurements, for most cases with higher feed rate have lower values and in the prediction model represent the worst scenario. The exception are samples with low feed rate, where, due to low radial cutting depth, the cutting tool cannot separate the material fully from the machined surface, which results in material build-up due to plastic deformation over the surface, increasing the total Sz parameter values.

However, considering all the process parameters and collecting first-hand information on the accuracy and particularities of the available equipment, this model provides an opportunity to predict the workpiece surface roughness and topography with a relatively high accuracy and reliability, if technological cutting process parameters are adapted to the selected technological process and workpiece material. Thus, this model could be used in an industrial application.

Other factors not considered in this research may be used to improve the accuracy of this mathematical model. One of them is plastic deformation and its influence on surface formation. Due to plastic deformation, surface topography values may differ from predicted ones. This model is still open for further improvements and subsequent research

10. REVIEW AND CONCLUSIONS

At the start of this research work, we proposed the main goal of the research. As a reminder, the main goal of this research project is to develop the mathematical methodology based on the calculation model for high-speed end-milling operations, to determine the surface topography parameter Sz.

To achieve the aforementioned goal, the following primary tasks were set for this research:

1. To review the literature to understand challenges and see the scope in the field of High-speed Machining and its behaviour and impact on surface quality.
2. To analyze the surface topography parameters and choose the most relevant surface topography parameters to describe the machined surface. To develop a mathematical model for this surface topography parameter, including all the most relevant milling process inaccuracies.
3. To plan and execute milling experiments, in order to test the hypothesis. In this way, milling strategies, cutting conditions and cutting system behaviour, etc. were selected.
4. To develop the mathematical surface topography formation model and predict the surface topography parameter Sz on a machined surface.
5. To make a comparative analysis of the developed mathematical model with real measurements, using experimentally machined samples.
6. To make a sound conclusions and provide the practical recommendations to dies and molds manufacturing industry.

   Taking into account the results described in previous chapters, the following general conclusions about this research work were drawn.

1. As a result of literature analysis, it was concluded that all surface topography prediction models can be ranked in two groups – Empirical and Theoretical. Empirical models are specifically developed for one machine and preset setting, changes are difficult or impossible to include. Only theoretical models can be used for reliable surface topography prediction model development. This is because a theoretical model contains variables for the physical and dynamic factors acting on the cutting process.

2. Cutting tool geometry and feed rate directly affect the topography parameter Sz. In the case of feed rate, its influence is directly proportionall to surface topography Sz. That was why this parameter was chosen as the basis for the developed topography prediction model.

3. Cutting forces in the normal and tangential directions against the peripheral cutting edge increase or decrease the defined feed rate value. This phenomenon was observed in surface topography images, with variations in distances between cutting marks. Accordingly, we believe that feed factor must be considered always together with cutting tool geometry, and change of cutting tool type, its sharpening or tool errors will always affect the final result of the machined surface.

4. As we saw from the ANOVA analysis, the type of material is another important parameter in the model. The mechanical properties of the material are decisive in surface topography formation.

5. An increase in the tool's concavity angle increases minimum surface topography proportionally. This effect is influenced by a higher feed rate, milling tool deflection and inclination components. The named components have the highest influence on the surface formation created by the rear cutting edge.

6. The tool inclination value changes due to cutting direction. This effect is related with milling machine installation accuracy and wear. If the milling machine has milling head alignment inaccuracies in relation to the milling table, or traverse bearings have significant wear, then the surface topography will represent machine inaccuracies.

7. Surface topography images confirm the existence of cutting tool deflection and its importance on surface topography formation. The cutting tool deflects along its axis due to the cutting forces and cutting vibrations. The first and secondary cutting edge intersection, or tip point, often change the position in relation to the working plane with some frequency, making irregular marks. Tool deflection depends on feed rate and cutting forces. Each cutting force affects the tool deflection in its representative, tangential and normal direction. Therefore, cutting tool deflection becomes one of most important factors that influence up to ¼ of total predicted Sz.

8. Analysis of the milling equipment's dynamic behaviour confirms the influence on equipment stiffness in surface topography formation. Milling machine table mass and natural frequency affect the topography parameter Sz. Until the introduction of the dynamic component, the predicted surface topography Sz value was proportionate to the selected factors (tool, material, cutting conditions). But as it has been demonstrated, the characteristics (mass increases damping) and the state of conservation of the machine affect the Sz value. To make the mathematical model independent from the environment, vibrations must be included. In some machines this influence may be negligible, but not in others.

9. Discrepancies between real measurements and the predicted model represent the influence of other effects working in the cutting process that are not considered in this work. One of the factors, revealed during the research process, was plastic deformation on the surface due to

chip formation. Plastic deformation has a significant effect on the surface with low cutting feed rate and changes the whole prediction process. This factor highlights the need for further research to improve the model accuracy and may be the first line for future research.

10. Another important aspect to be taken into account to check the reliability of the prediction model, and the measurements in general is the type of acquisition data performed by the topography measuring equipment. This is because the inclusion of anomalous data can end up falsifying all the results.

11. The final mathematical model achieved allows to predict the worst possible scenario for the parameter Sz. It means, if you know the state and behaviour of the machine (inclination error of the spindle axis, vibrations…) the mathematical model will calculate you the maximum Sz value (the top or limit for Sz). Of course, when you use this machine, you will select cut conditions, tool, clamping system, etc. to perform the machining operation in good conditions, in this case, your obtained Sz will always be better.

At the start of this research work, we developed a hypothesis to prove or refute during the research project, based on the conclusions made during the analysis. This hypothesis was:

The surface roughness, measured with different standardized parameters, has a direct relation with the topography of the surface. In the mechanical machining processes, the obtained topography is primarily related to the tool's footprint based on the paths of said tool. These paths are related to the kinematic parameters of the movement, as well as to the dynamic characteristics resulting from the efforts and deformations produced. It is possible to establish, according to physical behaviour models, a mathematical model that relates the topography obtained with the real paths of the tool. These paths can be determined based on working conditions (spindle speed, cut feed, number of teeth, etc.) and based on the dynamic behaviour model of the chain: tool-part-machine.

The previously outlined conclusions of this work confirm the hypothesis that it is possible to establish a mathematical model that relates surface topography with cutting tool paths based on working conditions (spindle speed, cut feed, number of teeth, etc.) and the equipment's dynamic behavior. Even if this model contains flaws and has insufficient accuracy in combination with certain technological parameters, it is still applicable for general surface topography prediction in flat-end milling applications, where the surface has been formed with the end of the cutting tool, as used in die and mold manufacturing processes. Most importantly, to develop an accurate prediction model for a wide selection of milling equipment and tools applied in the cutting process, all the properties of machining equipment need to be measured and considered in the model development beforehand, including geometry of the cutting tool. By knowing these parameters, an accurate surface topography prediction tool can be developed.

This proposal is different to others, provided by other authors in the literature review. When compared with others, it is more accurate than most, considering its direct relationship with the

geometrical properties of the cutting system. Some models developed by other authors still show better results, but they are not compared with other technological factors, so these models are not comparable.

11. RECOMMENDATIONS FOR DIE AND MOLD MANUFACTURUNG INDUSTRY AND FUTURE WORKS

Based on the previously stated conclusions, the author of this research can provide sound conclusions. These conclusions are aimed at die and mold manufacturers, cutting tool developers, students and everyone who works with High-Speed Milling operations and hard-to-cut materials.

1. The first, most important recommendation for die and mold manufacturers is to keep their machining equipment in a good condition and analyze machine stiffness behaviour, before using their machines for highly precise surface machining. As the results represent, milling equipment accuracy and stiffness affect the surface formation both directly and indirectly, and have a high impact on surface topography height.
2. Keep focused on the cutting conditions. Depending on machine accuracy, they still may affect surface topography formation the most. Especially cutting feed rate, cutting tool geometry and milling equipment dynamics. With increased feed rate, cutting forces increase and this affects the cutting process parameters directly, which affects the surface topography height formation. It is similar for the tool's geometrical properties.
3. Select the right cut strategy: as we have seen, the influence of tool inclination depends on cutting direction. Depending on the geometry, where possible, the right tool path can improve roughness.
4. Avoid using a Two Linear Path (TLP) cutting strategy, if the last overlap cutting depth is insufficient. Calculate the appropriate cutting depth, to ensure fully-fledged cutting process, with no up-rolling of the surface.
5. Check data from roughness measuring equipment. If the measurement technique generates a lot of invalid data, a filter should be used to avoid false roughness results.
6. When we have difficult (or expensive) parameters/values to achieve through the milling process, use of the Finite Element Method turns out to be a very useful tool. As we have had the opportunity to verify in this research, the results obtained from FEM are acceptable.
7. This mathematical model to predict Sz could be applied to calculate an average surface topography height that tends to the worst scenario. With improved balance between equipment natural vibration frequency, spindle speed and feed rate, the manufacturer could decrease the machine-tool-workpiece system vibration causes surface topography height error. The same goes for cutting tool and its geometry selection. Depending on

tool geometry, feed rate can be adjusted to decrease the surface height achieved by cutting tool geometry.

Considering these recommendations, die and mold manufacturers may improve the quality of the surface topography, performed during High-Speed Milling operations for hard-to-cut materials. But to improve the accuracy of the developed model, further improvements could be made. As discussed at the end of the conclusions chapter, one of the lines that could be moved forward is a more refined analysis of the plastic deformation. Due to plastic deformation, in the event of insufficient cutting depth, a blunt cutter or high cutting speed, surface topography may be deformed plastically. This would be an interesting factor to be included in the developed mathematical surface prediction model, to improve its accuracy.

Also, the number of samples for further research should be improved. This will improve the quality of the statistical analysis and may reveal certain unknown tool-part-machine system behavior that affects the surface topography formation.

12. PUBLICATIONS AND CONFERENCES RELATED WITH THE RESEARCH

All the results of this research work were submitted for peer-reviews in international scientific conferences. All the submitted publications have been successfully defended in the scientific conferences and experienced experts in the field valued the results. Papers have been published in conference proceedings as IMECE ASME, LEM3, DAAAM international and DAAAM Baltics. They represent the course and results of the study. Here is the list of these publications where all the results and calculations have been considered.

1. Logins, A.; Torims, T.; Gutierrez Rubert, S. C.; Rosado Castellano, P.; Torres, R. 9th "INFLUENCE OF THE HIGH-SPEED MILLING STRATEGY ON 3D SURFACE ROUGHNESS PARAMETERS", International DAAAM Baltic Conference "INDUSTRIAL ENGINEERING - 24-26 April 2014, Tallinn, Estonia, (SCOPUS, ISI Web of Science) 256.-261.lpp.

2. Torims, T.; Logins, A.; Rosado Castellano, P.; Gutierrez Rubert, S. C.; Torres, R., „THE DEPENDENCE OF 3D SURFACE ROUGHNESS PARAMETERS ON HIGH-SPEED MILLING TECHNOLOGICAL PARAMETERS AND MACHINING STRATEGY", Proceedings of the ASME 2014 International Mechanical Engineering Congress & Exposition IMECE2014, IMECE2014-37436, 2014. (SCOPUS, ISI Web of Science)

3. Andris Logins, Toms Torims „THE INFLUENCE OF HIGH-SPEED MILLING STRATEGY ON 3D SURFACE ROUGHNESS PARAMETERS", Proceedia Engineering, 25th DAAAM International Symposium on Intelligent Manufacturing and Automation, DAAAM 2014, 1253. - 1261., 2015, 10.1016/j.proeng.2015.01.491 (SCOPUS, ISI Web of Science)

4. A. Logins, T. Torims, S. C. Gutiérrez Rubert, P. Rosado Castellano, R. Torres Carot, F. Sergejev „STUDY OF COMBINED MACHINING PARAMETERS ON 3D ROUGHNESS

BEHAVIOUR IN MOULDS AND DIES", Proceedings of the 10th International Conference of DAAAM Baltic "Industrial Engineering" 39-44, 2015, 978-9949-23-804-0, 2015. (SCOPUS, ISI Web of Science)

5. A. Logins, T. Torims, S. C. Gutiérrez Rubert, P. Rosado Castellano, R. Torres Carot, F. Sergejev „EXPERIMENTAL ANALYSIS OF HOW THE INCLINATION ERROR OF FLAT-END MILLING TOOLS INFLUENCES 3D SURFACE TOPOGRAPHY PARAMETERS", Proceedings of the 11th International Conference of DAAAM Baltic "Industrial Engineering"1.-7. 2016,

6. A. Logins, T. Torims, S. C. Gutiérrez Rubert, P. Rosado Castellano, R. Torres Carot, F. Sergejev, „INFLUENCE OF TOOL DEFORMATIONS AND MOUNTING INACCURACIES ON 3D SURFACE TOPOLOGY", Thirteenth International Conference on HIGH SPEED MACHINING 2016, Metz, France, 4- October, 2016

7. A. Logins, T. Torims, P. Rosado Castellano, S. C. Gutiérrez Rubert, R. Torres Carot, "VIBRATION ANALYSIS OF HIGH-SPEED END MILLING OPERATIONS APPLIED TO INJECTION MOLD MATERIALS", Proceedings of the ASME 2017 International Mechanical Engineering Congress & Exposition IMECE2017, IMECE2017-72636, 2017, (SCOPUS, ISI Web of Science).

REFERENCES

[1] C. Tournier, "Usinage à grande vitesse: Technologies, modelisations et trajectoires". Dunod, 400 pgs., 2010.

[2] J. Vivancos, C. J. Luis, L. Costa, and J. A. Ortiz, "Optimal machining parameters selection in high speed milling of hardened steels for injection moulds," J. *Mater. Process. Technol.*, vol. 155–156, no. 1–3, pp. 1505–1512, 2004.

[3] G. Menges, W. Michaeli, and P. Mohren, "Georg Menges , Walter Michaeli , Paul Mohren How to Make Injection Molds." Hanser Gardner publications, Inc., 208pgs., 2000.

[4] F. Akbar, P. T. Mativenga, and M. A. Sheikh, "An evaluation of heat partition in the high-speed turning of AISI/SAE 4140 steel with uncoated and TiN-coated tools," *Proc. Inst. Mech. Eng. Part B J. Eng. Manuf.*, vol. 222, no. 7, pp. 759–771, 2008.

[5] T.-S. Jung, M.-Y. Yang, and K.-J. Lee, “A new approach to analysing machined surfaces by ball-end milling, part II:,” *Int. Journal of Advanced Manufacturing Technology*, vol. 25, no. 9, pp. 841–849, 2005.

[6] V. Kauppinen, “High-Speed Milling - a New Manufacturing Technology,” 4th International DAAAM Conference Industrial Engineering – Innovation As Competitive Edge For Sme, no. April, pp. 131–134, 2004.

[7] M. A. Davies, T. J. Burns, and T. L. Schmitz, “High-Speed Machining Processes: Dynamics on Multiple Scales,” *National Institute of Standards and Technology*, Vol 301, pp. 7–19, 1998.

[8] H. Onozuka, K. Utsumi, I. Kono, J. Hirai, Y. Numata, and T. Obikawa, “High speed milling processes with long oblique cutting edges,” *J. of Manufacturing Processes*, vol. 19, pp. 95–101, 2015.

[9] H. Schulz and T. Moriwaki, “High-speed Machining,” *CIRP Ann. - Manuf. Technol*., vol. 41, no. 2, pp. 637–643, 1992.

[10] M. Kronenberg, "Machining science and application: theory and practice for operation and development of machining processes", Oxford, New York, Pergamon Press, 1966.

[11] R. Pasko, L. Przybylski, and B. Slodki, “High speed machining (HSM)–The effective way of modern cutting,” *Proc. of 7th DAAAM Int. conf.* pp. 72–79, 2002.

[12] M. E. Martellotti, “An analysis of the Milling process", *ASME Transactions,* Vol 63,.” p. 667, 1941.

[13] W. A. Kline, R. E. DeVor, and I. A. Shareef, “The Prediction of Surface Accuracy in End Milling,” *J. Eng. Ind.*, vol. 104, no. 3, pp. 272–278, Aug. 1982.

[14] J.W. Sutherland, T.S. Babin, The geometry of a surface generated by the bottom of an end mill. *Proc. NAMRC* vol. 16, 202–208, 1988.

[15] S. Engin and Y. Altintas, “Mechanics and dynamics of general milling cutters. Part I : helical end mills,” *Int. J. Mach. Tools Manuf.*, vol. 41, pp. 2195–2212, 2001.

[16] D. K. Baek, T. J. Ko, and H. S. Kim, “Optimization of feedrate in a face milling operation using a surface roughness model,” *Int. J. Mach. Tools Manuf..*, vol. 41, no. 3, pp. 451–462, 2001.

[17] P. Franco, M. Estrems, and F. Faura, “Influence of radial and axial runouts on surface roughness in face milling with round insert cutting tools,” *Int. J. Mach. Tools Manuf.*, vol. 44, no. 15, pp. 1555–1565, 2004.

[18] E. Budak, “Analytical models for high performance milling. Part I: Cutting forces, structural deformations and tolerance integrity,” *Int. J. Mach. Tools Manuf.*, vol. 46, no. 12–13, pp. 1478–1488, 2006.

[19] S. H. Ryu, D. K. Choi, and C. N. Chu, “Roughness and texture generation on end milled surfaces,” *Int. J. Mach. Tools Manuf.*, vol. 46, no. 3–4, pp. 404–412, 2006.

[20] M. Wan, W. H. Zhang, G. Tan, and G. H. Qin, “New cutting force modeling approach for flat end mill,” *Chinese J. Aeronaut.*, vol. 20, no. 3, pp. 282–288, 2007.

[21] H. Jiang, X. Long, and G. Meng, “Study of the correlation between surface generation and cutting vibrations in peripheral milling,” *J. Mater. Process. Technol.*, vol. 208, no. 1–3, pp. 229–238, 2008.

[22] P. G. Benardos and G. C. Vosniakos, “Predicting surface roughness in machining: A review,” *Int. J. Mach. Tools Manuf.*, vol. 43, no. 8, pp. 833–844, 2003.

[23] J. Sutherland and R. DeVor, “A dynamic model of the cutting force system in the end milling process,” *Sensors and Controls for Manufacturing*, vol. PED-33. pp. 53–62, 1987.

[24] J. W. Dang, W. H. Zhang, Y. Yang, and M. Wan, “Cutting force modeling for flat end milling including bottom edge cutting effect,” *Int. J. Mach. Tools Manuf.*, vol. 50, no. 11, pp. 986–997, 2010.

[25] Y. Quinsat, L. Sabourin, and C. Lartigue, “Surface topography in ball end milling process: Description of a 3D surface roughness parameter,” *J. Mater. Process. Technol.*, vol. 195, no. 1–3, pp. 135–143, 2008.

[26] S. W. Kim, D. W. Lee, M. C. Kang, and J. S. Kim, “Evaluation of machinability by cutting environments in high-speed milling of difficult-to-cut materials,” *J. Mater. Process. Technol.* vol. 111, pp. 256–260, 2001.

[27] International organization for Standardization, ISO4287-1997, Geometrical Product Specifications (GPS) — Surface texture: Profile method — Terms, definitions and surface texture parameters, 25 pgs., 1997

[28] J. Vivancos, C. J. Luis, J. A. Ortiz, and H. A. González, “Analysis of factors affecting the high-speed side milling of hardened die steels,” *J. Mater. Process. Technol.*, vol. 162–163, pp. 696–701, 2005.

[29] M. Alauddin, M. A. El Baradie, and M. S. J. Hashmi, “Computer-aided analysis of a surface-roughness model for end milling,” *J. Mater. Process. Tech.*, vol. 55, no. 2, pp. 123–127, 1995.

[30] M. Alauddin, M. A. El Baradie, and M. S. J. Hashmi, “Optimization of surface finish in end milling Inconel 718,” *J. Mater. Process. Technol.*, vol. 56, no. 1–4, pp. 54–65, 1996.

[31] C. F. Yao, D. X. Wu, Q. C. Jin, X. C. Huang, J. X. Ren, and D. H. Zhang, “Influence of high-speed milling parameter on 3D surface topography and fatigue behavior of TB6 titanium alloy,” *Trans. Nonferrous Met. Soc. China (English Ed.*, vol. 23, no. 3, pp. 650–660, 2013.

[32] N. S. K. Reddy and P. Venkateswara Rao, “Selection of optimum tool geometry and cutting conditions using a surface roughness prediction model for end milling,” *Int. J. Adv. Manuf. Technol.*, vol. 26, no. 11–12, pp. 1202–1210, 2005.

[33] B. Ozcelik and M. Bayramoglu, “The statistical modeling of surface roughness in high-speed flat end milling,” *Int. J. Mach. Tools Manuf.*, vol. 46, no. 12–13, pp. 1395–1402, 2006.

[34] X. Da Qin, S. Hua, X. L. Ji, S. M. Chen, and W. Y. Ni, “Surface Roughness Model for Helical Milling of Die-Steel Based on Response Surface Methodology,” *Key Eng. Mater.*, vol. 431–432, pp. 346–350, 2010.

[35] J. Sun and Y. B. Guo, “A comprehensive experimental study on surface integrity by end milling Ti-6Al-4V,” *J. Mater. Process. Technol.*, vol. 209, no. 8, pp. 4036–4042, 2009.

[36] R. H. Yuan, J. Sun, J. F. Li, L. Y. Song, and Y. W. Zhang, “Experimental Study on Surface Roughness and Residual Stress by End Milling 69111-Stainless Steel,” *Adv. Mater. Res.*, vol. 97–101, pp. 1257–1260, 2010.

[37] W. Zhang, M. L. Zheng, M. M. Cheng, and Q. Wan, “Experiment Research of Cutter Edge and Cutting Parameters Influence on Machined Surface Roughness for High Speed Milling Hardened Steel,” *Adv. Mater. Res.*, vol. 136, pp. 86–90, 2010.

[38] D. Begic-Hajdarevic, A. Cekic, and M. Kulenovic, “Experimental study on the high speed machining of hardened steel,” *Procedia Eng.*, vol. 69, pp. 291–295, 2014.

[39] C. K. Toh, “Surface topography analysis in high speed finish milling inclined hardened steel,” *Precis. Eng.*, vol. 28, no. 4, pp. 386–398, 2004.

[40] H. Y. Cao, L. H. Guo, and C. Chen, “Study on Surface Roughness of High-Speed Cutting of Ni-Base Superalloy under Different Cutting Media,” *Adv. Mater. Res.*, vol. 102–104, pp. 758–761, 2010.

[41] F. Jiang, J. Li, L. Yan, J. Sun, and S. Zhang, “Optimizing end-milling parameters for surface roughness under different cooling/lubrication conditions,” *Int. J. Adv. Manuf. Technol.*, vol. 51, no. 9–12, pp. 841–851, 2010.

[42] M. S. Lou, J. C. Chen, and C. M. Li, “Surface roughness prediction technique for CNC end-milling,” *J. Ind. Technol.*, vol. 15, no. 1, pp. 1–6, 1998.

[43] M.-Y. Wang and H.-Y. Chang, “Experimental study of surface roughness in slot end milling AL2014-T6,” *Int. J. Mach. Tools Manuf.*, vol. 44, pp. 51–57, 2004.

[44] A. M. Zain, H. Haron, and S. Sharif, “Prediction of surface roughness in the end milling machining using Artificial Neural Network,” *Expert Syst. Appl.*, vol. 37, no. 2, pp. 1755–1768, 2010.

[45] A. M. Zain, H. Haron, and S. Sharif, “Application of GA to optimize cutting conditions for minimizing surface roughness in end milling machining process,” *Expert Syst. Appl.*, vol. 37, no. 6, pp. 4650–4659, 2010.

[46] B. Lela, D. Bajić, and S. Jozić, “Regression analysis, support vector machines, and Bayesian neural network approaches to modeling surface roughness in face milling,” *Int. J. Adv. Manuf. Technol.*, vol. 42, no. 11–12, pp. 1082–1088, 2008.

[47] Y. Ding, W. Liu, X. Bin Wang, L. J. Xie, and J. Han, “Experimental Study on the Relationship between Surface Roughness and Cutting Parameters when Face Milling High Strength Steel,” *Adv. Mater. Res.*, vol. 139–141, pp. 782–787, 2010.

[48] C. Croarkin, “Engineering Statistics Handbook.” Statistical Engineering Division, Information Technology Laboratory, NIST, 2003

[49] X. W. Yu and X. H. Ma, “Prediction Model of Surface Roughness for 2A70 Alloy Based on Orthogonal Test,” *Key Eng. Mater.*, vol. 458, pp. 179–184, 2010.

[50] B. C. Routara, A. Bandyopadhyay, and P. Sahoo, “Roughness modeling and optimization in CNC end milling using response surface method: Effect of workpiece material variation,” *Int. J. Adv. Manuf. Technol.*, vol. 40, no. 11–12, pp. 1166–1180, 2009.

[51] S. Alam, A. K. M. Nurul Amin, M. Konneh, and A. U. Patwari, “Surface roughness prediction in high speed flat end milling of Ti-6AL-4V and optimization by desirability function of RSM,” *Int. Conf. Adv. Mater. Process. Technol. AMPT 2009*, vol. 264–265, pp. 1166–1173, 2011.

[52] S. Al-Zubaidi, J. A. Ghani, and C. H. Che Haron, “Application of ANN in milling process: A review,” *Model. Simul. Eng.*, vol. 2011, 2011.

[53] B. Ozcelik, H. Oktem, and H. Kurtaran, “Optimum surface roughness in end milling Inconel 718 by coupling neural network model and genetic algorithm,” *Int. J. Adv. Manuf. Technol.*, vol. 27, no. 3–4, pp. 234–241, 2005.

[54] H. Oktem, T. Erzurumlu, and F. Erzincanli, “Prediction of minimum surface roughness in end milling mold parts using neural network and genetic algorithm,” *Mater. Des.*, vol. 27, no. 9, pp. 735–744, 2006.

[55] P. T. B. Huang, J. C. Chen, and Y. T. Jou, “A Regression Neural Model for In-Process Surface Roughness Monitoring in End Milling Operations,” *Key Eng. Mater.*, vol. 419–420, pp. 369–372, 2009.

[56] H. Öktem, T. Erzurumlu, and M. Çöl, “A study of the Taguchi optimization method for surface roughness in finish milling of mold surfaces,” *Int. J. Adv. Manuf. Technol.*, vol. 28, no. 7–8, pp. 694–700, 2006.

[57] P. G. Benardos and G. C. Vosniakos, “Prediction of surface roughness in CNC face milling using neural networks and Taguchi ’ s design of experiments,” vol. 18, pp. 343–354, 2002.

[58] E. S. Topal, “The role of stepover ratio in prediction of surface roughness in flat end milling,” *Int. J. Mech. Sci.*, vol. 51, no. 11–12, pp. 782–789, 2009.

[59] Y. L. Chen, B. L. Zhang, W. R. Long, and H. Xu, “Research on Surface Roughness Prediction Model for High-Speed Milling Inclined Plane of Hardened Steel,” *Adv. Mater. Res.*, vol. 97–101, pp. 2044–2048, 2010.

[60] M. F. F. A. Rashid and M. R. A. Lani, “Surface Roughness Prediction for CNC Milling Process using Artificial Neural Network,” Proceedings of the World Congress on Engineering, vol. 3, pp 1-6, 2010.

[61] Y. Liu, Z. Jiang, and Z. Li, “Impact of cutting parameters on surface roughness in milling aluminum alloy 6061 using ANN models,” *Appl. Mech. Mater.*, vol. 63–64, pp. 412–415, 2011.

[62] B. Gan, Y. J. Huang, and G. X. Zheng, “Prediction of Surface Roughness Profiles for Milling Process with Fractal Parameters Based on LS-SVM,” *Adv. Mater. Res.*, vol. 97–101, pp. 1186–1193, 2010.

[63] M. R. Razfar, R. Farshbaf Zinati, and M. Haghshenas, “Optimum surface roughness prediction in face milling by using neural network and harmony search algorithm,” *Int. J. Adv. Manuf. Technol.*, vol. 52, no. 5–8, pp. 487–495, 2010.

[64] J. P. Hu, Y. Li, and J. C. Zhang, “Surface Roughness Prediction of High Speed Milling Based on Back Propagation Artificial Neural Network,” *Adv. Mater. Res.*, vol. 201–203, pp. 696–699, 2011.

[65] G. Quintana, M. L. Garcia-Romeu, and J. Ciurana, “Surface roughness monitoring application based on artificial neural networks for ball-end milling operations,” *J. Intell. Manuf.*, vol. 22, no. 4, pp. 607–617, 2011.

[66] B. J. L. Yang, J. C. Chen, “A Systematic Approach for Identifying Optimum Surface Roughness Performance in End-Milling Operations A Systematic Approach for Identifying Optimum Surface Roughness Performance in End-Milling Operations,” *J. Ind. Technol.*, vol. 17, no. 2, pp. 1–8, 2001.

[67] J. Z. Zhang, J. C. Chen, and E. D. Kirby, “Surface roughness optimization in an end-milling operation using the Taguchi design method,” *J. Mater. Process. Technol.*, vol. 184, no. 1–3, pp. 233–239, 2007.

[68] S. Podrug, N. Architecture, “Design of Experiments, Application in the Optimization of Milling Process,” *J. Metalurgija* vol. 49, no. 2, pp. 123–126, 2010.

[69] K. Yusuf *et al.*, “Effect of cutting parameters on the surface roughness of titanium alloys using end milling process,” *Sci. Res. Essays*, vol. 5, no. 11, pp. 1284–1293, 2010.

[70] J. A. Speedie, I. Black, and J. M. Ritchie, “Finding the optimum cutting conditions for face milling 13% manganese steel using the Taguchi design method and predictive equations,” *6th Int. Conf. Process. Manuf. Adv. Mater. - THERMEC’2009*, vol. 89–91, pp. 527–532, 2010.

[71] Y. W. Wang, S. Zhang, J. F. Li, and T. C. Ding, “Optimal Cutting Parameters for Desired Surface Roughness in End Milling Inconel 718,” *Adv. Mater. Res.*, vol. 126–128, pp. 911–916, 2010.

[72] T. Ding, S. Zhang, Y. Wang, and X. Zhu, “Empirical models and optimal cutting parameters for cutting forces and surface roughness in hard milling of AISI H13 steel,” *Int. J. Adv. Manuf. Technol.*, vol. 51, no. 1–4, pp. 45–55, 2010.

[73] T. C. Ding, S. Zhang, Z. M. Li, and Y. W. Wang, “Optimization of Cutting Parameters for Desirable Surface Roughness in End-Milling Hardened AISI H13 Steel under a Certain Metal Removal Rate,” *Adv. Mater. Res.*, vol. 188, pp. 307–313, 2011.

[74] N. Tosun and H. Pihtili, “Gray relational analysis of performance characteristics in MQL milling of 7075 Al alloy,” *Int. J. Adv. Manuf. Technol.*, vol. 46, no. 5–8, pp. 509–515, 2010.

[75] B. Jiang, Y. J. Yang, X. L. Liu, C. X. Qi, and X. F. Zhao, “Incidence Analysis on Characteristic of High Speed Ball-end Milling Hardened Steel,” *Science (80-.).*, vol. 188, pp. 1–6, 2011.

[76] H. Öktem, T. Erzurumlu, and H. Kurtaran, “Application of response surface methodology in the optimization of cutting conditions for surface roughness,” *J. Mater. Process. Technol.*, vol. 170, no. 1–2, pp. 11–16, 2005.

[77] Y. Z. Pan, J. Zhao, X. L. Fu, and X. Ai, “Optimization of Surface Roughness Based on Multi-Linear Regression Model and Genetic Algorithm,” *Adv. Mater. Res.*, vol. 101, pp. 3050–3054, 2010.

[78] C. Prakasvudhisarn, S. Kunnapapdeelert, and P. Yenradee, “Optimal cutting condition determination for desired surface roughness in end milling,” *Int. J. Adv. Manuf. Technol.*, vol. 41, no. 5–6, pp. 440–451, 2009.

[79] M. Brezocnik, M. Kovacic, and M. Ficko, “Prediction of surface roughness with genetic programming,” *J. Mater. Process. Technol.*, vol. 157–158, no. SPEC. ISS., pp. 28–36, 2004.

[80] Y. Yang, X. Li, P. Jiang, and L. Zhang, “Prediction Of Surface Roughness In End Milling With Gene Expression Programming,” *Proc. 41st Int. Conf. Comput. Ind. Eng.*, pp. 441–446, 2011.

[81] O. Çolak, C. Kurbanoğlu, and M. C. Kayacan, “Milling surface roughness prediction using evolutionary programming methods,” *Mater. Des.*, vol. 28, no. 2, pp. 657–666, 2007.

[82] H. Öktem, “An integrated study of surface roughness for modelling and optimization of cutting parameters during end milling operation,” *Int. J. Adv. Manuf. Technol.*, vol. 43, pp. 852–861, 2009.

[83] K. V. M. K. Raju, G. R. Janardhana, P. N. Kumar, and V. D. P. Rao, “Optimization of cutting conditions for surface roughness in CNC end milling,” *Int. J. Precis. Eng. Manuf.*, vol. 12, no. 3, pp. 383–391, 2011.

[84] K. Kadirgama, M. M. Noor, and A. N. Abd Alla, “Response ant colony optimization of end milling surface roughness,” *Sensors*, vol. 10, no. 3, pp. 2054–2063, 2010.

[85] T. S. Babin, J. M. Lee, J. W. Sutherland, S. G. Kapoor, "A model for end milled surface topography", *Manufacturing Engineering Transactions PublisherSME, North American Manufacturing Research Inst*. p 362-368., 1985.

[86] I. Buj-Corral, J. Vivancos-Calvet, and H. González-Rojas, “Influence of feed, eccentricity and helix angle on topography obtained in side milling processes,” *Int. J. Mach. Tools Manuf.*, vol. 51, no. 12, pp. 889–897, 2011.

[87] I. Buj-Corral, J. Vivancos-Calvet, and A. Dom??nguez-Fern??ndez, “Surface topography in ball-end milling processes as a function of feed per tooth and radial depth of cut,” *Int. J. Mach. Tools Manuf.*, vol. 53, no. 1, pp. 151–159, 2012.

[88] K. Yong, M. Chang, Y. Ho, D. Woo, and J. Suk, “Simulation of surface roughness and pro ® le in high-speed end milling,” *J. Mater. Process. Technol* vol. 113, pp. 410–415, 2001.

[89] S. H. Ryu, D. K. Choi, and C. N. Chu, “Surface Generation Mechanism in Flat End Milling,” *American Society for Precision Engineering*, Annual 1999 pp. 3–6., 1999.

[90] J. P. Costes and V. Moreau, “Surface roughness prediction in milling based on tool displacements,” *J. Manuf. Process.*, vol. 13, no. 2, pp. 133–140, 2011.

[91] M. Arizmendi *et al.*, “Model for surface topography prediction in peripheral milling considering tool vibration,” *CIRP Ann. - Manuf. Technol.*, vol. 58, no. 1, pp. 93–96, 2009.

[92] M. Arizmendi, J. Fernández, A. Gil, and F. Veiga, “Effect of tool setting error on the topography of surfaces machined by peripheral milling,” *Int. J. Mach. Tools Manuf.*, vol. 49, no. 1, pp. 36–52, 2009.

[93] M. Arizmendi J. Fernandez, L. N. López de Lacalle, A. Lamiki., “Model development for the prediction of surface topography generated by ball-end mills taking into account the tool parallel axis offset. Experimental validation,” *CIRP Ann. - Manuf. Technol.*, vol. 57, no. 1, pp. 101–104, 2008.

[94] Y. Quinsat, S. Lavernhe, and C. Lartigue, “Characterization of 3D surface topography in 5-axis milling,” *Wear*, vol. 271, no. 3–4, pp. 590–595, 2011.

[95] A. Duroobi, “Pick-Interval Scallop Height Estimation Using Three Types of Geometrical end Mill Cutters on CNC Milling Machine", J. Eng. & Tech. vol. 31, no. 8, pp. 1580–1600, 2013.

[96] G. Peigne, H. Paris, D. Brissaud, and A. Gouskov, “Impact of the cutting dynamics of small radial immersion milling operations on machined surface roughness,” *Int. J. Mach. Tools Manuf.*, vol. 44, no. 11, pp. 1133–1142, 2004.

[97] Y. Altintaş and E. Budak, “Analytical Prediction of Stability Lobes in Milling,” *CIRP Ann. - Manuf. Technol.*, vol. 44, no. 1, pp. 357–362, 1995.

[98] E. Budak, “Mechanics and dynamics of milling thin walled structures,” Thesis, Vancouver: University of British Columbia Library, 284pgs., 1994.

[99] H. Paris, G. Peigne, and R. Mayer, “Surface shape prediction in high speed milling,” *Int. J. Mach. Tools Manuf.*, vol. 44, no. 15, pp. 1567–1576, 2004.

[100] D. Kyun Baek, T. Jo Ko, and H. Sool Kim, “A dynamic surface roughness model for face milling,” *Precis. Eng.*, vol. 20, no. 97, pp. 171–178, 1997.

[101] Z. Shi, L. Luning, L. Zhanqiang, “Influence of dynamic effects on surface roughness for face milling process", *Int. J. Adv. Manuf. Technol,* vol. 80, 1823-1831, 2015.

[102] S. J. Zhang and S. To, “A theoretical and experimental study of surface generation under spindle vibration in ultra-precision raster milling,” *Int. J. Mach. Tools Manuf.*, vol. 75, pp. 36–45, 2013.

[103] A. Weremczuk, R. Rusinek, and J. Warminski, “The Concept of Active Elimination of Vibrations in Milling Process,” *Procedia CIRP*, vol. 31, pp. 82–87, 2015.

[104] S. Wojciechowski, P. Twardowski, M. Pelic, R. W. Maruda, S. Barrans, and G. M. Krolczyk, “Precision surface characterization for finish cylindrical milling with dynamic tool displacements model,” *Precis. Eng.*, vol. 46, pp. 158–165, 2016.

[105] International organization for Standardization, ISO 25178-2:2012 Geometrical product specifications (GPS) — Surface texture: Areal — Part 2: Terms, definitions and surface texture parameters, 47pgs., 2012.

[106] F. Blateyron, “The Areal Field Parameters,” *Characterisation Areal Surf. Texture*, no. Springer Berlin Heidelberg, pp. 15–43, 2013.

[107] B. Griffiths, "Manufacturing Surface Technology: Surface Integrity and Functional Performance", Book, *Elsevier Science,* 256pgs. 2001.

[108] A. Logins, Master thesis “Influence of The High-Speed Milling Strategy on 3D Surface Roughness Parameters”, Master thesis, Riga Technical University, Faculty of Transport and mechanical engineering, Riga, 122 p., 2014.

[109] T. Torims, A. Logins, P. Castellano Rosado, S. Gutiérrez, and R. Torres, “The Dependence of 3d Surface Roughness Parameters on High-Speed Milling Technological Parameters And Machining Strategy,” *Proc. ASME 2014 Int. Mech. Eng. Congr. Expo.*, vol. IMECE2014, pp. 1–9, 2014.

[110] A. Logins, T. Torims, S. C. G. Rubert, P. R. Castellano, and R. Torres, “Influence of The High-Speed Milling Strategy on 3d Surface Roughness Parameters,” *9th Int. DAAAM Balt. Conf. "INDUSTRIAL Eng.* -, vol. 24–26 Apri, pp. 1–6, 2014.

[111] A. Logins, T. Torims, S. C. Gutiérrez Rubert, P. Rosado Castellano, R. Torres Carot, F. Sergejev, „Influence of Tool Deformations and Mounting Innacuracies on 3D Surface Topology”, Thirteenth International Conference on HIGH SPEED MACHINING 2016, Metz, France, 4- October, 2016

[112] A. Logins and T. Torims, “The influence of high-speed milling strategies on 3D surface roughness parameters,” in *Energy Procedia*, vol. 100, pp. 1253-1261, 2015.

[113] A. Logins, T. Torims, S. C. G. Rubert, P. R. Castellano, and R. Torres, “Study of Combined Machining Parameters on 3D Roughness Behaviour in Moulds and Dies,” *10th Int. DAAAM Balt. Conf. “INDUSTRIAL Eng.*, no. May, p. 2–7, 2015., pp. 2–7, 2015.

[114] Michigan Metrology, “3D surface roughnes and wear measurements, analysis and inspection, [Online], Available: https://www.michmet.com/3d_s_height_parameters.htm 25.11.2018

[115] Pearson correlation coefficient”, [Online] Available: https://www.spss-tutorials.com/pearson-correlation-coefficient, 27.06.2019.

[116] Taylor Hobson, “Form Talysurf Intra Brochure,” 2012, [Online], Available: http://www.ilusionideasweb.com.ar/vaccaro/pdfs/Form-Talysurf-Intra.pdf, 26.06.2019.

[117] Independent Academia, Descriptive Statistics, [Online], Available: https://www.academia.edu/32445911/CHAPTER_1_DESCRIPTIVE_STATISTICS, 26.06.2019.

[118] J. S. Armstrong, “Illusions in Regression Analysis,” *Int. J. Forecast.*, no. July 2012.

[119] D. M. Lane, “Analysis of Variance”, Online statistics education, [Online], Available: http://onlinestatbook.com/2/analysis_of_variance/anova.pdf, 26.06.2019.

[120] Bussines research methodology, Systematic sampling, [Online], https://research-methodology.net/sampling-in-primary-data-collection/systematic-sampling, 26.06.2019.

[121] Product catalogue: Mitsubishi Materials Corporation, “Impact Miracle Coating Coating Technology,” [Online], Available: https://www.mitsubishicarbide.com/en/technical_information/tec_rotating_tools/tec_solid_end_mills/tec_solid_end_mills_coating_top/tec_solid_end_mills_coating, 18.05.2019.

[122] J. Global, S. Home, P. Information, G. Information, and R. Blanks, “16.10.2015. MITSUBISHI MATERIALS CORPORATION – Solid Carbide Rotary Blanks»Grade Information (Rotary Blanks),” pp. 1–5, 2015.

[123] Mitsubishi Materials Corporation, Coated Carbide(Cvd&Pvd), pp. 3–5, 2015, [Online], Available: http://www.mitsubishicarbide.net/contents/mht/enuk/html/product/technical_information/grade/milling/f_cvd_pvd.html, 12.06.2019.

[124] International organization for Standardization, ISO 6983-1:1982 Numerical Control Of Machines -- Program Format And Definition Of Address Woriso 6983-1:1982 Numerical Control Of Machines - Program Format And Definition Of Address Words - Part 1: Data Format For Positioning, Line Motion And Contouring, 1982,

[125] Ø. Langsrud, “ANOVA for Unbalanced Data: Use Type II Instead of Type III Sums of Squares”, *Statistics and Computing*, p. 163–167., 2003.

[126] Heavy tailed distribution, [Online], Available: https://www.statisticshowto.com/heavy-tailed-distribution/, 12.09.2018.

[127] Real Statistics Using Excel, Analysis of Skewness and Kurtosis, Online Course, [Online], Available: http://www.real-statistics.com/tests-normality-and-symmetry/analysis-skewness-kurtosis, 02.01.2020.

[128] IBM support, Test Between subjects, [Online] Available: https://www-01.ibm.com/support/docview.wss?uid =swg21475419 , 11.08.2019.

[129] H. Moradi, G. Vossoughi, M. R. Movahhedy, and M. T. Ahmadian, "Forced vibration analysis of the milling process with structural nonlinearity, internal resonance, tool wear and process damping effects," *Int. J. Non. Linear. Mech.*, vol. 54, pp. 22–34, 2013.

[130] S. Wojciechowski, P. Twardowski, and M. Pelic, "Cutting forces and vibrations during ball end milling of inclined surfaces," *Procedia CIRP*, vol. 14, pp. 113–118, 2014.

[131] Product Catalogue, MITSUBISHI Materials UK, "Guide to solid carbide end mills, catalogue, [Online], Available: https://www.mitsubishicarbide.net/webcatalog/OMB04F001BLogic.do?srs_id=10000222&mkt_rykshu=mhg&gng_rykshu=enuk&ctgr_rykshu=solid_end_mills&ngs_tni=M&hskzi_ini=&inst_ybkgu=&inst_zish_mi=&row=20&startIndex=60, 05.4.2020.

[132] H. P. Gavin, "Vibrations of Single Degree of Freedom Systems," *Struct. Dyn.*, pp. 1–28, 2010.

[133] T. Hsu, "Application of Second Order Differential Equations in Mechanical Engineering Analysis", ME130 Applied Engineering Analysis. Notes. 59 pp. 2017.

[134] R. Szalai, B. Mann, G. Stepan, and A. Enigineering, "Period-two and Quasi-periodic Vibrations of High-speed Milling." Proceedings of the 9th CIRP International Workshop on Modeling of Machining Operations. 107-114, 2006.

[135] Product catalogue, FORZA MORDAZA, [Online] https://www.primeraocasion.com/es/mordaza-modular-de-precision-vertex-vmp-5/, 25.12.2018

[136] ANOVA statistics, [Online], Available: https://www.statisticshowto.datasciencecentral.com/probability-and-statistics/f-statistic-value-test/, 14.09.2019

APPENDIXES

A - Copy of publications

1. INFLUENCE OF THE HIGH-SPEED MILLING STRATEGY ON 3D SURFACE ROUGHNESS PARAMETERS" - https://drive.google.com/open?id=1cwfGMyRoWtMjujooozG62phDPDo66GnE

2. „THE DEPENDENCE OF 3D SURFACE ROUGHNESS PARAMETERS ON HIGH-SPEED MILLING TECHNOLOGICAL PARAMETERS AND MACHINING STRATEGY" - https://drive.google.com/open?id=1fbgj4n0HimL0NDKiDMlaxwa4hHeQS4L9

3. „THE INFLUENCE OF HIGH-SPEED MILLING STRATEGY ON 3D SURFACE ROUGHNESS PARAMETERS" –

https://drive.google.com/open?id=1jw_wIKIzj26yZcXq6s-e6v9n1Gn1n0IP

4. „STUDY OF COMBINED MACHINING PARAMETERS ON 3D ROUGHNESS BEHAVIOUR IN MOULDS AND DIES" – https://drive.google.com/open?id=1romllNMg0sapJ-oJksuFaF4Kro2bwwXV

5. „EXPERIMENTAL ANALYSIS OF HOW THE INCLINATION ERROR OF FLAT-END MILLING TOOLS INFLUENCES 3D SURFACE TOPOGRAPHY PARAMETERS" - https://drive.google.com/open?id=1cc0NRu04FmAfY6HxP_pvjGzeFxJ4-V6F

6. „INFLUENCE OF TOOL DEFORMATIONS AND MOUNTING INACCURACIES ON 3D SURFACE TOPOLOGY" – https://drive.google.com/open?id=1JrcTd9saXuJH48MxxtAhKuQVcCvxTVfh

7. "VIBRATION ANALYSIS OF HIGH-SPEED END MILLING OPERATIONS APPLIED TO INJECTION MOLD MATERIALS" - https://drive.google.com/open?id=1Sr0bbS6tPD3rK-8I0w5O8b4Nyjnndg5u

B - Design of experiments

Coordinates			
Start point		End point	
X	Y	X	Y
-5	5	-39	5
-39	5	-39	26
-39	26	-5	26
-5	26	-5	5

D mill, mm:	10
Vc , mm/min:	150
n, r/min:	4774,65
f, mm/min:	F, mm/teeth:
954,9	0,1

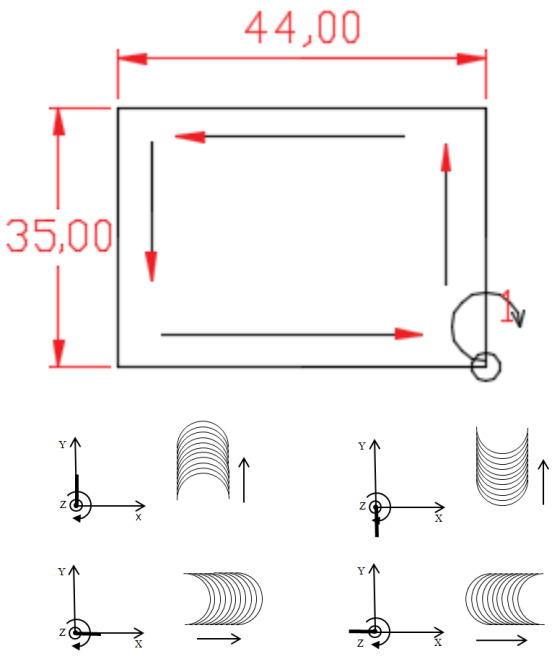

Fig. B-1. Representation of cutting tool movement and representative marks

ID Number: 2

NC program code

N10	G53 XYZ
N20	G53
N30	T4.4
N40	M6
N50	G0X-15Y15 S4775 M3
N60	G0Z1
N70	G1Z-0.3F50
N80	G1Y16F954.9
N90	G1X-29
N100	G1Y15
N110	G1X-15
N120	G0Z1
N130	G0X-15Y5
N140	G1Z-0.3
N150	G3X-5Y15F954.9
N160	G1Y16
N170	G3X-15Y26
N180	G1X-29
N190	G3X-39Y16
N200	G1Y15
N210	G3X-29Y5
N220	G1X-15
N230	G0Z100
N240	M30

Design of experiment for all other samples was designed in the same way, with appropriate cutting conditions and cutting path on specific specimen. Actual spreadsheets with design of experiments for every part of research project are available here: https://drive.google.com/open?id=11-pnaC-mwJBu6ae51J4bJVSFpqZAfGOy

C - Surface topography measurements and images

In this attachment we include 3D surface topography measurement analysis samples from each of study research parts. First part represents 3D surface topography, where flat end milling model was introduced. Second part represents 3D surface topography, where vibrational behavior was analyzed. And third part represents 3D surface topography, where validation model was tested. All other sample 3D surface topography measurements can be reached with the link below. Please, copy this link in your browser manually. Otherwise bowser will block Your access.

https://drive.google.com/drive/folders/11qKgcQJPGa7iZWMmF04WIEA391e8khvy?usp=sharing

Topography represented in these files agrees with standard measurement equipment analysis filters. Topography parameters used for research was filtered for each sample additionally.

Sample 67, KONDIA B500 milling machine, Flat end milling, SOUTH cutting direction:

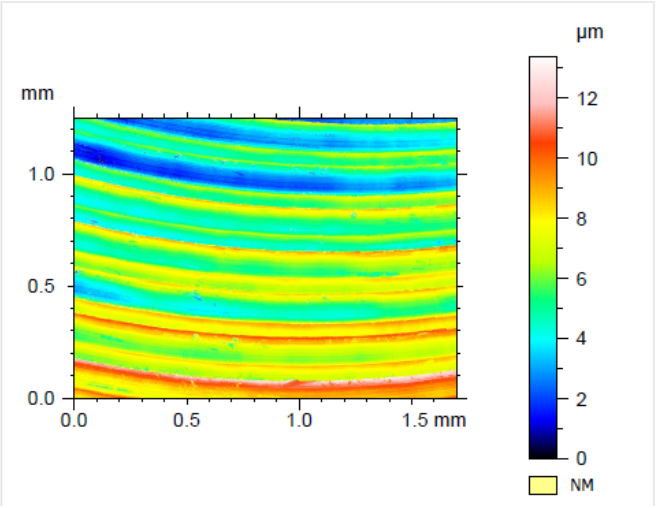

Identity card			
Filename:	C:\A…\1.1.2_x5_speed1_W0.22_THRO5_30_30.OPD		
Axis:	**X**		
Length:	1.70	mm	
Size:	2295	points	
Spacing:	0.741	µm	
Axis:	**Y**		
Length:	1.25	mm	
Size:	1687	lines	
Spacing:	0.741	µm	
Axis:	**Z**		
Length:	13.4	µm	
Spacing:	0.836	nm	

Fig. C-1. Identification of sample measurement – dimensions of data array

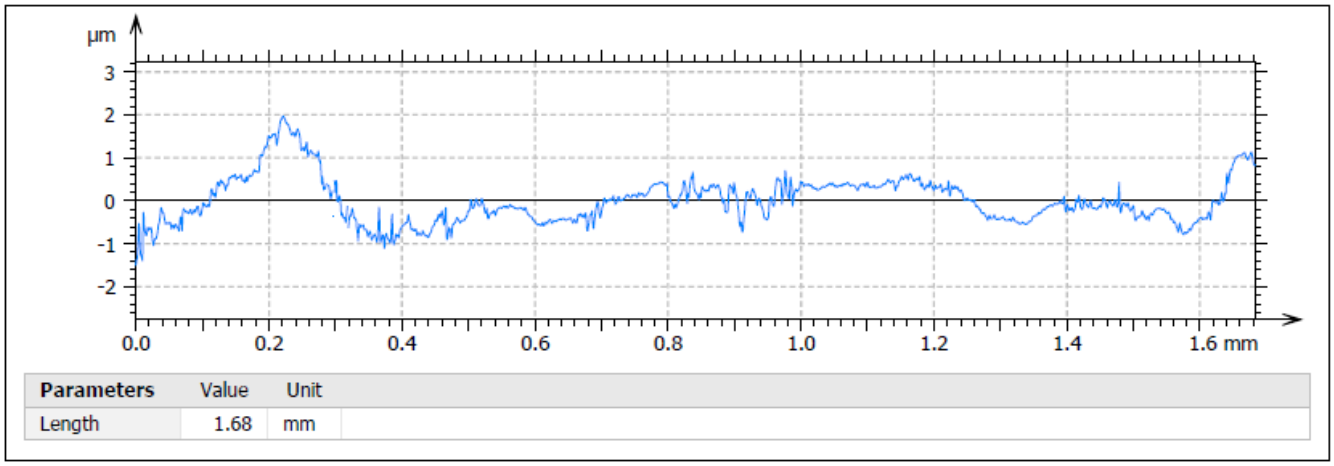

FIG. C-2. Surface profile

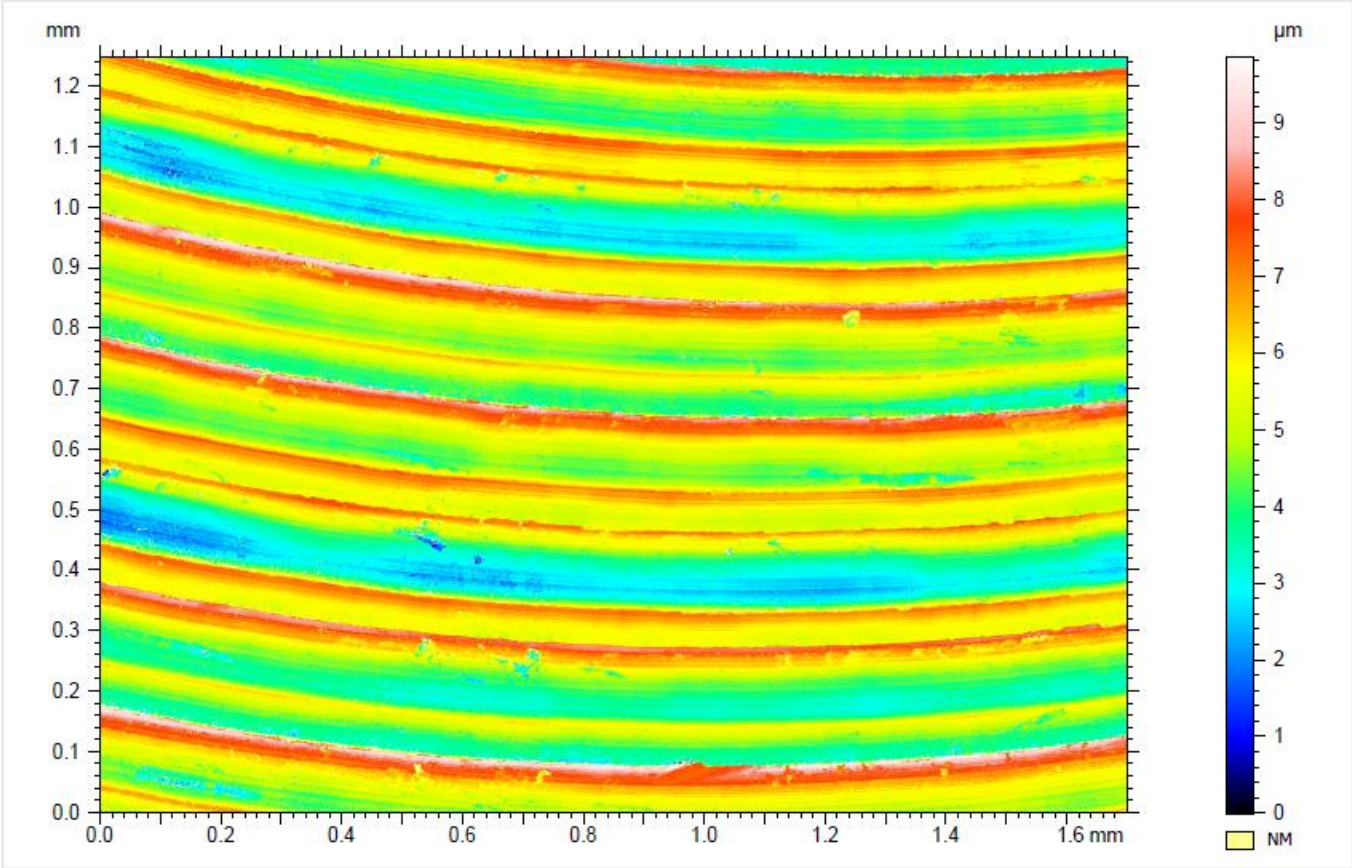

Fig. C-3. Surface topography – top view.

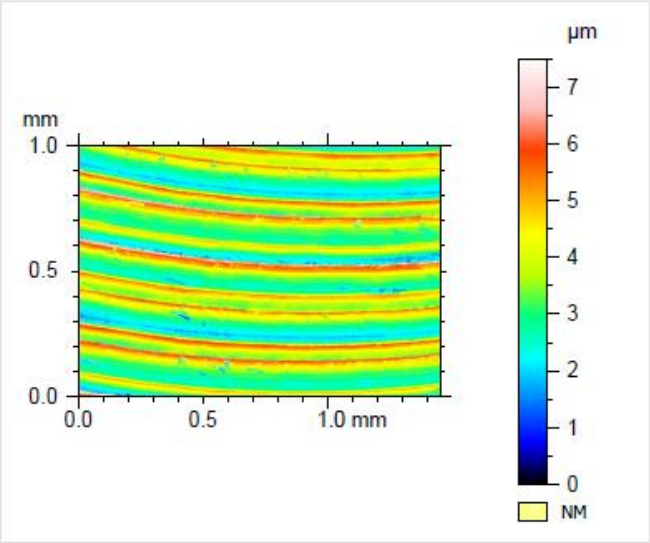

Fig. C-4. Surface topography – with removed form

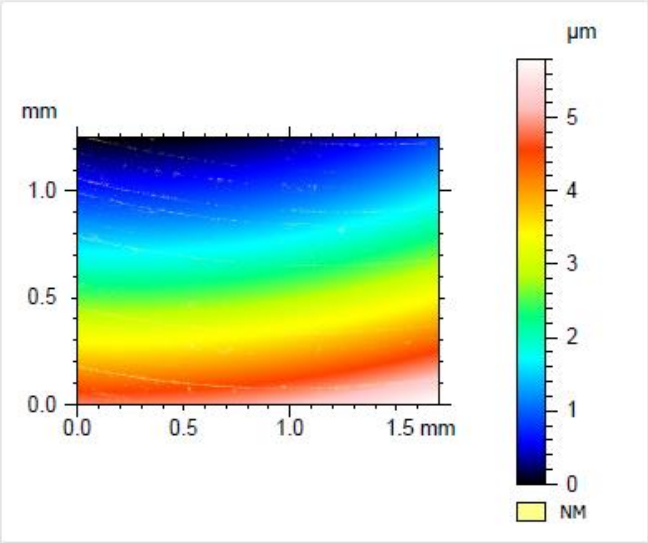

Fig. C-5. Removed form

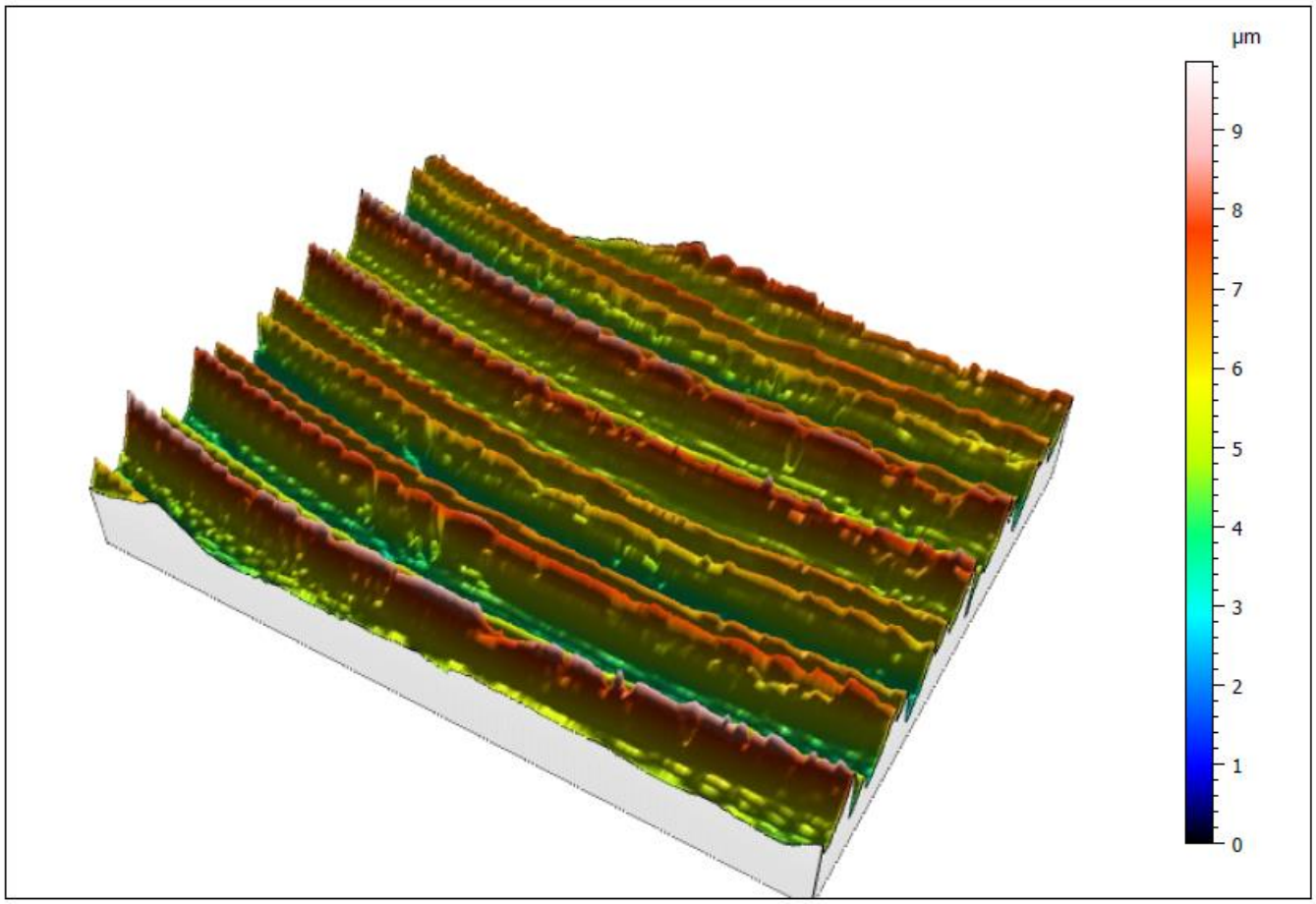

Fig. C-6. 3D Surface topography

Table C-1. Surface topography parameters.

ISO 25178				
Height Parameters				
Sq	1.07	µm		*Root-mean-square height*
Ssk	0.502			*Skewness*
Sku	2.67			*Kurtosis*
Sp	3.86	µm		*Maximum peak height*
Sv	3.65	µm		*Maximum pit height*
Sz	7.50	µm		*Maximum height*
Sa	0.877	µm		*Arithmetic mean height*
Functional Parameters				
Smr	0.642	%	*c = 1 µm under the highest peak*	*Areal material ratio*
Smc	1.56	µm	*p = 10%*	*Inverse areal material ratio*
Spatial Parameters				
Sal	0.0212	mm	*s = 0.2*	*Autocorrelation length*
Str	0.0606		*s = 0.2*	*Texture-aspect ratio*
Std	176	°	*Reference angle = 0°*	*Texture direction*
Hybrid Parameters				
Sdq	*****			*Root-mean-square gradient*
Sdr	*****	%		*Developed interfacial area ratio*
Functional Parameters (Volume)				
Vm	5.07e-005	mm³/mm²	*p = 10%*	*Material volume*
Vv	0.00161	mm³/mm²	*p = 10%*	*Void volume*
Vmp	5.07e-005	mm³/mm²	*p = 10%*	*Peak material volume*
Vmc	0.000962	mm³/mm²	*p = 10%, q = 80%*	*Core material volume*
Vvc	0.00153	mm³/mm²	*p = 10%, q = 80%*	*Core void volume*
Vvv	7.98e-005	mm³/mm²	*p = 80%*	*Pit void volume*
EUR 15178N				
Functional Indices				
Sbi	0.565			*Surface bearing index*
Sci	1.58			*Core fluid retention index*
Svi	0.370			*Valley fluid retention index*
ASME B46.1				
3D Parameters				
St	7.50	µm		*Maximum height*
Sp	3.86	µm		*Maximum peak height*
Sv	3.65	µm		*Maximum pit height*
Sq	1.07	µm		*Root-mean-square height*
Sa	0.877	µm		*Arithmetic mean height*
Ssk	0.502			*Skewness*
Sku	2.67			*Kurtosis*
SWt	*****	µm	*Gaussian filter, 0.8 mm*	*Area waviness height*

Sample 113, GENTIGER GT-66, Flat end milling, WEST cutting direction:

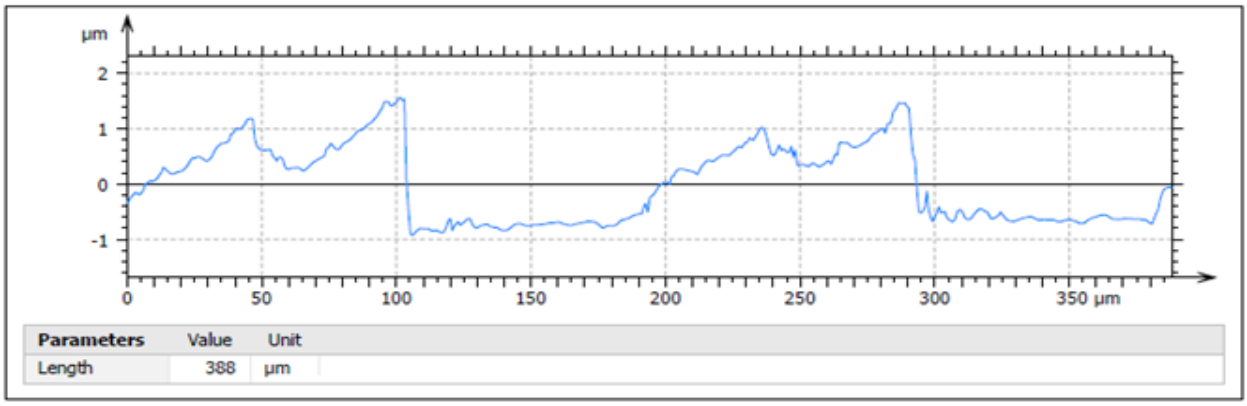

Fig. C-7. Surface profile

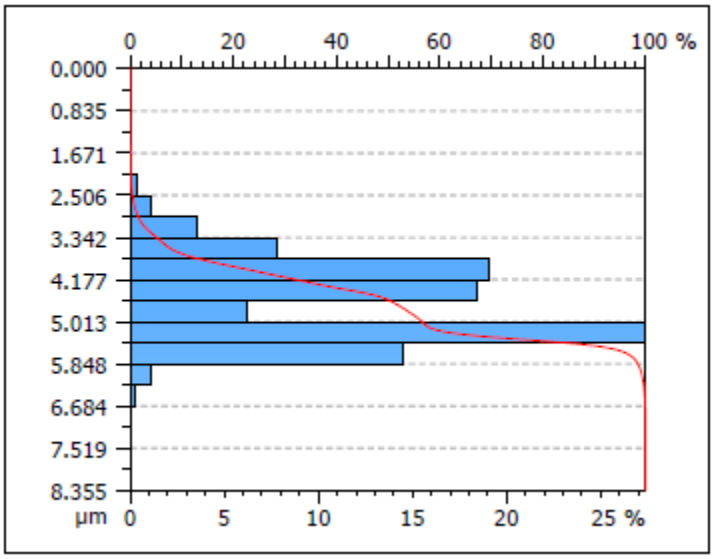

Fig. C-8. Surface profile height histogram

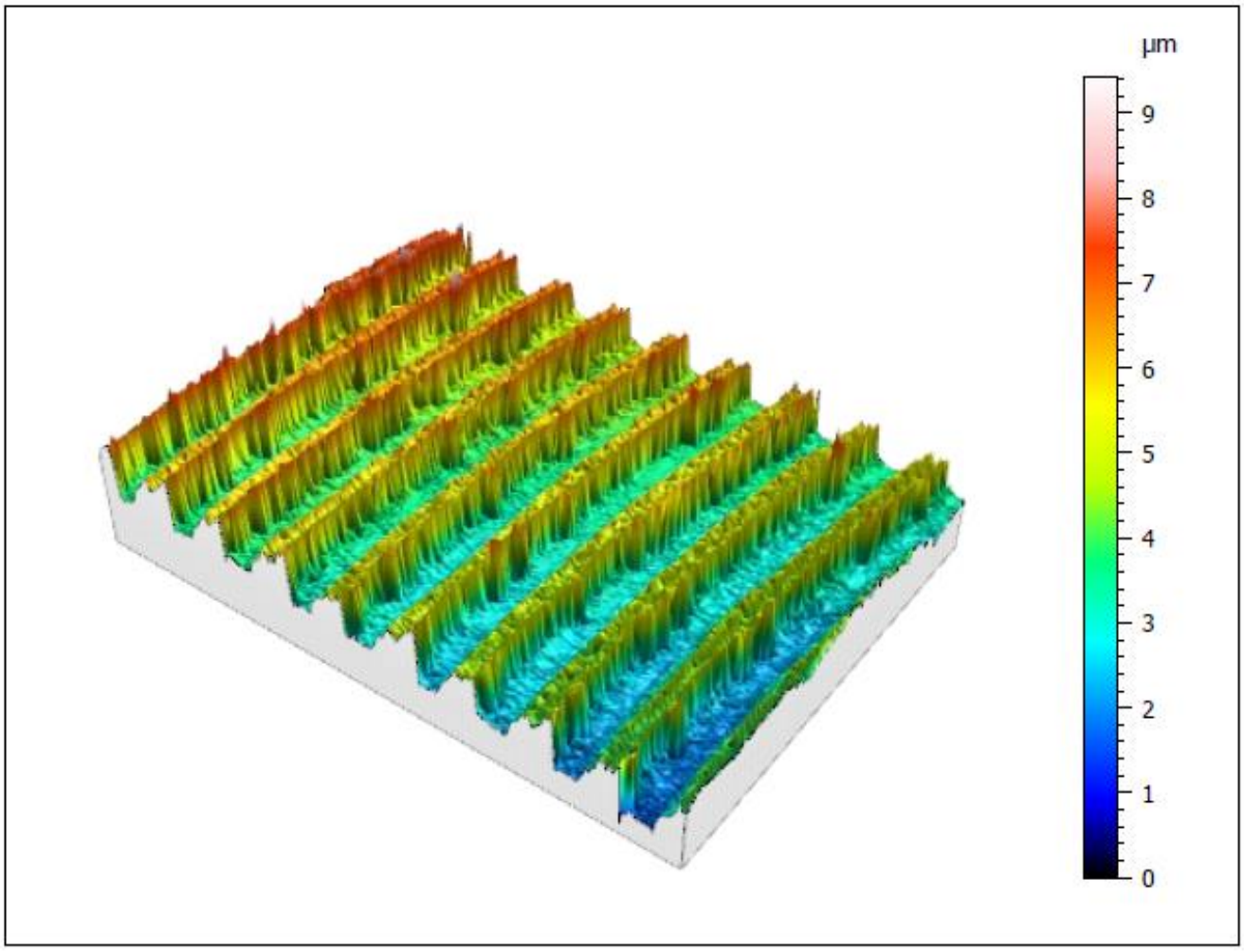

Fig. C-9. 3D surface topography

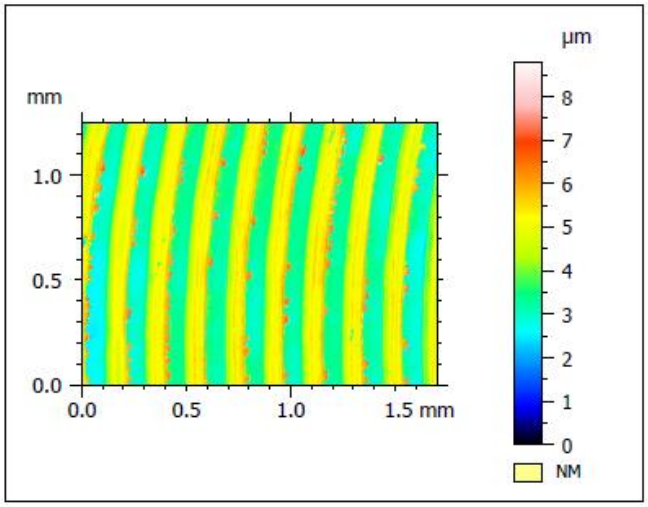

Fig. C-10. Surface topography – with removed form

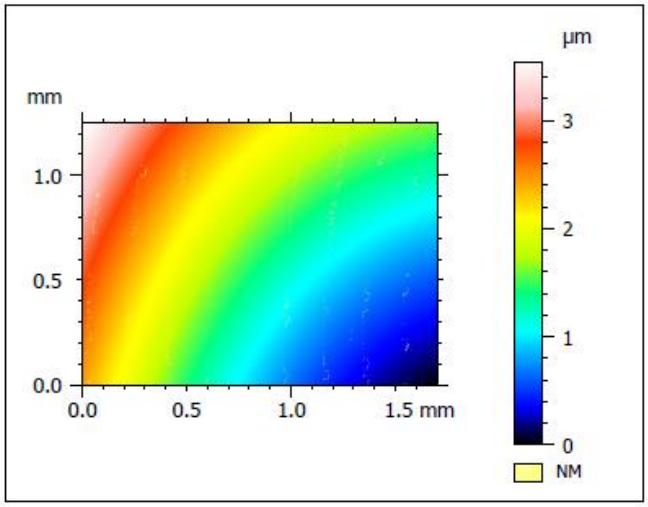

Fig. C-11. Removed form

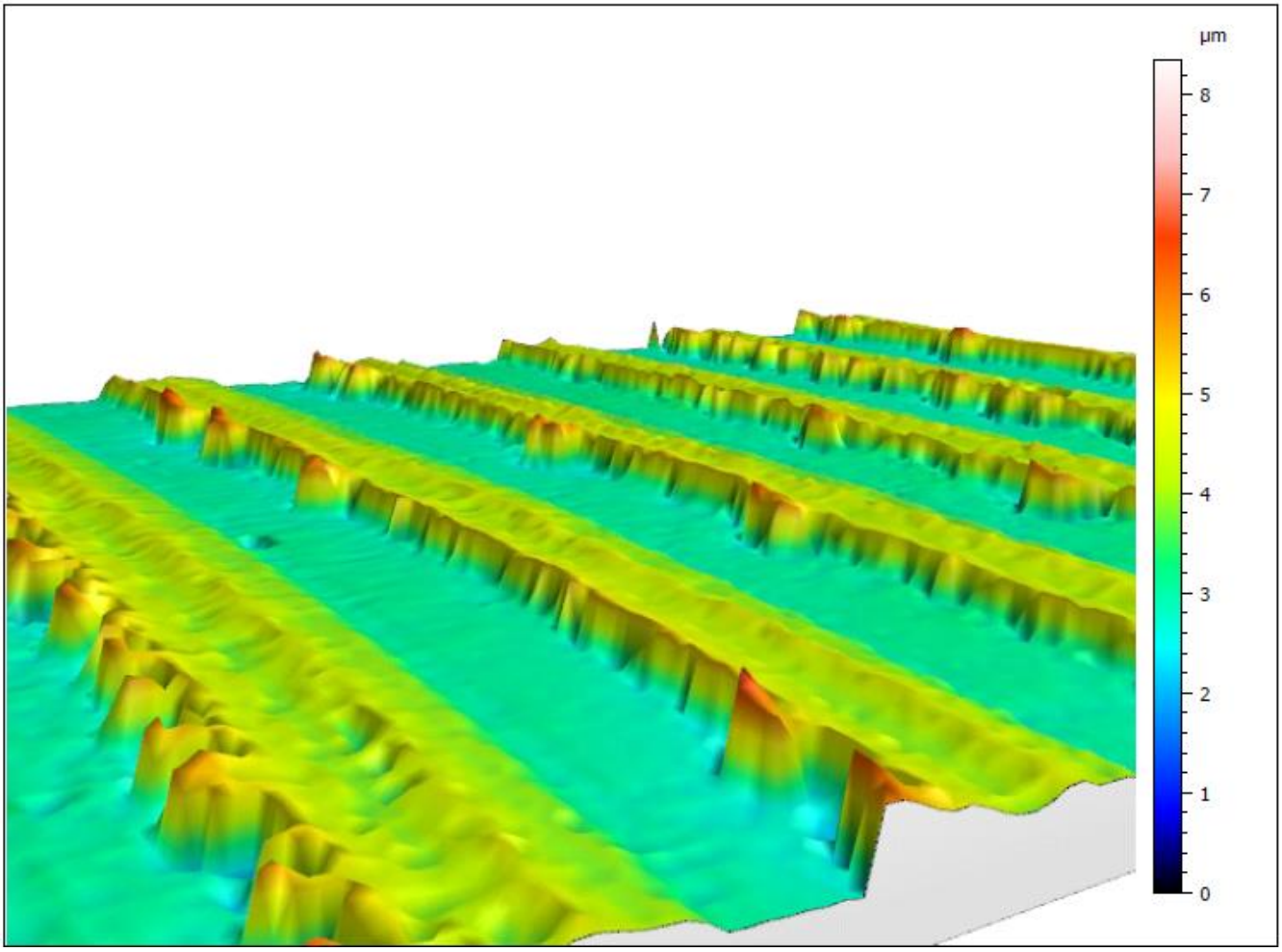

Fig. C-12. 3D surface topography

Table C-2. Surface topography parameters.

ISO 25178				
Height Parameters				
Sq	0.783	µm		*Root-mean-square height*
Ssk	0.344			*Skewness*
Sku	2.40			*Kurtosis*
Sp	4.64	µm		*Maximum peak height*
Sv	3.71	µm		*Maximum pit height*
Sz	8.35	µm		*Maximum height*
Sa	0.688	µm		*Arithmetic mean height*
Functional Parameters				
Smr	0.003	%	*c = 1 µm under the highest peak*	*Areal material ratio*
Smc	0.979	µm	*p = 10%*	*Inverse areal material ratio*
Spatial Parameters				
Sal	0.0314	mm	*s = 0.2*	*Autocorrelation length*
Str	0.0867		*s = 0.2*	*Texture-aspect ratio*
Std	86.0	°	*Reference angle = 0°*	*Texture direction*
Hybrid Parameters				
Sdq	*****			*Root-mean-square gradient*
Sdr	*****	%		*Developed interfacial area ratio*
Functional Parameters (Volume)				
Vm	4.05e-005	mm³/mm²	*p = 10%*	*Material volume*
Vv	0.00102	mm³/mm²	*p = 10%*	*Void volume*
Vmp	4.05e-005	mm³/mm²	*p = 10%*	*Peak material volume*
Vmc	0.000744	mm³/mm²	*p = 10%, q = 80%*	*Core material volume*
Vvc	0.000986	mm³/mm²	*p = 10%, q = 80%*	*Core void volume*
Vvv	3.36e-005	mm³/mm²	*p = 80%*	*Pit void volume*
EUR 15178N				
Functional Indices				
Sbi	0.235			*Surface bearing index*
Sci	1.58			*Core fluid retention index*
Svi	0.208			*Valley fluid retention index*
ASME B46.1				
3D Parameters				
St	8.35	µm		*Maximum height*
Sp	4.64	µm		*Maximum peak height*
Sv	3.71	µm		*Maximum pit height*
Sq	0.783	µm		*Root-mean-square height*
Sa	0.688	µm		*Arithmetic mean height*
Ssk	0.344			*Skewness*
Sku	2.40			*Kurtosis*
SWt	*****	µm	*Gaussian filter, 0.8 mm*	*Area waviness height*

Sample 183, KONDIA B500, Flat end milling, SOUTH cutting direction:

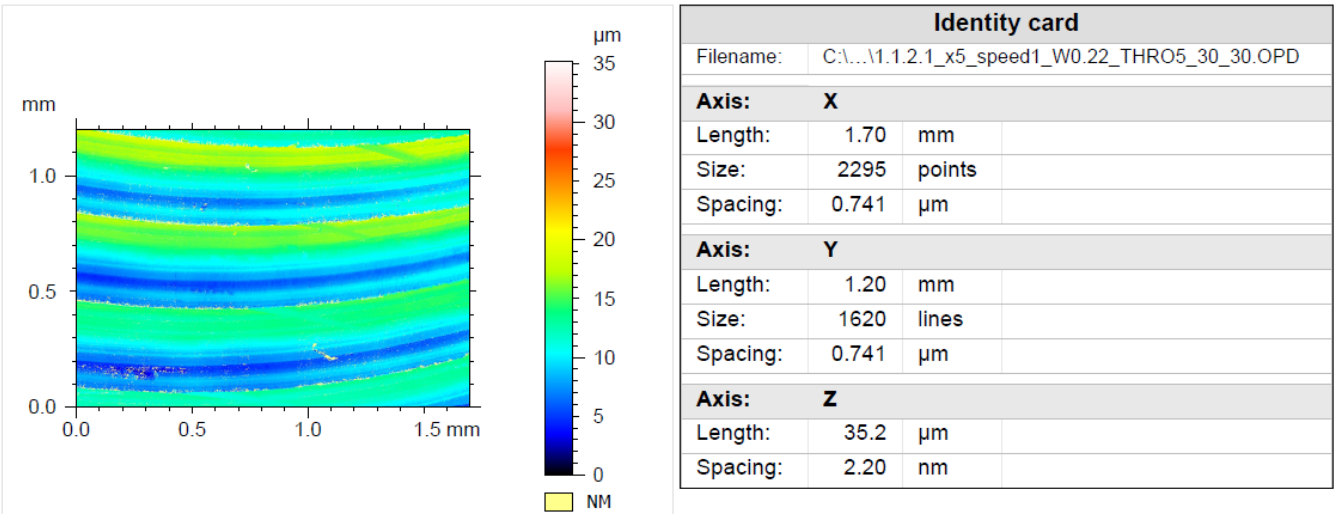

Identity card		
Filename:	C:\...\1.1.2.1_x5_speed1_W0.22_THRO5_30_30.OPD	
Axis:	**X**	
Length:	1.70	mm
Size:	2295	points
Spacing:	0.741	µm
Axis:	**Y**	
Length:	1.20	mm
Size:	1620	lines
Spacing:	0.741	µm
Axis:	**Z**	
Length:	35.2	µm
Spacing:	2.20	nm

Fig. C-12. Identification of sample measurement – dimensions of data array

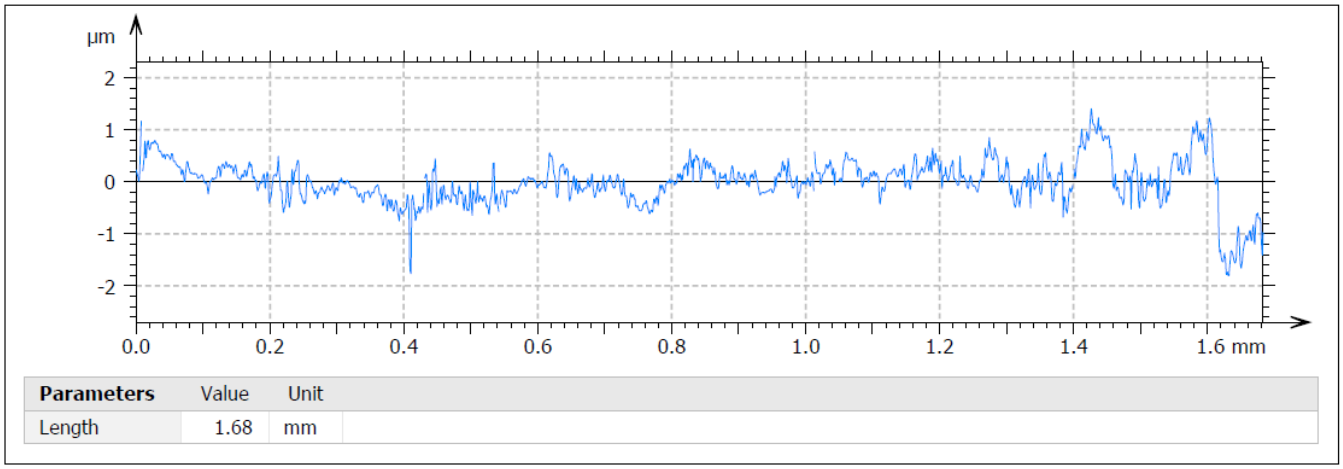

Parameters	Value	Unit
Length	1.68	mm

Fig. C-14. Surface profile

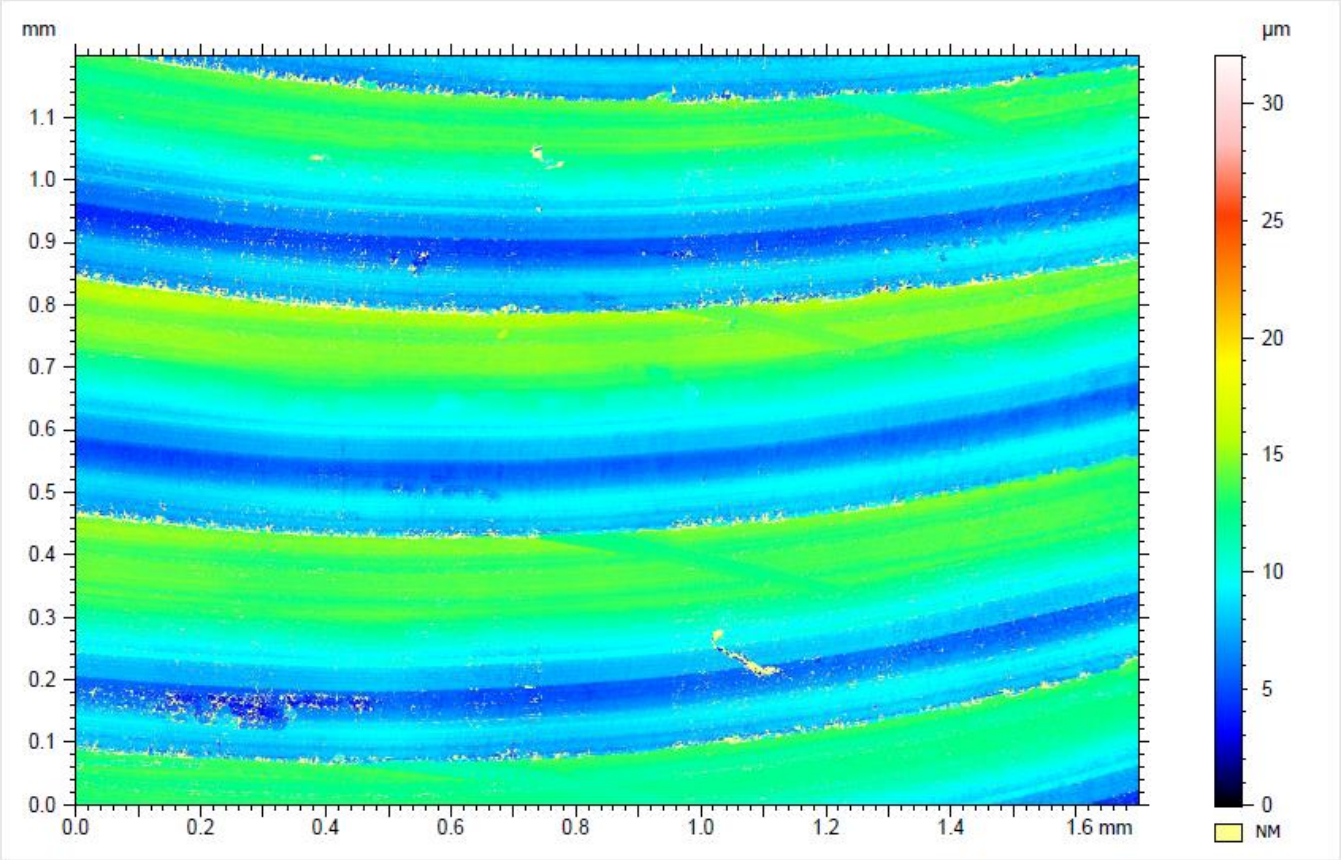

Fig. C-15. Surface topography – top view

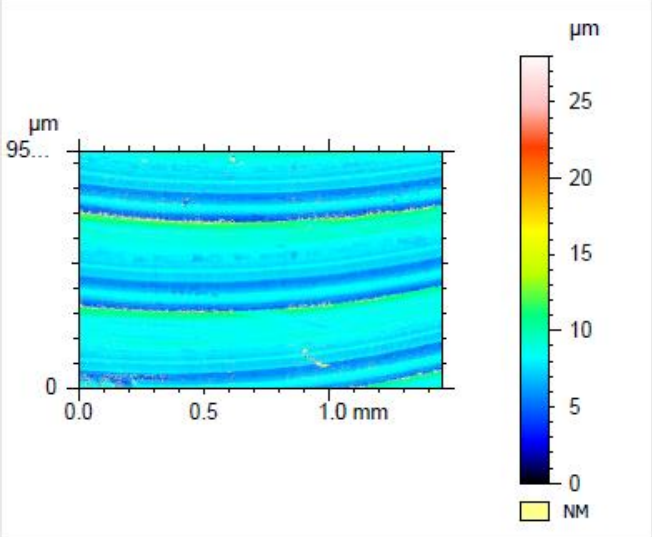

Fig. C-16. Surface topography – with removed form

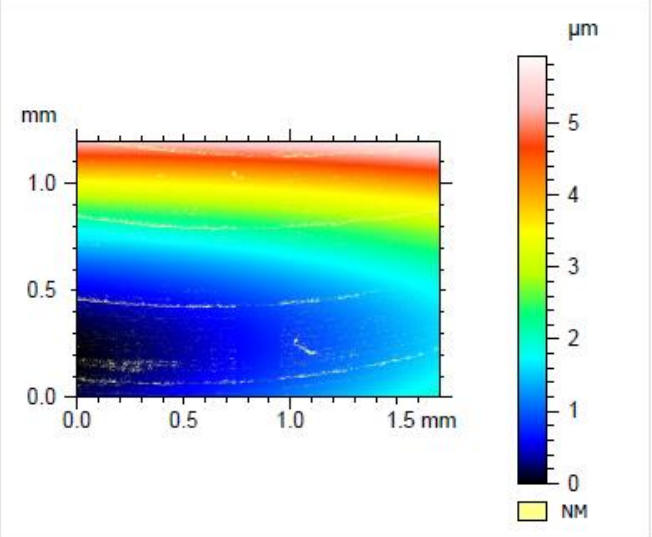

Fig. C-17. Removed form

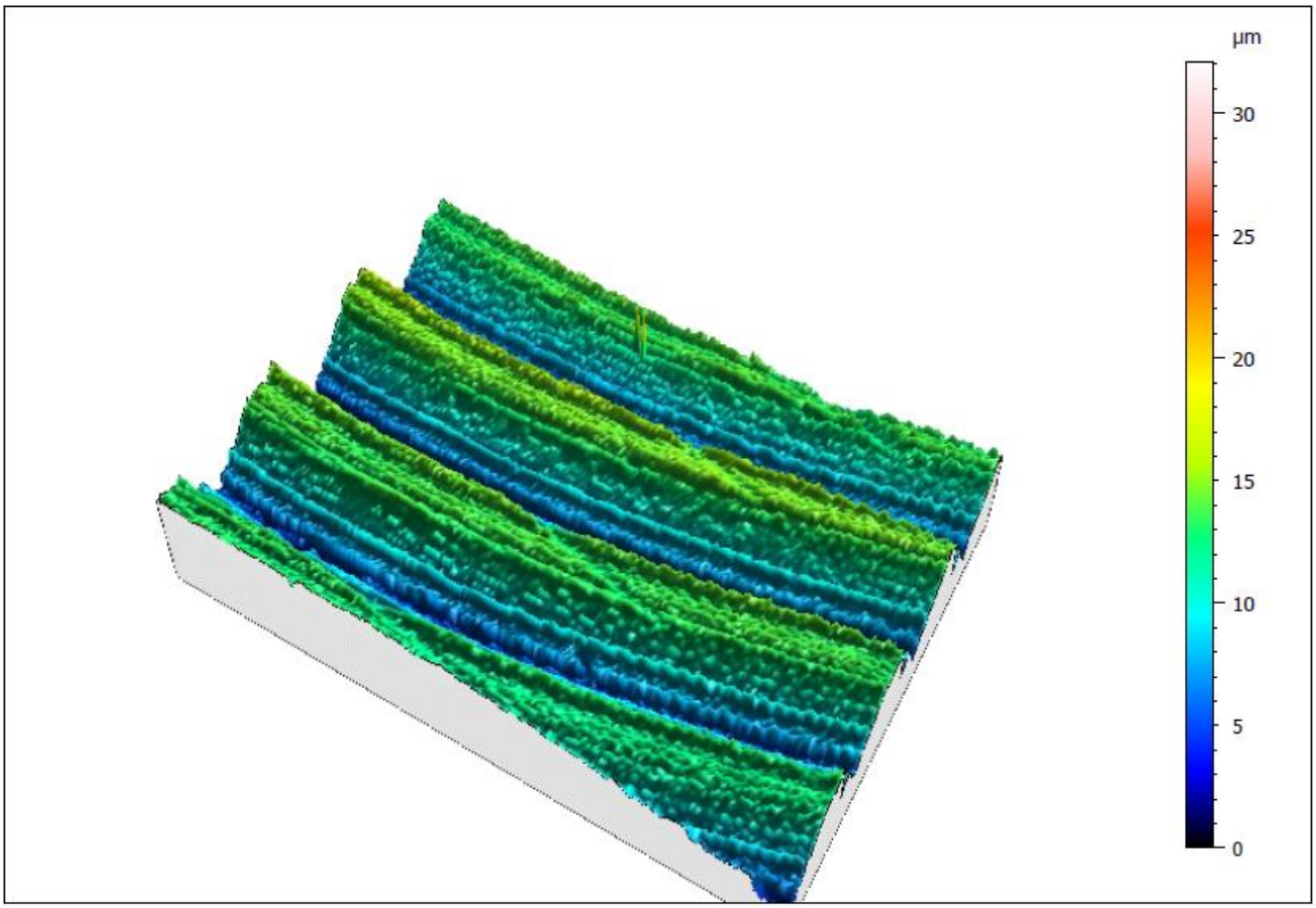

Fig. C-18. 3D Surface topography

Table C-3. Surface topography parameters.

ISO 25178				
Height Parameters				
Sq	1.33	µm		*Root-mean-square height*
Ssk	0.0598			*Skewness*
Sku	4.71			*Kurtosis*
Sp	20.3	µm		*Maximum peak height*
Sv	7.72	µm		*Maximum pit height*
Sz	28.0	µm		*Maximum height*
Sa	1.00	µm		*Arithmetic mean height*
Functional Parameters				
Smr	0.00184	%	*c = 1 µm under the highest peak*	*Areal material ratio*
Smc	1.45	µm	*p = 10%*	*Inverse areal material ratio*
Spatial Parameters				
Sal	0.0221	mm	*s = 0.2*	*Autocorrelation length*
Str	0.0306		*s = 0.2*	*Texture-aspect ratio*
Std	3.25	°	*Reference angle = 0°*	*Texture direction*
Hybrid Parameters				
Sdq	*****			*Root-mean-square gradient*
Sdr	*****	%		*Developed interfacial area ratio*
Functional Parameters (Volume)				
Vm	9.39e-005	mm³/mm²	*p = 10%*	*Material volume*
Vv	0.00154	mm³/mm²	*p = 10%*	*Void volume*
Vmp	9.39e-005	mm³/mm²	*p = 10%*	*Peak material volume*
Vmc	0.00106	mm³/mm²	*p = 10%, q = 80%*	*Core material volume*
Vvc	0.00134	mm³/mm²	*p = 10%, q = 80%*	*Core void volume*
Vvv	0.000198	mm³/mm²	*p = 80%*	*Pit void volume*
EUR 15178N				
Functional Indices				
Sbi	0.0732			*Surface bearing index*
Sci	0.990			*Core fluid retention index*
Svi	0.738			*Valley fluid retention index*
ASME B46.1				
3D Parameters				
St	28.0	µm		*Maximum height*
Sp	20.3	µm		*Maximum peak height*
Sv	7.72	µm		*Maximum pit height*
Sq	1.33	µm		*Root-mean-square height*
Sa	1.00	µm		*Arithmetic mean height*
Ssk	0.0598			*Skewness*
Sku	4.71			*Kurtosis*
SWt	*****	µm	*Gaussian filter, 0.8 mm*	*Area waviness height*

D - Mathematical calculation of minimum surface, cutting forces and tool deflection, cutting tool inclination and vibration model

In this example one sample surface topography calculation model is described. The same principle was used for all other samples, with different cutting process parameters. Fig. D-1 represent end milling tool ”barrel” with rotation axis O, Cutting tool tip point A and other designated points for tool tip point displacement calculations.

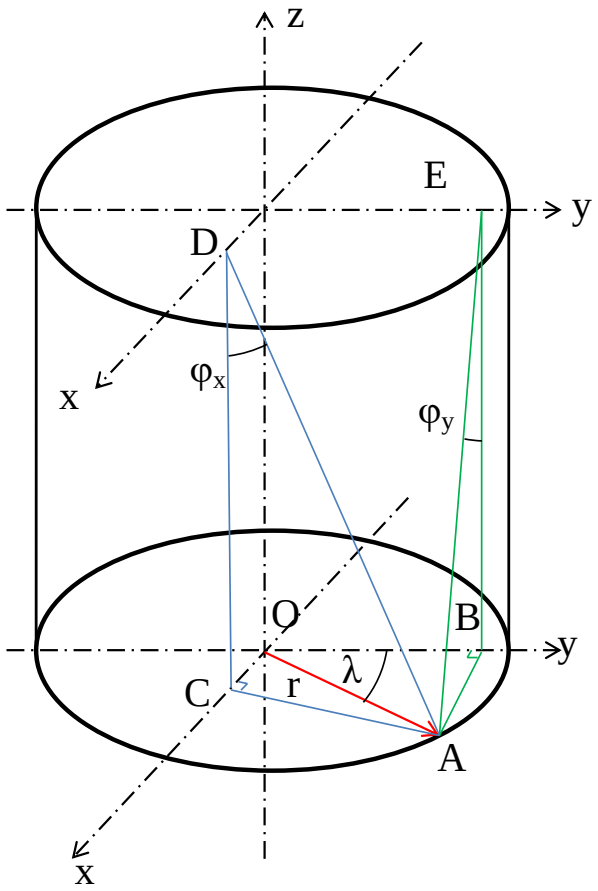

Fig. D-1. Cutting tool “barrel” with representative angles and calculation points.

First of all, geometrical calculation was done for Cutting tool tip point geometrical particularities. Minimum surface topography height was calculated by equation 6.1 in Chapter 6. Effect of minimum surface topography is represented in Fig. D-2.

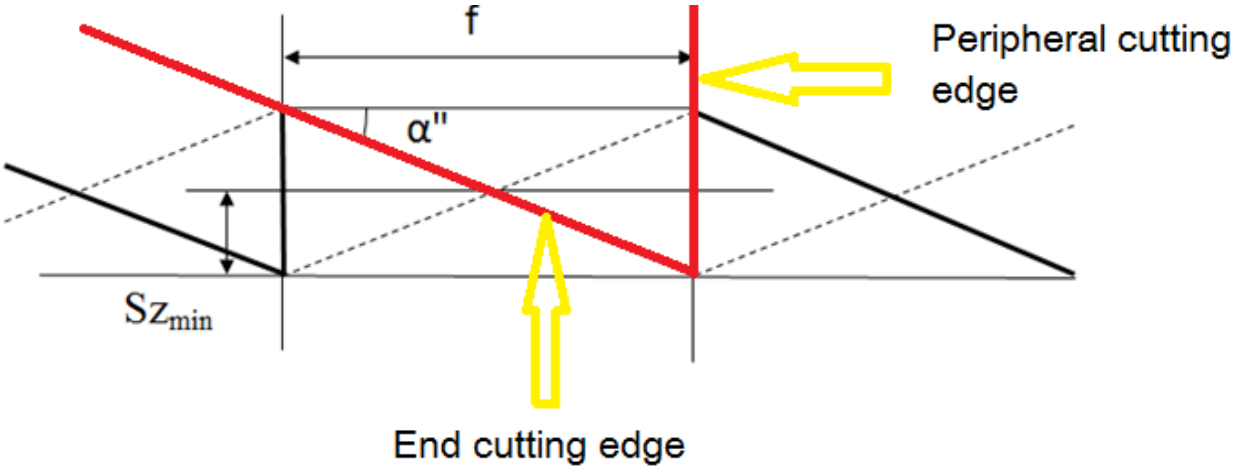

Fig. D-2. Minimum surface topography height formation.

edges

$$Sz(min) = \frac{1}{2} * \tan(\alpha) * f \qquad \text{Eq. D-1}$$

Sz_{minF2} = 3,492077 µm;

The next parameter added to surface topography formation calculations is Cutting force model and its caused cutting tool deflection component. To do this, cutting forces was simulated first. Simulation results are represented in Table D-1.

Table D-1 Cutting force *Fc* peak values according to selected feed rate

FEED RATE *f*, mm/ tooth	**CUTTING FORCE F_C, N**
0,1	136,3

Deflection model was calculated with help of MathCAD software tool, to model the cutting forces and use their influence against the cutting tool stiffness. According cutting conditions was selected for calculation and cutting tool immersion angle, with certain step was defined for use of calculation.

Deflection model was calculated with help of MathCAD software tool, to model the cutting forces and use their influence against the cutting tool stiffness. According cutting conditions was selected for calculation and cutting tool immersion angle, with certain step was defined for use of calculation.

Designations: f- cutting feed rate, r - cutting tool radius, h- cutting tool length out of the tool length, j – number of cutting edges, n – spindle speed, ap- cutting depth, θ – immersion angle, tc – un-cutted chip thickness. Kt is the cutting pressure for tangential force, Kn and Ka are cutting pressure for normal and axial forces.

$f := 0.1 \quad r := 5 \quad H := 34.8$

$Kt := 4395$

$\beta := \frac{30 \cdot \pi}{180} \quad z := 0, 0.1 .. 0.3$

$Kn := 1.034$

$Ka := 0.436$

$n := 4775 \quad ap := 0.3 \quad j := 2$

$\theta := 0, 0.00001 \cdot \pi .. \pi$

Fig. D-3. represents change of un-cutted chip thickness during the immersion angle increase. Selected immersion angle for analysis is half turn of cutting tool, to cover complete chip separation process for one cutting tool edge. The uncutted chip cross section tc, depends on feed, f, cut depth, ap and tool immersion angle, and is expressed as:

$$tc(\lambda) := (f \cdot \sin(\lambda)) \cdot ap \qquad \text{Eq. D-2}$$

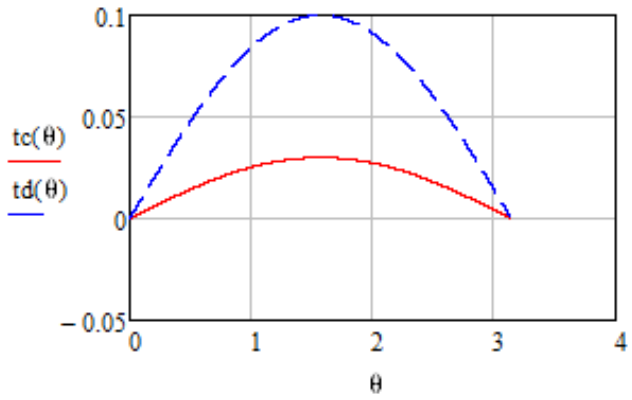

Fig. D-3. Un-cutted chip thickness along the cutting tool immersion angle

Next, for cutting force determination general, well known cutting force model was used. First local cutting force components from coefficients was determined:

$$Ft(\lambda) := Kt \cdot tc(\lambda) \qquad \text{Eq. D-3}$$

$$Fn(\lambda) := Kn \cdot (Kt \cdot tc(\lambda)) \qquad \text{Eq. D-4}$$

$$Fa(\lambda) := Ka \cdot (Kt \cdot tc(\lambda)) \qquad \text{Eq. D-5}$$

$$Fx(\lambda) := -Ft(\lambda) \cdot \cos(\lambda) - Fn(\lambda) \cdot \sin(\lambda) \qquad \text{Eq. D-6}$$

$$Fy(\lambda) := Ft(\lambda) \cdot \sin(\lambda) - Fn(\lambda) \cdot \cos(\lambda) \qquad \text{Eq. D-7}$$

Eq. D-8

$$Fz(\lambda) := Fa(\lambda)\cdot \sin(\lambda)$$

Cutting force coefficient change during the cutting process and cutting tool immersion angle is represented in Fig. D-4.

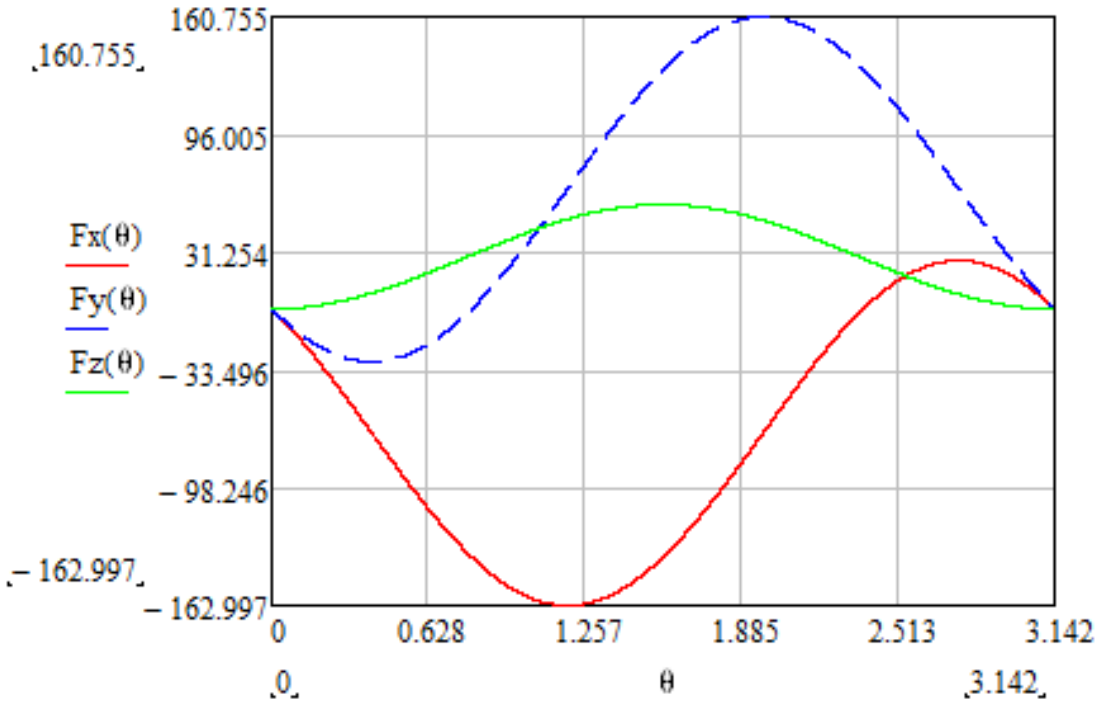

Fig. D-4. Cutting force changes along the cutting tool rotation from immersion till the end of cut

After, cutting force coefficients was multiplied by cutting tool stiffness coefficients, to obtain the geometrical tool tip point deflection from its start point:

Table D-2. Cutting tool MS2MSD1000 material (WC) rigidity coefficients (depends on tools geometry)

Force applied direction	**Deformation direction**	**Stiffness coefficient, N/mm**
Tangential	Tangential	M_t = 8146,374
Normal	Normal	M_n = 11334,784
Axial	Tangential	$M_{z(t)}$ = 40150,968
	Normal	$M_{z(n)}$ = 57703,738
	Axial	$M_{z(a)}$ = 15885,716

$$\delta X(Fx(\lambda)) = -Ft(\lambda) * \frac{1}{Mt} * \cos(\lambda) - Fn(\lambda) * \frac{1}{Mn} * \sin(\lambda) \quad \text{Eq. D-9}$$

$$\delta Y(Fy(\lambda)) = Ft(\lambda) * \frac{1}{Mt} * \sin(\lambda) - Fn(\lambda) * \frac{1}{Mn} * \cos(\lambda) \quad \text{Eq. D-10}$$

$$\delta Z(F(\lambda)) = \left(-Ft(\lambda) * \frac{1}{Mz(t)}\right) + \left(-Fn(\lambda) * \frac{1}{Mz(n)}\right) + \left(Fa(\lambda) * \frac{1}{Mz(a)}\right) \quad \text{Eq. D-11}$$

In our case, deflection in Z axis direction is most important, to analyze, how cutting tool end cutting edge performs cutting surface, and how it affect the surface topography formation.

Table D-3. Cutting tool deflection in axial – Z direction according to applied cutting force

FEED RATE *f*, mm/ tooth	**CUTTING FORCE F_c, N**	**TOOL's AXIAL DEFLECTION, mm**
0,1	136,3	0,0036188

The next cutting process parameter to add to our mathematical model is cutting tool axis inclination model, that may become from milling machine spindle alignment or construction inaccuracy and wear out. Inclination of Machine spindle axis is represented in Fig. D-5. Following equation D11 was used for calculation of milling axis inclination caused surface topography height changes.

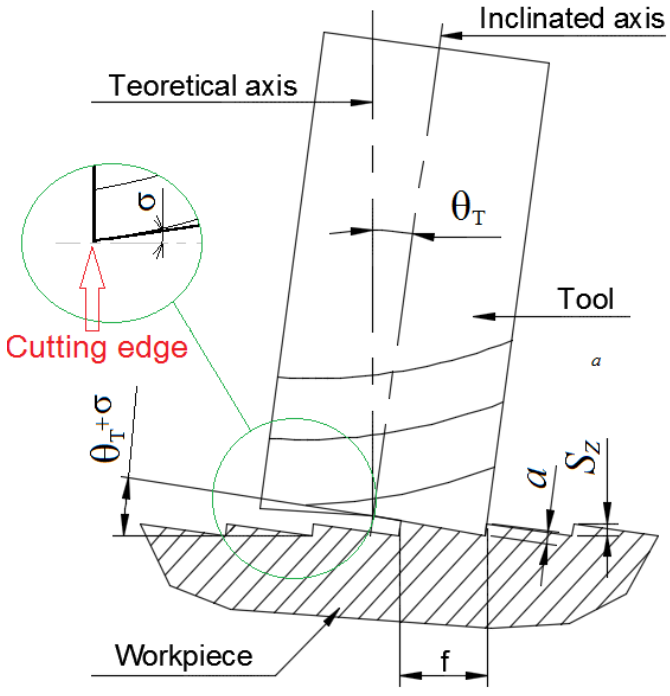

Fig. D-5. Representation of milling machine spindle axis inclination

$$Sz_{\mathrm{T}}(\lambda) = \frac{\mathrm{t}(\lambda)*\tan(\theta_T+\sigma)}{1+\tan(\theta_T+\sigma)*\tan(\theta)}$$ Eq. D-12

Calculation results for KONDIA B500 milling machine is represented here in Table D-4:

CUTTING DIRECTION, *DIR*	**INCLINATION ANGLE θ_T, degrees (KONDIA)**
SOUTH	-0,2422552
NORTH	0,2422552
WEST	-1,5153107
EAST	1,5153107

The last component added to this calculation model is Vibration component. Vibration component was calculated thanks to the MathCAD solving tool that allows determining vibration amplitude and providing a graph with milling table deviations. Forced vibrations dynamical displacement function was solved to obtain the deviations of milling equipment.

$$M \times \left(\frac{d^2}{dt^2}y(t)\right) + C \times \left(\frac{d}{dt}y(t)\right) + K \times y(t) = f(t)$$ Eq. D-13

$$f(t) = Ft(\lambda(t)) * sin(\lambda(t))$$ Eq. D-14

Volume of Milling table (calculated with SOLIDWORKS from CAD drawing):

$$M = \delta_{tool} \times \mathrm{V}_{table}$$ Eq. D-15

Spring and dampening coefficients was derived from milling equipment vibration measurements done for milling table and spindle base construction. Fig. D-6 represents the milling table deviations in Z axis due to initiated cutting force and constructive particularities. The magnitude of milling table displacement is used for surface topography formation model development. They directly influence surface topography formation after end milling operation. The results of solved function are represented in table D-5. Maximum value of deviation is selected as it represents the worst scenario of milling system dynamical behavior in Z axis direction.

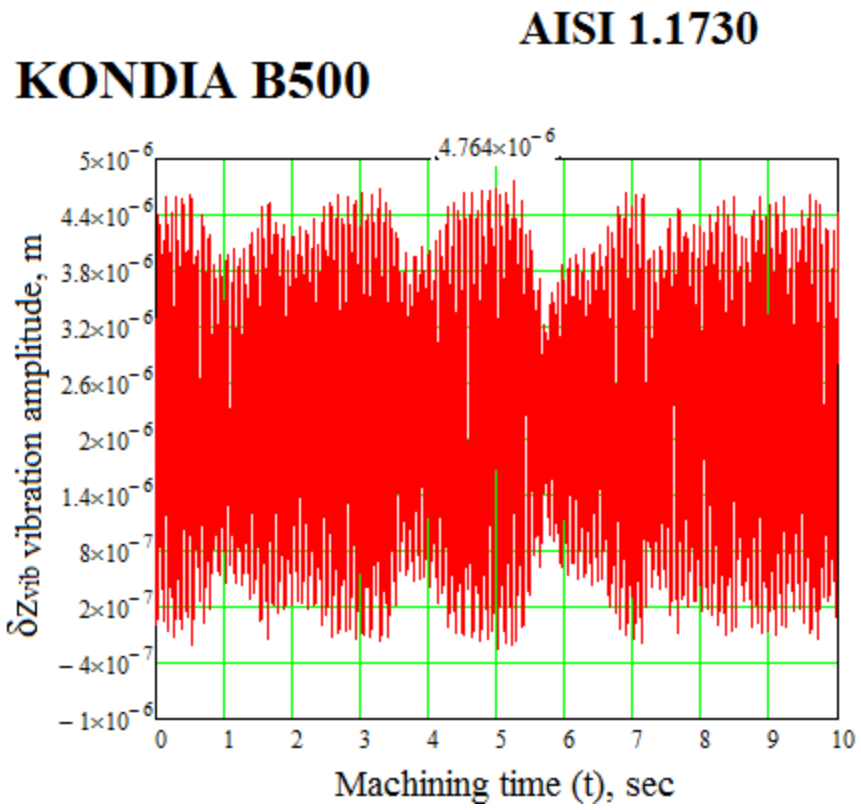

Fig. D-6. Plot of solved second order vibration system equation (KONDIA B500 machine, feed F2 = 0,1 mm/tooth.)

Table D-5. KONDIA B500 milling machine vibration amplitude on *Z* axis due to cutting force F_Z

MATERIAL TYPE	FEED 2, 0,1 mm/t
DIN 1.1730	0,0047643 mm

Total surface height variation in the Z axis direction, $\delta S_Z(\lambda)$, is calculated as the sum of each calculated component. This is S_Z – predicted value in μm. The model has been improved by including the machine-tool-workpiece system's natural frequency, causing tool tip point displacement in the Z axis. The addition of this will give a more accurate surface maximum height in the scale-limited surface area parameter S_Z, Eq. D-16. Results are presented in Table D-6.

$$\delta Sz(\lambda) = Sz_{min} + \delta Sz\big(\mathrm{F}(\lambda)\big) + \delta Sz_{\mathrm{T}}(\lambda) + \delta \mathrm{z}_{\mathrm{vib}} \qquad \text{Eq. D-16}$$

Table D-6. Measured and predicted surface topography parameters analysis for KONDIA B500 milling machine, DIN 1.1730 material and cutting feed F1 = 0,1mm/tooth.

Feed direction	S_Z measured, µm	S_Z mean value, µm	S_Z predicted, µm	Difference between measured average and predicted, µm, %	Difference between directions, %	
					Measured	Predicted
1. SOUTH	14,3043	14,837155	11,4524294	3,3847256 22,8 %	5,4 %	6,9 %
	15,3700					
3. NORTH	16,1740	15,682900	12,2979246	3,207314 25,7 %		
	15,1918					
2. WEST	13,7202	12,441450	9,2341359	3,384975 21,6 %	46,6 %	36,4 %
	11,1627					
4. EAST	16,4806	23,321250	14,5162181	8,805032 37,8 %		

The same principle was used for all other samples with appropriate cutting conditions.

E - Vibration analysis of KONDIA B500 and GENTIGER GT66V High speed milling machines

VIBRATIONS KONDIA B500 MILLING MACHINE

Results of the measurements at 15/07/2016

First trial: FRF milling head

Frequency response function (FRF) is calculated by hit by hammer against the machine spindle and measuring response on it. FRF is measured in $m/s^2/N$.

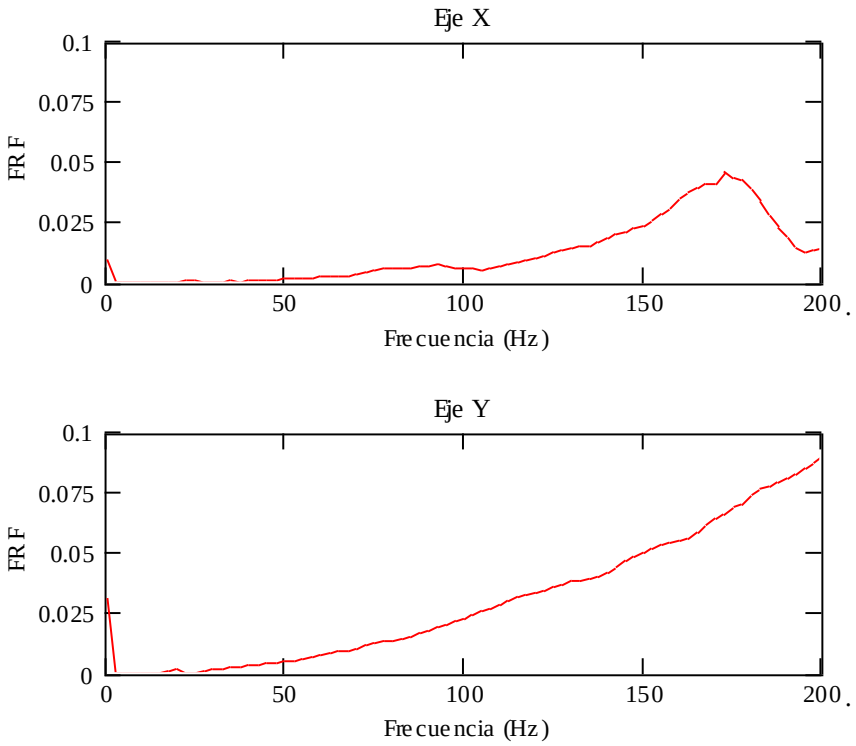

Fig. E-1. Resonance in X axis direction is 172 Hz at the spindle working frequency range.

Second trial: FRF milling table

Hitting and measuring the response of KONDIA B500 milling table:

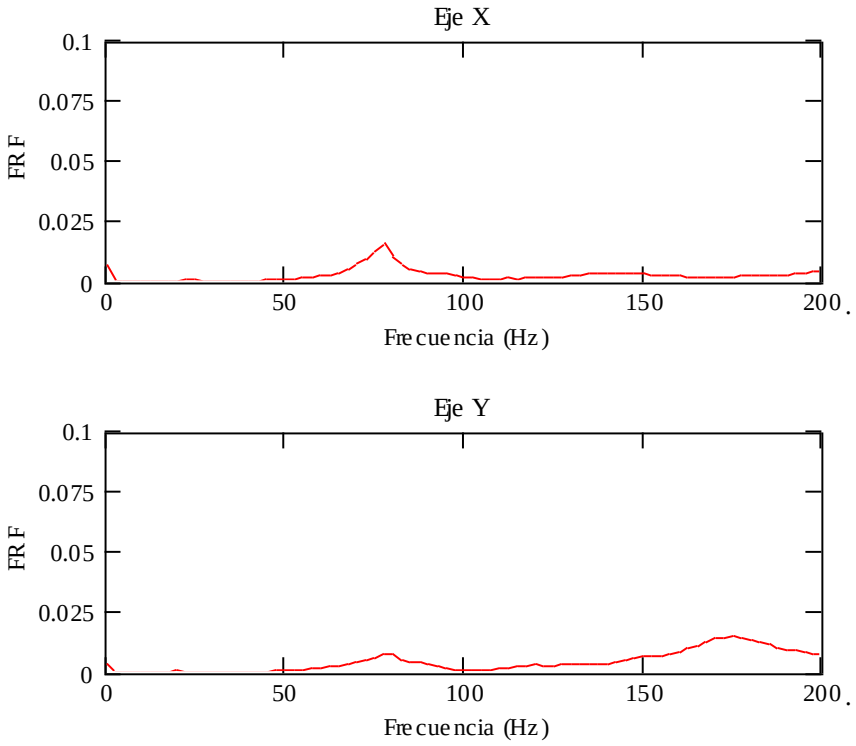

Fig. E-2. The highest resonance of milling table is 77 Hz.

Third trial: amplitude of response function

Response of the milling head was measured on both orthogonal directions (X and Y) and the same for milling table. It was swept in increments of 100 r/min from 3000 to 5000 r/min.

The measurement results are recorded in videos. Vibration measured by acceleration in m/s^2 and with the calculation of the associated peak displacement in microns.

The maximum displacement at spindle appears at frequency equal to 1.3 times of rotation – spindle speed. When the 4300 - 4400 r/min of the spindle is reached and a frequency of 5600 - 5700 cpm is excited, that is around 94 Hz.

The maximum displacement at milling table in the X direction appears again at a frequency equal to 1.3 times of rotation when the head is reached 3400 - 3500 r/min and a frequency of 4500 - 4600cpm is excited, that is around 76 Hz. It coincides with the resonance excitation measured at excited impact on the milling table.

The maximum displacement at milling table in the Y direction appears again at a frequency equal to 1.3 times that of rotation frequency, when the 3600 r/min of the spindle is reached and a frequency of 4700 cpm is excited, that is around 78 Hz.

VIBRATIONS GENTIGER GT66 MILLING MACHINE

Results of the measurements at 21/09/2016

First trial: FRF milling head

Frequency response function (FRF) is calculated by hit by hammer against the machine milling table and measuring response on it. FRF is measured in $m/s^2/N$.

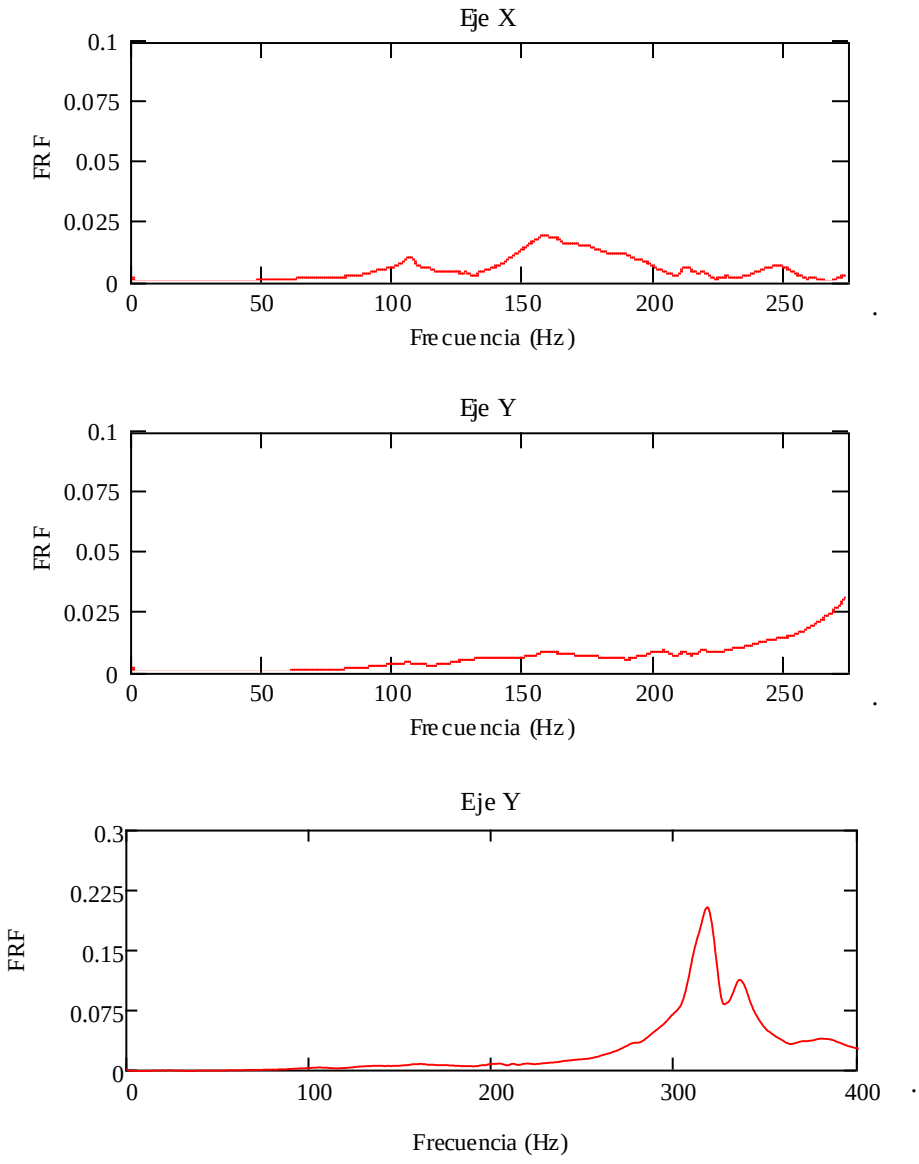

Fig. E-3. Resonance in X axis direction is 158 Hz at the spindle working frequency range.

Response amplitudes at each frequency lower than those obtained at the KONDIA milling machine. At Y there is significant resonance at 317 Hz (19,000 r/min), with significant FRF amplitude from 290 Hz (17400 r/min).

Second trial: FRF milling table

Hitting and measuring the response of GENTIGER GT-66 milling table:

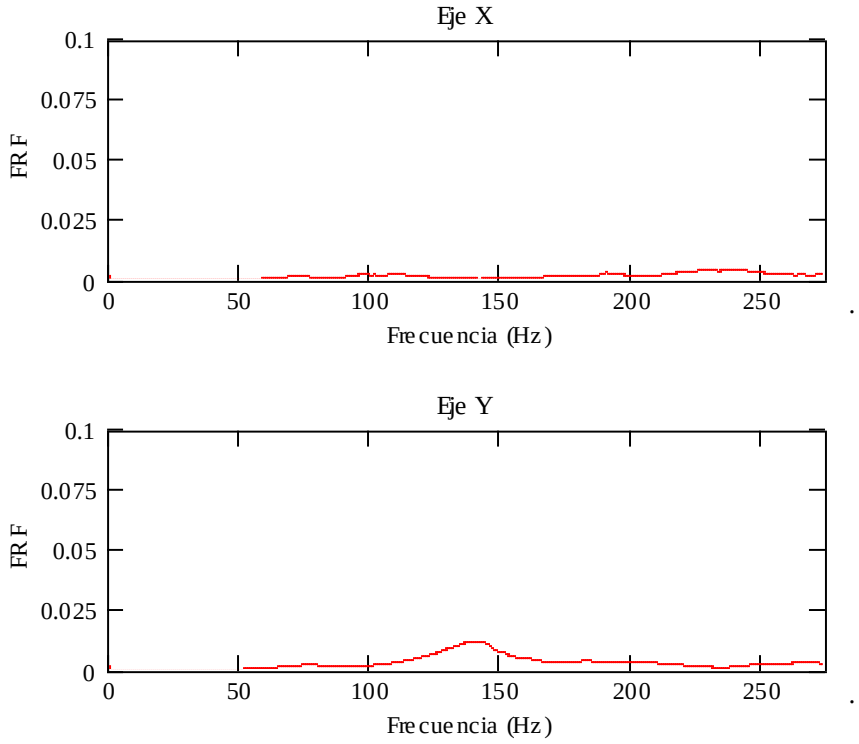

Fig. E-4. Highest resonance of milling table Y direction is 139 Hz.

Third trial: amplitude of response function

Response of the milling head was measured on both directions - X and Y, while at table in Y direction. It was swept in increments of 100 r/min from 3000 to 5000 r/min.

The measurement results recorded in videos. Vibration measured by acceleration in m/s^2 and with the calculation of the associated peak displacement in microns.

In X direction there is no significant vibration at milling head unit. Only vibration fixed at a fixed frequency of 50 Hz (3000 cpm) from some auxiliary equipment.

In Y direction milling head vibration is very low (less than 0.1 micron) at the turning frequency and twice the turning frequency. At the rotational frequency, the machine frame as a whole has a similar vibration amplitude in the Y axis direction.

Response was measured in the X and Y direction of milling head as well as in the rear structure of the machine in the Y direction, sweeping in increments of 100 r/min from 14000 to 16000 r/min.

The recorded acceleration caused the loss of contact of the accelerometers with the head unit when reaching 15000 r/min. In the videos of the peak amplitude it is observed that the amplitude between 14000 and 15000 r/min remains below 0.5 microns at the points of the head where the accelerometers were located.

CALCULATION OF VIBRATION AMPLITUDE

This is a description of MathCAD based prediction model, how we obtained vibration amplitude, considering the SPRING/DAMPENING coefficients were obtained from Measurement calculation, using solving tool of Excel.

f- cutting feed rate, r - cutting tool radius, h - cutting tool length out of the tool length, j – number of cutting edges, n – spindle speed, a_p- cutting depth, θ – immersion angle, t_c – uncutted chip thickness.

$f := 0.1 \quad r := 5 \quad H := 34.8$

$Kt := 4395$

$\beta := \frac{30 \cdot \pi}{180} \quad z := 0, 0.1 .. 0.3$

$Kn := 1.034$

$Ka := 0.436$

$n := 4775 \quad ap := 0.3 \quad j := 2$

$\theta := 0, 0.00001 \cdot \pi .. \pi$

Figure D-3. represents change of un-cutted chip thickness during the immersion angle increase. Selected immersion angle for analysis is half turn of cutting tool, to cover complete chip separation process for one cutting tool edge. The uncutted chip cross section tc, depends on feed, f, cut depth, ap and tool immersion angle, and is expressed as:

$$tc(\lambda) := (f \cdot \sin(\lambda)) \cdot ap \qquad \text{Eq. D-2}$$

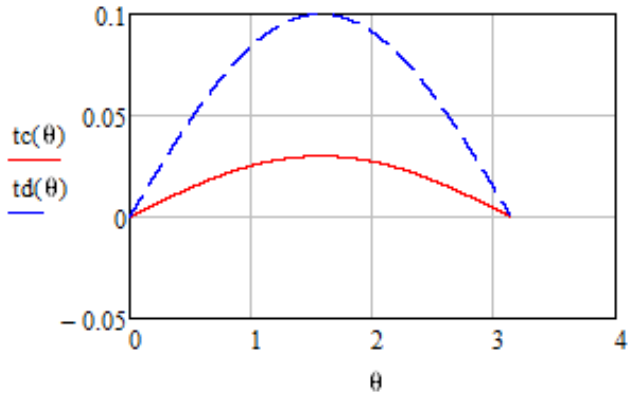

Fig. D-3. Un-cutted chip thickness along the cutting tool immersion angle

Next, for cutting force determination general, well known cutting force model was used. First local cutting force components from coefficients was determined:

$$Ft(\lambda) := Kt \cdot tc(\lambda) \qquad \text{Eq. D-3}$$

$$Fn(\lambda) := Kn \cdot (Kt \cdot tc(\lambda)) \qquad \text{Eq. D-4}$$

$$Fa(\lambda) := Ka \cdot (Kt \cdot tc(\lambda)) \qquad \text{Eq. D-5}$$

$$Fx(\lambda) := -Ft(\lambda) \cdot \cos(\lambda) - Fn(\lambda) \cdot \sin(\lambda) \qquad \text{Eq. D-6}$$

$$Fy(\lambda) := Ft(\lambda) \cdot \sin(\lambda) - Fn(\lambda) \cdot \cos(\lambda) \qquad \text{Eq. D-7}$$

$$Fz(\lambda) := Fa(\lambda) \cdot \sin(\lambda) \qquad \text{Eq. D-8}$$

Cutting force coefficient change during the cutting process and cutting tool immersion angle is represented in Fig. D-4.

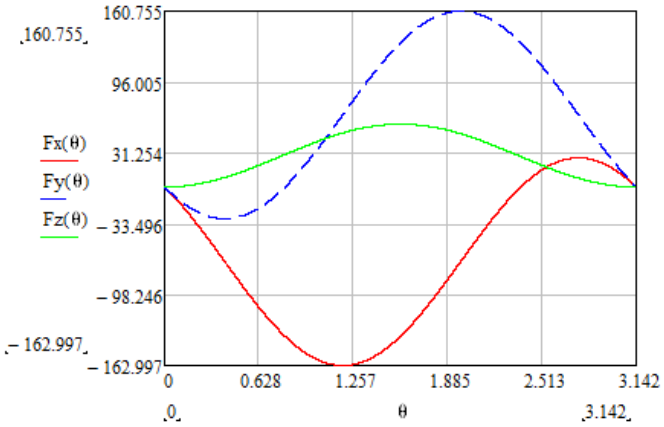

Fig. D-4. Cutting force changes along the cutting tool rotation from immersion till the end of cut

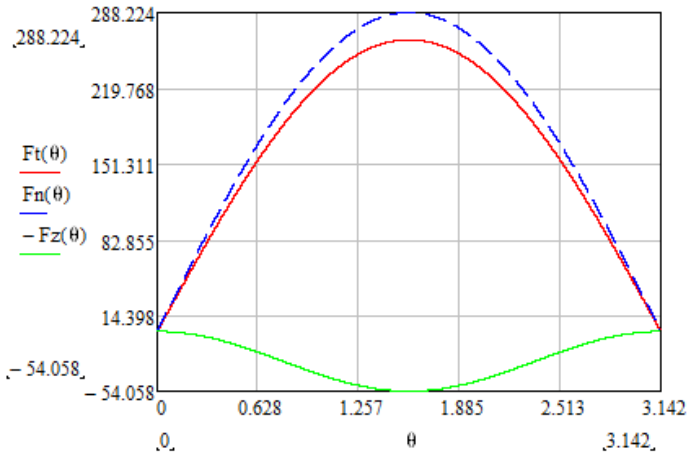

Fig. E-5. Cutting force changes along the cutting tool rotation from immersion till the end of cut

In Mathcad software, numerical solution was applied to the differential equation of motion. Below is represented view from MathCad software where the procedure of motion differential equation solving was executed to obtain system vibration amplitudes.

NUMERICAL SOLUTION

Given

$M := 168.2$ $C := 1000$ $tm := 10$ Table mass, demping force, solving time

$fn := 139$ $n := 4775$

$fex := \frac{4774}{60}$ Natural and exitation freq

$\omega n := fn \cdot 2 \cdot \pi$ Natural angular frequency

$\omega ex := \pi \cdot fex \cdot 2 \cdot 2 = 999.864$ Exitation frequency

$y'(0) = 0$

$y(0) = 0$

$Fa(\omega ex \cdot t) \cdot \sin(\omega ex \cdot t)$

$K := \omega n^2 \cdot M = 1.283 \times 10^8$

$f(t) := 115$ Cutting force on axis

$$M \cdot \frac{d^2}{dt^2} y(t) + C \cdot \left(\frac{d}{dt} y(t) \right) + K \cdot y(t) = f(t)$$

$y := Odesolve(t, tm)$

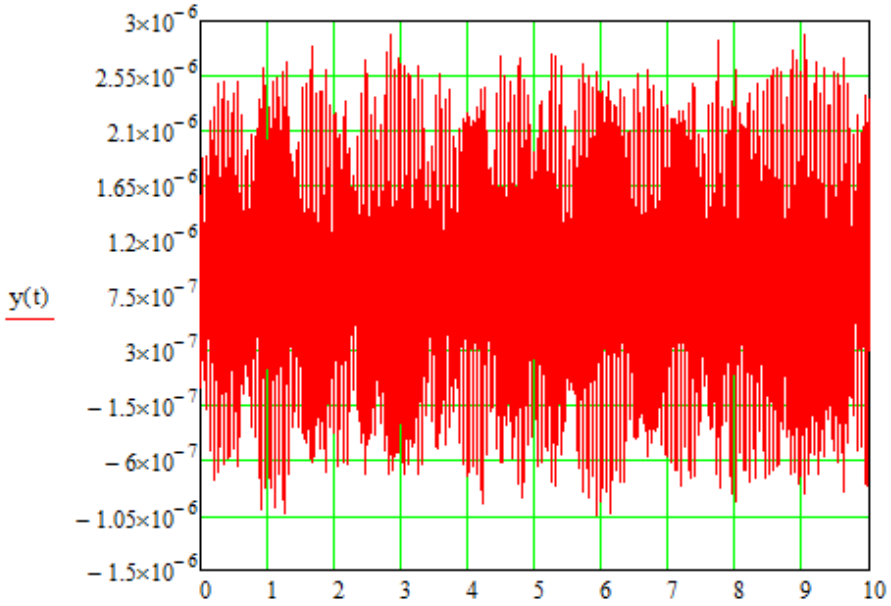

Fig. E-6. Milling table vibration amplitude in *Z* axis direction.

Table E-1. Results of predicted vibration amplitude in μm for GENTIGER GT66 milling machine

GENTIGER GT66						Gentiger Vibration Amplitude, μm
Material	Sample Nr.	Yield strenght, N/mm2	Feed rate, mm/t	Cutting direction	Measured Sz, μm	
1.1730	8.1	560	0,04	SOUTH	14,669580	2,2020
1.1730	8.2	560	0,04	WEST	5,560960	2,2020
1.1730	8.3	560	0,04	NORT	7,181510	2,2020
1.1730	8.4	560	0,04	EAST	9,947900	2,2020
1.1730	10.1	560	0,1	SOUTH	9,940090	2,4290
1.1730	10.2	560	0,1	WEST	12,535850	2,4290
1.1730	10.3	560	0,1	NORT	9,236980	2,4290
1.1730	10.4	560	0,1	EAST	8,256570	2,4290
1.1730	15.1	560	0,2	SOUTH	10,693360	2,5140
1.1730	15.2	560	0,2	WEST	12,593170	2,5140
1.1730	15.3	560	0,2	NORT	11,623720	2,5140
1.1730	15.4	560	0,2	EAST	14,890640	2,5140
1.2312	24.1	820	0,04	SOUTH	3,904490	2,2920
1.2312	24.2	820	0,04	WEST	3,514940	2,2920
1.2312	24.3	820	0,04	NORT	6,792110	2,2920
1.2312	24.4	820	0,04	EAST	4,259040	2,2920
1.2312	26.1	820	0,1	SOUTH	4,790890	2,2201
1.2312	26.2	820	0,1	WEST	8,281630	2,2201
1.2312	26.3	820	0,1	NORT	8,219480	2,2201
1.2312	26.4	820	0,1	EAST	4,601300	2,2201
1.2312	31.1	820	0,2	SOUTH	21,905520	2,3630
1.2312	31.2	820	0,2	WEST	12,029410	2,3630
1.2312	31.3	820	0,2	NORT	18,587170	2,3630
1.2312	31.4	820	0,2	EAST	11,853460	2,3630

Table E-2. Results of predicted vibration amplitude in μm for KONDIA B500 milling machine

KONDIA B500						Kondia Vibration Amplitude, μm
Material	Sample Nr.	Yield strenght, N/mm2	Feed rate, mm/t	Cutting direction	Measured Sz, μm	
1.1730	2.1	560	0,04	SOUTH	16,028090	3,307
1.1730	2.2	560	0,04	WEST	12,447170	3,307
1.1730	2.3	560	0,04	NORT	10,808250	3,307
1.1730	2.4	560	0,04	EAST	11,915360	3,307
1.1730	7.1	560	0,1	SOUTH	11,965270	4,7643
1.1730	7.2	560	0,1	WEST	14,935230	4,7643

1.1730	7.3	560	0,1	NORT	10,316150	4,7643
1.1730	7.4	560	0,1	EAST	12,115000	4,7643
1.1730	1.1	560	0,2	SOUTH	30,297970	5,1899
1.1730	1.2	560	0,2	WEST	22,432550	5,1899
1.1730	1.3	560	0,2	NORT	20,034520	5,1899
1.1730	1.4	560	0,2	EAST	11,289970	5,1899
1.2312	18.1	820	0,04	SOUTH	7,869790	3,5154
1.2312	18.2	820	0,04	WEST	11,870090	3,5154
1.2312	18.3	820	0,04	NORT	8,668390	3,5154
1.2312	18.4	820	0,04	EAST	5,543330	3,5154
1.2312	23.1	820	0,1	SOUTH	11,217830	4,1958
1.2312	23.2	820	0,1	WEST	11,688370	4,1958
1.2312	23.3	820	0,1	NORT	8,961290	4,1958
1.2312	23.4	820	0,1	EAST	13,980070	4,1958
1.2312	17.1	820	0,2	SOUTH	24,209540	4,578
1.2312	17.2	820	0,2	WEST	43,962470	4,578
1.2312	17.3	820	0,2	NORT	27,663840	4,578
1.2312	17.4	820	0,2	EAST	24,336890	4,578